CHARACTERIZATION AND UTILIZATION OF ACTIVATEDTAMARIND KERNEL POWDER IN INDUSTRIAL WASTE - WATER TREATMENT

BY

ABRAHAM DANLADI ADAMS

P14SCTX8016

A DISSERTATION SUBMITTED TO THE SCHOOL OF POSTGRADUATE STUDIES,

AHMADU BELLO UNIVERSITY, ZARIA

NIGERIA

IN PARTIAL FULFILLMENT OF THE REQUIREMENTS FOR THE AWARD OF MASTER OF SCIENCE IN COLOUR CHEMISTRY AND TECHNOLOGY

DEPARTMENT OF POLYMER AND TEXTILE SCIENCE

AHMADU BELLO UNIVERSITY,

ZARIA, NIGERIA

MAY, 2017

DECLARATION

I hereby declare that the work in this dissertation entitled "CHARACTERIZATION AND UTILIZATION OF TAMARIND KERNEL POWDER IN INDUSTRIAL WASTEWATER TREATMENT" has been carried out by me in the Department of Polymerand Textile Science. The information derived from the literature has been duly acknowledged in the text and a list of references provided. No part of this thesis was previously presented for another degree or diploma at this or any other institution.

---------- ---------- ----------

Student Name Signature Date

CERTIFICATION

This dissertation entitled CHARACTERIZATION AND UTILIZATION OF TAMARIND KERNEL POWDER IN INDUSTRIAL WASTE-WATER TREATMENT by ABRAHAM DANLADI ADAMS meets the regulations governing the award of the degree of Master of Science in Colour Chemistry and Technology of the Ahmadu Bello University, and is approved for its contribution to knowledge and literary presentation.

---------- ----------

Professor Olufemi Sunmonu Date

Chairman, Supervisory Committee

---------- ----------

Professor Umaru S. Ishiaku Date

Member, Supervisory Committee

---------- ----------

Dr. Elaoyi David Paul Date

Member, Supervisory Committee

---------- ----------

Prof. Abu S. Lawal Date

Head of Department

---------- ----------

Prof. Sadiq Z. Abubakar Date

Dean, Postgraduate School

DEDICATION

This research work is dedicated to God Almighty and to the Mother I never met.

ACKNOWLEDGEMENT

To God Almighty, for everything He has done for me, His love, and faithfulness which he has freely bestowed upon my life; I say thank you Jehovah.

To my distinguished team of supervisors, Professor Olufemi Sunmonu, Professor Umaru S. Ishiaku and Dr. Elaoyi David Paul, I say thank for your intellectual support and encouragement.

To my parents, guardians and relations I express my sincere appreciation, may God Almighty continue to keep and sustain you throughout your days on earth.

To my lecturers at the Departments of Chemistry and Textile Science, I say thank you for the hard work you have put in to help transform our minds into that of researchers.

To my friends and colleagues, I say thank you for the support and encouragement you offered me throughout my research.

Finally, I want to say thank you to the members of staff of laboratory unit of Science laboratory technology Department, Nigerian Institute of Leather and Science Technology (NILEST) Zaria, and the Multi User Laboratory, Ahmadu Bello University Zaria, may God Almighty bless and sustain you in Jesus Name, Amen.

ABSTRACT

Activated tamarind kernel powderwas prepared from tamarind seed(Tamarindus indica);and utilized for the removal of Acid Red 1, Reactive Orange 20 and Reactive blue 29 dyes from their aqueous solutions. The powder was activated using 4M nitric acid (HNO_3). The effect of various parameters which include; pH, adsorbent dosage, ion concentration, and contact time were studied to identify the adsorption capacity of the activated tamarind kernel powder under the above conditions. The percentage of dye adsorbed is seen to be dependent on these factors. The result obtained indicated that the adsorption of Acid Red 1 (AR1), Reactive Orange 20 (RO20) and Reactive Blue 29 (RB29) decreased with increase in initial concentration but increased with increase in temperature. At equilibrium, all three dyes showed highest dye uptake at initial dye concentration of 20 mg/l, pH 2, adsorbent dose of 1.0 g, and at a contact time range of 80-100 min. The Langmuir, Freundlich, Temkin and Dubinin Radushkevichisotherm models measured at a temperature range of 298-328K are fitted into the graphs. The Temkin isotherm model is best-fitted into the experimental data with R^2 values ranging between 0.913-0.987 for Acid Red 1, 0.865-0.969 for Reactive Orange 20 and 0.942-0.992 for Reactive Blue 29. The next in line for best fitting is the Langmuir isotherm with R^2 values ranging between 0.859-0.995 for Acid Red 1 dye, 0.825-0.974 for Reactive Orange 20 and 0.971-0.989 for Reactive Blue 29. This is followed by Dubinin Radushkevich isotherm with R^2 values ranging between 0.931-0.974 for Acid Red 1, 0.923-0.989 for Reactive Orange 20 and 0.789-0.923 for Reactive Blue 29. Lastly is the Freundlich isotherm with R^2 values ranging between 0.803-0.931 for Acid Red 1, 0.856-0.964 for Reactive Orange 20 and 0.982-0.995 for Reactive Blue 29. The pseudo-first order and pseudo-second order kinetic models were also fitted into the graphs, but pseudo-second order was best fitted into the experimental data. The thermodynamic parameters such as enthalpy, entropy, and free energy which were determined using the Van't Hoff equations were found to

provide the clues necessary to predict the nature of the adsorption process. The values of the activation energy (E_A) obtained indicated that the adsorption of AR1, RO20 and RB29 on activated tamarind kernel powder (ATKP) is a physical process.The negative free energy (ΔG) indicatedthat the adsorption process is feasible and spontaneous, the negative enthalpy (ΔH) indicatedthat the reaction is exothermic in nature and the negative entropy (ΔS) indicated that there is decreased randomness at the solid/solution interphase during the adsorption process. The chemical functional groups of the ATKP adsorbent were studied by Fourier Transform Infrared (FTIR) spectroscopy which helped in the identification of possible adsorption sites on the adsorbent surface. Characterization of the activated tamarind kernel powder which was carried out using standard methods, showed that the values of the parameters of interest such as moisture and dry matter content, ash content, pH and bulk density; fall within acceptable range. Therefore, activated tamarind kernel powder has proven to be a very good adsorbent for the removal of acid dyes and reactive dyes.

TABLE OF CONTENTS

	Page
Title Page	i
Declaration	ii
Certification	iii
Dedication	iv
Acknowledgements	v
Abstract	vi
Table of Contents	viii
List of Figures	xiv
List of Tables	xix
List of Appendices	xxi
List of Plates	xxiii
Abbreviations	xxiv

CHAPTER ONE INTRODUCTION

1.1	Background of Study	1
1.2	Statement of Research Problem	3

1.3 Justification for the Research 3

1.4 Aim and Objectives 4

CHAPTER TWO LITERATURE REVIEW 5

2.1 Dyes 5

2.1.1 Acid Dyes 5

2.1.2 Reactive Dyes 6

2.1.2.1 C.I. Reactive Blue 29 6

2.1.2.2 C.I. Reactive Orange 20 7

2.2 Tamarind 8

2.2.1 Taxonomy 9

2.2.2 Botanical Description 10

2.2.3 Common/Vernacular Names 10

2.2.4 Fruits and Seeds 10

2.2.5 Origin and Geographical Distribution 11

2.3 Polymers 11

2.4 Adsorption 13

2.4.1 Types of Adsorption 14

2.4.1.1 Chemisorption 14

2.4.1.2 Physisorption 14

2.4.3 Extent of Adsorption 15

2.4.4 Adsorption Rate 16

2.4.4 Adsorption Isotherms 16

2.4.4.1 Langmuir Isotherm 17

2.4.4.2 Freundlich Isotherm 18

2.4.4.3 Temkin Isotherm 20

2.4.4.4 Dubinin Radushkevich Isotherm 20

2.4.5 Adsorption Thermodynamics 21

2.4.5.1 Van't Hoff Plot 21

2.4.5.2 Development of Van't Hoff Plot 22

2.4.6 Adsorption Kinetics 23

2.4.6.1 Pseudo-First Order Kinetics 23

2.4.6.2 Pseudo-Second Order Kinetics 23

2.5 Tamarind kernel Polysaccharide 24

2.5.1 Industrial Utilization of Tamarind Kernel Powder 25

2.5.1.1 Pharmaceutical Applications of TKP 25

2.5.2 Tamarind Kernel Powder as Composite Material 26

2.5.2.1 Hydroxyapatite (Hap)/Tamarind Kernel Powder (TKP) Composite 26

2.5.2.2 Fourier Transform Infrared Spectroscopy of TKP/HAp Nano Composites 26

2.5.3. Tamarind Kernel Powder in Diary Waste water Treatment 27

CHAPTER THREE MATERIALS AND METHODS29

3.1 Materials 29

3.1.1 Sample Collection, Identification and Treatment 29

3.1.2 Preparation of 0.1M HCl 29

3.1.3 Preparation of 0.1 M NaOH 29

3.1.4 Preparation of 4 M HNO_3 29

3.1.5 Adsorbate Preparation 30

3.2 Methods 30

3.2.1 Preparation of Adsorbent 30

3.2.2 Characterization of ATKP 30

3.2.2.1Moisture and Dry Matter Content 30

3.2.2.2Ash Content 31

3.2.2.3 pH measurement 31

3.2.2.4 Bulk Density 32

3.2.3FTIR Analysis 32

3.2.4 Adsorption Experiment 33

3.2.4.1 Effect of initial Dye Concentration 33

3.2.4.2 Effect of Adsorbent Dose 34

3.2.4.3 Effect of pH 34

3.2.4.4 Effect of Contact Time 34

3.2.4.5 Effect of Temperature 34

3.2.4.6 Adsorption Isotherms 35

3.2.4.7 Adsorption Kinetics 35

3.2.4.8 Adsorption Thermodynamics 35

CHAPTER FOUR RESULTS 37

4.1 Characterization of ATKP 37

4.2 FTIR Analysis of ATKP 37

4.3 Adsorption Studies 37

4.4 Adsorption Isotherms 37

4.4.1 Langmuir Isotherms 37

4.4.2 Freundlich Isotherms 67

4.4.3 Temkin Isotherms 67

4.4.4 Dubinin-Radushkevich Isotherms 67

4.5 Adsorption Kinetics 67

4.6 Adsorption Thermodynamics 67

CHAPTER FIVE DISCUSSION 122

5.1 Characterization of ATKP 122

5.1.1 Moisture and Dry Matter Content 122

5.1.2 Bulk Density 122

5.1.3 Ash Content of ATKP 123

5.1.4 pH of ATKP 123

5.2 FTIR Analysis of ATKP 123

5.3 Adsorption Studies 125

5.3.1 Effect of pH 125

5.3.2 Effect of Adsorbent Dose 126

5.3.3 Effect of Contact Time 126

5.3.4 Effect of initial Concentration 127

5.3.5 Adsorption Isotherm Modelling 128

5.3.5.1Langmuir Isotherm 128

5.3.5.2 Freundlich Isotherm 130

5.3.5.3 Temkin Isotherm 132

5.3.5.4 Dubinin Radushkevich 134

5.4 Adsorption Kinetics 136

5.5 Adsorption Thermodynamics 138

CHAPTER SIX SUMMARY, CONCLUSION AND RECOMMENDATIONS 139

6.1 Summary and Conclusion 139

6.2 Recommendations 140

6.3 Contributions to Knowledge 141

REFERENCES 142

APPENDICES 158

LIST OF FIGURES

Figures

4.1	FTIR of Raw ATKP	43
4.2	FTIR of AR1 treated ATKP	44
4.3	FTIR of RO20 treated ATKP	45
4.4	FTIR of RB29 treated ATKP	46
4.5	Effect of pH Plot	47
4.6	Effect of Adsorbent Dose Plot	48
4.7	Effect of Contact Time Plot	49
4.8	Effect of initial Concentration Plot	50
4.9	Langmuir isotherm Plot for AR1 at 298K	51
4.10	Langmuir isotherm Plot for AR1 at 308K	52
4.11	Langmuir isotherm Plot for AR1 at 318K	53
4.12	Langmuir isotherm Plot for AR1 at 323K	54
4.13	Langmuir isotherm Plot for AR1 at 328K	55
4.14	Langmuir isotherm Plot for RO20 at 298K	56
4.15	Langmuir isotherm Plot for RO20 at 308K	57

4.16 Langmuir isotherm Plot for RO20 at 318K 58

4.17 Langmuir isotherm Plot for RO20 at 323K 59

4.18 Langmuir isotherm Plot for RO20 at 328K 60

4.19 Langmuir isotherm Plot for RB29 at 298K 61

4.20 Langmuir isotherm Plot for RB29 at 308K 62

4.21 Langmuir isotherm Plot for RB29 at 318K 63

4.22 Langmuir isotherm Plot for RB29 at 323K 64

4.23 Langmuir isotherm Plot for RB29 at 328K 65

4.24 Separation Factor Plot 66

4.25 Freundlich isotherm Plot for AR1 at 298K 68

4.26 Freundlich isotherm Plot for AR1 at 308K 69

4.27 Freundlich isotherm Plot for AR1 at 318K 70

4.28 Freundlich isotherm Plot for AR1 at 323K 71

4.29 Freundlich isotherm Plot for AR1 at 328K 72

4.30 Freundlich isotherm Plot for RO20 at 298K 73

4.31 Freundlich isotherm Plot for RO20 at 308K 74

4.32 Freundlich isotherm Plot for RO20 at 318K 75

4.33 Freundlich isotherm Plot for RO20 at 323K 76

4.34 Freundlich isotherm Plot for RO20 at 328K 77

4.35 Freundlich isotherm Plot for RB29 at 298K 78

4.36 Freundlich isotherm Plot for RB29 at 308K 79

4.37 Freundlich isotherm Plot for RB29 at 318K 80

4.38 Freundlich isotherm Plot for RB29 at 323K 81

4.39 Freundlich isotherm Plot for RB29 at 328K 82

4.40 Temkin isotherm Plot for AR1 at 298K 83

4.41 Temkin isotherm Plot for AR1 at 308K 84

4.42 Temkin isotherm Plot for AR1 at 318K 85

4.43 Temkin isotherm Plot for AR1 at 323K 86

4.44 Temkin isotherm Plot for AR1 at 328K 87

4.45 Temkin isotherm Plot for RO20 at 298K 88

4.46 Temkin isotherm Plot for RO20 at 308K 89

4.47 Temkin isotherm Plot for RO20 at 318K 90

4.48 Temkin isotherm Plot for RO20 at 323K 91

4.49 Temkin isotherm Plot for RO20 at 328K 92

4.50 Temkin isotherm Plot for RB29 at 298K 93

4.51 Temkin isotherm Plot for RB29 at 308K 94

4.52 Temkin isotherm Plot for RB29 at 318K 95

4.53 Temkin isotherm Plot for RB29 at 323K 96

4.54 Temkin isotherm Plot for RB29 at 328K 97

4.55 Dubinin Radushkevich isotherm Plot for AR1 at 298K 98

4.56 Dubinin Radushkevich isotherm Plot for AR1 at 308K 99

4.57 Dubinin Radushkevich isotherm Plot for AR1 at 318K 100

4.58 Dubinin Radushkevich isotherm Plot for AR1 at 323K 101

4.59 Dubinin Radushkevich isotherm Plot for AR1 at 328K 102

4.60 Dubinin Radushkevich isotherm Plot for RO20 at 298K 103

4.61 Dubinin Radushkevich isotherm Plot for RO20 at 308K 104

4.62 Dubinin Radushkevich isotherm Plot for RO20 at 318K 105

4.63 Dubinin Radushkevich isotherm Plot for RO20 at 323K 106

4.64 Dubinin Radushkevich isotherm Plot for RO20 at 328K 107

4.65 Dubinin Radushkevich isotherm Plot for RB29 at 298K 108

4.66 Dubinin Radushkevich isotherm Plot for RB29 at 308K 109

4.67 Dubinin Radushkevich isotherm Plot for RB29 at 318K 110

4.68 Dubinin Radushkevich isotherm Plot for RB29 at 323K 111

4.69 Dubinin Radushkevich isotherm Plot for RB29 at 328K 112

4.70 Pseudo-First order Plot for AR1 113

4.71 Pseudo-First order Plot for RO20 114

4.72 Pseudo-First order Plot for RB29 115

4.73 Pseudo-Second order Plot for AR1 116

4.74 Pseudo-Second order Plot for RO20 117

4.75 Pseudo-Second order Plot for RB29 118

4.76 Van’t Hoff Plot for AR1 119

4.77 Van’t Hoff Plot for RO20 120

4.78 Van’t Hoff Plot for RB29 121

LIST OF TABLES

Tables

2.1	Common Names of Tamarind	10
2.2	Chemical composition of TKP	26
4.1	Physicochemical Parameters of ATKP	38
4.2	FTIR of Raw ATKP	39
4.3	FTIR of AR1 treated ATKP	40
4.4	FTIR of RB29 treated ATKP	41
4.5	FTIR of RO20 treated ATKP	42

LIST OF APPENDICES

Appendix		Page
1	Standard Calibration Curve for AR1	158
2	Standard Calibration Curve for RB29	159
3	Standard Calibration Curve for RO20	160
4	Experimental Data for AR1	161
5	Experimental Data for RO20	162
6	Experimental Data for RB29	163
7	Equilibrium Data for AR1Langmuir Plot	164
8	Equilibrium Data for RO20 Langmuir Plot	165
9	Equilibrium Data for RB29 Langmuir Plot	166
10	Equilibrium Data for AR1Freundlich Plot	167
11	Equilibrium Data for RO20Freundlich Plot	168
12	Equilibrium Data for RB29 Freundlich Plot	169
13	Equilibrium Data for AR1 Temkin Plot	170
14	Equilibrium Data for RO20 Temkin Plot	171
15	Equilibrium Data for RB29 Temkin Plot	172

16 Equilibrium Data for AR1 Dubinin Radushkevich Plot 173

17 Equilibrium Data for RO20 Dubinin Radushkevich Plot 174

18 Equilibrium Data for RB29 Dubinin Radushkevich Plot 175

19 Equilibrium Data for Pseudo-First and Pseudo-Second order Plot 176

20 Equilibrium Data for Van't Hoff Plot 177

21 Effect of pH 178

22 Effect of Adsorbent Dose 179

23 Effect of Contact Time 180

24 Effect of Initial Concentration 181

25 Langmuir Isotherm Constants 182

26 Freundlich Isotherm Constants 183

27 Temkin Isotherm Constants 184

28 Dubinin Radushkevich Isotherm Constants 185

29 Pseudo-First Order Constants 186

30 Pseudo-Second Order Constants 187

31 Thermodynamic Parameters 188

LIST OF PLATES

Plates

I	Coloured Effluent Discharge	189
II	Dye Polluted Water Body	190
III	Prepared Stock Solutions of AR1, RO20 and RB29 dyes	191
IV	Prepared Concentrations of AR1, RO20 and RB29 dyes	192
V	Treatment of dye samples using ATKP	193
VI	Temperature controlled treatment of dye samples on ATKP	194
VII	Uv/Visible Spectrophotometric analysis of treated dye samples	195

ABBREVIATIONS AND SYMBOLS

TKP	Tamarind Kernel Powder
ATKP	Activated Tamarind Kernel Powder
FTIR	Fourier Transform Infrared
CI	Colour Index
AR1	Acid Red 1
RO20	Reactive Orange 20
RB29	Reactive Blue 29
q_e	Equilibrium Adsorbate Concentration
q_t	Equilibrium Adsorbate Concentration at time T
q_e(calc)	Calculated Equilibrium Adsorbate Concentration
K_{eq}	Equilibrium Constant
R_L	Separation Factor
R^2	Correlation Coefficient
b	Langmuir Constant
k_f	Freundlich Constant
q_D	Dubinin Radushkevich Constant

b_T	Temkin Constant
k_1	Pseudo-First order Constant
k_2	Pseudo-Second order Constant
ΔG	Gibbs free energy Change
ΔH	Enthalpy Change
ΔS	Entropy Change
% R	Percent dye Adsorbed

CHAPTER ONE

INTRODUCTION

1.1 Background of Study

Environmental pollution control is said to be amatter of utmost concern in many countries. However, air and water pollution constitute the major environmental pollution in several countries. Consequently, open burning leads to air pollution, while industrial effluent and domestic sewage leads to water pollution. Water pollution results to bad effects on public water supplies which can cause health problem, while air pollution can cause lung diseases, burning eyes, cough, and chest tightness. The environmental issues surrounding the presence of colour in effluent is a continuous problem for dye stuff manufacturers, dyers, finishers, and water companies (Kesari *etal.*, 2011).

The contaminants such as dyes, heavy metal, cyanide, toxic organics, nitrogen, phosphorus, phenols, suspended solids, colour, and turbidity from industries and untreated sewage sludge from domestics, are becoming of great concern to the environmental and public health. Therefore, the treatment of these pollutants is very important (Cheremisinoff, 1993).

Residual dyes from different sources (e.g., textile industries, paper and pulp industries, dye and dye intermediates industries, pharmaceutical industries, tannery, and Kraft bleaching industries and others) are considered a wide variety of organic pollutants introduced into the natural water resources or wastewater treatment systems. One of the main sources with severe pollution problems worldwide is the textile industry and its dye-containing wastewaters (i.e. 10,000 different textile dyes with an estimated annual production of 7.105 metric tonnes are commercially available worldwide; 30% of these dyes are used in excess of 1,000 tonnes per annum, and 90% of the textile products are used at the level of 100 tonnes per annum or less) (Baban *et al*., 2010; Robinson *et al*., 2001; Soloman *et al*., 2009). About 10-25% of textile dyes are lost during the dyeing process, and 2-20% is directly discharged as aqueous effluents

in different environmental components. In particular, the discharge of dye-containing effluents into the water environment is undesirable, not only because of their colour, but also because many of the dyes released and their breakdown products are toxic, carcinogenic or mutagenic to life forms mainly because of carcinogens, such as benzidine, naphthalene and other aromatic compounds (Suteu *et al*., 2009; Zaharia *et al*., 2009). Without adequate treatment these dyes can remain in the environment for a long period of time. For instance, the half-life of hydrolysed Reactive Blue 19 is about 46 years at pH 7 and 298 K (Hao*et al.*, 2000).

In addition to the aforementioned problems, the textile industry consumes large amounts of potable and industrial water as processing water (90-94%) and a relatively low percentage as cooling water (6-10%) in comparison with the chemical industry where only 20% is used as process water and the rest for cooling. The recycling of treated wastewater has been recommended due to the high levels of contamination in dyeing and finishing processes (i.e. dyes and their breakdown products, pigments, dyeintermediates, auxiliary chemicals and heavy metals, and others(Bertea and Bertea, 2008; Bisschops and Spanjers, 2003; Correia *et al*., 1994; Orhon *et al*., 2001).

Synthetic dyes have been increasing in textile industries for dyeing natural and synthetic fibres. Discharge of dye- bearing waste-water makes an adverse effect on aquatic environment because the dyes give water undesirable colour (Ibrahim *et al.,* 2010) and reduce light penetration and photosynthesis (Al-Degs *et al.,* 2004; Wang *et al.,* 2005; Oei *et al.,* 2009). Conventional methods used to treat coloured effluents are oxidation, coagulation and flocculation, biological treatment, membrane filtration. However, the single conventional treatment is unable to remove certain forms of colour, particularly those arising from reactive dyes as a result of their high solubility and low biodegradability (Vijayaraghavan *et al.,* 2009).

1.2 Statement of Research Problem

One of the major problems concerning textile and leather wastewaters is coloured effluent (Ramakrishna, *et al;* 1997). This wastewater contains a variety of organic compounds and toxic substances, which are harmful to fish and other aquatic organisms. Dyes even in low concentrations affect the aquatic life and food web. Since many organic dyes are harmful to human beings, the removal of colour from process or waste effluents becomes environmentally important. Due to the large degree of organics present in these molecules and the stability of modern dyes, conventional physicochemical and biological treatment methods are ineffective for their removal (Mckay, 1995).

1.3 Justification for the Research

Activated carbon is a widely used adsorbent due to its high adsorption capacity, high surface area, microporous structure, and high degree of surface reactivity, but there are some problems associated with its use,it is expensive and regeneration results in a 10–15% loss of adsorbent and its uptake capacity and therefore this adds to the operational costs. This led to a search for cheaper, easily obtainable materials for the adsorption of dye from industrial effluent (Waranusantigul*et al.,* 2003). As a result, the use of natural waste products and plants has increased considerably during the past years for pollution control applications (Kumar *et al*., 2009).

Tamarind Kernel is a biological waste material which is readily available and relatively cheap. It can be collected and powdered. (Shanthi and Mahalakshmi,2012).It has excellent potential for the removal of dye from coloured effluent (Patel and Vashi, 2010).TKP has been used to remove dyes from the binary mixture of their aqueous solution (Shanthi and Mahalakshmi,2012).It has also found excellent application in the reduction of Chemical oxygen demand (COD), Total dissolved solids; Sulphates and Turbidity from diary waste water (Shoba*et al*., 2015).

1.4 Aim and Objectives

The aim of this research is to characterize and utilize Activated Tamarind Kernel Powder (ATKP) in the treatment of Industrial waste water.

This aim will be achieved by the following objectives:

i. To isolate, carbonize and activate the tamarind kernel powder
ii. To determine some physicochemical parameters which include pH, contact time, adsorbent dose and initial concentration of the ATKP adsorbent
iii. To run the FTIR Spectra of the activated ATKP adsorbent before and after treatment with Acid Red 1, Reactive Orange 20 and Reactive Blue 29 (AR1, RO20 and RB29) in order to identify the functional groups responsible for the adsorption of each dye molecule unto the ATKP surface
iv. To analyse the effect of Initial concentration, Initial pH, Contact time, Adsorbent dose and operating Temperature in order to determine the optimum conditions for maximum adsorption of the dyes (AR1, RO20 and RB29) from their aqueous solutions
v. To examine the adsorption efficiency of ATKP for AR1, RO20 and RB29 by analysing the adsorption isotherms (Langmuir, Freundlich, Temkin and Dubinin-Radushkevich)
vi. To examine the rate of adsorption by studying the adsorption Kinetics (Lagagren Pseudo-First order and Pseudo-Second order)
vii. To examine the spontaneity of adsorption of AR1, RO20 and RB29 on ATKP through the determination of the thermodynamics parameters (Standard Gibbs free energy, Activation Energy, Enthalpy and Entropy)

CHAPTER TWO

LITERATURE REVIEW

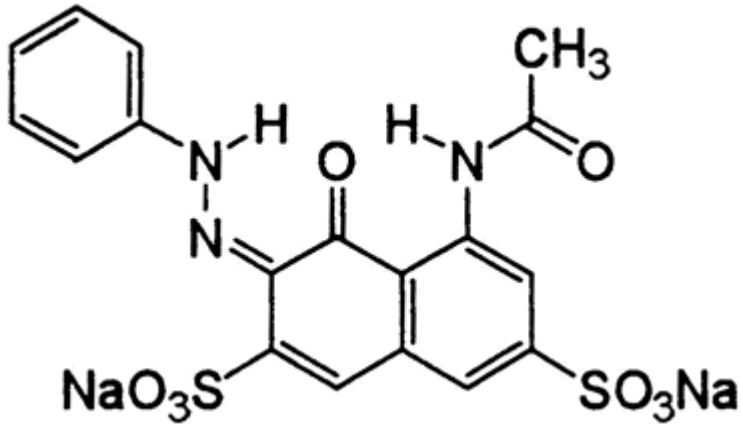
2.1Dyes

Dye is a natural or synthetic colouring material, whether soluble or insoluble which impacts its colour to a material by staining or being imbibed by it, and which is employed from a solution of fine dispersion, sometimes with the aid of mordant. Many types of dyes used in textile industries are direct, reactive, acid, and basic dyes. However, these dyes are invariably left in the industrial wastes. They are widely used in textile, paper, leather, and mineral processing industries to colour their product. Their presence in wastewater causes adverse effects in human and aquatic life when disposed into the environment (Wang *et al*., 2005). This is because they have synthetic origin and complex aromatic molecular structures, which makes them inert and difficult to biodegrade when discharged into waste streams. Also,people overlook their undesirable nature. Some dyes and their degradation products may be carcinogens and toxins, which are important sources of water pollution. Thus, their treatment becomes a major problem to environmental managers. Some dyes are harmful to aquatic life in rivers where they are discharged, because they can reduce light penetration into water, decrease the efficiency of photosynthesis in aquatic plant, and have adverse effect on their growth (Gurses *et al*., 2006). Furthermore, dyes can also cause severe damage to human beings such as the malfunctioning of kidney, reproductive system, liver, brain, and the central nervous system (Andre *et al*., 2011).

2.1.1 Acid dyes

Acid dyes are highly water soluble, and have better light fastness than basic dyes. The textile acid dyes are effective for protein fibres such as silk, wool, nylon and modified acrylics. They contain sulphonic acid groups, which are usually present as sodium sulphonate salts. These increase solubility in water, and give the dye molecules a negative charge. In an acidic

solution, the -NH_2 functionalities of the fibres are protonated to give a positive charge $^{+}NH_3$. This charge interacts with the negative dye charge, allowing the formation of ionic interactions. As well as this, Van-der-Waals bonds, dipolar bonds and hydrogen bonds are formed between dye and fibre. As a group, acid dyes can be divided into two sub-groups: acid-levelling or acid-milling. These dyes are normally very complex in structure but have large aromatic molecules, having a sulphonyl or amino group which makes them soluble in water. Most of the acid dyes belong to one of the following three main structural molecules, namely anthraquinone, azo and triphenylmethane type(www.Textilelearner.blogspot.com.ng 2012). A common example of acid dye is C.I. Acid Red 1. This dye is synthesised by diazotizing aniline and coupling the salt with 4-acetamido-5-hydroxynaphthalene-2,7-disulfonicacid (www.worlddyevariety.com/acidred1, 2013)



C.I. Acid Red 1

2.1.2 Reactive Dyes

Reactive dyes are coloured organic compounds that are capable of forming a covalent bond between reactive groups of the dye molecule and nucleophilic groups on the polymer chains within the fibre (Tailor *et al.*, 2006). Consequently, the dyes become chemically part of the

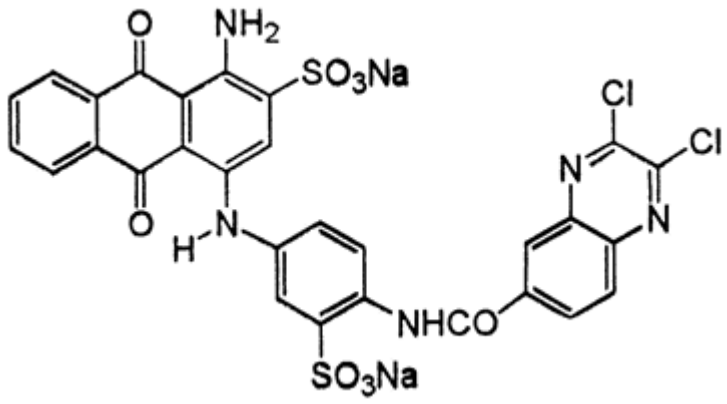
fibre by producing dye-polymer linkages (Dolby, 1977; Nkeonye, 1988). In this regard, covalent dye-polymer bonds are formed, for instance, with the hydroxyl groups of cellulose, the amino, hydroxyl and mercapto groups of proteins, and the amino groups of polyamides (Patel *et al*., 2002).

The possibility of forming a covalent bond between dyes and fibres had long been attractive to dye chemists, since attachment by physical adsorption and by mechanical retention had the disadvantage of either low wash fastness or high cost (Beech, 1970; Ahmed, 1995). It was anticipated that the covalent attachment of the dye molecules to the fibre would produce very high washfastness because covalent bonds are the strongest known binding forces between molecules (Nkeonye, 1988; Bhattacharya and Paschal, 1984). The energy required to break this bond would be of the same order as that required to break covalent bonds in the fibre itself (Lewis, 1982).

Reactive dyes were initially introduced commercially for application to cellulosic fibres, and this is still their most important use (Christie, 2001; Ratee, 1984). The growth rate of reactive dyes for cellulosic fibres is expected to continue increasing, because reactive dyes continue to gain market share at the expense of other dye types such as azoic dyes (Dolby, 1977). Reactive dyes have also been developed for application on protein and polyamide fibres. In addition, investigations into the development of reactive dyes for polyester and polypropylene fibres have been demonstrated to the level of technical possibility but such dyes are not yet of commercial interest (Christie, 2001; Ratee, 1984).

2.1.2.1 C.I. Reactive Blue 29

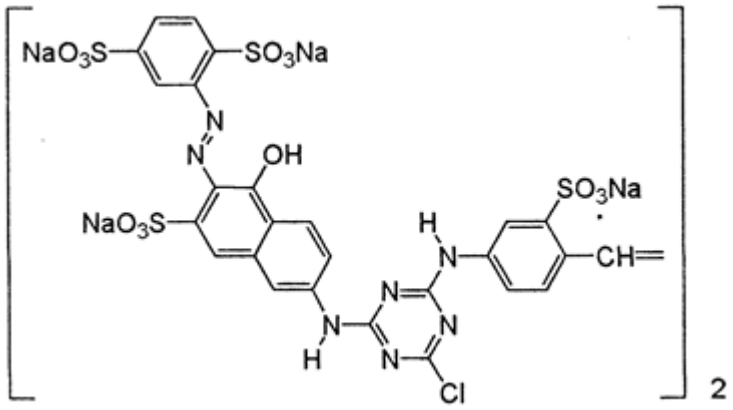
Reactive Blue 29 is synthesised from the condensation reaction of 1-amino-4-bromo-9,10-dihydroanthracene-2-sulfunic acid and 2,5-diaminobenzene sulfonic acid and then reacting the product by condensation with 2,3-dicholoroquinoxaline-6-carboxylchloride(www.worlddyevariety.com/reactiveblue29, 2013).



C.I. Reactive Blue 29

2.1.2.2 C.I. Reactive Orange 20

Reactive Orange 20 is synthesised by diazotization of 2-aminobenzene-1,4-disulfonic acid and coupling with 7-amino-4-hydroxynaphthalene-2-sulfonic acid and then reacting the product by condensation with 1,2-bis (4-amino-2-sulfophenyl) ethane (www.worlddyevariety.com/reactiveorange20, 2013).



C.I. Reactive Orange 20

2.2 Tamarind

Tamarind (*Tamarindus indica* L) is a multipurpose tropical fruit tree used chiefly for its fruits, which are eaten fresh or processed for non-food uses. It is widely grown as a subsistence crop for meeting local demands. It is also grown for commercial application in food, pharmaceutical and textile industries (Purseglove 1987).

2.2.1 Taxonomy

Tamarind is a monotypic genus containing the only species *T. indicus*. It is thought that Linnaeus gave the specific epithet indicus because the name Tamarind itself was derived from Arabic which combined Tamar meaning 'date' with the Hindi meaning 'of India'. The full Arabic name was TamarU'l-Hind and the word 'data' was included because of the brown appearance of Tamarind pulp. No systematic cytogenetic stitches have been carried out for Tamarind although diploid chromosomes number (2n) has been reported (Purseglove, 1987).

The Nomenclature of Tamarind is as follows:

Kingdom	:	Plantae (plants)
Sub-Kingdom	:	Tracheobionta (vascular plants)
Super-division	:	Spermatophyta (seed plants)
Division	:	Magnoliophyta (flowering plants)
Class	:	Magnoliopsida (dicotyledanae)
Subclass	:	Rosidae
Order	:	Fabales
Family	:	Fabaceae
Genus	:	Tamarindus
Species	:	indica L (http://plants.usda.gov/, Rudd1991).

2.2.2 Botanical Description

Tamarind is a long-lived, large, evergreen or semi-evergreen tree, 20-30m tall with a thick trunk that can reach 1.5-2m diameter. The trunk is sometimes multi-stemmed with widely spreading branches. The bank is brownish-grey, rough and scaly. Young twigs are slender and puberulent. Tamarind produces a deep taproot and an extensive lateral root system (El-Siddig *et al*.,2006).

2.2.3 Common/Vernacular Names

Tamarind is known by a variety of common/vernacular names that vary both within and from country to country, mainly because of its importance, distribution, multiple uses and popularity among the people (Gunasena and Hughes 2000).

Table 2.1some common names of Tamarind by country

Country/Language	Common/Vernacular Name
English	Tamarind, Indian date
China	Khaam, Mak, Khan
French	Tamarin, Tamarainer
Hindi	Ambli, Auli, Inuli
Nigeria	Tsamiya
Kenya	Mkwaju, Oran

2.2.4 Fruits and Seeds

The fruits are pods 5-16cm long x 2cm broad, oblong, curved or straight, with rounded ends, somewhat compressed and indehiscent although brittle. The pod has an outer epicarp which is light grey or brown and scary. Within is firm but the soft pulp is thick and blackish brown.

The pulp is traversed by formed seed cavities, which contain the seeds. The outer surface of the pulp has three tough branched fibres from the base to the apex. Each pod contains 1-12 seeds which are flattered, glossy, and orbicular to rhomboid, each 3-10 x 1.3 cm and the centre of each flat side of the seed is marked with a large central depression. Seeds are hard, red to purple brown, non arillate and exalbuminous. Seed chambers are lived with a parchment like membrane. Cotyledons are thick (El-Siddig *et al*; 2006). Pods ripen about 10 months after flowering and can remain on the tree until the next flowering period, unless harvested (Rama Rao, 1975; Chaturvedi, 1985).

2.2.5 Origin and Geographical Distribution

Various geographical areas have been proposed for the origin of Tamarind; India (Morton, 1987) or the far east of Africa but the consensus is that it is Africa, placed it in Ethiopia, but others considered it indigenous to the drier savannahs of tropical Africa, from Sudan, Ethiopia, Kenya and Tanzania, West-ward though Sub Sahelian Africa to Senegal (El-Siddig *et al*; 2006; NAS, 1979). It is thought to have been introduced to South and Southeast Asia a very long time ago (Brenan, 1967; NAS, 1979) and naturalized in many areas where it was introduced (Purseglove, 1987; Coronel, 1991).

According to Simons *et al.,* (2005) the native distribution of Tamarind is as follows: Burkina Faso, Cameroon, Central African Republic, Chad, Ethiopia, Gambia, Guinea, Guinea-Bissau, Kenya, Madagascar, Mali, Niger, Nigeria, Senegal, Sudan, Tanzania, Uganda, Cape Verde.

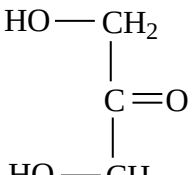
2.3 Polymers

Polymers are macromolecules composed of a large number of repeating monomer units. Polymers can be natural or synthetic, and are usually high molecular weight compounds with regularly arranged smaller units. Natural polymers are usually polysaccharides and are widely

used as excipients in oral drug delivery dosage forms. These natural materials have advantages over synthetic polymers, since they are chemically inert, nontoxic, less expensive, biodegradable, widely available, have less chance of adverse effects and have better patient acceptance (Jani*et al*., 2009). Natural polymers like gums and mucilages are plant-based hydrocolloids abundant in Nature and common in higher plants. Gums are considered to be pathological products formed following an injury to the plant or as a result of some pathological condition, while mucilages are physiological and normal products of metabolism (Malviya*et al*; 2011).

The term "carbohydrate" is derived from the $C_n(H_2O)_n$ general chemical formula exhibited by most of these molecules. Carbohydrates are the most common organic molecules, and are far more common than any other type of biological compound. Carbohydrates have a variety of roles. Carbohydrates are important components of extracellular molecules, including secreted soluble proteins, cell-surface proteins, and various types of extracellular matrix molecules. In the form of cellulose, carbohydrates act as one of the main structural components in plants. Carbohydrates are also used in bacterial cell walls, and form the major components of arthropod exoskeletons. Carbohydrates are used as energy sources in essentially all organisms. Glucose polymers, such as starch in plants and glycogen in animals and bacteria, are critical energy storage molecules. In addition, glucose is a source of biosynthetic intermediates for nearly all anabolic pathways. Most carbohydrate nomenclature is based on historical trivial names. However a few general rules are commonly used. The word saccharide (from the Sanskrit word śarkarā via the Greek word sakcharon (σακχαρον), meaning "sugar") is also used to refer to carbohydrates. It is primarily used to refer to the size of the molecule. "Monosaccharide" refers to the individual carbohydrates; "oligosaccharide" and "polysaccharide" refer to carbohydrate polymers of varying sizes. The suffix "-ose" designates a carbohydrate. The number of carbon atoms is designated by a prefix for some

forms of the compound names (e.g., triose and hexose). Some carbohydrates contain ketones; these are termed ketoses, and are sometimes (but not always) identified by the "-ulose" suffix. Most other carbohydrates are termed aldoses, because they contain aldehydes. The simplest carbohydrate, dihydroxyacetone, is a ketotriose, with the molecular formula $C_3(H_2O)_3$.



Dihydroxyacetone

With the exception of dihydroxyacetone (which is a symmetrical molecule), all carbohydrates are chiral molecules. In general, aldoses have (n – 2) chiral centres, while ketoses have (n – 3) chiral centres (Mark-Brandt, 2011).

2.4 Adsorption

Adsorption is actually a mechanism in which the forces of interaction between surface atoms and the adsorbate molecules are similar to Van der Waals forces that exist between all adjacent molecules. There are both attractive forces and repulsive forces with the net force depending on the distance between the surface of the adsorbent and the adsorbate molecule (Cooney,1999).

In other words, adsorption is a process in which a soluble chemical (the adsorbate) is removed from a fluid (liquid) or gas by contact with a solid surface (the adsorbent).It is the trapping of impurities by strong physical bond within the porous structure of Carbon. It is one of the many processes used to purify, concentrate, or separate components (Glenn,1993) and competes with other processes like evaporation, solvent extraction, distillation, sublimation, drying, sedimentation, filtration, screening, ion exchange, centrifugation, and absorption (Glenn,1993).It is used in industry for product separation and waste treatment. In general,

adsorption is the process by which a component moves from one phase to another while crossing some boundaries. It was found that the observed effect of adsorption was achieved within porous solids and that adsorption was the result of interactive forces of physical attraction between the surface of porous solids and component molecules being removed from the bulk phase (Arun, 2002).

2.4.1 Types of Adsorption

2.4.1.1 Chemisorption

Chemisorption can be seen to result from chemical interaction between the adsorbate and the adsorbing medium. The bonding force associated is much stronger and the heat liberated during the process is much larger than that in physisorption. Typically, the enthalpy values are in the region of 200kJ mol^{-1} (Atkins, 2003). The energy needed for the chemisorbed molecule to react with other molecular species may be considerably less than the energy required when the two species react directly in the gas phase. This lower energy requirement is the basis of explanation of the catalytic effect of solid surfaces in enhancing the rate of some chemical reactions. Chemisorption is an irreversible process; on desorption, the substance undergoes a chemical change (Bhatia, 2006). On a general note, monolayer is formed in chemisorption due to the short-range chemical forces between the adsorbate and adsorbent (Atkins, 2003; Oladunni, 2012).

2.4.1.2 Physisorption

In physisorption, the molecules adhere to the surface of the solid adsorbent as a result of intermolecular attractive forces (Vander Waals forces) between them. The adsorption process is exothermic and liberates heat depending upon the magnitude of the attractive force. The advantage of physisorption is that the process is reversible. The adsorbed material can be easily removed or desorbed by reducing the pressure or by increasing the temperature without any change in chemical composition. Another desirable characteristic of physisorption is that

the rate generally is quite rapid (Bhatia, 2006). The enthalpy of physisorption can be measured by monitoring the rise in temperature of a sample of known heat capacity, and typical values are in the region of 20kJmol^{-1} (Atkins 2003; Oladunni 2012).

The major factors which affect physical adsorption include the surface area of the adsorbent, pore structure of the adsorbent, surface chemistry of the adsorbent, nature of the adsorbate, pH of the solution, and the presence of competing adsorbates. It is due to these factors that physical adsorption is considered to be a complex phenomenon. Surface area of the adsorbent is one of the most important factors on which adsorption greatly depends. The surface area is comprised of two types, the external surface area and the internal surface area (pore walls). When molecules are larger than the pore diameter, lesser adsorption would take place because of steric hindrances (LaGrega*et al.*, 1994; Cooney, 1999).

2.4.2 Extent of Adsorption

The surface of an adsorbent is typically composed of various surface functional groups (SFG). Adsorption of organic adsorbate is greatly dependent on the amount and nature of surface oxide groups (Cooney, 1999). Surface functional groups (carbon/oxygen) are created by oxidation occurring during the activation process of an adsorbent. Some of the common basic functional groups created are lactones, quinones, and carboxylates (Arun, 2002). Some of the common acidic functional groups created are phenolic, hydroxyl, carbonyl, and carboxylic acids (Arun, 2002). The presence of oxygen-containing basic groups are a key factor in promoting irreversible adsorption (Vidic *et al.*, 1993).Strongly dissociated adsorbates are weakly adsorbed when compared to non-dissociated adsorbates (Cooney, 1999). The more non polar an adsorbate, the higher the adsorption capacity. This is attributed to the fact thatthese adsorbate molecules tend to prefer the adsorbent surface rather than being in the solution (Cooney, 1999). It has also been shown that an increase in the molecular weight of the adsorbate will generally enhance adsorption until the size of the adsorbate is

larger than the pore size of the adsorbent. Typically, aromatic compounds are more adsorbable than aliphatic compounds of similar molecular size and branched-chain molecules are generally more adsorbable than straight-chain molecules (Cooney, 1999). In addition, solubility of the adsorbate is also an important factor. In general, the lower the solubility of the adsorbate, the higher the adsorption capacity since the forces of attraction between the adsorbate molecules and the adsorbent surface molecules will be greater than the forces of attraction between the adsorbate and the solvent molecules (Cooney, 1999).

The extent of surface coverage is normally expressed as the fractional coverage, θ. It represents the extent of adsorption:

$$\theta = \frac{Number\ of\ Adsorption\ sites\ occupied}{Number\ of\ Adsorption\ sites\ available} \qquad 2.1$$

The fraction coverage can also be expressed in terms of volume of adsorbate (Atkins, 2003).

2.4.3 Adsorption Rate

The rate of adsorption, ($d\theta/dt$) is the rate change of surface coverage with time and can be determined by observing the change of fractional coverage overtime (Atkins, 2003).

2.4.4 Adsorption Isotherms

Adsorption Isotherms are empirical relationship used to predict how much solute can be adsorbed by activated carbon (Steve and Erika, 1998). Chilton *et al.*,(2002) defined Adsorption isotherm as a graphical representation showing the relationship between the amount adsorbed by a unit weight of adsorbent (eg activated carbon) and the amount of adsorbate remaining in a test medium atequilibrium. It maps the distribution of adsorbable solute between the liquid and solid phases at various equilibrium concentration (Chilton *et al.,* 2002).The adsorption isotherm is based on data that are specific for each system and the isotherm must be determined for every application. An adsorption isotherm besides providing a panorama of the course taken by the system under study in a concise form, it also

indicateshow efficiently an estimate of the economic feasibility of the carbons' commercial application for the specific solute can be obtained (Chilton *et al.,* 2002).

2.4.4.1 Langmuir Isotherm

The Langmuir adsorption model explains adsorption by assuming an adsorbate behaves as an ideal gas at isothermal conditions. At these conditions, the adsorbates partial pressure is related to its volume when adsorbed onto a solid adsorbent. The adsorbent is assumed to be an ideal solid surface composed of series of distinct sites capable of binding the adsorbate. The adsorbate binding is treated as a chemical reaction between the adsorbate molecule and an empty site. This reaction yields an adsorbed complex with an associated equilibrium constant K_{eq} (Dorian *et al.,* 2014).

The non-linear expression of Langmuir isotherm model can be illustrated as Equation (2.2) (Langmuir, 1916):

$$q_e = q_m K_L \ C_e/1+K_L C_e \quad (2.2)$$

where C_e is the concentration of solution at equilibrium (mg/L); qe is the corresponding adsorption capacity (mg/g); q_m(mg/g) and K_L (L/mg) are constants which are related to adsorption capacity and energy or net enthalpy of adsorption, respectively.Linear forms of the isotherms models are also widely adopted to determine the isotherm parameters or the most fitted model for the adsorption system due to the mathematical simplicity. The linear forms of the Langmuir are as follows:

$$C_e/q_e = 1/q_m K_L + C_e/q_m \quad (2.3)$$

$$1/q_e = [1/q_m K_L]1/C_e + 1/q_m \quad (2.4)$$

$$q_e = q_m - [1/K_L]q_e/C_e \quad (2.5)$$

$$q_e/C_e = K_L q_m - K_L q_e \quad (2.6)$$

Among the four linear forms which will result in different parameter estimates, the type I (eq. 2.3) is one of the most popular linear forms used in literatures, due to the minimal deviations

from the fitted equation (Kinniburgh, 1986; Ho, 2005). Hence by plotting C_e/q_e against Ce it is possible to obtain the value of the Langmuir constant K_L and q_m.

Langmuir model made the following assumptions:

(i) The adsorption is an equilibrium process

(ii) Adsorption cannot proceed beyond monolayer coverage

(iii) Each adsorption site is equivalent in terms of energy of adsorption and uniform i.e. the surface is perfectly flat on a microscopic scale

(iv) There are no interactions between adjacent adsorbate molecules

Although the theory is more appropriate for the description of chemisorption, it is adopted for a number of systems where the coverage is low. Thus, Langmuir adsorption isotherm is applicable to monolayer adsorption onto a surface having homogenously distributed identical binding sites over the sorbent surface.

Langmuir isotherm study has been carried out on the adsorption of various substances on tamarind kernel powder (Kinniburgh, 1986; Ho, 2005).

The equilibrium parameter R_L, which is a dimensionless constant, is referred to as separation factor and is given by:

$$R_L = \frac{1}{1+(1+bC_o)} \qquad (2.7)$$

Where; C_o is the initial concentration and b is the Langmuir equilibrium constant. The R_L values indicate the adsorption to be favourable if ($0< R_L<1$), unfavourable if ($R_L>1$), linear if ($R_L=1$) or irreversible if ($R_L=0$).

2.4.4.2 Freundlich Isotherm

A fairly satisfactory empirical isotherm, which can be applied to adsorption of gases with considerable success but has been used principally for adsorption from solution, has been discussed by H. Freundlich.

The Freundlich adsorption isotherm (Ozacar and Sengil, 2003) is given by:

$$q_e = K_f C_e^{1/n} \quad (2.8)$$

A linear form of the expression above is written as:

$$\log q_e = \log K_f + 1/n \log C_e \quad (2.9)$$

where q_e is the amount of adsorbate per unit weight of adsorbent, K_F is Freundlich constant measuring adsorption capacity, C_e is the equilibrium concentration of the adsorbate in solution, n is a constant related to adsorption efficiency and energy of adsorption intensity of adsorbent. K_f and n can be obtained from the intercepts and slopes of the linear plot of $\log q_e$ against $\log C_e$. The magnitude of adsorption intensity n gives an indication of the favourability of the adsorption process. Ho and Chang (2001) reported that the favourability of the process is achieved if n lies in the range of 1–10.The Freundlich equation is basically empirical but is often useful as a means for data description. This is because the equation is adequate to describe non-linear adsorption in a narrow range of adsorbate concentration. The mathematical simplicity of the equation enables it to be used easily. It describes the adsorption processes on surface adsorption sites that are energetically heterogeneous. However, theoretically, the amount of adsorbed solute may become infinite as bulk solute concentration increases and this is a disadvantage.The adsorption isotherm is useful for predicting the capacity that an adsorbent has for adsorbing adsorbate. The steeper the isotherm, the more effective is the adsorbent. As the concentration increases, the higher will be the effective capacity at the concentration level desired for adsorption (Weber, 1973).

The Langmuir and Freundlich equations provide mathematical description of the experimentally observed dependence of the on concentration. The adsorption isotherm relates to an equilibrium condition. However, the practical retention times used in many water treatment applications do not provide sufficient time for true equilibrium to be obtained (Weber, 1973).

2.4.4.3 Temkin Isotherm model

This model assumes that the adsorption heat of all molecules decreases linearly with the increase in coverage of the adsorbent surface and that adsorption is characterized by a uniform distribution of binding energy. (Piccin*et al*., 2011).

The Temkin isotherm (Aharoni and Sparks, 1991) is given by:

$$qe = RT/b\ln(A_T C_e) \quad (2.10)$$

The linear form of Temkin isotherm can be expressed as:

$$q_e = (RT/b_T)\ln A_T + (RT/bT)\ln C_e \quad (2.11)$$

where A_T is the Temkin isotherm equilibrium binding constant (L/g); b_T is the Temkin isotherm constant; R is the universal gas constant (8.314J/mol/K); T is the temperature at 298K; and $C_e$is the equilibrium concentration (mg/L). Temkin isotherm constant $b_T$and Temkin isotherm equilibrium binding constant $A_T$are obtained from the intercepts and slopes of the linear plot of q_e versus lnC_e.

2.4.4.4 The Dubinin-Radushkevich (D-R) Isotherm Model

This considers that adsorbent size is comparable to the micropore size and the adsorption equilibrium relation for a given adsorbate-adsorbent combination can be expressed independently of temperature by using the adsorption potential (ε)

$$\varepsilon = \mathrm{RT}\ln\left(1 + \frac{1}{\mathrm{Ce}}\right) \quad (2.12)$$

The D-R isotherm assumes a Gaussian-type distribution for the characteristic curve and the model can be described as follows

$$\ln q_e = \ln q_s - B\varepsilon^2 \quad (2.13)$$

whereq_s is the D-R constant (mol/g) and B gives the activation energy (E_A) (kJ/mol) per molecule of adsorbate at the moment of its transfer to the solid surface from the bulk solution and can be computed using the equation:

$$E_A = \frac{1}{(2B)^{\frac{1}{2}}} \quad (2.14)$$

Values of q_s and B can be determined through linearization of the D-R isotherm by plotting ln q_e versus ε^2.

The activation energy,E_A reveals the nature of adsorption. Thus, if the value of activation energy E_A is less than 8 kJ/mol, adsorption process is physical; but if it is ranged from 8 to 16 kJ/mol, it is a chemical adsorption.

2.4.5 Adsorption Thermodynamics

Adsorption thermodynamics are determined from the thermodynamic equilibrium coefficients obtained at different temperatures and initial concentrations in order to verify possible adsorption mechanisms (Crini and Badot, 2008). The aim of thermodynamic study is to determine the spontaneity of the adsorption process by the use of thermodynamic parameters such as free energy change (ΔG), enthalpy change (ΔH), and entropy change (ΔS). ΔG determines if the process is feasible and spontaneous or not; ΔH determines if the process is exothermic or endothermic; and ΔS is used to determine the increase or decrease in randomness of the process at the solid/solution interface. Reactions occur spontaneously at a given temperature if ΔG is a negative quantity (Abdessalem *et al.*, 2012). The thermodynamic parameters were calculated based on the following equations:

$$\Delta G = -RT\ln(K) \quad (2.15)$$

$$\Delta G = \Delta H - T\Delta S \quad (2.16)$$

where T is the absolute temperature (K), R is the universal gas constant (8.314J/mol/K) and K is the Langmuir constant. The Gibbs free energy of adsorption (ΔG) can be related with the equilibrium constant K (L/mol), corresponding to the reciprocal of the Langmuir constant b (Oladoja*et al.*, 2008 In: Okoli *et al*., 2015).

2.4.5.1 Van't Hoff Plot

The Van't Hoff equation provides information about the temperature dependence of the equilibrium constant. The Van't Hoff equation may be derived from the Gibbs-Helmholtz

equation, which gives the temperature dependence of the Gibbs free energy. For the standard Gibbs free energy, the Gibbs-Helmholtz equation is:

$$\left(\frac{\partial(\Delta G/T)}{\partial(1/T)}\right) P = \Delta H \qquad (2.17)$$

Substituting the expression and dividing both sides by –*R*, the first form of the Van't Hoff equation is obtained,

$$\left(\frac{\partial lnK}{\partial(1/T)}\right) P = -\Delta H/R \qquad (2.18)$$

From this form of the Van't Hoff equation, we see that at constant pressure, a plot with lnK_{eq}on the *y*-axis and 1/ T on the *x*-axis has a slope given by –ΔH/R.This is the origin of LeChatelier's Principle for the heat absorbed or evolved during the course of a chemical reaction. For an endothermic reaction, the slope is negative and so as the temperature increases, the equilibrium constant increases. While for an exothermic reaction, the slope is positive and so as temperature increases, the equilibrium constant decreases (Jean, 2015).

2.4.5.2 Development of Van't Hoff equation from Thermodynamics

From the definition of Gibbs free energy

$$\Delta G = \Delta H - T\Delta S \qquad (2.19)$$

where *S* is the entropy of the system, and from the Gibbs free energy isotherm equation.

$$lnK = -\Delta H/RT + \Delta S/R \qquad (2.20)$$

these equations are combined to obtain

$$lnK = -\Delta H/RT + \Delta S/R \qquad (2.21)$$

Differentiation of this expression with respect to the variable *T* yields the Van't Hoff equation (Dickerson and Gies, 1976).

2.4.6 Adsorption Kinetics

Kinetic tests show the time-concentration profile for adsorption. The adsorption reaction itself is inherently an extremely fast one. It is mainly the particle mass transfer which controls the overall adsorption kinetics (adsorbent particle size, porosity, adsorbate size and mixing in the adsorption system). The adsorption kinetics constitutes a criterion in the determination of adsorption processes (Volesky *et al*., 1999). Kinetics studies are carried out by mixing an amount of adsorbent with a given concentration of metal solution, with varying contact time (Bhatti*et al*., 2006).

2.4.6.1 Pseudo-First Order

The pseudo-first order equation (Lagergren, 1898) is generally expressed as (McKay and Ho, 1999):

$$dq/dt = k_1(q_e-q_t) \quad (2.22)$$

where q_e and q_t are the amount of adsorbate adsorbed on adsorbent at equilibrium (mg/g) and time t, respectively, and k_1 is the rate constant of pseudo-first order adsorption (min-1). Integrating equation (15) for the boundary conditions t=0 to t=t is the following:

$$\log(q_e-q_t) = \log q_e - k_1 t/2.303 \quad (2.23)$$

The plot of $\log(q_e-q_t)$ versus t will give a straight line and the value of k_1 can be obtained from the slope of the graph while qe (calculated) is obtained from the intercept of the graph (Gupta and Rastogi, 2007).

2.4.6.2 Pseudo-Second Order

The pseudo-second order kinetic model is expressed as:

$$dq/dt = k_2(q_e-q_t)^2 \quad (2.24)$$

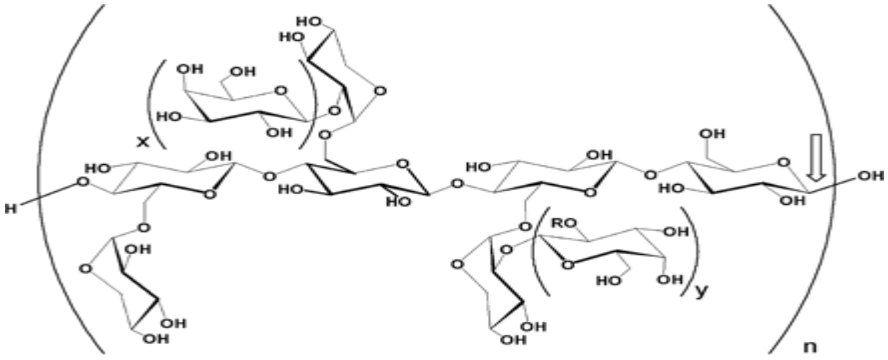
where k_2 is the pseudo-second order rate constant of adsorption (g./mg.min). The linearized integrated form of equation---is given as:

$$t/q_t = 1/k_2q_e^2 + 1/q_e\, t \quad (2.25)$$

If the pseudo-second order kinetics is applicable to the system, then the plot of t/q_t versus t will give a linear relationship with $1/q_e$ and $1/k_2q_e^2$ as the slope and intercept and there is no need to know any parameter beforehand. The pseudo-second order kinetics model has been successfully applied to several adsorption systems (Mckay and Ho, 1999; Oladunni, 2012).

2.5 Tamarind Kernel Powder

The composition of tamarind kernel powder resembles cereals with 12.7-15.4% of protein, 3-7.5% of oil, 7-8.4% of crude fibre, 61-72.2% carbohydrates, and 2.45-3.3% of ash. All of this was measured on dry weight basis (Gerard *et al*., 1980). Chemically, tamarind kernel powder is a highly branched carbohydrate polymer. TKP is a polymer with an average molecular weight of 52350 daltons and a monomer of mainly three sugars- glucose, galactose and xylose in a molar ratio of 3:2:1. The polymer consists of cellulose-type spine which carries xylose and galactoxylose substituents. About 80% of glucose residues are substituted by xylose residues (1-6 linked), which themselves are partially substituted by p-1-2 galactose residues. The exact sequential distribution of branches is not known. TKP is a branched polysaccharide with a main chain of Â-D-1-glucopyrynosyl units, with a side chain consisting of single D-xylopyranosyl unit attached to every 2nd, 3rd and 4th D glucopyrynosyl unit through1-6 linkage (Rao and Srivastava,1973). Native TKP exhibits a strong tendency to self-aggregate when dispersed in aqueous solvents. The aggregates consist of lateral assemblies of single polysaccharide strands, showing a behaviour that could be well described by the wormlike chain or the Kuhn's model. Static light scattering data on these particles show that their stiffness is determined by the number of aggregated strands. High degree of substitution of glucan chain produces a stiff extended conformation for tamarind polysaccharide molecule, with large volume occupancy in a solution (Glicksman, 1996).



Chemical structure of Tamarind kernel powder

2.5.1 Industrial Utilization of Tamarind Kernel Powder

2.5.1.1 Pharmaceutical Applications of TKP

Over the last two decades, muco-adhesion has attracted considerable attention for a range of reasons like its potential to optimize localized drug delivery by retaining a dosage form at the site of action (e.g. within gastrointestinal tract) and in case of systemic delivery by maintaining the formulation in intimate contact with the absorption site (e.g. the buccal cavity, stomach). Various studies have been conducted on buccal delivery of drugs using muco-adhesive polymers mainly polysaccharides (Bottari *et al*., 1975). Although Tamarind kernel powder (TKP) is used as an ingredient in food materials, it has not been extensively evaluated till date for its utility in pharmaceuticals formulations. TKP is a galactoxyloglucan isolated from seed kernel of *Tamarindus indica*. It possesses properties like high viscosity, broad pH tolerance and adhesivity (Rao *et al*., 1973). These properties led to its application as stabilizer, thickener, gelling agent, and binder in food and pharmaceutical industries. In addition to these, other important properties of TKP have been identified recently which include non-carcinogenicity (Sano *et al*., 1996), muco-adhesivity, biocompatibility (Burgalassi *et al*., 1996), high drug holding capacity (Kulkarni *et al*., 1997) and high thermal stability (Datta and Bandopadhyay,2006). These led to its application as excipient in the hydrophilic drug delivery system (Burgalassi *et al*., 1996; Kulkarni *et al*., 1997). Polysaccharides, such as hydroxy ethyl cellulose, ethyl cellulose and TKP are expected to

reside in the target area for relatively prolonged periods, in virtue of their muco-adhesivity and/or viscosity, which slows down the clearance from the site of application and this can be utilized to reduce the hepatic first pass metabolism and local degradation of the drug (Ucello-Berrata *et al*., 2008).TKP is an interesting candidate for pharmaceutical use. It is used as a carrier for variety of drugs for controlled release applications. Many techniques have been used to manufacture the TKP-based delivery systems, which makes it an exciting and promising excipient for the pharmaceutical industry for the present and future applications.

Table 2.2Chemical Compositions of TKP from different Location

Area	Uthaithani	Ang.Thong	NakhonSawan	India
Moisture %	9.69	9.09	9.63	10.78
Ash %	0.05	0.05	0.05	0.39
Protein %	13.46	13.95	13.61	12.53
Fat %	6.52	7.48	7.71	5.64
Polysaccharide %	79.97	78.52	78.63	81.62

(KittiyaKlahal*et al.*,2012)

2.5.2. Tamarind Kernel Powder as Composite Material

2.5.2.1. Hydroxyapatite (Hap)/Tamarind Kernel Powder (TKP) Composite

Hydroxyapatite has attracted much interest as a biomaterial for use in prosthetic application due to its similarity in crystallography and chemical composition to that of human hard tissue.(Rauli *et al*., 2011) Its outstanding properties like biocompatibility, bioactivity, osteo conductivity, non-toxicity and non-inflammatory nature.(Liu *et al*., 1997). This bio ceramic has got a variety of applications which include: bone tissue engineering, restoration of periodontal defects,(Meffert *et al*., 1985) edentulous ridge augmentation (Piecuch *et al*., 1986)orthopaedic and dental implant coating.(Munting *et al*., 1990) HAp is widely used for hard tissues repair, as a result, this inorganic phosphate has been studied extensively for

medical application in the form of powders, composite or even coatings (Khelendra *et al*., 2011). Although many routes have been explored for synthesis of hydroxyapatite powders such as hydrothermal methods (Yoshimura *et al*., 1994; Chye *et al*., 2008), sol-gel process (Sanosh*et al.,* 2009), reaction in solid state, microwave processing (Arita*et al.,* 1995), the chemical precipitation route has proven to be popular because of its versatile and economic advantages, and thus has been extensively reported (Yang *et al*., 2005).

2.5.2.2. Fourier Transform Infrared Spectroscopy of TKP/HAp Nano Composites

The Fourier transform infrared (FT-IR) Spectra is recorded on a Perkin elemer Spectrometer, in the range of 400 cm^{-1} to 4000 cm^{-1}. The spectra show the absorbance bands at 3425.82 cm^{-1} and 3609.39 cm^{-1}correspond to the presence of hydroxyl group in the composite. Absorbance bands at 1669.95 cm^{-1},1600.51 cm^{-1} and 1414.83 cm^{-1},1417.25cm^{-1} reveals the presence of C=O and CH_2 asymmetric bending and bands at 1036.51 cm^{-1},1035.53 cm^{-1} and 564.98 cm^{-1} 565.74 cm^{-1} shows the presence of phosphate group in the HAp/TKP nano composite. In an isolated state the compound of HAp shows a broad band at 3425 cm^{-1}, indicates the presence of intermolecular H-bonding. The sharp peak occurs in the region of 3609 cm^{-1} indicates the presence of free O-H, and there is no inter molecular H-bonding between the molecules of HAp.

2.5.3. Tamarind Kernel Powder Dairy Waste water Treatment

The effectiveness of Tamarind kernel powder, a cheap agro-based product, as an adsorbent to remove chemical oxygen demand (COD), total solids, turbidity and sulphate present in a dairy industry wastewater has been evaluated by Shoba *et al*., (2015). Maximum removal of COD, total solids, turbidity and sulphate was obtained at an optimum dosage of 4g/l (turbidity-57%, total solids- 77.14%,COD-68.18%, sulphates-71.42%), optimum rapid mixing contact time of 15 minutes (turbidity-73%, total solids 76.19%, COD- 79.5%,

sulphates- 85.71%) and an optimum slow mixing contact time of 40 minutes (turbidity- 78.8%, total solids- 80.95%, COD -92.05%, sulphates – 88.57%)(Shoba *et al*., 2015).

CHAPTER THREE

MATERIALS AND METHODS

3.1 Materials

3.1.1 Sample Collection, Identification and Treatment

Tamarind kernel fruit was collected from the local market at Samaru, Sabongari Local Government Area of Kaduna state. After collection it was taken to Biological Sciences Department of Ahmadu Bello University where it was identified as *Tamarindus indica*. The Tamarind kernel seeds were washed thoroughly with water to remove the adhering materials. Then, the reddish testa of the seeds wasremoved by heating seeds in an oven at 80^0C for 2 hours. The kernelswere tamped and placed in the oven at a temperature of 300 ^{0}C for 3 hours for the tamped powder to carbonize completely. The powder was sieved through 400 microns to get uniform geometrical size for use. The Acid Red 1, Reactive Orange 20 and Reactive Blue 29 dye samples were supplied by Sigma Aldrich Company.

3.1.2 Preparation of 0.1 M HCl

Exactly 8.3 ml of concentrated $HCl_{(aq)}$ (37% w/v) with specific gravity of 1.19 g/cm^3, was measured into a 1 L volumetric flask and made up to mark with double distilled water.

3.1.3 Preparation of 0.1 M NaOH

Exactly 4.0 g of sodium hydroxide pellets were dissolved indouble distilled water in a 100 ml volumetric flask and made up to mark with double distilled water.

3.1.4 Preparation of 4 M HNO_3

Exactly 69.44 ml of HNO_3 (65% w/v) with specific gravity of 1.4 g/cm^3, was measured into a 250 ml volumetric flask and made up to mark with double distilled water.

3.1.5 Adsorbate Preparation

Stock solutions (1.0 g/L) of Acid Red 1, Reactive Blue 29 and Reactive Orange 20 were prepared by dissolving about 1gram each of the dyes in 1 L of distilled water. All test solutions of the desired concentrations were prepared by successive dilutions to get the required initial experimental concentration (20–100 mg/L).

3.2 Methods

3.2.1 Preparation of Activated Tamarind Kernel Powder

The activated tamarind kernel powder was prepared as described by Shanthi and Mahalakshmi (2012). About 200g of the sieved carbon above was mixed with 200 ml 4M nitric acid. The mixture was transferred into an oven at 105 ^{0}C for 30min with occasional stirring before it was removed and left overnight. After cooling, the activated tamarind kernel powder was repeatedly washed with double distilled water until the pH of the filtrate fell between 6 - 6.5, the adsorbent was then dried in an oven at 105 ^{0}C for 1 hour and stored in a desiccator.

3.2.2Characterization of the Adsorbent

3.2.2.1 Moisture and Dry Matter Content

Clean silica crucibles were dried in a desiccator and weighed. Exactly 1g of the dry tamarind kernel powder was weighed as W_1. It was dried in an air-circulated oven at 105 ^{0}C for 3 hours after which it was cooled in a desiccator and then the final weight taken as W_2 (Gimba *et al.,* 2009).

$$Moisture\ (\%) = \frac{W_1 - W_2(g)}{W_1(g)} \times 100 \qquad 3.1$$

$$Dry\ matter\ (\%) = \frac{W_2\ (g)}{W_1\ (g)} \times 100 \qquad 3.2$$

3.2.2.2 Ash Content Determination

This was done using ASTM E1755-01. Copper crucible was heated in a furnace at 575^{0}C for four hours, cooled in a desiccator and weighed. Oven dried sample from the moisture content determination was used. The crucible containing the dry sample was placed in a muffle furnace and temperature was allowed to rise to 575^{0}C. After about 6 hours, it was removed and allowed to cool in a desiccator and the weight was taken as W_3. It was then placed back into the furnace at 575 ^{0}C for one hour until a constant weight of ± 0.3g was obtained(ASTM, 2003).

Calculation

$$Ash\ (\%) = \frac{W_3(g)}{W_1(g)} \times 100 \qquad 3.3$$

3.2.2.3 pH Measurements

The activated TKP sample was boiled in double distilled water using a reflux condenser to recycle water vapour. The particles of TKP were filtered out; after which the filtrate was cooled to 50°C and the pH of the filtrate was determined by electrometric measurement(ASTM, 1996).

3.2.2.4 Bulk Density

Displacement method was used for this analysis. This was done by measuring the volume of double distilled water displaced when known weight (2g) of the sample was transferred into a 50 ml of double distilled water in a 100 ml graduated measuring cylinder (Allen, 1974; Oladunni *et al*; 2012).

Procedure

A 100 ml calibrated measuring cylinder was washed and dried. Exactly 50 ml of the water was added to the measuring cylinder and the volume was noted. 2g of the sample was transferred into the measuring cylinder and volume of the increased water level was recorded. Care was taken to ensure there were no air bubbles before taking volume measurements.

Calculation

Volume of water displaced (ml) = Final – initial volume.

$$Bulk\ Density\ \left(\frac{g}{cm^3}\right) = \frac{Ma}{Va} \qquad 3.4$$

where Ma is the mass of the adsorbent (g) and Va is the volumeof water displaced (Oladunni *et al*., 2012).

3.2.3 Fourier Transform Infrared (FTIR) Analysis

To study the mechanism of dye removal by activated TKP, the active chemical groups on the adsorbent surface before and after respective dye adsorption were evaluated by FTIR spectroscopy. The FTIR spectrum was recorded on an Agilent Fourier Transform Infrared Spectrophotometer (FTIR) at the Multi-User Laboratory Ahmadu Bello University Zaria. 16 scans were collected at the range of 4000-650 cm^{-1} with resolution of 8 cm^{-1}.

3.2.4 Adsorption Experiment

3.2.4.1 Effect of Initial Dye Concentration

The adsorption experiment was carried out by batch method (Oladunni *et al*; 2012). The experiment was done at ambient temperature (298 K) with a basic reciprocating shaker using 120 ml glass bottle as the reactor. The working initial dye concentrations are 20, 40, 60, 80 and 100 mg/L.

Procedure

The effect of initial dye concentration was analysed. Exactly 50 ml of each of the working solution was measured using a measuring cylinder into 100 ml conical flasks; 0.2 g of the adsorbent was transferred into each conical flask. The mixtures were then transferred into the reactor bottles where they were agitated (at the same time) with a mechanical shaker at about 150 rpm for about 2 hours and left undisturbed on the desk for 24 hours to equilibrate. At the end of 24 hours, the mixture was filtered through a whatman filter paper into another 120 ml glass bottle. The first 5 ml of the filtrate was discarded to allow for proper saturation of the filter paper by the solution. The concentration of the dye remaining in the solution was determined using anAgilent Cary 300 UV/visible spectrophotometer. The amount of dye adsorbed was calculated using the equation:

$$qe = V\frac{(Co - Ce)}{W} \qquad 3.5$$

where q_e is the amount of dye adsorbed by the adsorbent, V is the volume of the solution, C_o is the initial dye concentration, C_e is the residual dye concentration and W is the weight of the adsorbent. The percentage dye removed (% Rem) was determined using the equation:

$$\%Rem = \frac{(Co - Ce)}{Co} \times 100 \qquad 3.6$$

3.2.4.2 Effect of Adsorbent Dose

The effect of the adsorbent dosage was determined at a constant pH of 6, initial dye concentration of 20 mg/L and agitation time of 2 hours. The adsorbent dosage was varied as follows: 0.4, 0.6, 0.8, 1.0 and 1.2 g.

3.2.4.3 Effect of Initial pH

The effect of initial pH was determined by altering the pH at constant temperature (298 K), adsorbent dosage (0.2 g), initial concentration (20 mg/L) and agitation time (2 hours). The pH was varied at 2,4,6,8 and 10 using 0.1M HCl and 0.1M NaOH to either increase or decrease the pH of the solution.

3.2.4.4 Effect of Contact Time

The effect of contact time is an important factor in adsorption studies as it helps in the study of the kinetics of adsorption. The effect of contact time was determined by agitating the mixture at varied time intervals. The agitation was carried out at constant temperature (298 K), adsorbent dosage (0.2 g), initial concentration (20 mg/L) and pH (pH 6). The contact time was varied at 20,40,60,80 and 100 mins.

3.2.4.5 Effect of Temperature

The effect of Temperatureis important to this study as it helps in generating the data needed for adsorption thermodynamic study. This was determined by agitating the mixture at varying temperatures and initial dye concentrations. The agitation was carried out at constant adsorbent dosage (0.2 g), and pH (pH 6) and contact time of 2 hours. The different temperatures used were 298, 308, 318, 323 and 328 K.

3.2.4.6 Adsorption Isotherms

The adsorption isotherms used in this research have been described in chapter 2.4.5.

Langmuir adsorption isotherm was obtained by plotting C_e/q_e against Ce and the Langmuir constant K_L and q_m were obtained from the intercept and slope respectively of the Langmuir plot.

Freundlich adsorption isotherm was obtained by plotting $\log q_e$ against $\log C_e$.K_f and n are Freundlich constants obtained from the intercepts and slopes of the Freundlich plot.

Temkin isotherm was obtained by a linear plot of q_e versus $\ln C_e$. The Temkin constant b_T and the Temkin isotherm equilibrium binding constant $A_T$were obtained from the intercepts and slopes of the Temkin plot.

The Dubinin Radushkevich isotherm was obtained by plotting ln q_e versus ε^2.Values of q_s and B were determined from the slope and intercepts of the D-R plot.

3.2.4.7 Adsorption Kinetics

The adsorption kinetics used in this research has been described in chapter 2.4.6.

The Pseudo first order plot was obtained by plotting log (q_e-q_t) against t and the value of k_1 was obtained from the slope of the graph while qe (calculated) was obtained from the intercept of the graph.

The Pseudo second order plot was obtained by plotting t/q_t against t with $1/q_e$ and $1/k_2q_e^2$ as the slope and intercept respectively.

3.2.4.8 Adsorption Thermodynamics

The adsorption thermodynamics used in this research has been described in chapter 2.4.5.

The thermodynamics parameters described in chapter 2.4.5 were obtained from the Van't Hoff equation, and a graph of $\ln K_{eq}$ on the *y*-axis and 1/ T on the *x*-axis was plotted where ΔHand ΔSwere obtained from the slope and intercept respectively of the plot.

CHAPTER FOUR

RESULTS

4.1 Characterization of Activated Tamarind Kernel Powder

Table 4.1 shows the values obtained from the physicochemical characterization that was carried out on the activated tamarind kernel powder.

4.2 FTIR Analysis of ATKP

Tables 4.2 to 4.5 show the results obtained from the FTIR analysis of pure activated tamarind kernel powder, Acid Red 1treated, Reactive Blue 29 treated and Reactive Orange 20 treated activated tamarind kernel powder respectively. Also the FTIR spectra from the analysis stated above are represented in Figures 4.1 to 4.4 in the same order as above.

4.3 Adsorption Studies

Figures 4.5 to 4.8 shows the plots obtained from the batch adsorption experiment in which the effect of initial pH, adsorbent dose, contact time, and initial concentrationwere determined.

4.4 Adsorption Isotherm Studies

4.4.1 Langmuir Isotherms

Figures 4.9 to 4.13 show the Langmuir isotherm plots for Acid Red 1 at a temperature of 298-328K respectively, figures 4.14 to 4.18 show the Langmuir isotherm plots for Reactive Orange 20 at temperature of 298-328K respectively, figures 4.19 to 4.23 show the Langmuir isotherm plots for Reactive Blue 29 at temperatures of 298-328K respectively. Figure 4.24 shows the Separation factor (R_L) variation with concentration on Adsorption of Acid Red 1, Reactive Orange 20 and Reactive Blue 29.

Table 4.1: Physicochemical Parameters of Tamarind Kernel Powder

Parameters	TKP
Dry matter content (%)	96.55
Moisture content (%)	3.45
pH	6.40
Bulk Density ($g.cm^{-3}$)	0.40
Ash content (%)	5.30

Table 4.2: FTIR Analysis of Raw Activated TKP

Group frequency (cm^{-1})	Funtional group Assignment
3261.4	O-H Stretch, Carboxylic acid
2922.2	H-C-H Stretch alkanes
2855.1	H-C-H Stretch alkanes
2109.7	$-C\equiv C-$ Stretch alkynes
1699.7	$-C=C-$ Stretch alkenyl
1606.5	$-C=C-$ Stretch conjugated
1237.5	C-N Stretch aromatic amines
1159.2	C-N Stretch aromatic amines
1028.7	C-O Stretch, Primary alcohol

Table 4.3: FTIR Analysis of AR1 Activated TKP

Group frequency (cm^{-1})	Functional group Assignment
3261.4	O-H (broad) Hydroxyl group, H-bonded OH Stretch
2926.0	Methyl C-H asymmetric/symmetric Stretch
2855.1	Methyl C-H asymmetric/symmetric Stretch
2113.4	—C≡≡C— terminal alkyne (monosubstituted)
1699.7	Aromatic combination bands
1606.5	Open chain Azo , Primary amine (NH bend)
1438.8	Aromatic nitro compounds
1241.2	Aromatic Phosphates (P-O-P stretch)
1159.2	—C=N Stretch, tertiary amine
1032.5	C-O Stretch, Primary alcohol

Table 4.4: FTIR Analysis of RB29 Activated TKP

Group frequency (cm^{-1})	Funtional group Assignment
3257.7	O-H (broad) Hydroxyl group, H-bonded OH Stretch
2926.0	Methyl C-H asymetric/symetric Stretch
2855.1	Methyl C-H asymetric/symetric Stretch
2109.7	—C≡≡C— terminal alkyne (monosubstituted)
1923.3	Aromatic combination bands
1703.4	Carboxylic acid
1606.5	Quinone or conjugated ketone
1241.2	Aromatic Phosphates (P-O-P stretch)
1159.2	Sulfonates
1028.7	(P-O-C stretch) Aliphatic Phosphate

Table 4.5: FTIR Analysis of RO20 Activated TKP

Group frequency (cm^{-1})	Funtional group Assignment
3343.4	O-H (broad) Hydroxyl group, H-bonded OH Stretch
2922.2	Methyl C-H asymetric/symetric Stretch
2855.1	Methyl C-H asymetric/symetric Stretch
2113.4	—C≡≡C— terminal alkyne (monosubstituted)
1703.4	Aromatic combination bands
1617.7	Open chain Azo , Primary amine (NH bend)
1438.8	Carbonate ion
1241.2	Aromatic ethers, Aryl-O Stretch
1159.2	Secondary amine CN stretch
1028.7	(P-O-C stretch) Aliphatic Phosphate

Agilent Technologies

Sample ID:ACTIVATED TKP
Sample Scans:16
Background Scans:16
Resolution:8
System Status:Good

Method Name:Transmittance Method
User:Admin
Date/Time:2016-07-25T11:52:39.149+01:00
Range:4000 - 650
Apodization:Happ-Genzel

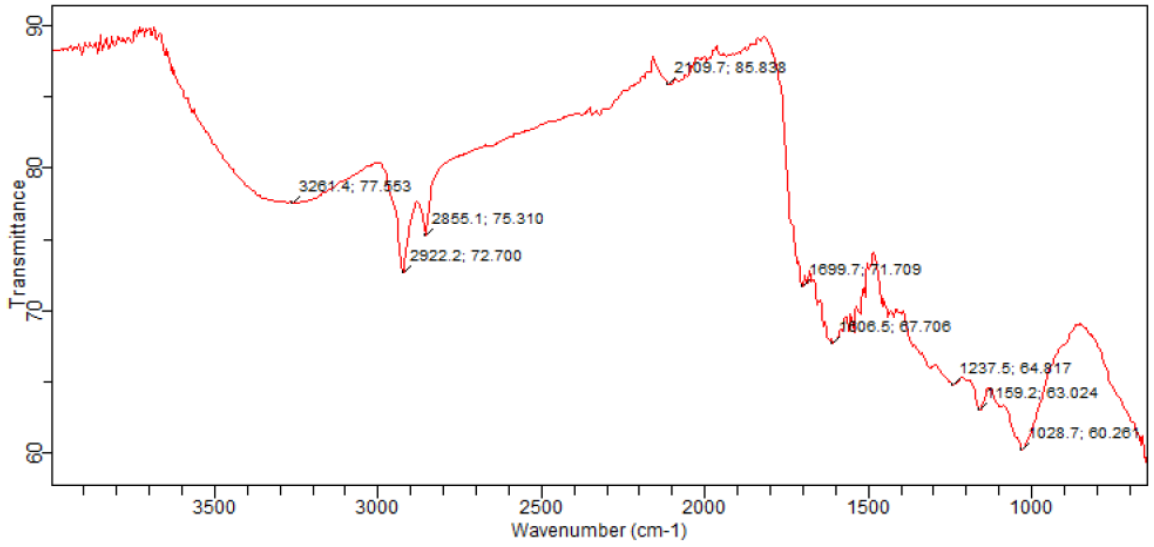


Figure 4.1: FTIR Spectrum of Activated Tamarind Kernel Powder

Agilent Technologies

Sample ID:AR1 TREATED
Sample Scans:16
Background Scans:16
Resolution:8
System Status:Good

Method Name:Transmittance Method
User:Admin
Date/Time:2016-07-25T11:39:07.344+01:00
Range:4000 - 650
Apodization:Happ-Genzel

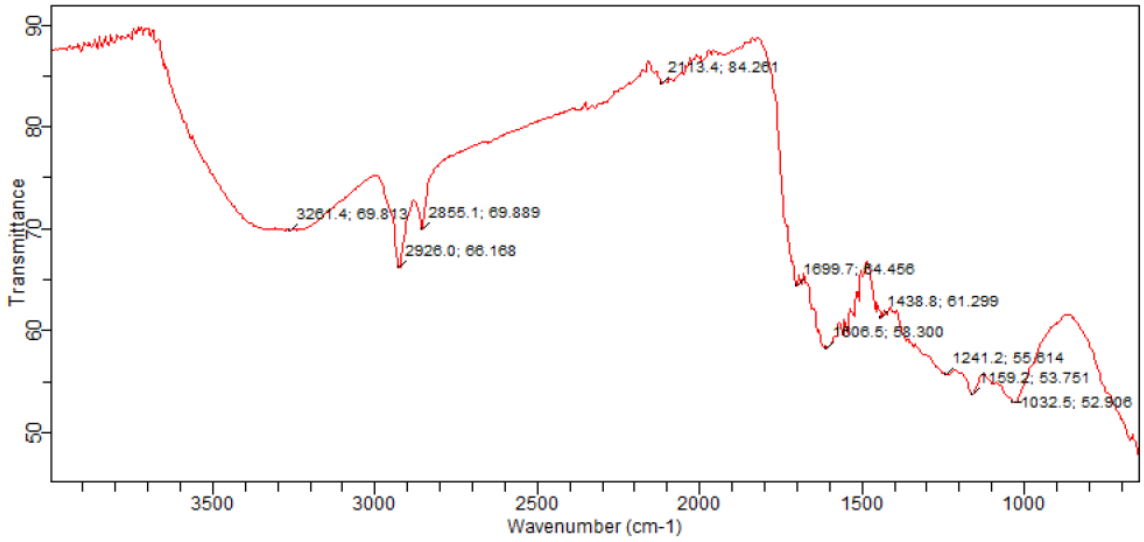


Figure 4.2: FTIR Spectrum of Acid Red 1 Treated TKP

Agilent Technologies

Sample ID:RO20 TREATED
Sample Scans:16
Background Scans:16
Resolution:8
System Status:Good

Method Name:Transmittance Method
User:Admin
Date/Time:2016-07-25T11:45:12.619+01:00
Range:4000 - 650
Apodization:Happ-Genzel

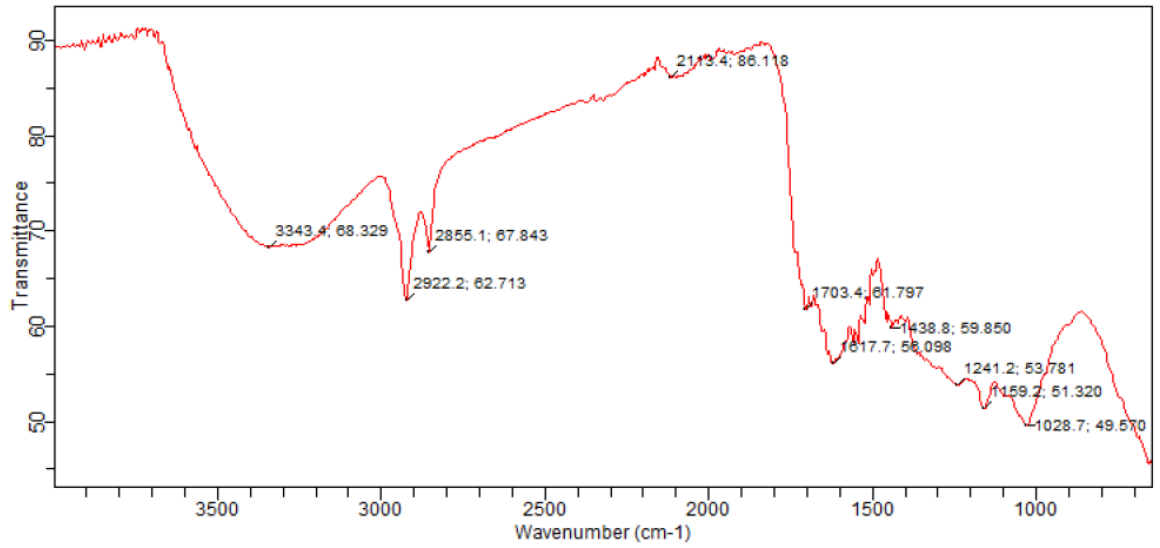


Figure 4.3: FTIR Spectrum of Reactive Orange 20 Treated TKP

Agilent Technologies

Sample ID:RB29 TREATED
Sample Scans:16
Background Scans:16
Resolution:8
System Status:Good

Method Name:Transmittance Method
User:Admin
Date/Time:2016-07-25T11:43:03.107+01:00
Range:4000 - 650
Apodization:Happ-Genzel

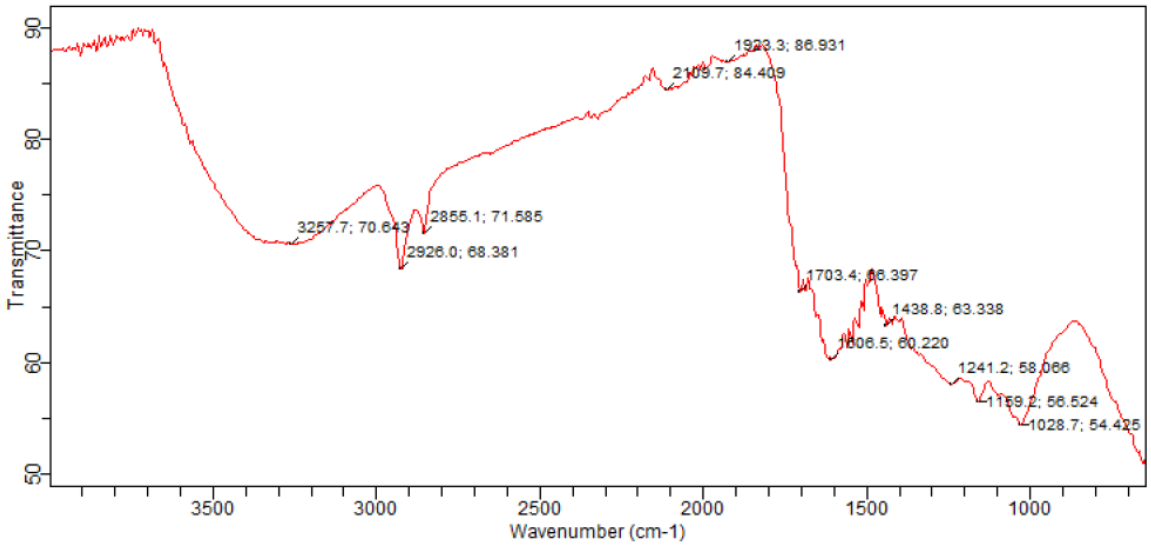


Figure 4.4: FTIR Spectrum of Reactive Blue 29 Treated TKP

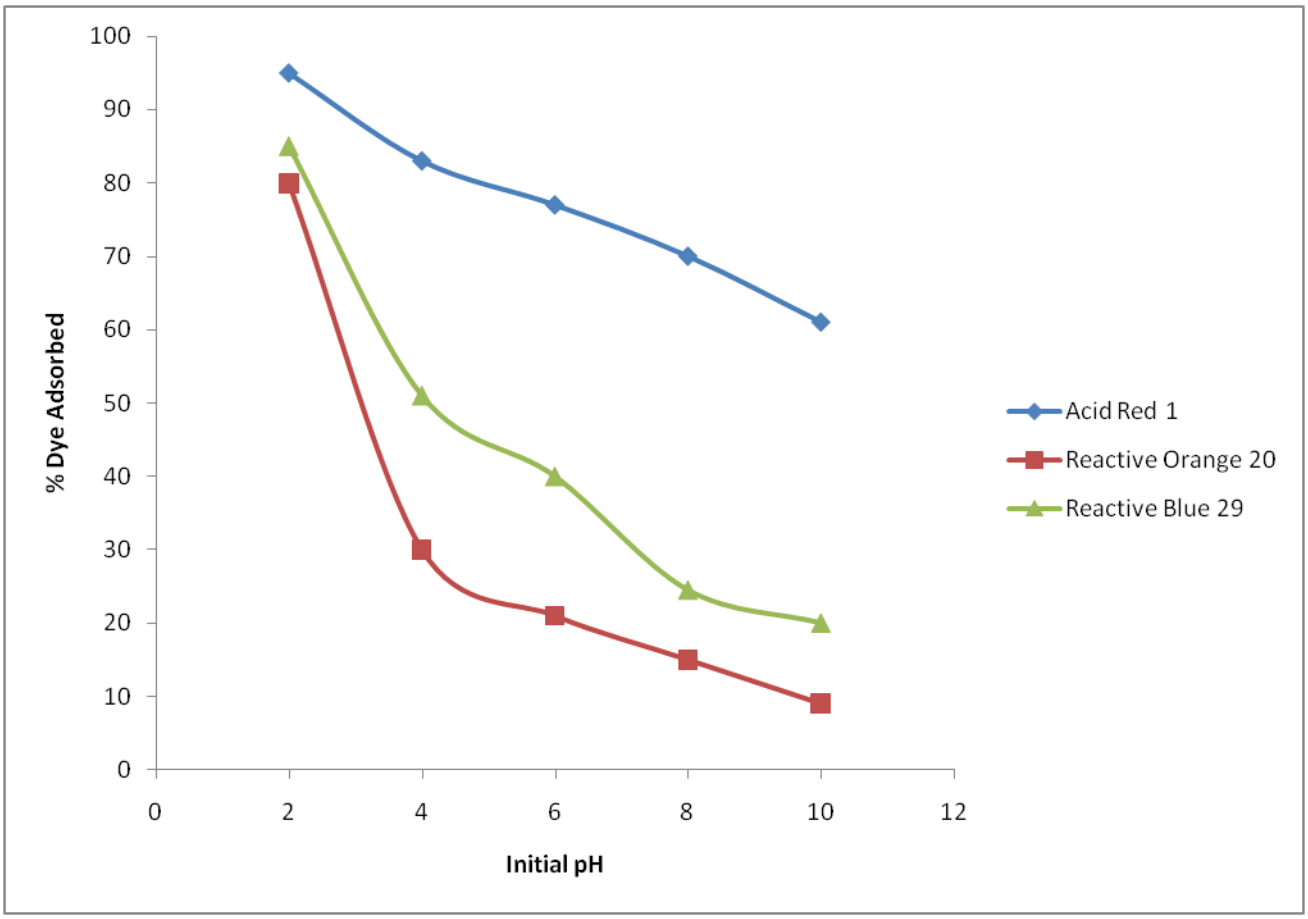


Figure 4.5: Effect of pH on Dye Adsorption onto TKP

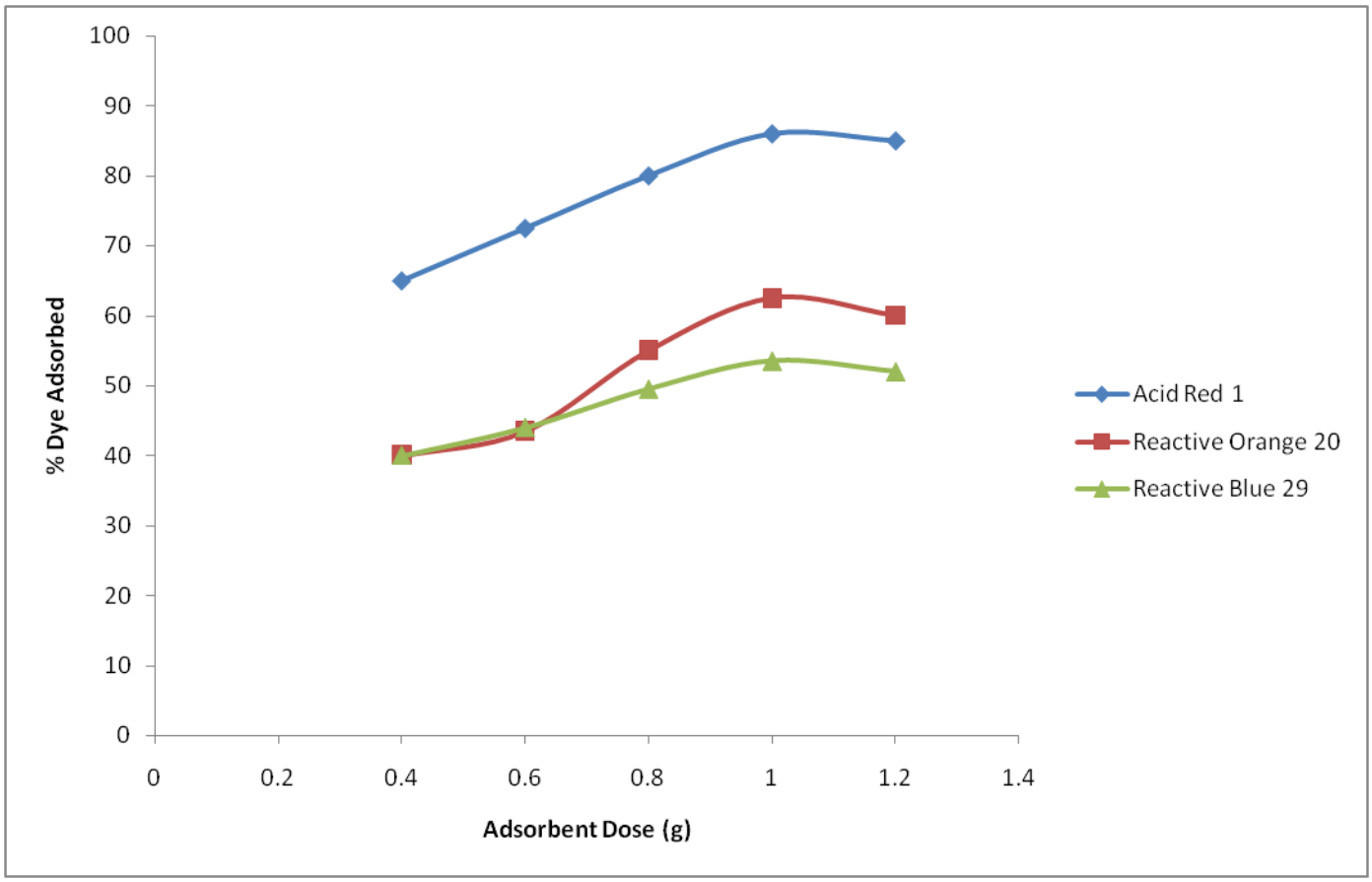


Figure 4.6: Effect of Adsorbent Dose on Dye Adsorption onto TKP

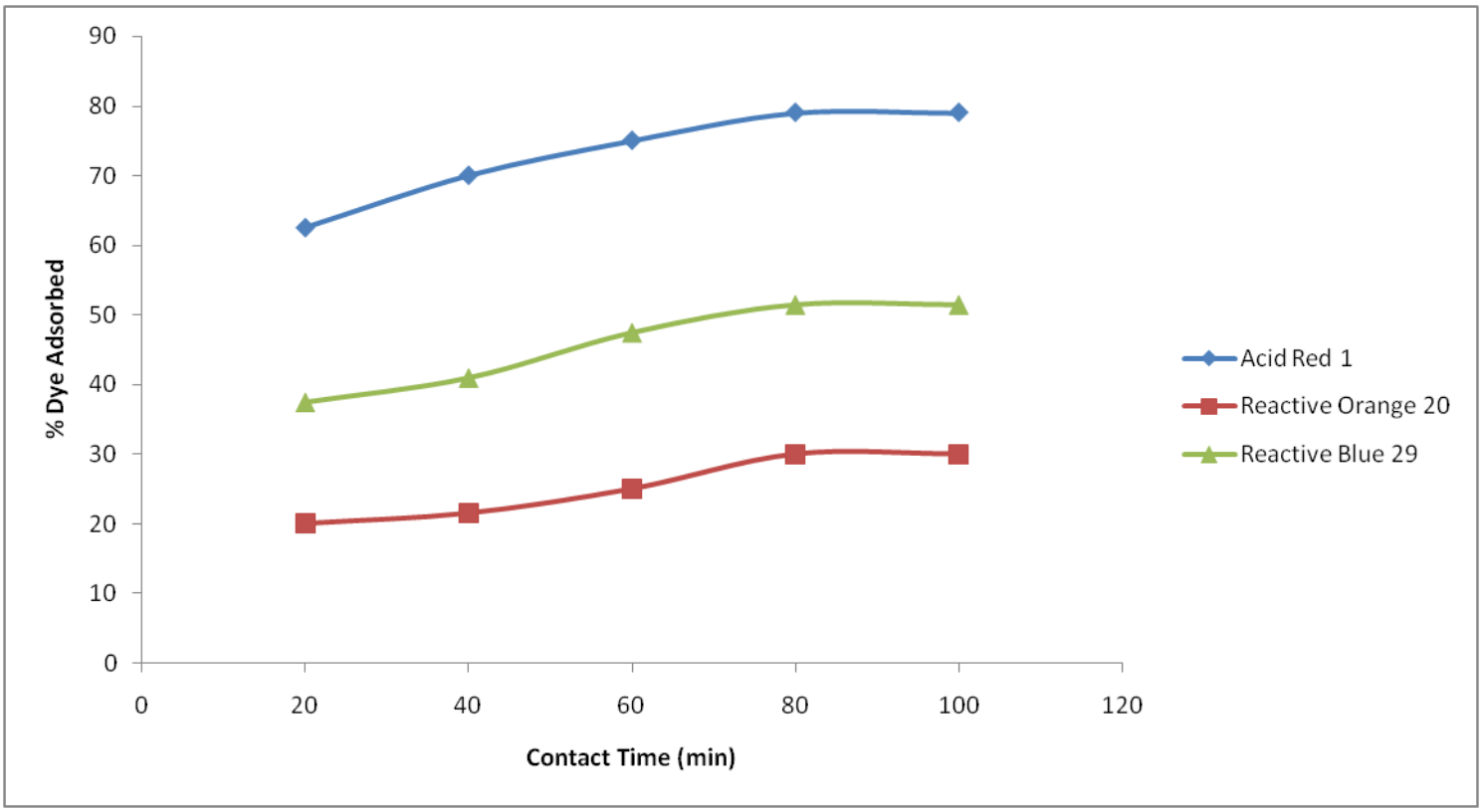


Figure 4.7: Effect of Contact Time on Dye Adsorption onto TKP

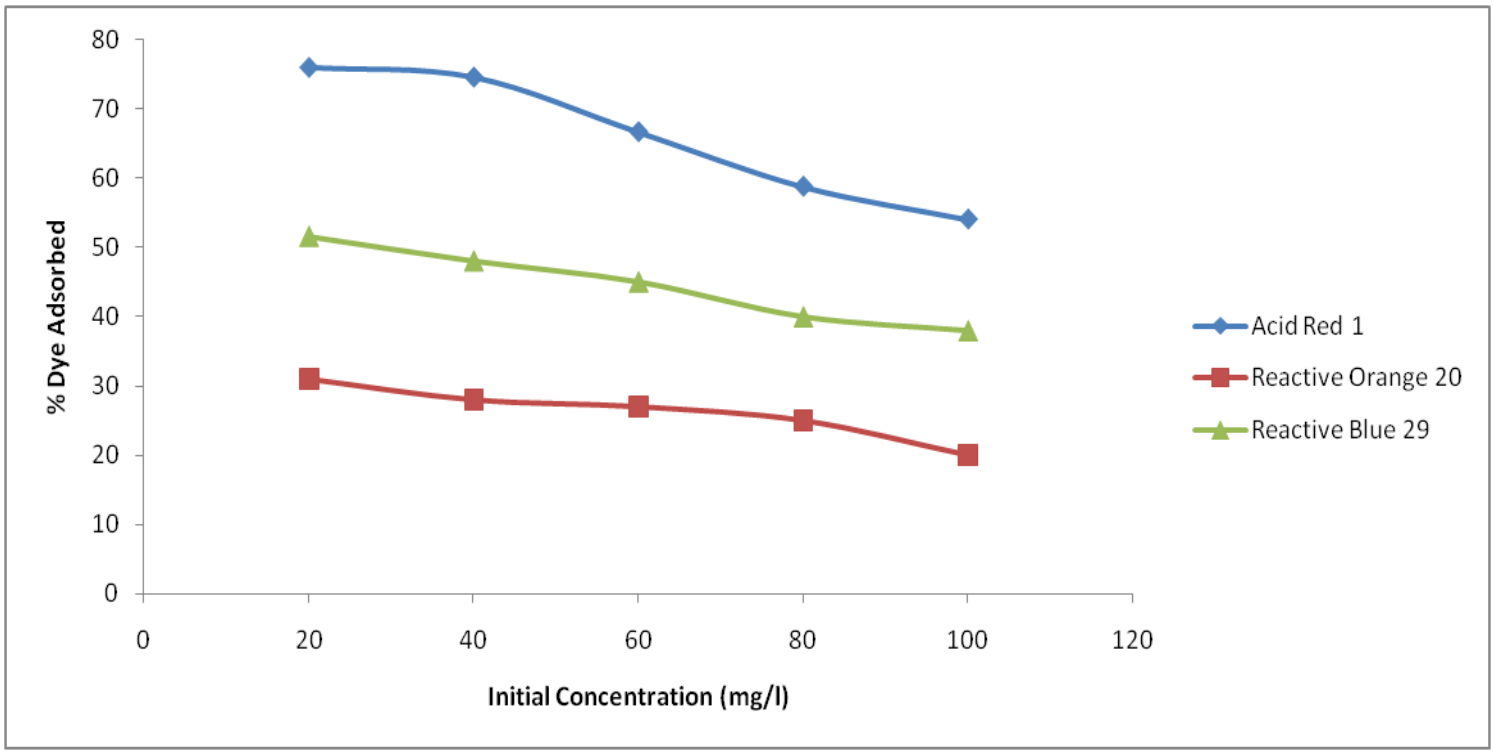


Figure 4.8: Effect of Initial Dye Concentration on Dye Adsorption onto TKP

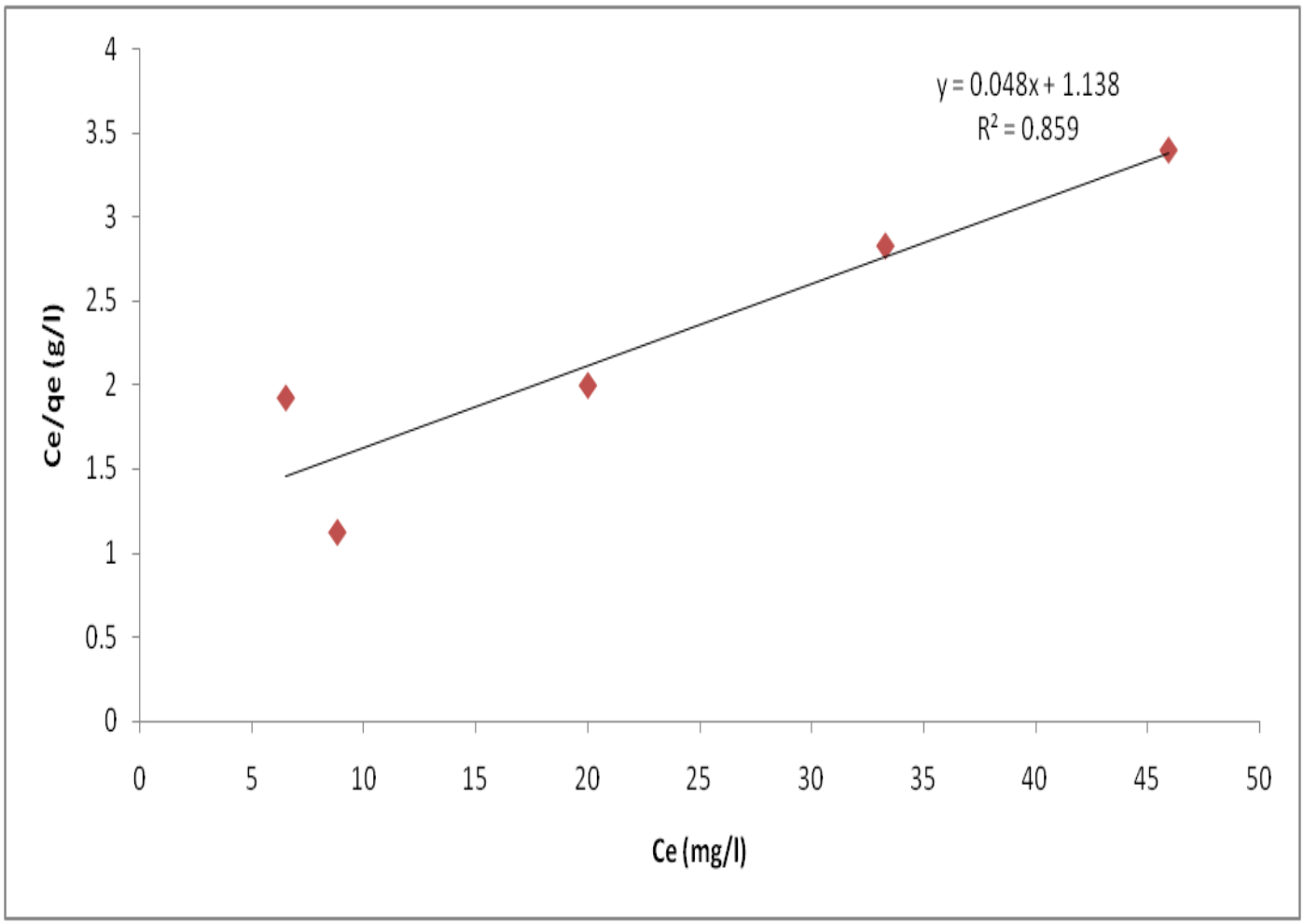


Figure 4.9: Langmuir Isotherm for AR1 Adsorption on TKP at 298 K

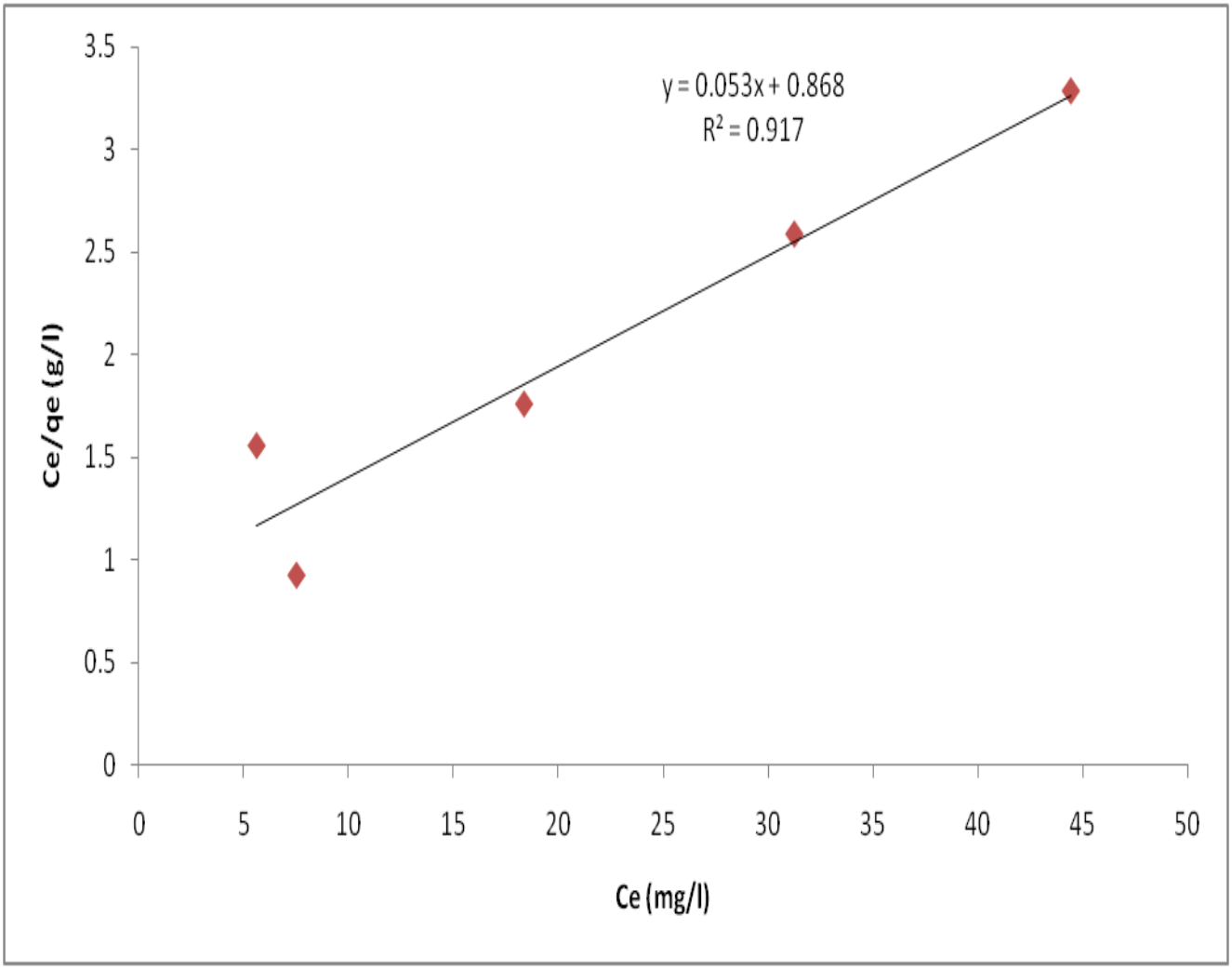


Figure 4.10: Langmuir Isotherm for AR1 Adsorption on TKP at 308 K

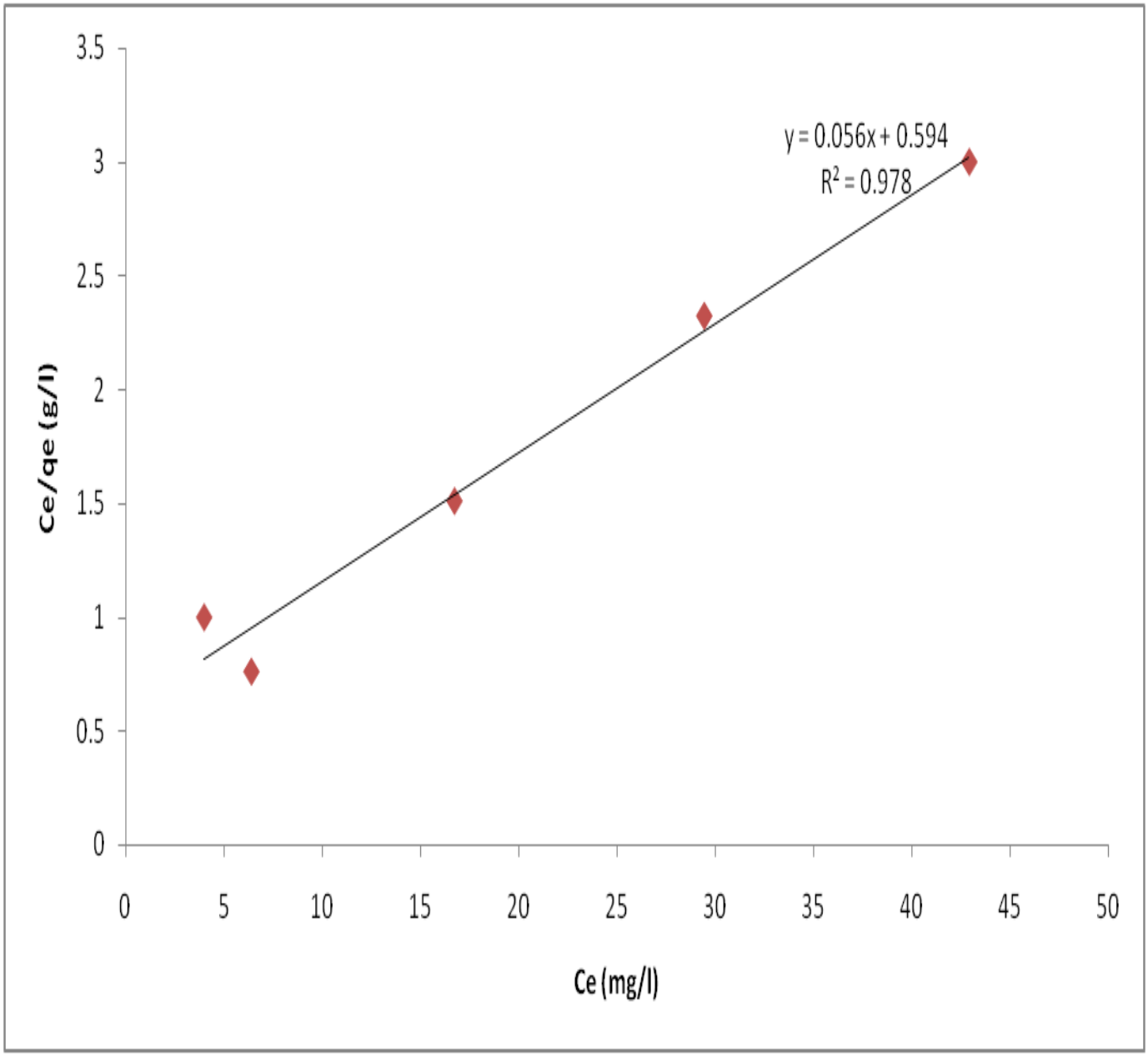


Figure 4.11: Langmuir Isotherm for AR1 Adsorption on TKP at 318 K

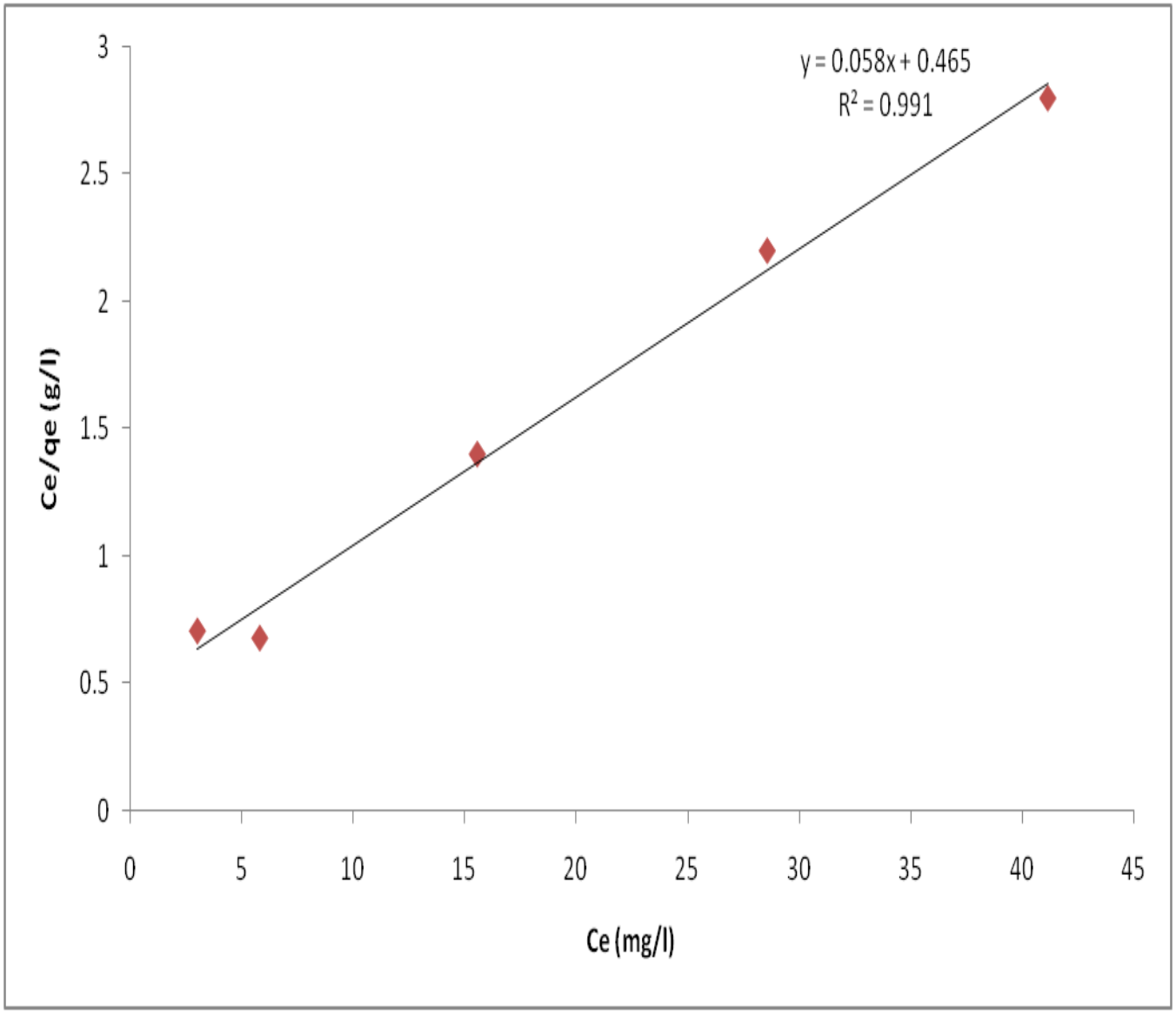


Figure 4.12: Langmuir Isotherm for AR1 Adsorption on TKP at 323 K

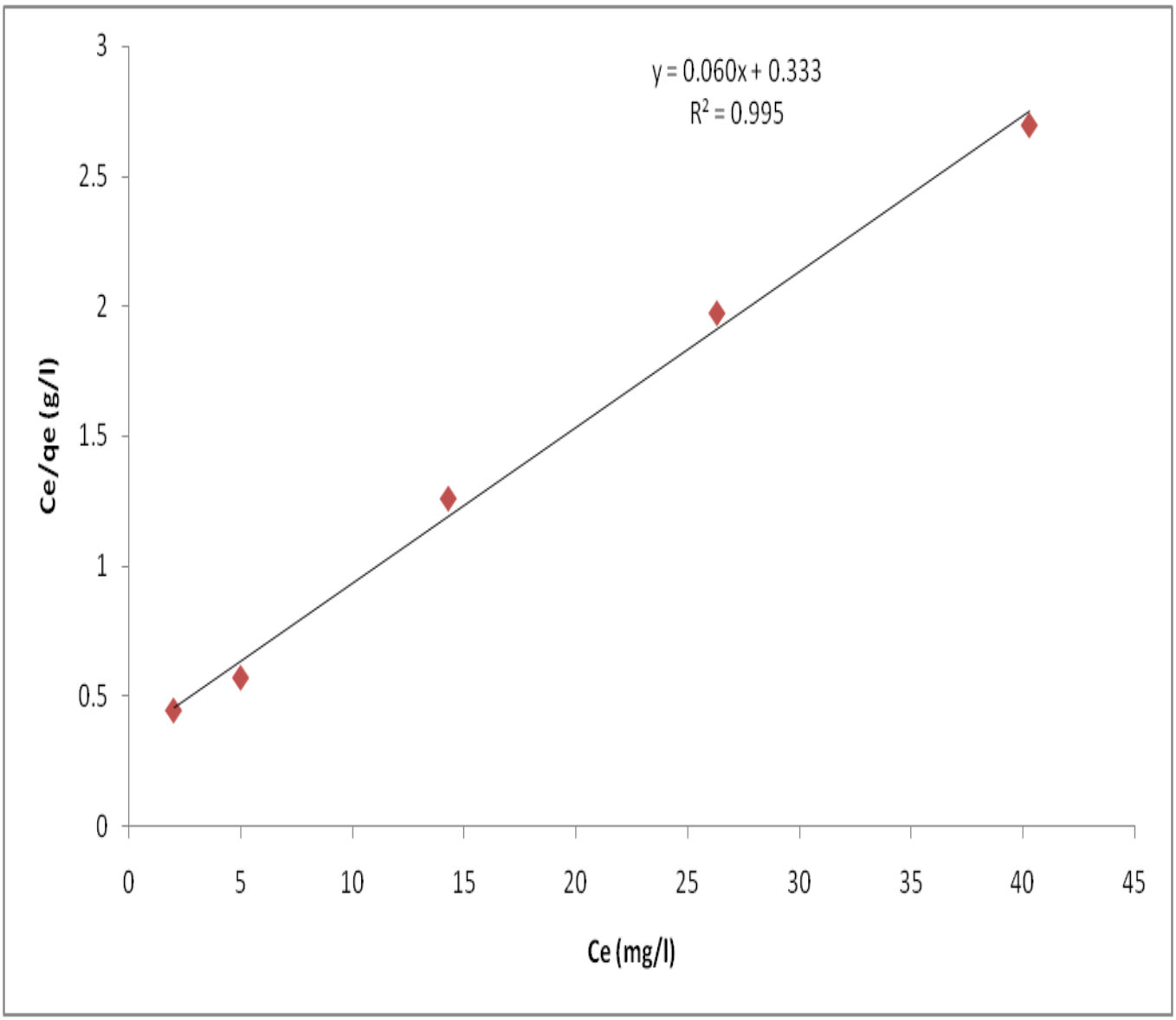


Figure 4.13: Langmuir Isotherm for AR1 Adsorption on TKP at 328 K

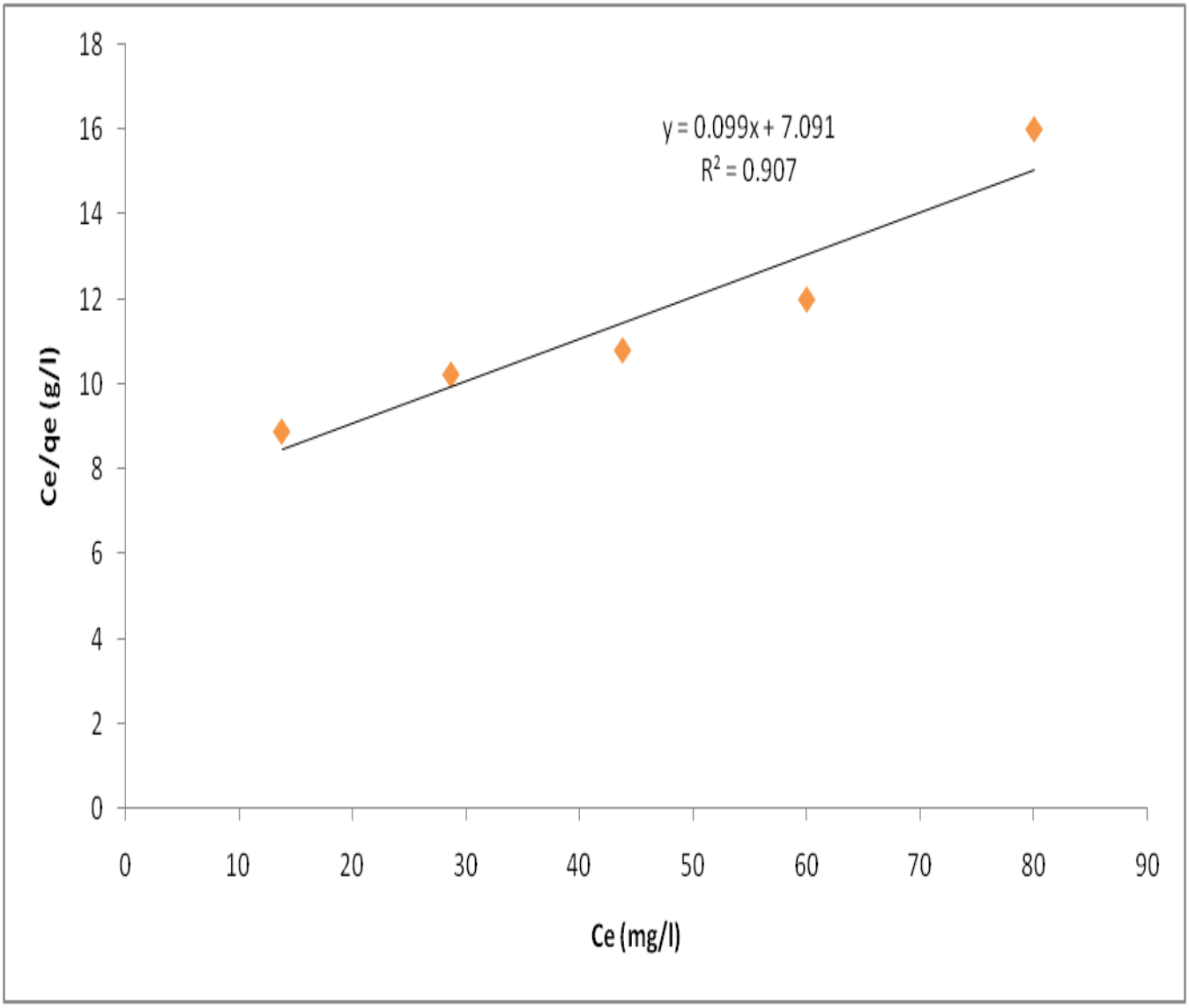


Figure 4.14: Langmuir Isotherm for RO20 Adsorption on TKP at 298 K

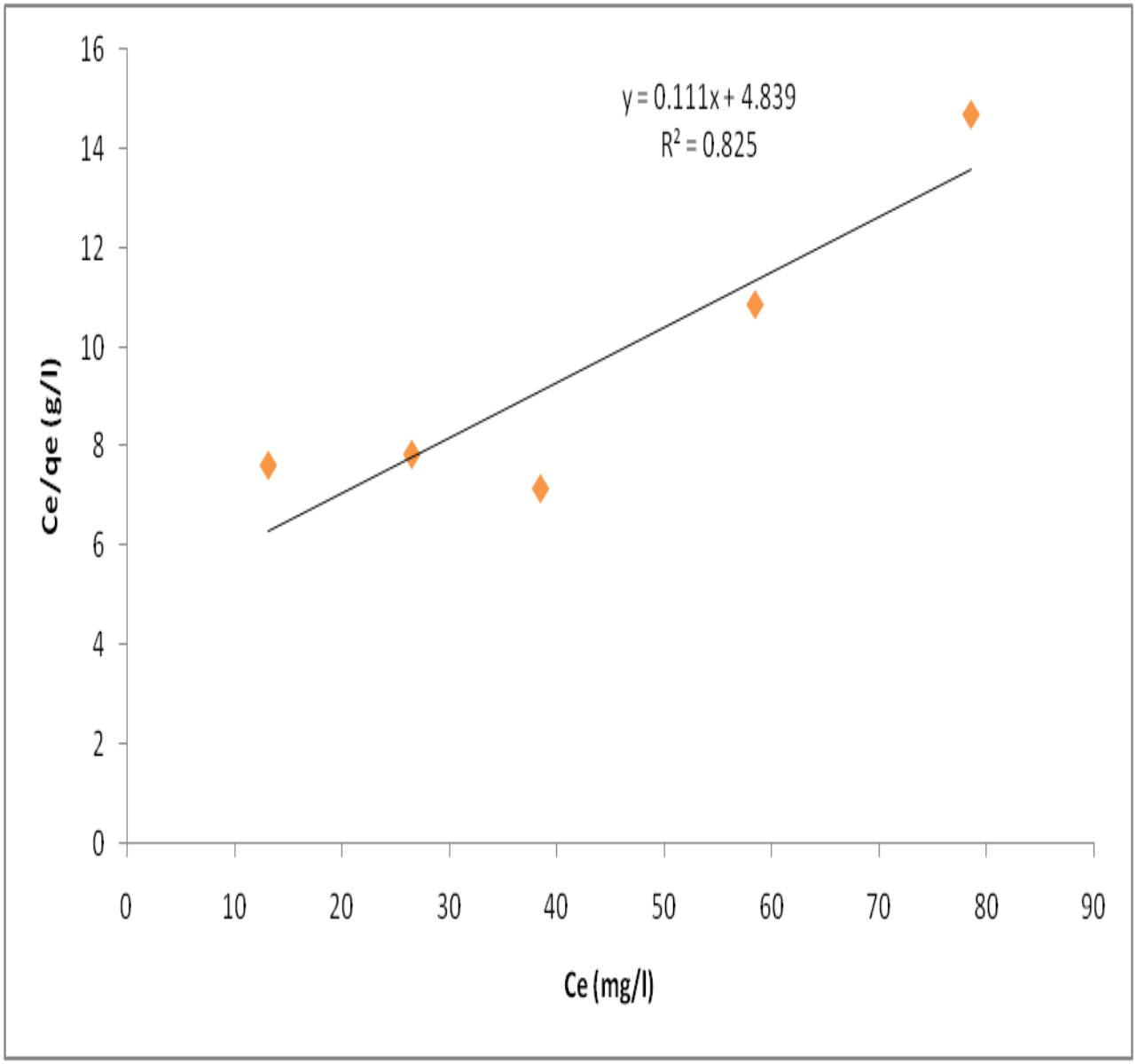


Figure 4.15: Langmuir Isotherm for RO20 Adsorption on TKP at 308 K

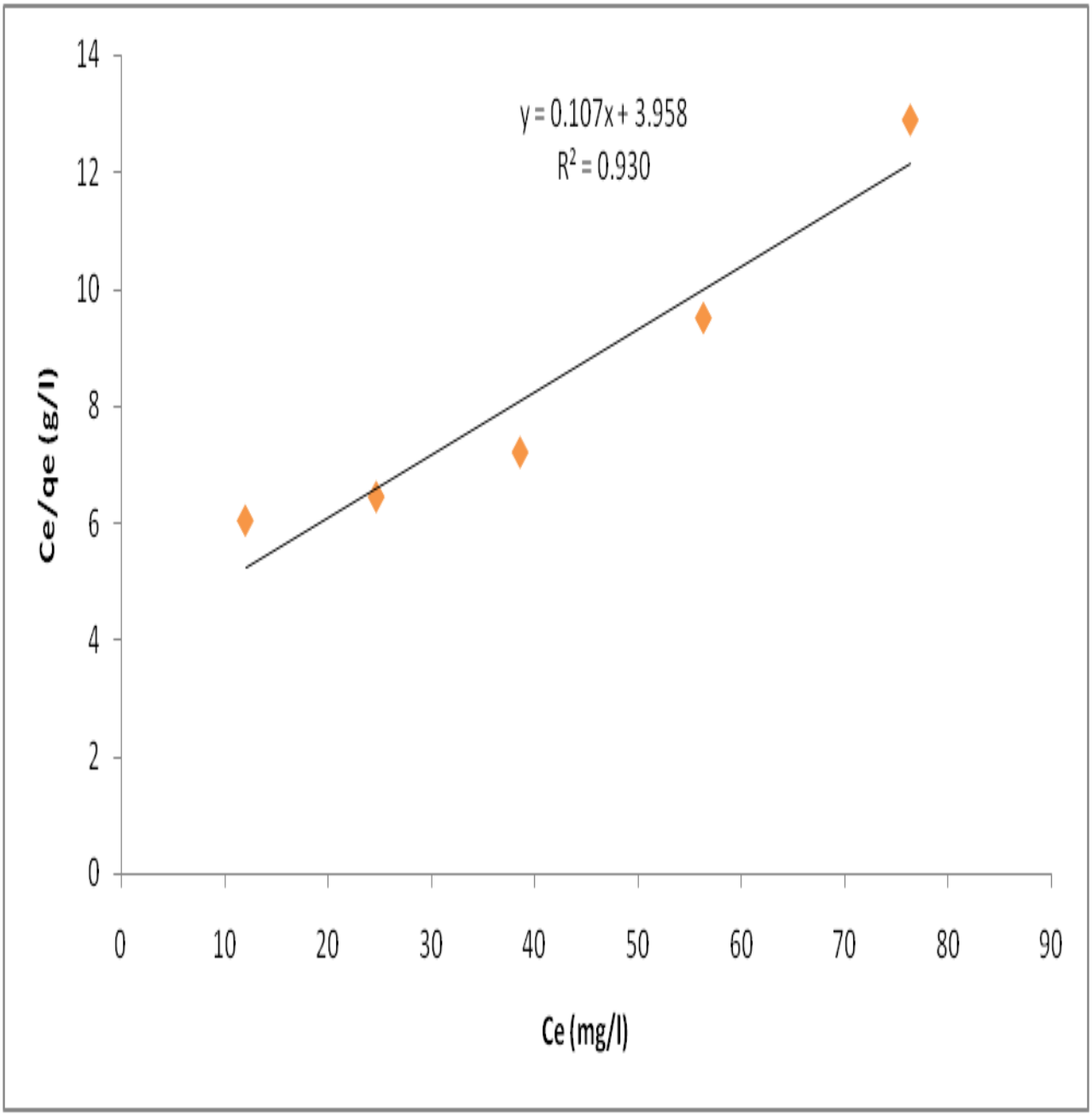


Figure 4.16: Langmuir Isotherm for RO20 Adsorption on TKP at 318 K

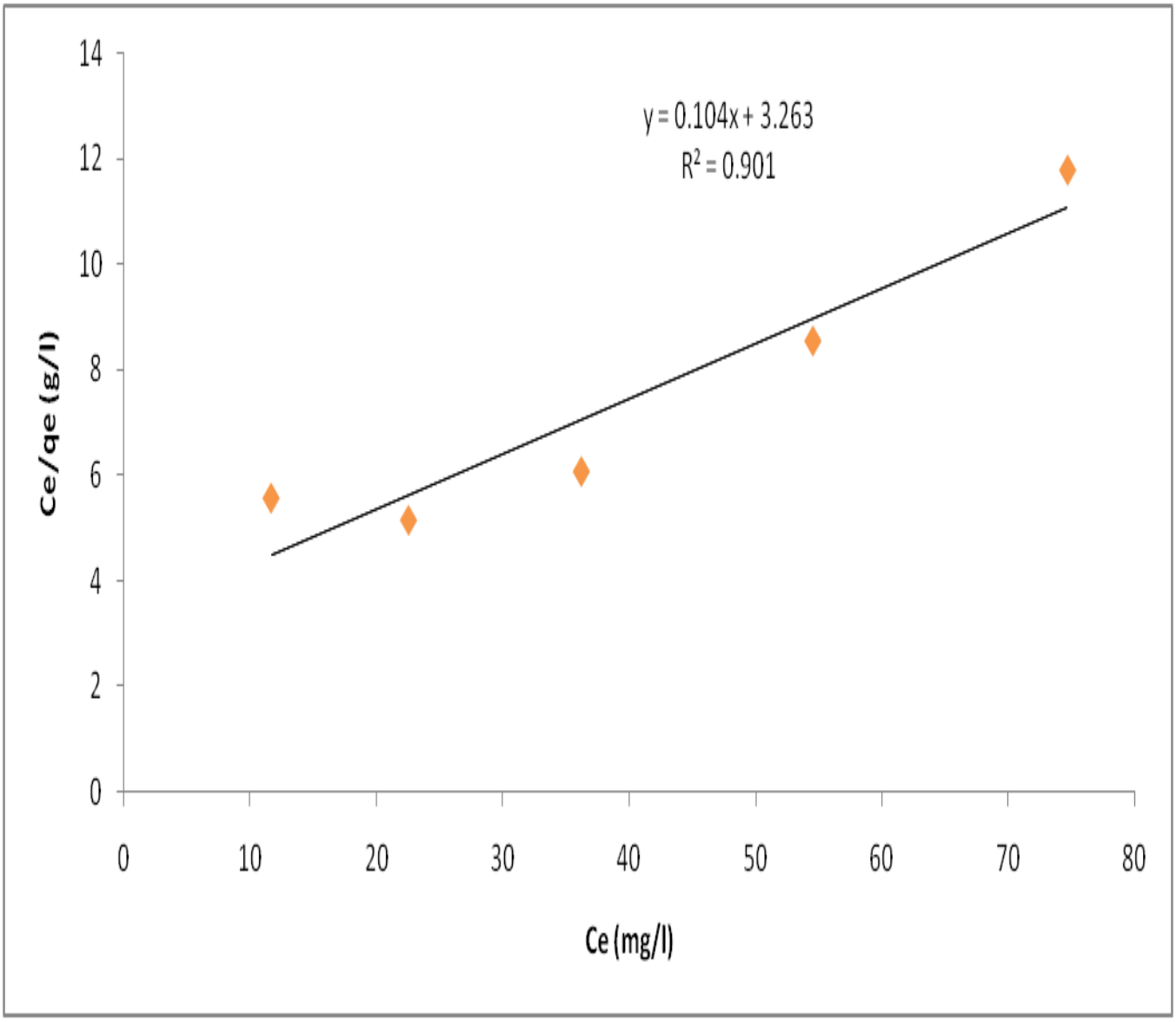


Figure 4.17: Langmuir Isotherm for RO20 Adsorption on TKP at 323 K

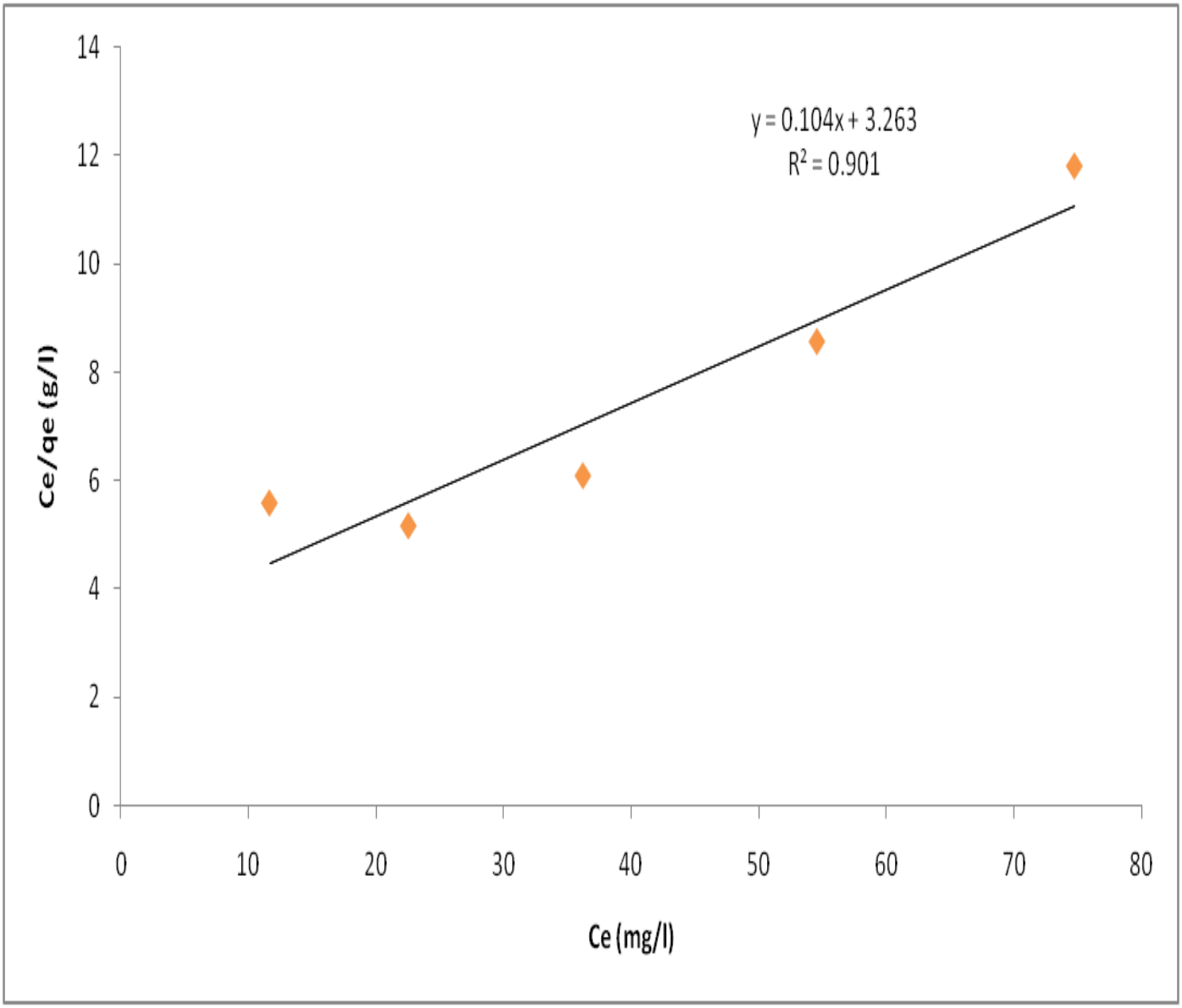


Figure 4.18: Langmuir Isotherm for RO20 Adsorption on TKP at 328 K

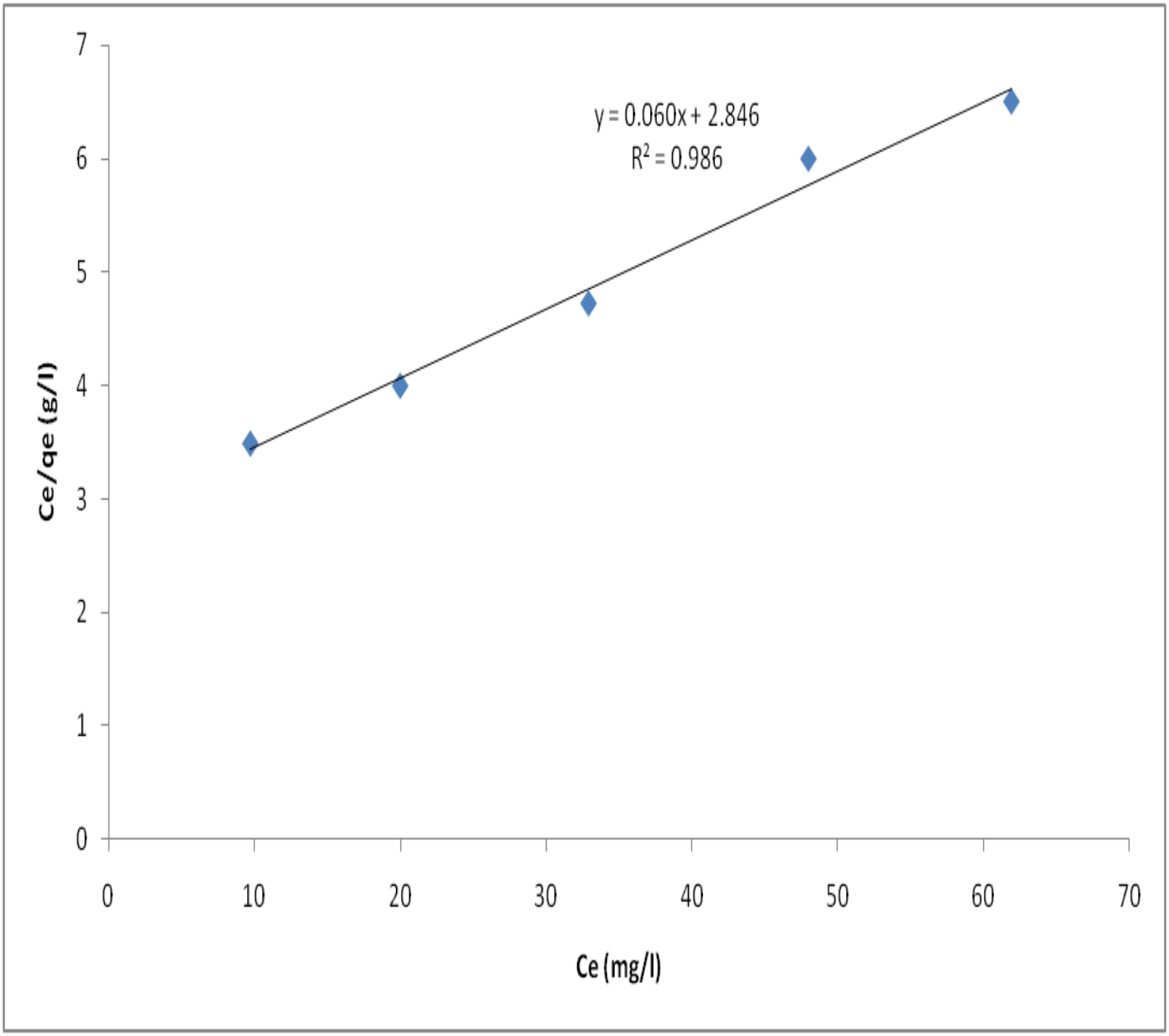


Figure 4.19: Langmuir Isotherm for RB29 Adsorption on TKP at 298 K

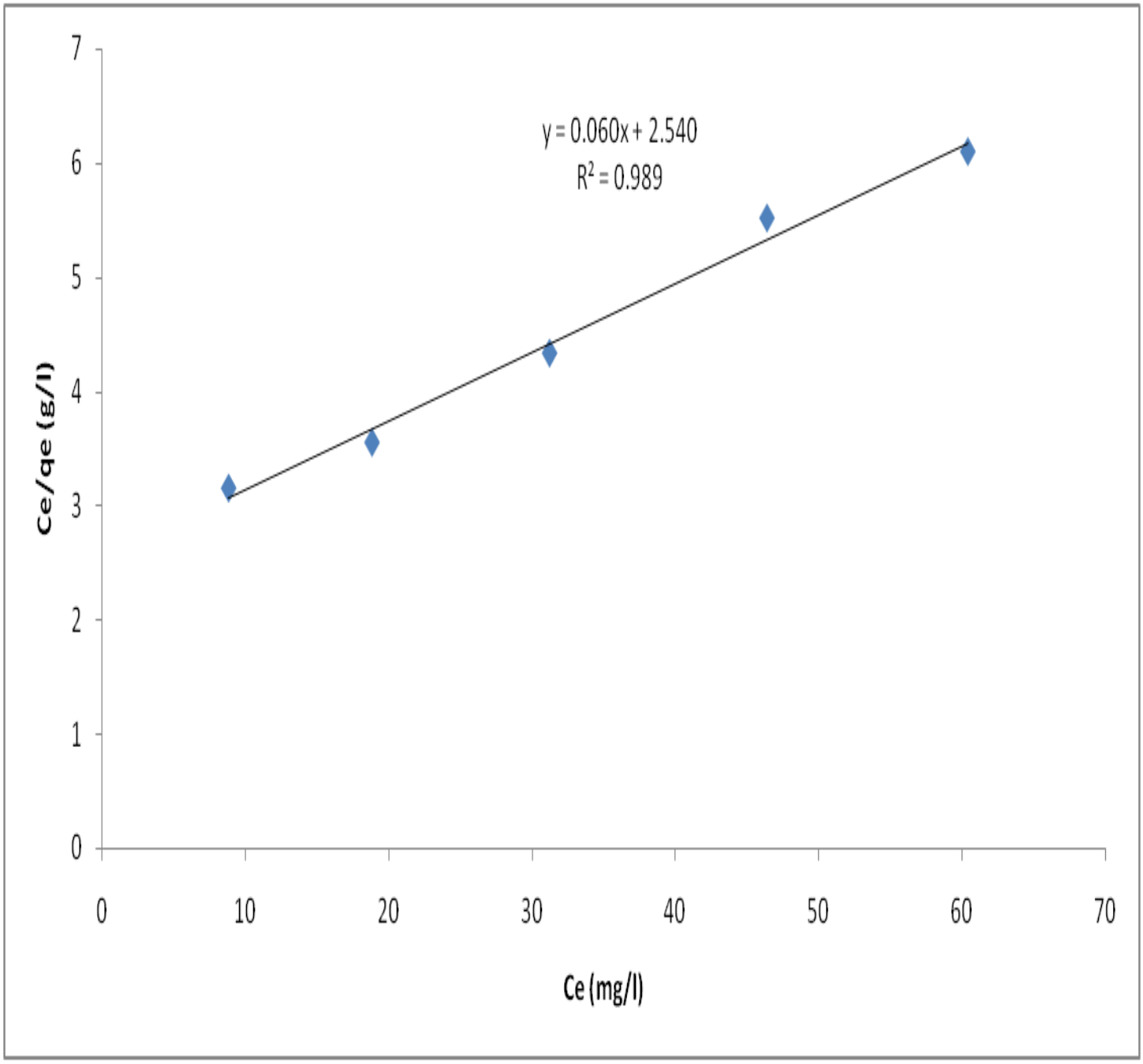


Figure 4.20: Langmuir Isotherm for RB29 Adsorption on TKP at 308 K

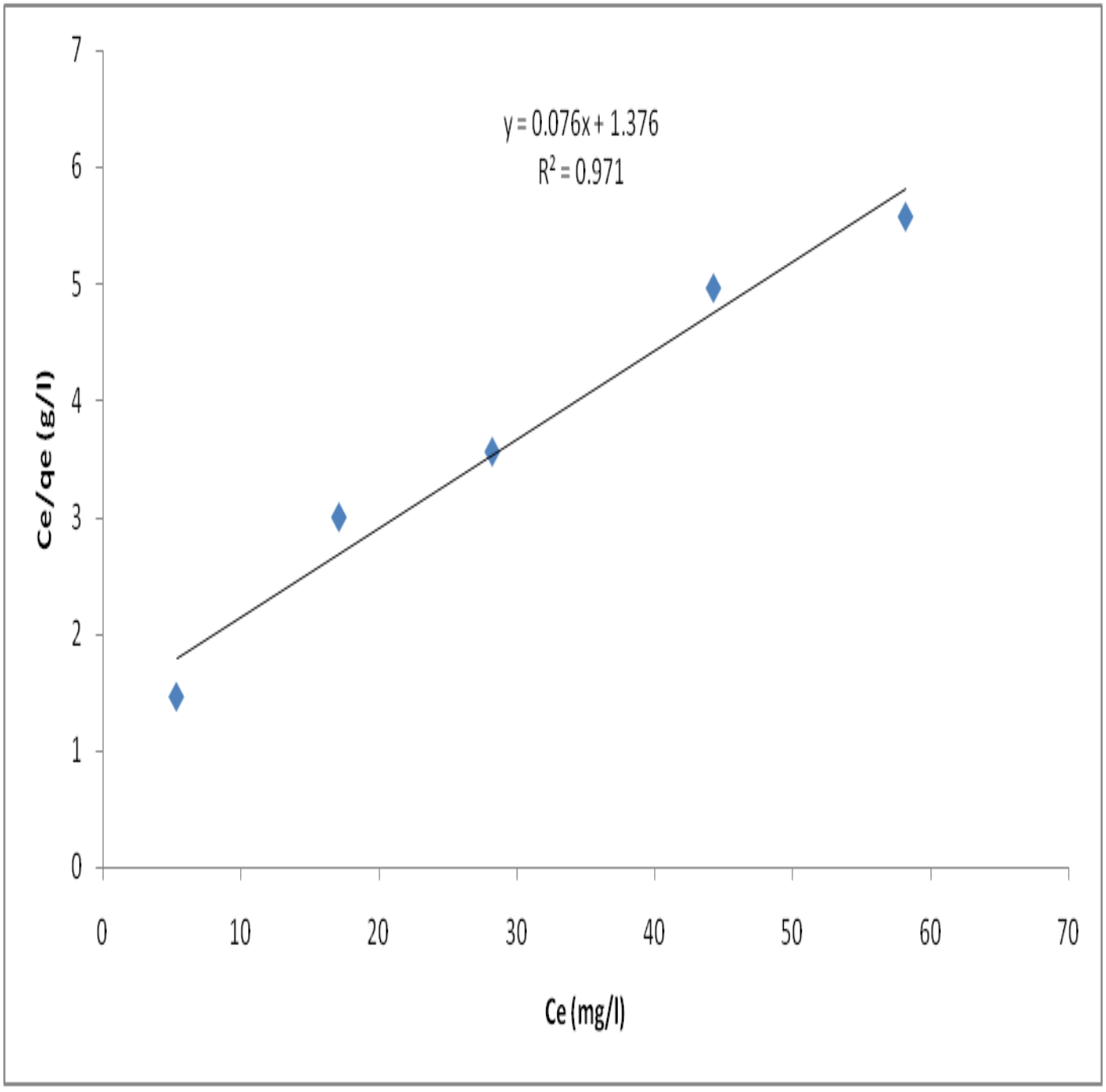


Figure 4.21: Langmuir Isotherm for RB29 Adsorption on TKP at 318 K

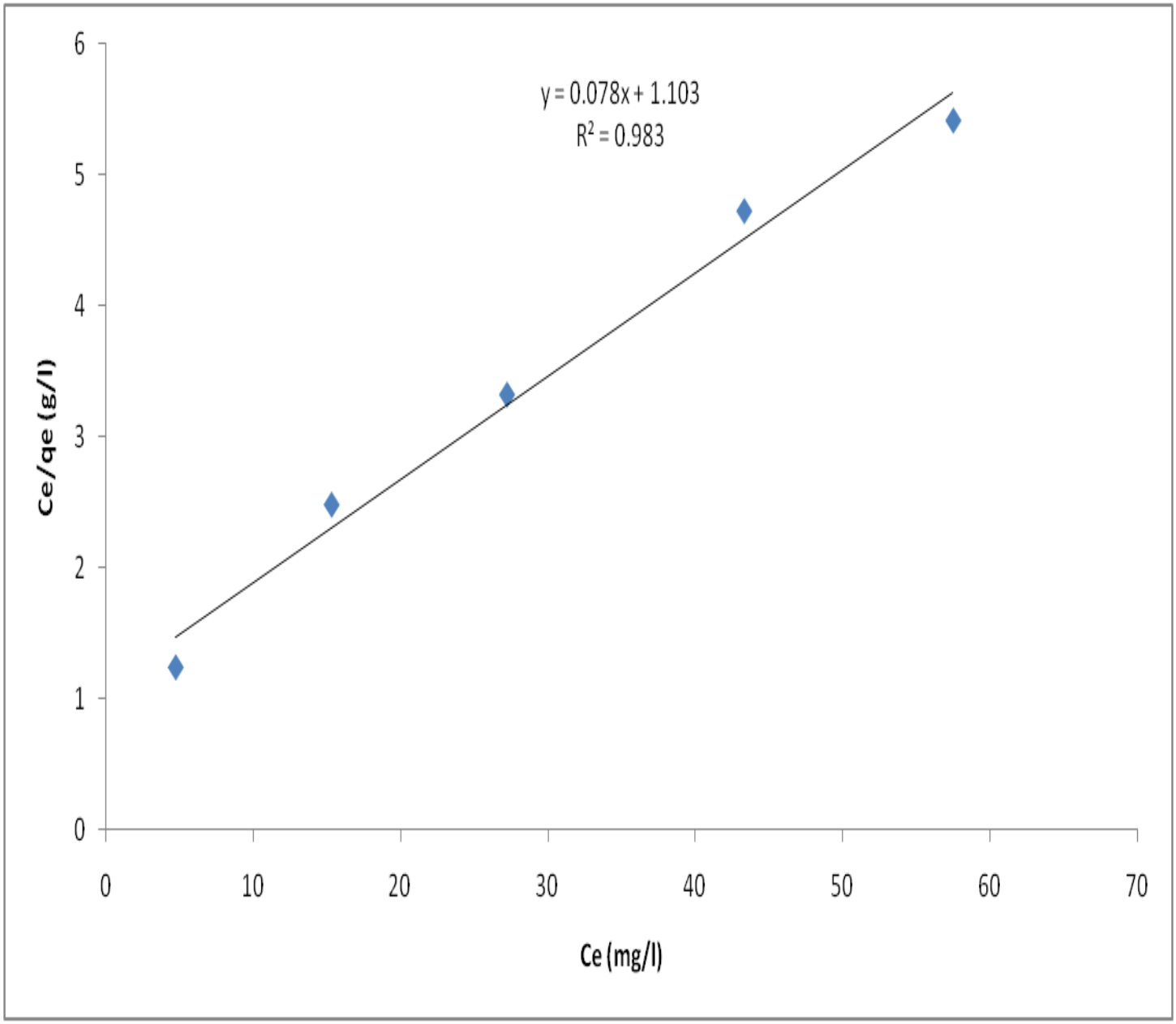


Figure 4.22: Langmuir Isotherm for RB29 Adsorption on TKP at 323 K

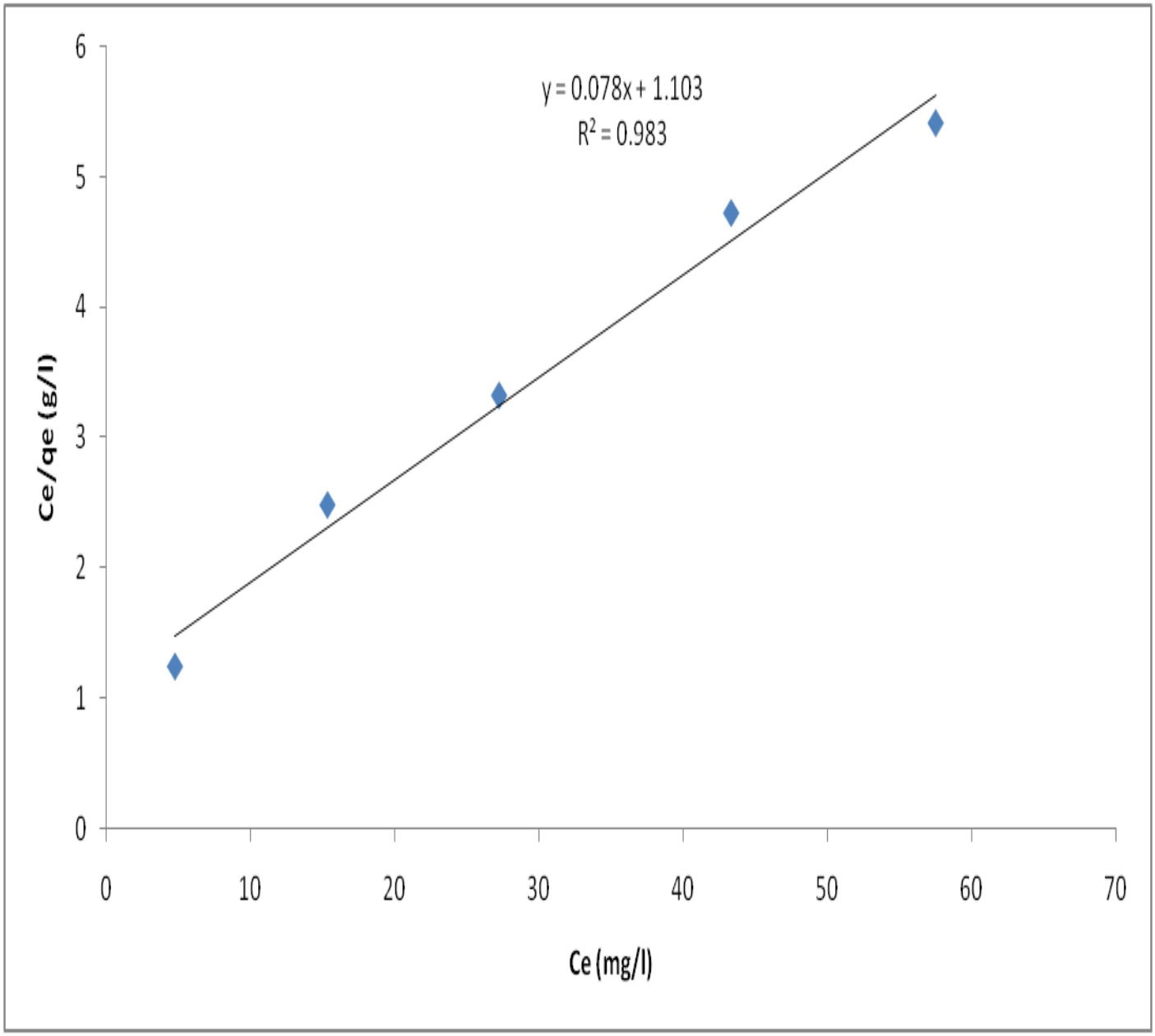


Figure 4.23: Langmuir Isotherm for RB29 Adsorption on TKP at 328 K

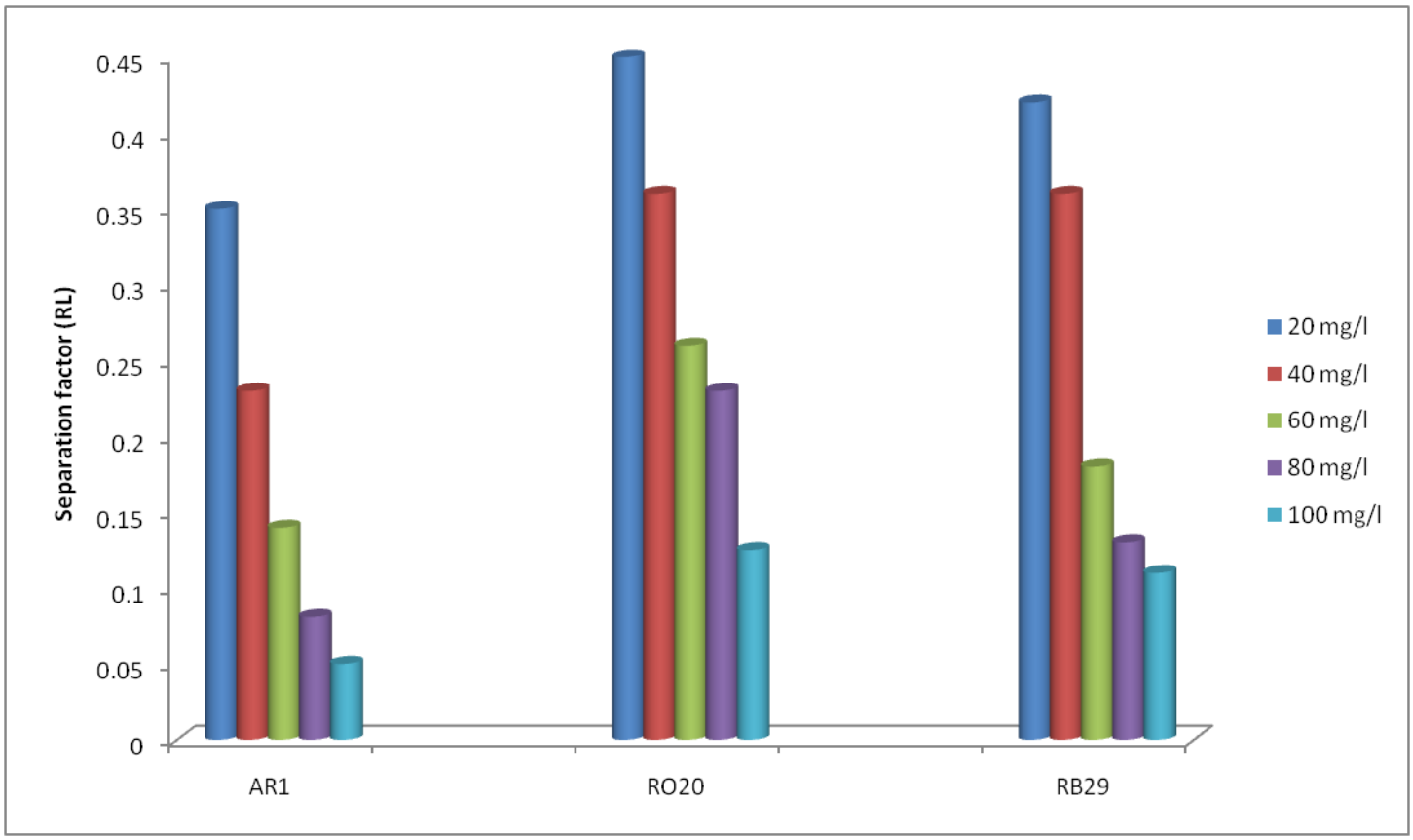


Figure 4.24: Separation Factor (R_L) Variation with Concentration (mg/l) on Adsorption of AR1, RO20 and RB29

4.4.2 Freundlich Isotherms

Figures 4.25 to 4.29 show the Freundlich isotherm plots for Acid Red 1 at temperatures of 298-328K respectively, figures 4.30 to 4.34 show the Freundlich isotherm plots for Reactive Orange 20 at a temperature of 298-328K respectively, figures 4.35 to 4.39 show the Freundlich isotherm plots for Reactive Blue 29 at temperatures of 298-328K respectively.

4.4.3 Temkin Isotherms

Figures 4.40 to 4.44 show the Temkin isotherm plots for Acid Red 1 at a temperature of 298-328K respectively, figures 4.45 to 4.49 show the Temkin isotherm plots for Reactive Orange 20 at a temperature of 298-328K respectively, figures 4.50 to 4.54 show the Temkin isotherm plots for Reactive Blue 29 at a temperature of 298-328K respectively.

4.4.4 Dubinin-Radushkevich Isotherms

Figures 4.55 to 4.59 show the Dubinin-Radushkevich isotherm plots for Acid Red 1 at a temperature of 298-328K respectively, figures 4.60 to 4.64 show the Dubinin-Radushkevich isotherm plots for Reactive Orange 20 at a temperature of 298-328K respectively, figures 4.65 to 4.69 show the Dubinin-Radushkevich isotherm plots for Reactive Blue 29 at a temperature of 298-328K respectively.

4.5 Adsorption Kinetics

Figures 4.70 to 4.72 show the Pseudo-First order plots for Acid Red 1, Reactive Orange 20 and Reactive Blue 29 respectively. Figures 4.73 to 4.75 show the Pseudo-Second order plots for Acid red 1, Reactive Orange 20 and Reactive Blue 29 respectively.

4.6 Adsorption Thermodynamics

Figures 4.76 to 4.78 show the thermodynamic plots for Acid Red 1, Reactive Orange 20 and Reactive Blue 29 treatment on activated tamarind kernel powder.

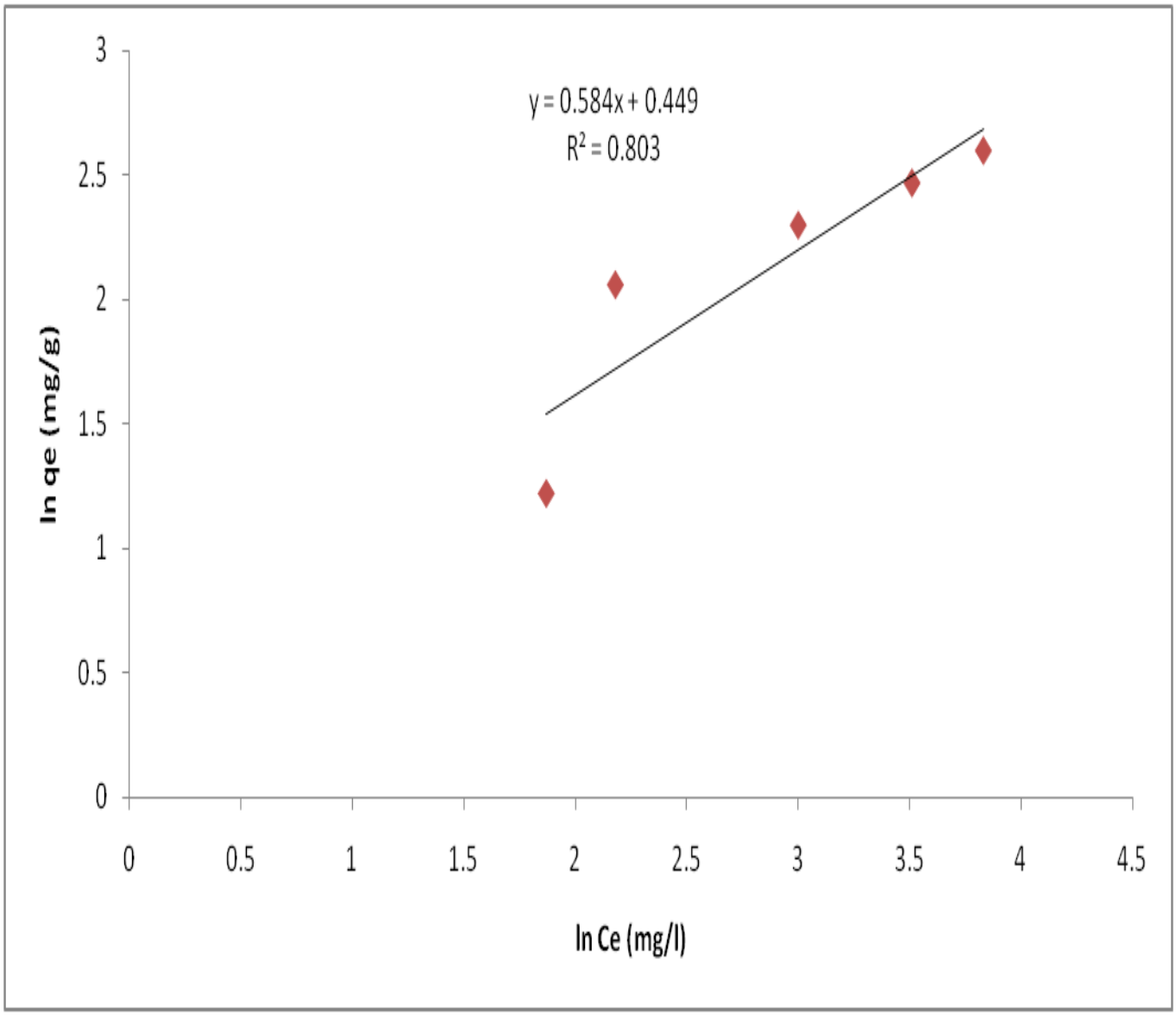


Figure 4.25: Freundlich Isotherm for AR1 Adsorption on TKP at 298 K

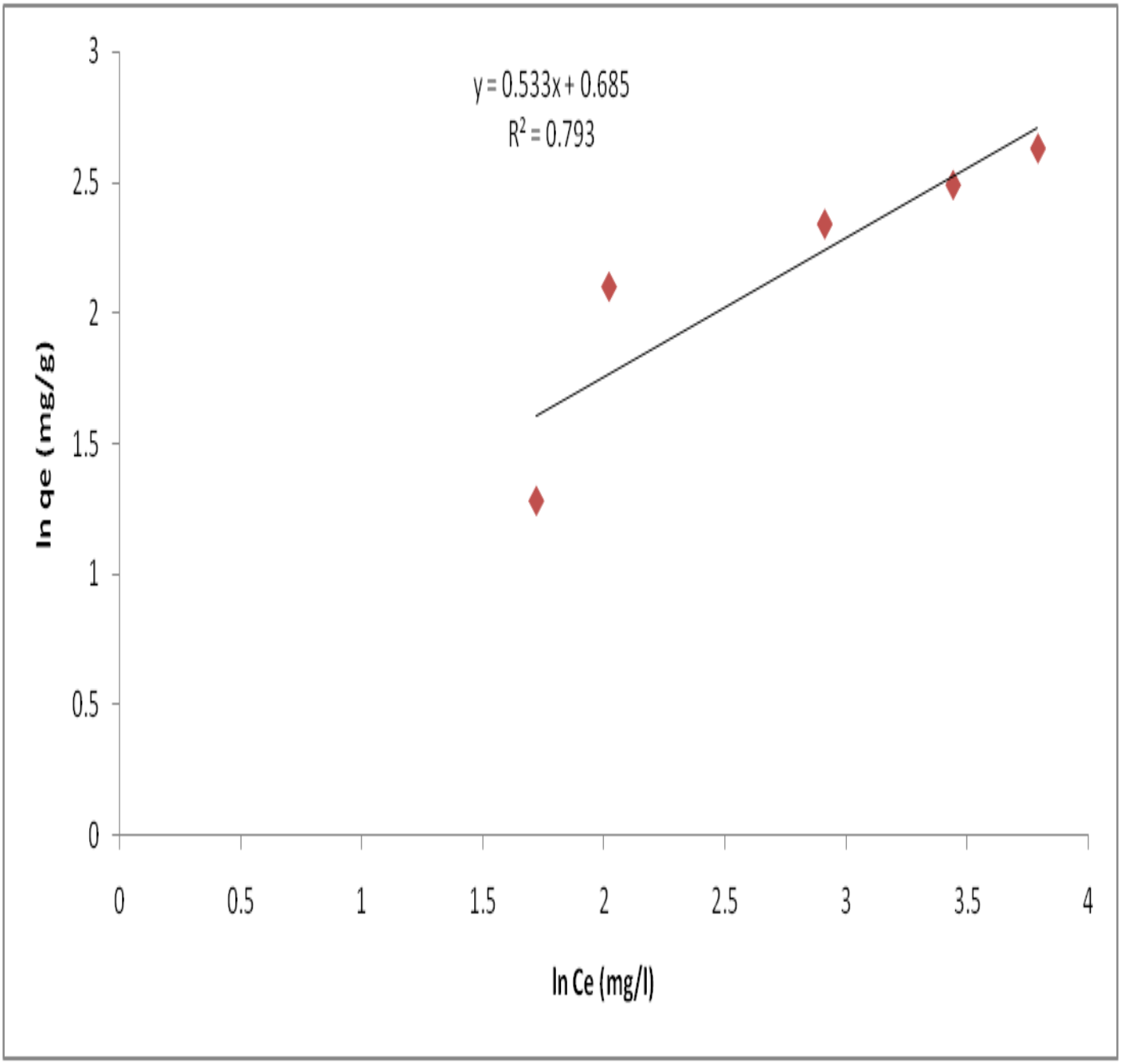


Figure 4.26: Freundlich Isotherm for AR1 Adsorption on TKP at 308 K

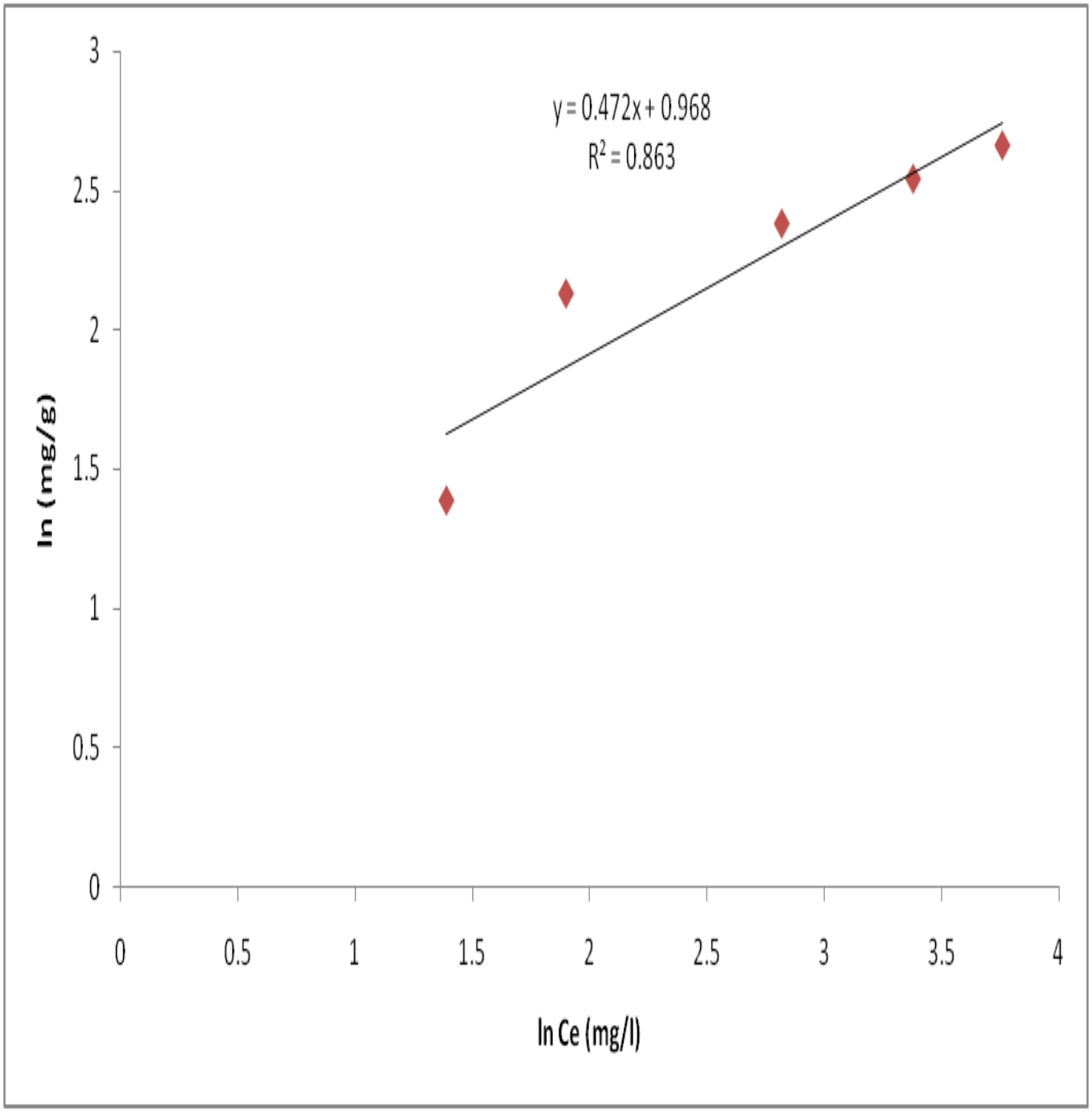


Figure 4.27: Freundlich Isotherm for AR1 Adsorption on TKP at 318 K

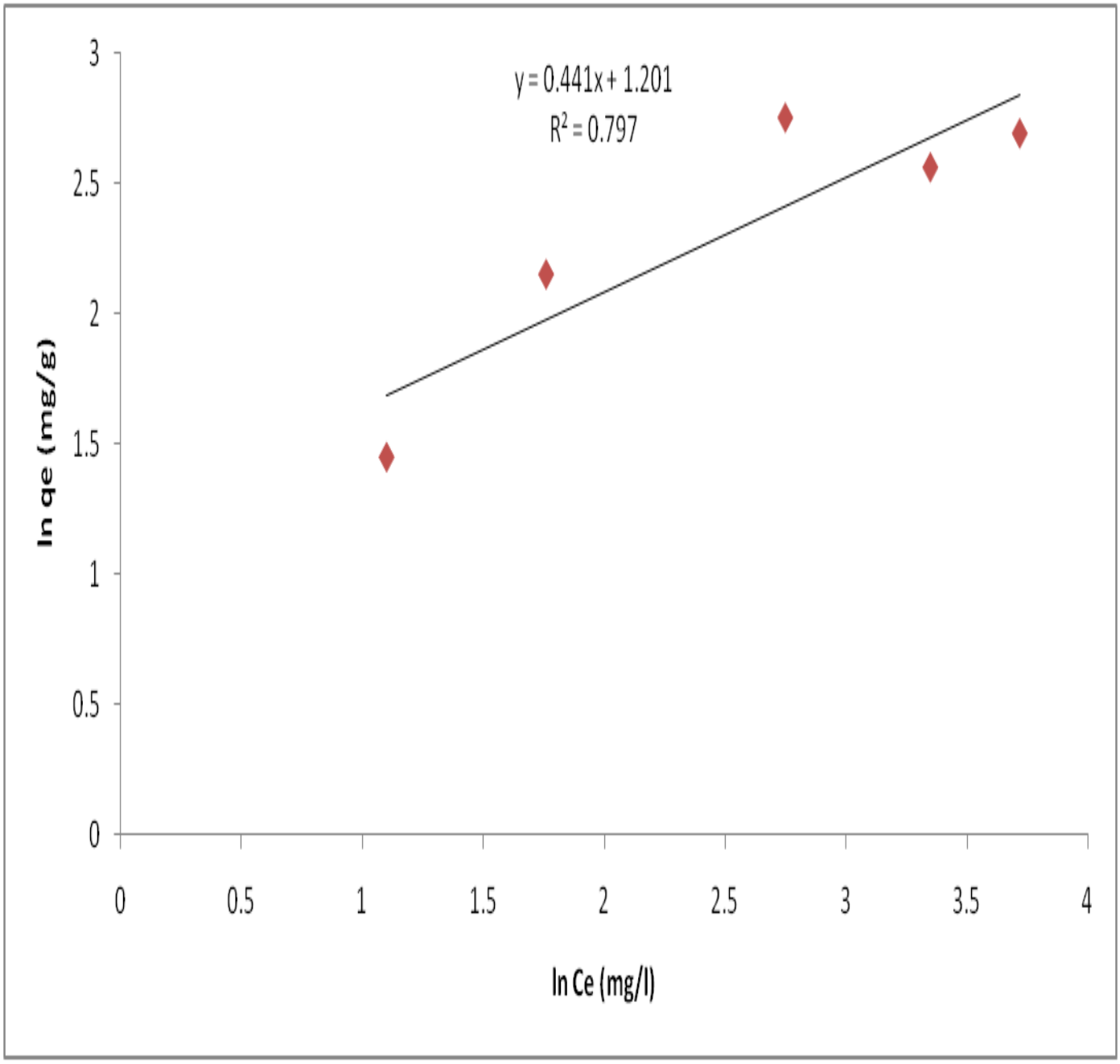


Figure 4.28: Freundlich Isotherm for AR1 Adsorption on TKP at 323 K

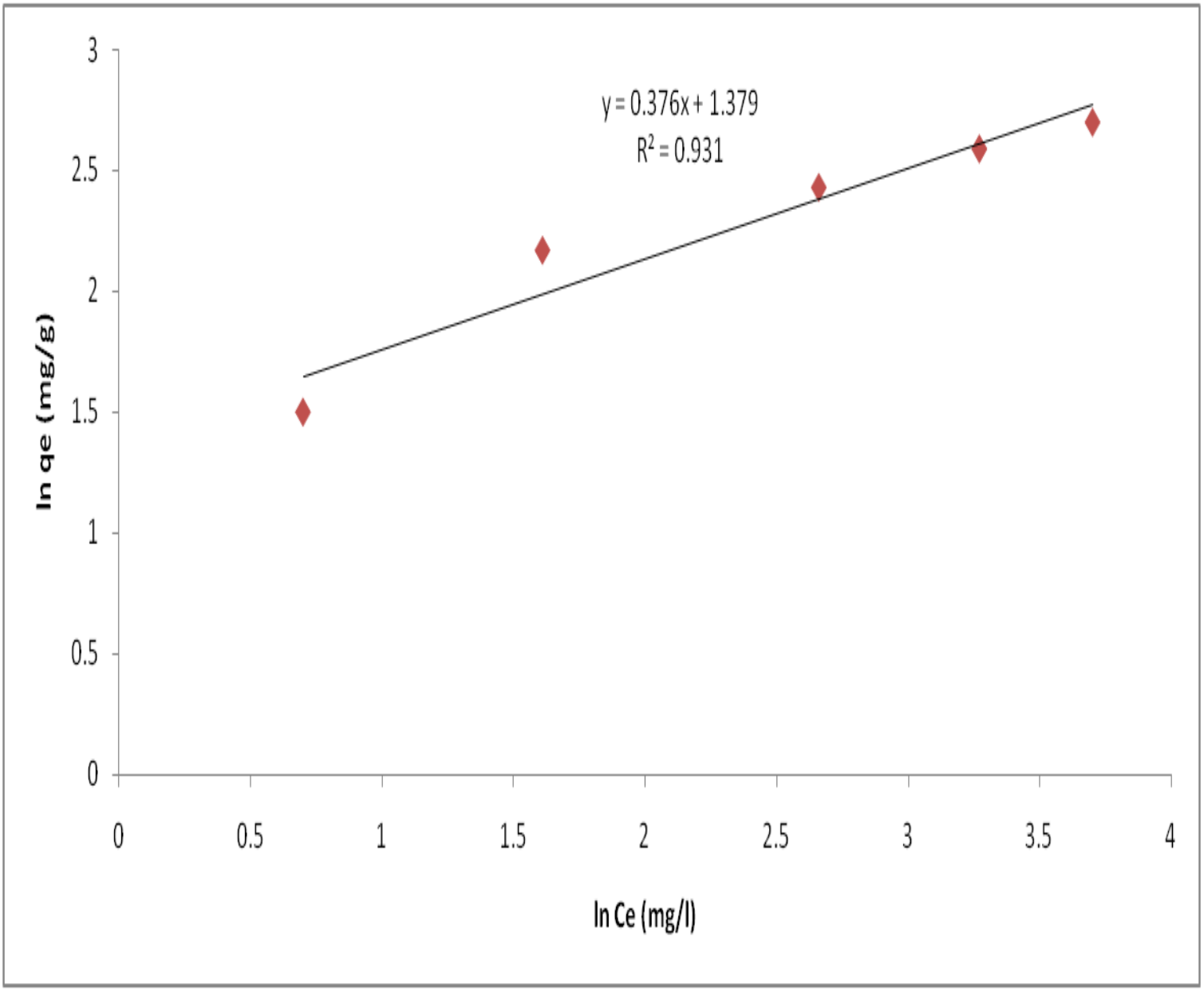


Figure 4.29: Freundlich Isotherm for AR1 Adsorption on TKP at 328 K

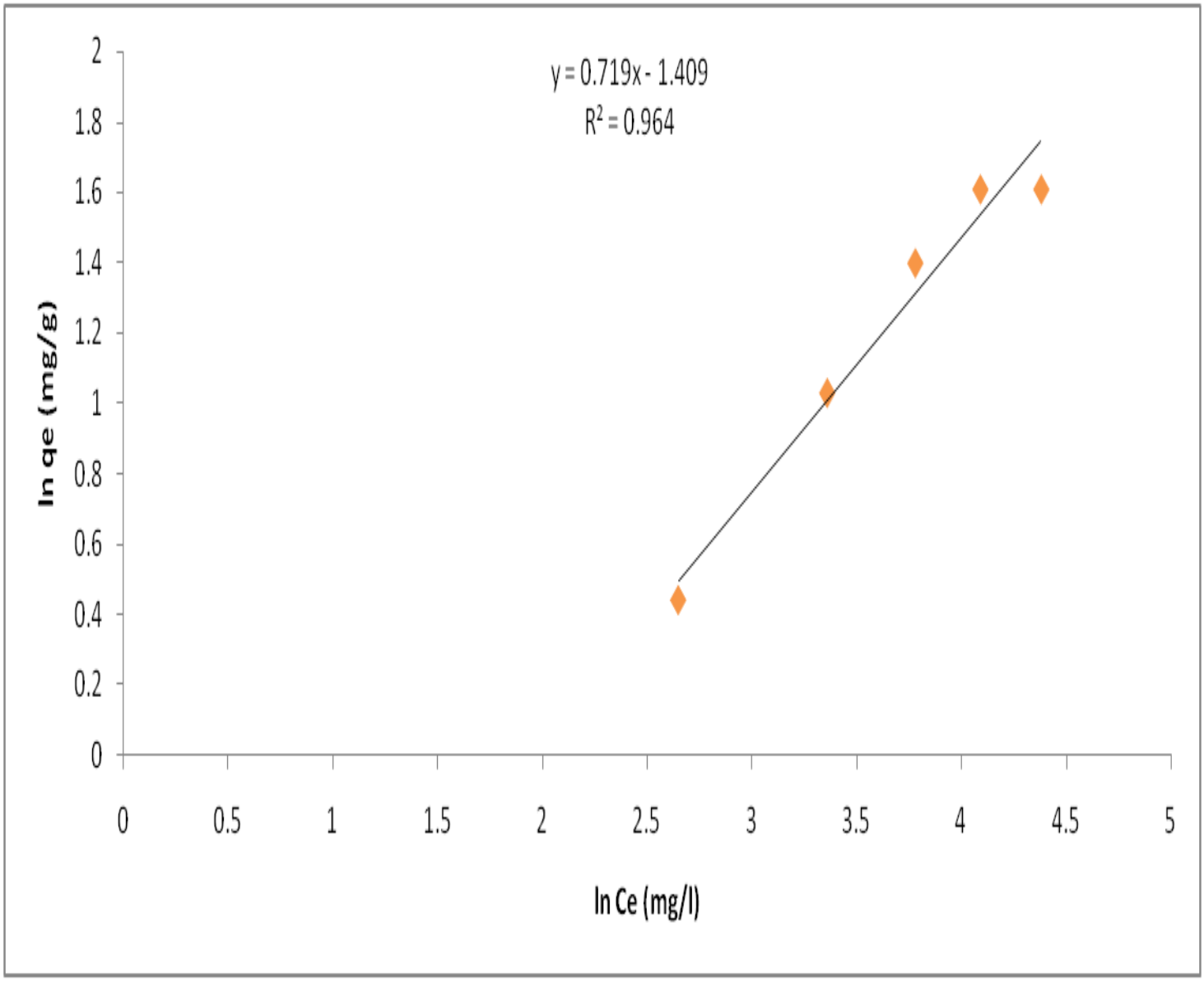


Figure 4.30: Freundlich Isotherm for RO20 Adsorption on TKP at 298 K

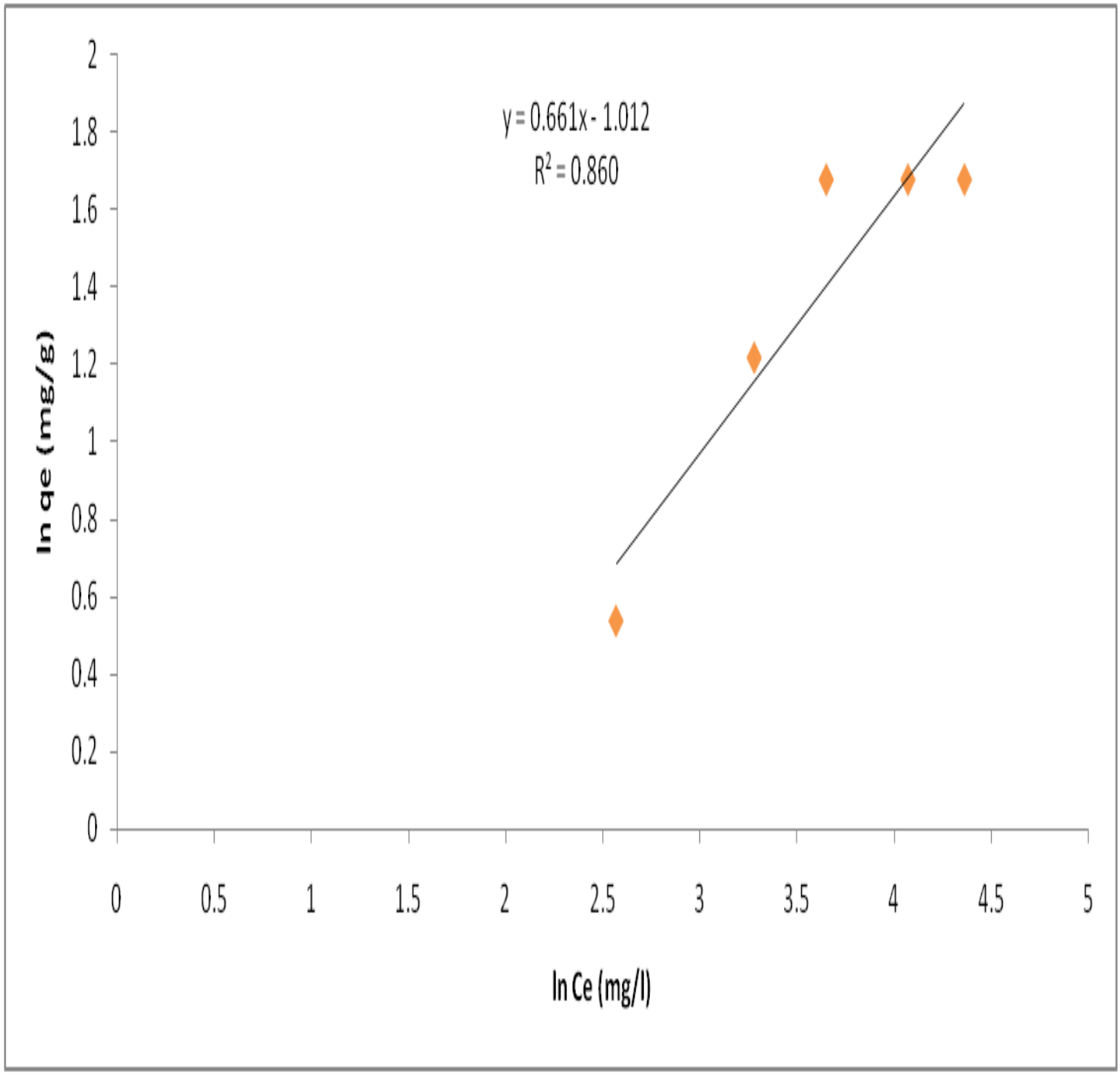


Figure 4.31: Freundlich Isotherm for RO20 Adsorption on TKP at 308 K

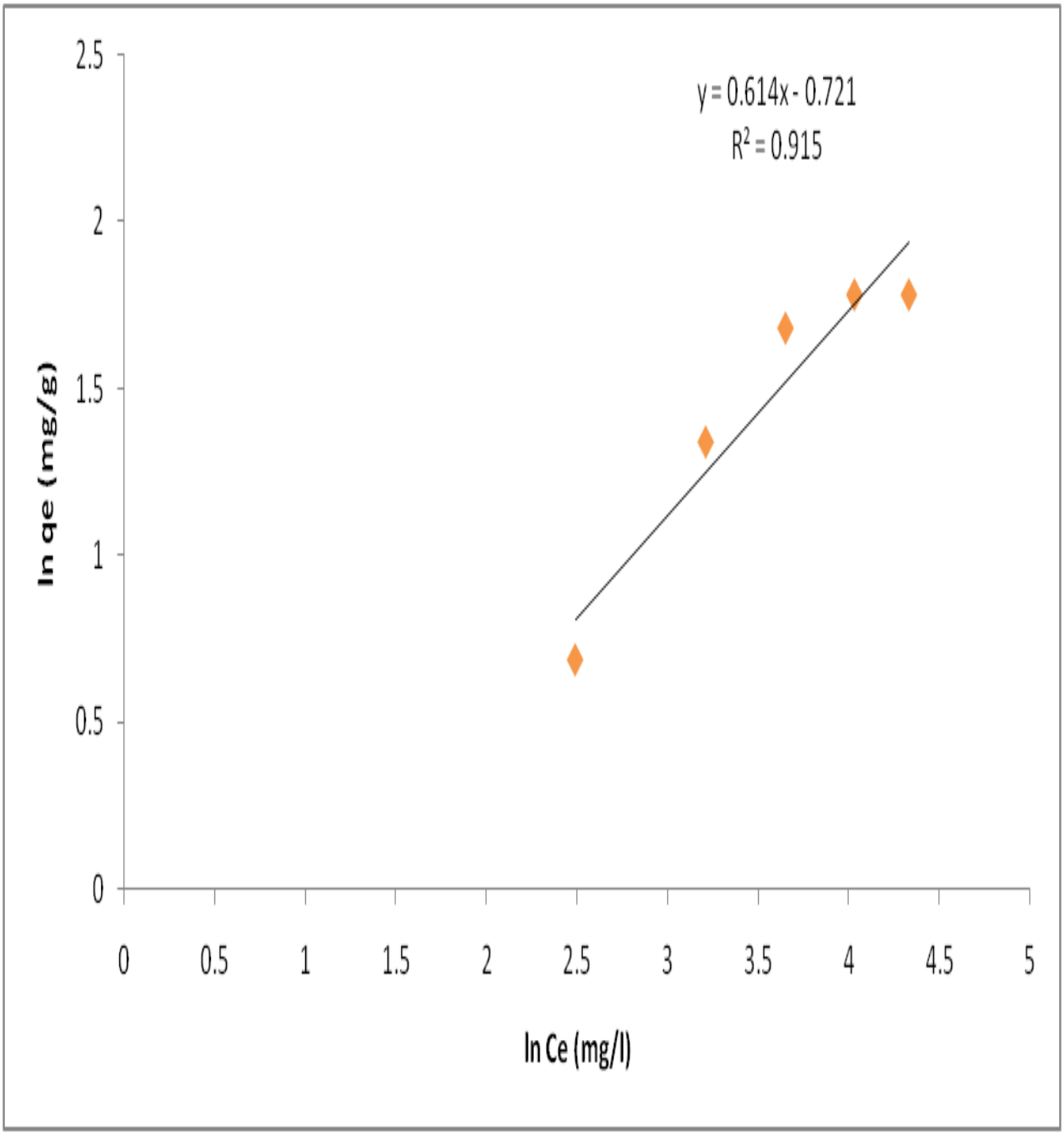


Figure 4.32: Freundlich Isotherm for RO20 Adsorption on TKP at 318 K

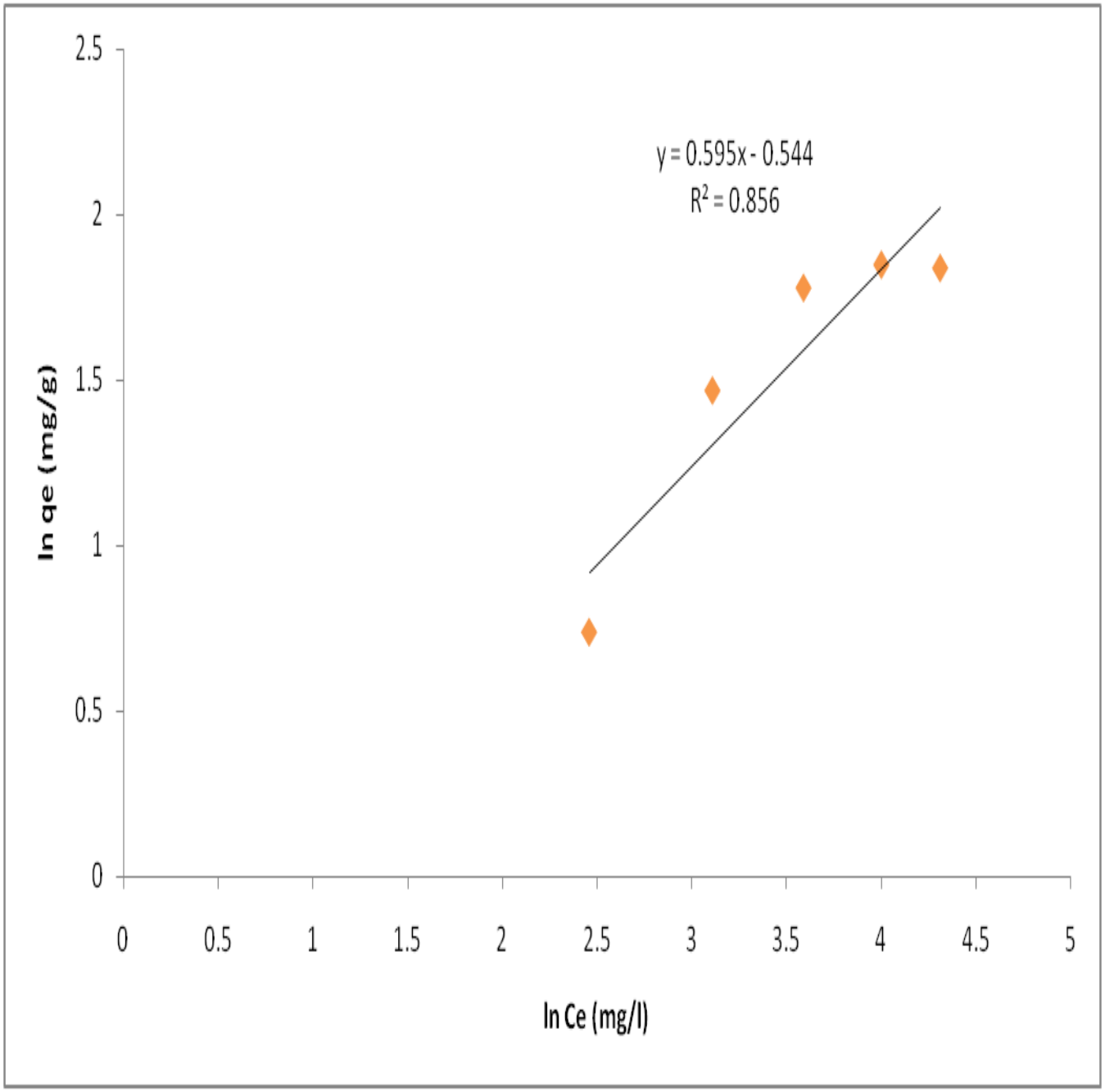


Figure 4.33: Freundlich Isotherm for RO20 Adsorption on TKP at 323 K

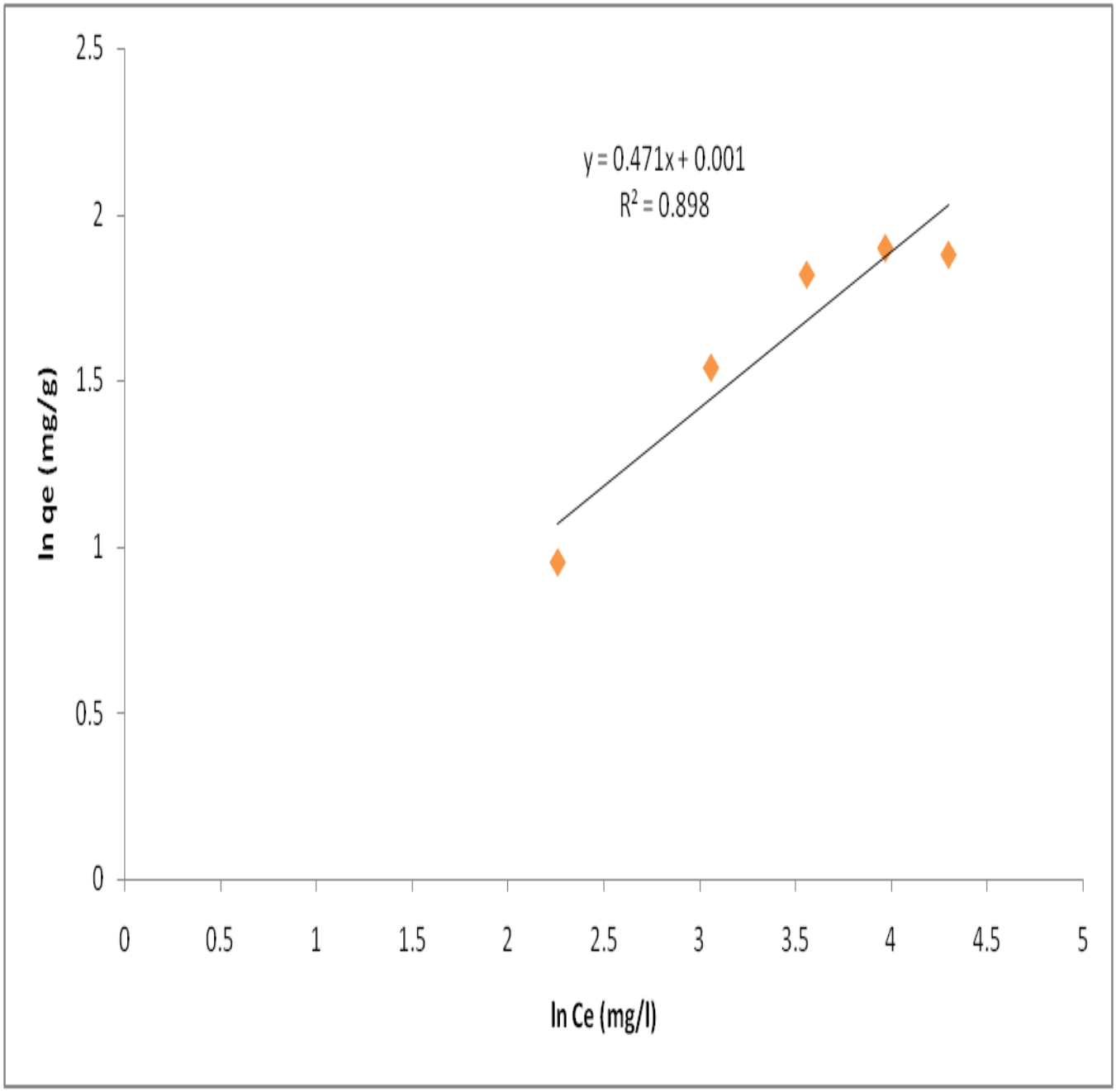


Figure 4.34: Freundlich Isotherm for RO20 Adsorption on TKP at 328 K

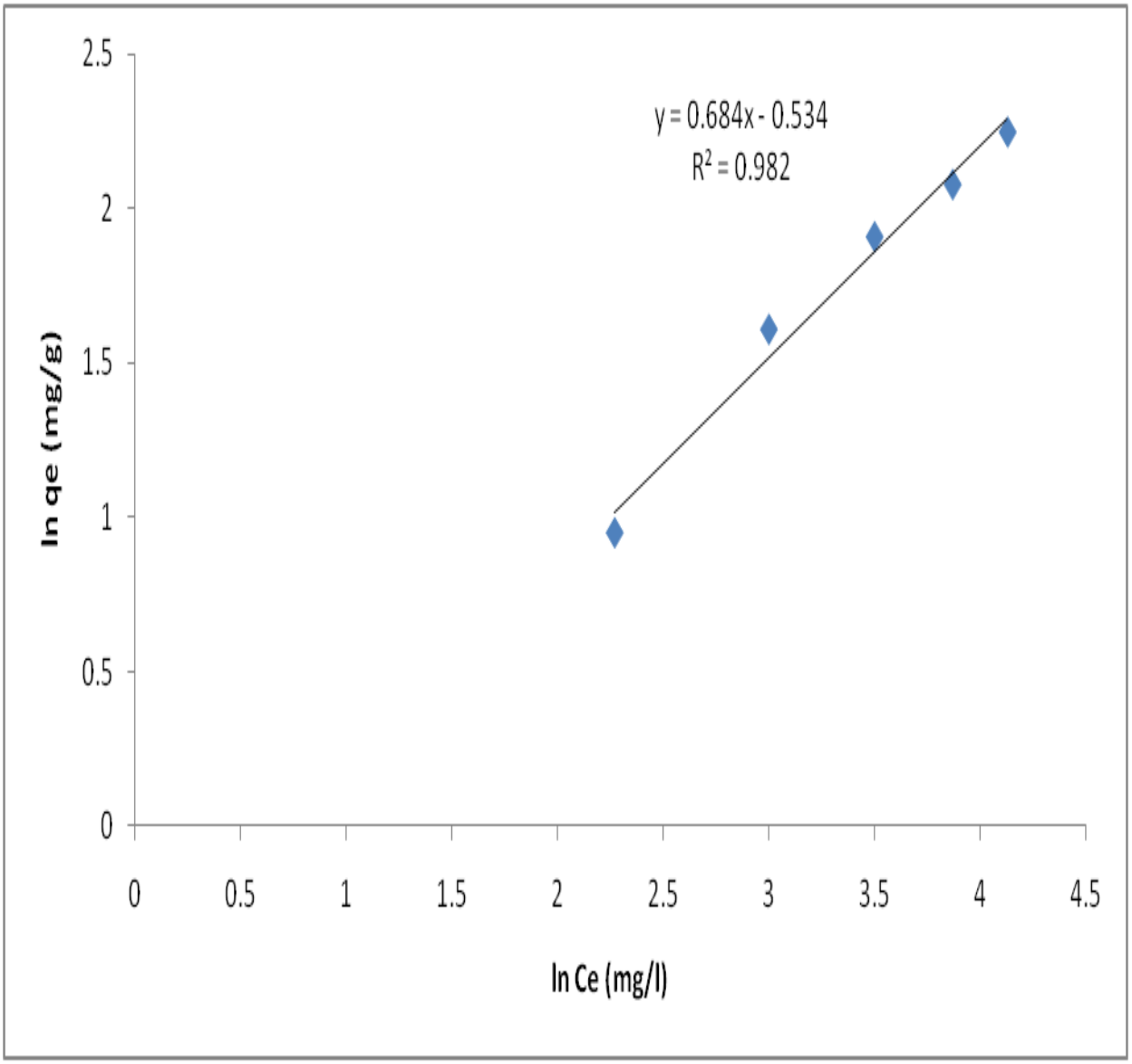


Figure 4.35: Freundlich Isotherm for RB29 Adsorption on TKP at 298 K

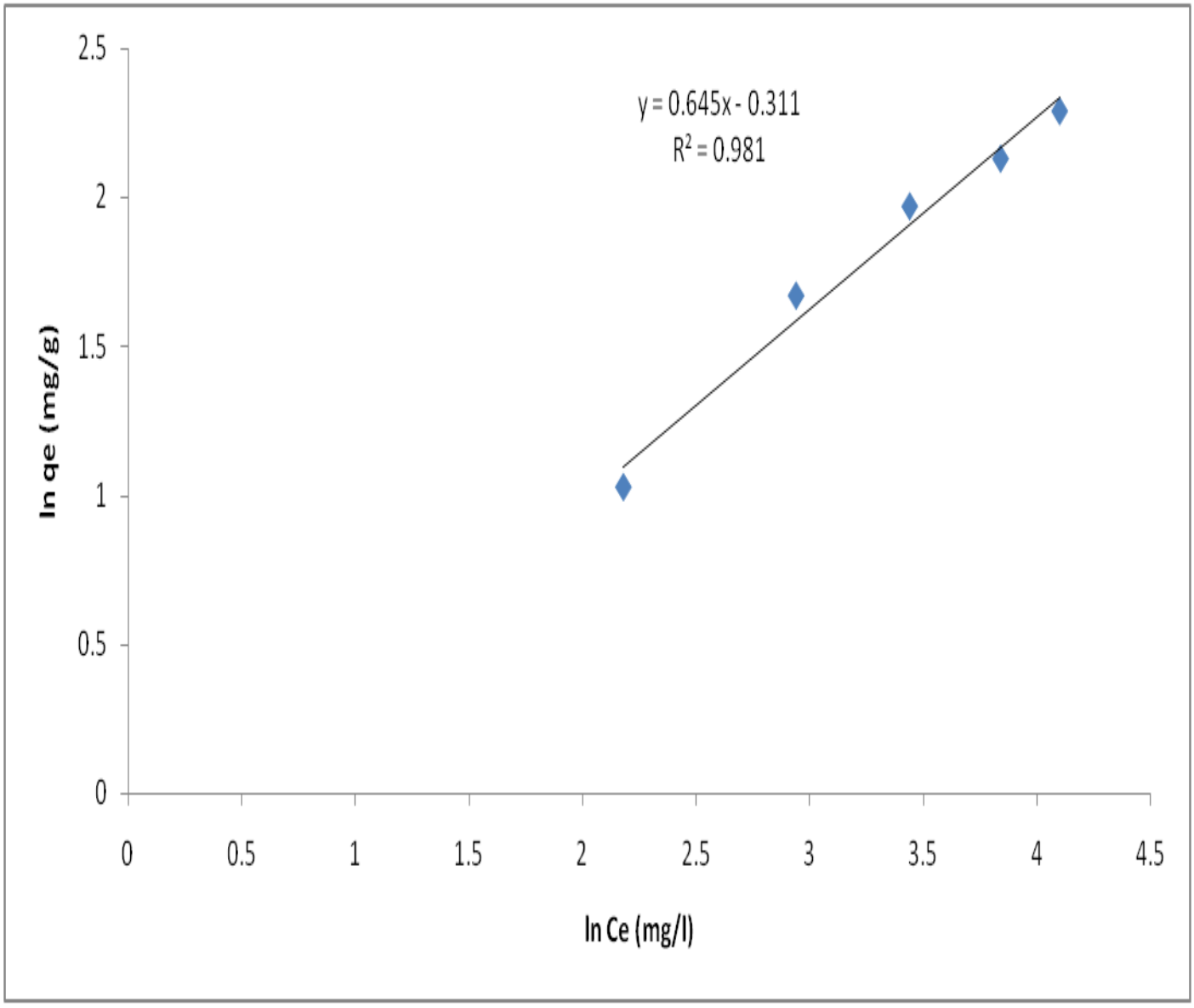


Figure 4.36:Freundlich Isotherm for RB29 Adsorption on TKP at 308 K

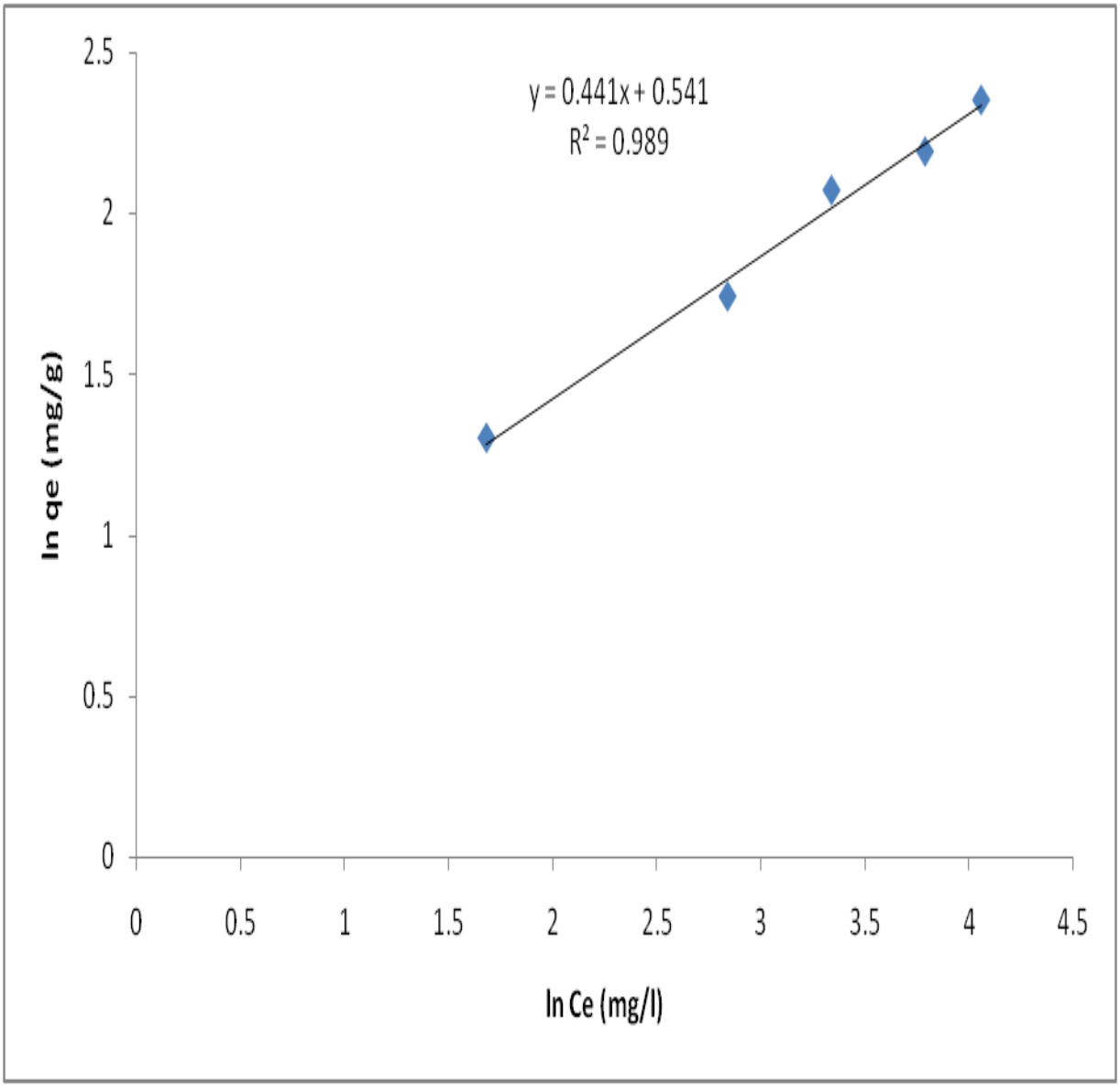


Figure 4.37: Freundlich Isotherm for RB29 Adsorption on TKP at 318 K

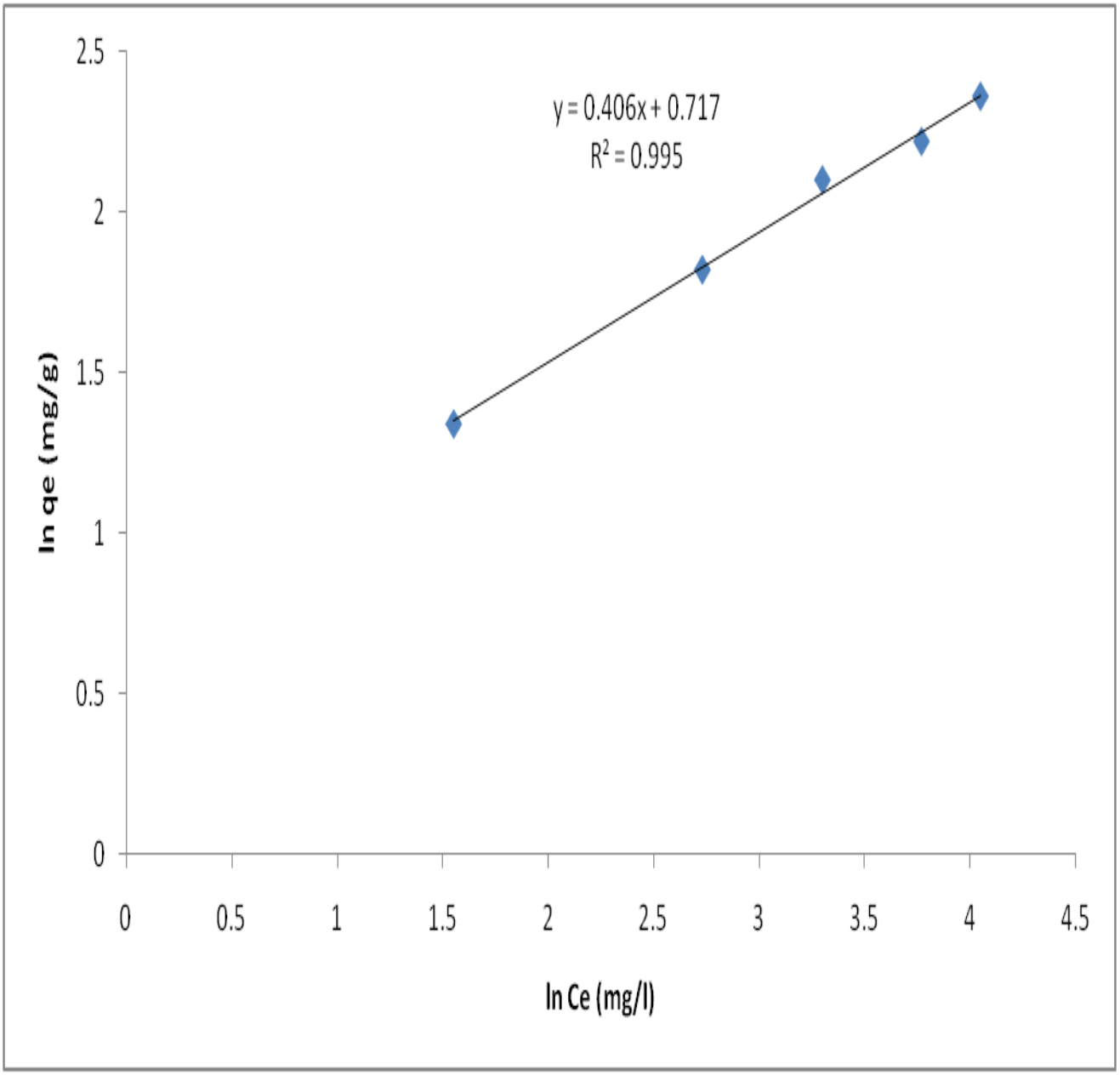


Figure 4.38: Freundlich Isotherm for RB29 Adsorption on TKP at 323 K

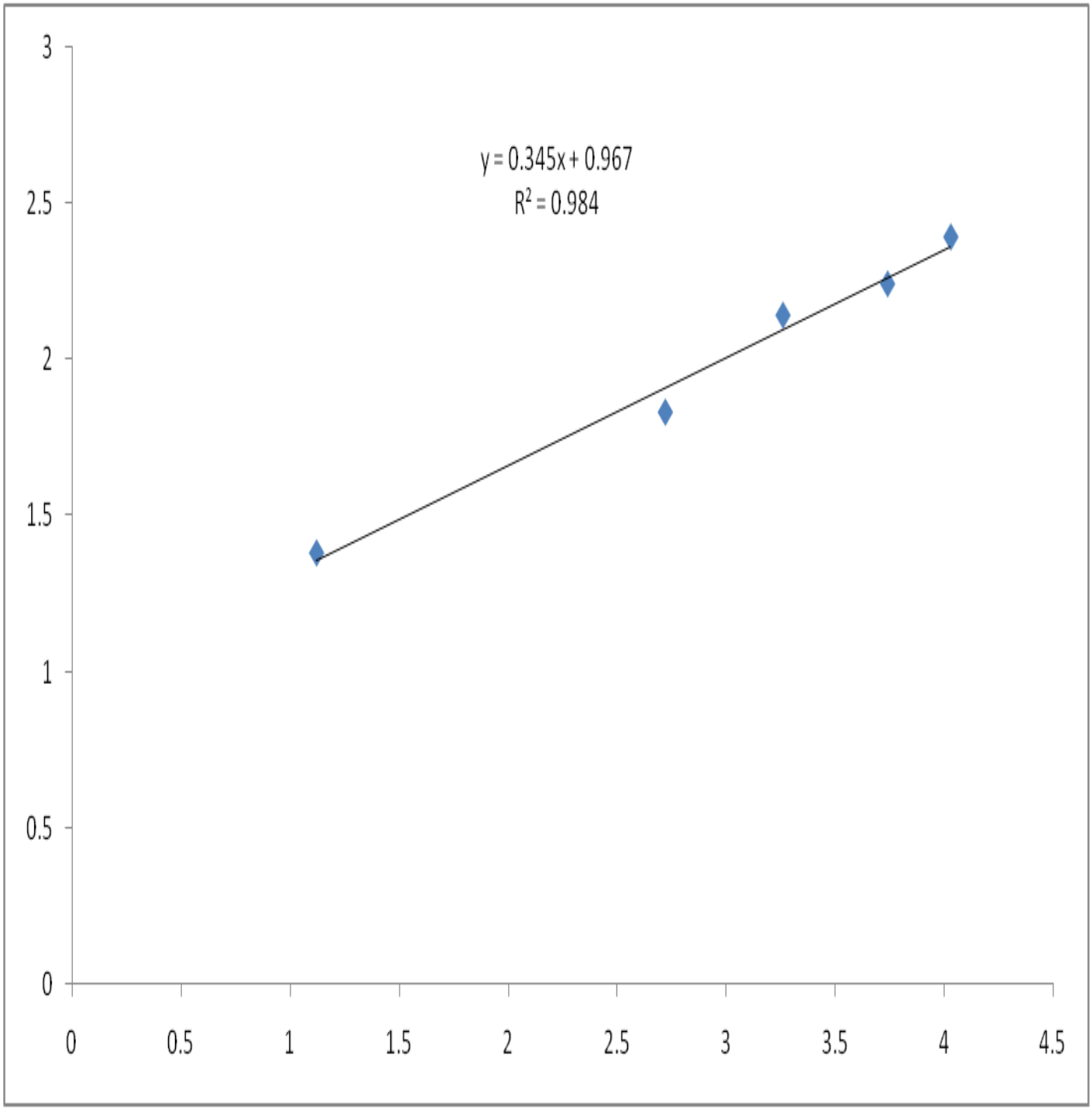


Figure 4.39: Freundlich Isotherm for RB29 Adsorption on TKP at 328 K

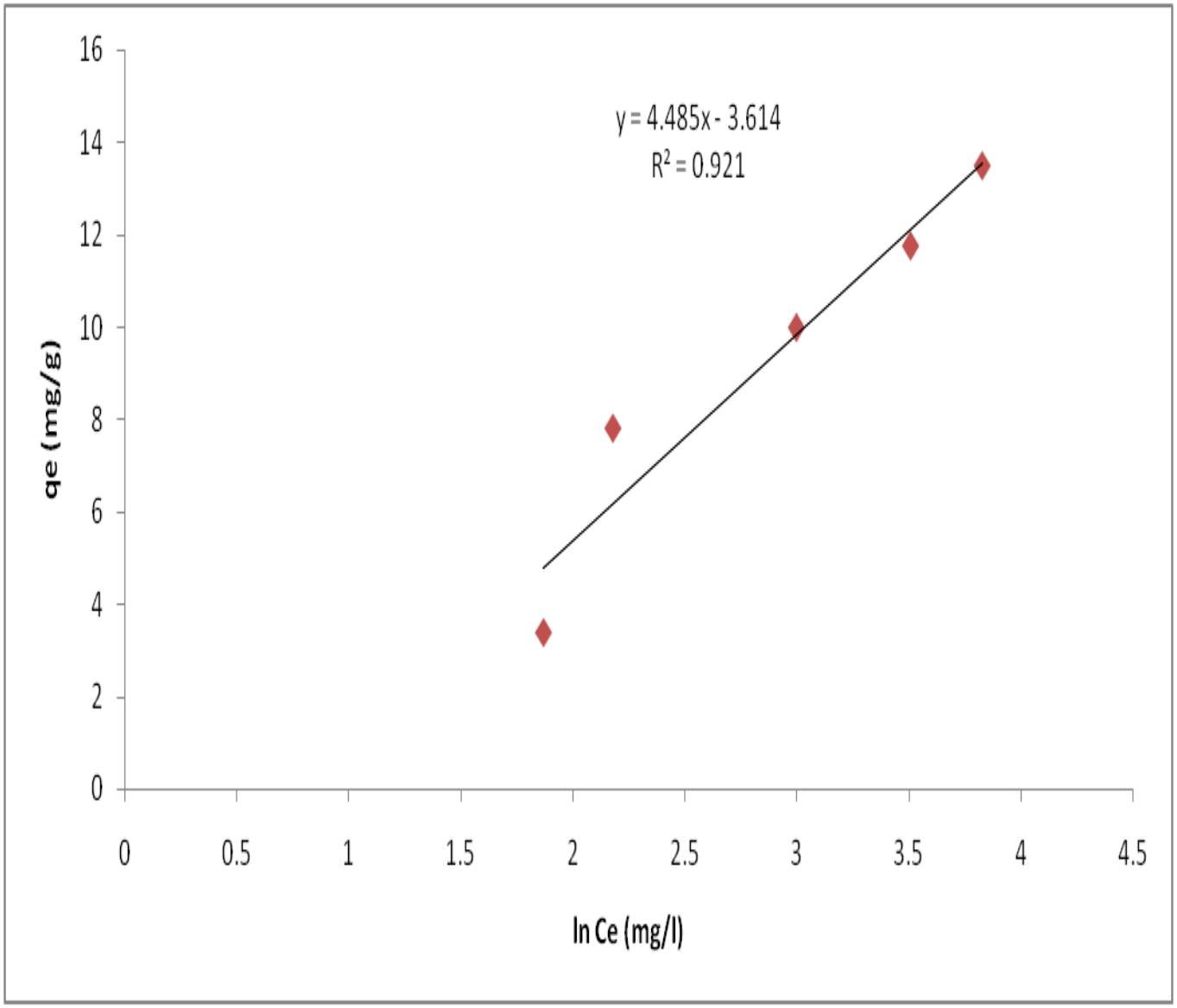


Figure 4.40: Temkin Isotherm for AR1 Adsorption on TKP at 298 K

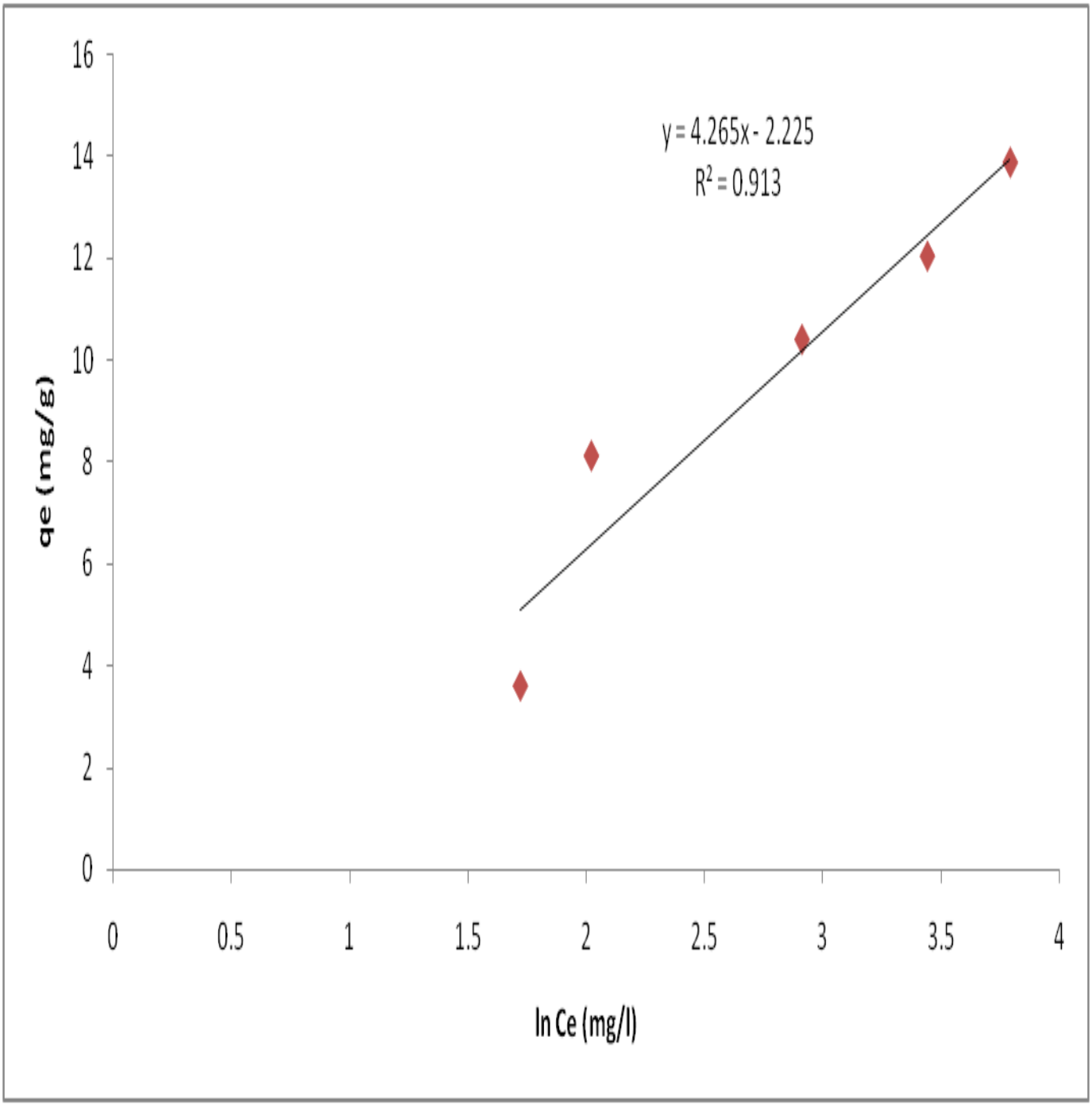


Figure 4.41: Temkin Isotherm for AR1 Adsorption on TKP at 308 K

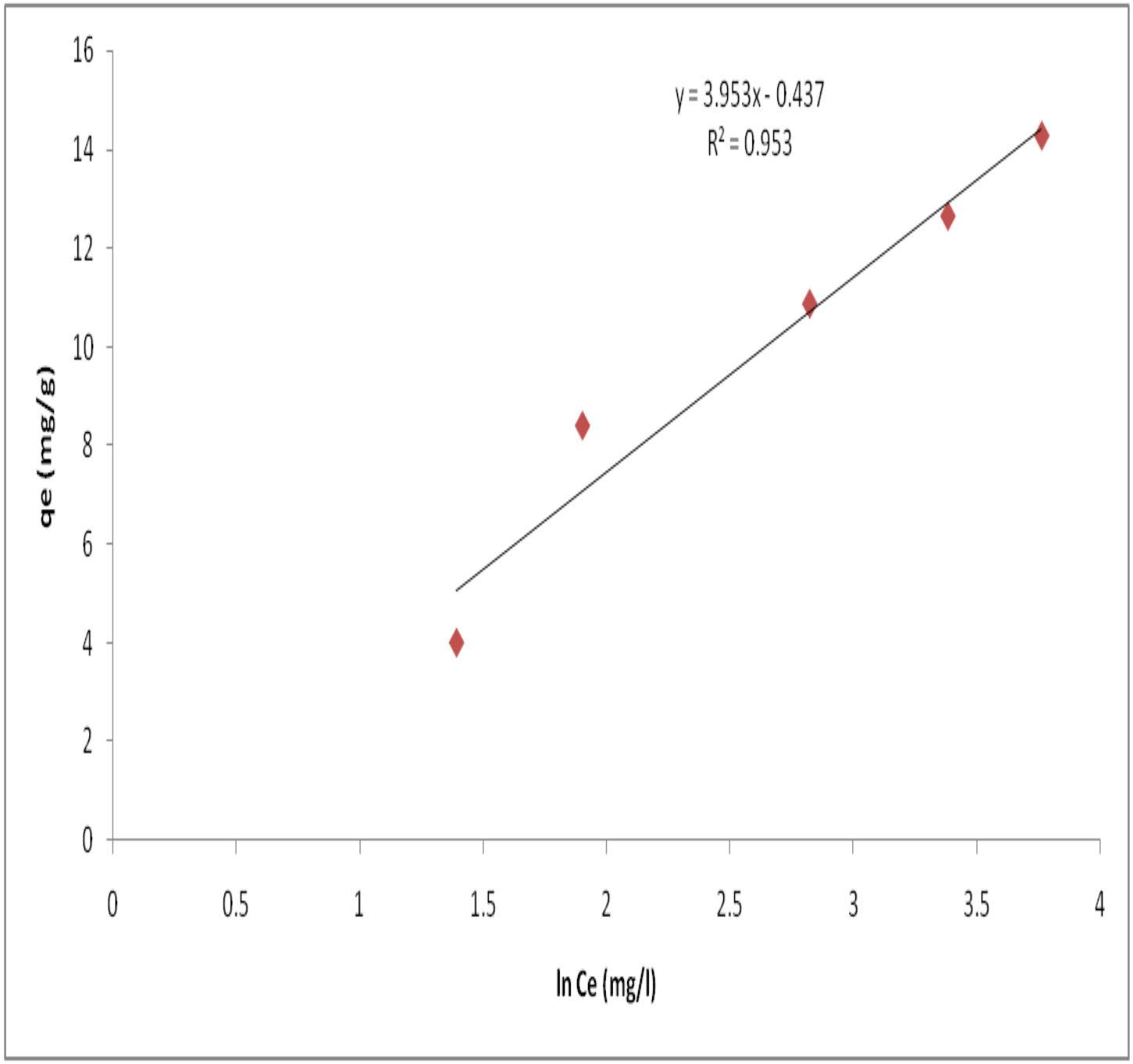


Figure 4.42: Temkin Isotherm for AR1 Adsorption on TKP at 318 K

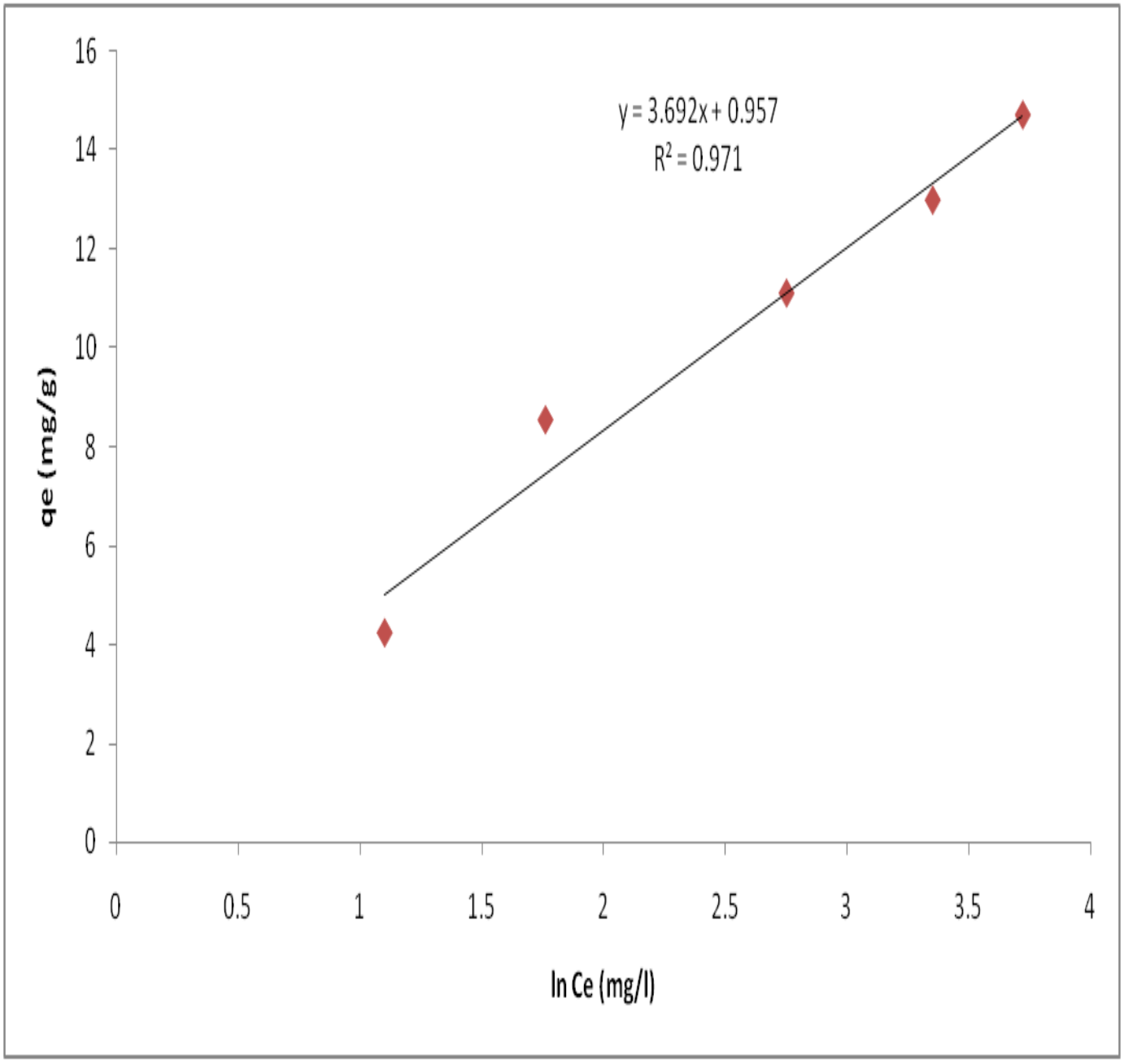


Figure 4.43: Temkin Isotherm for AR1 Adsorption on TKP at 323 K

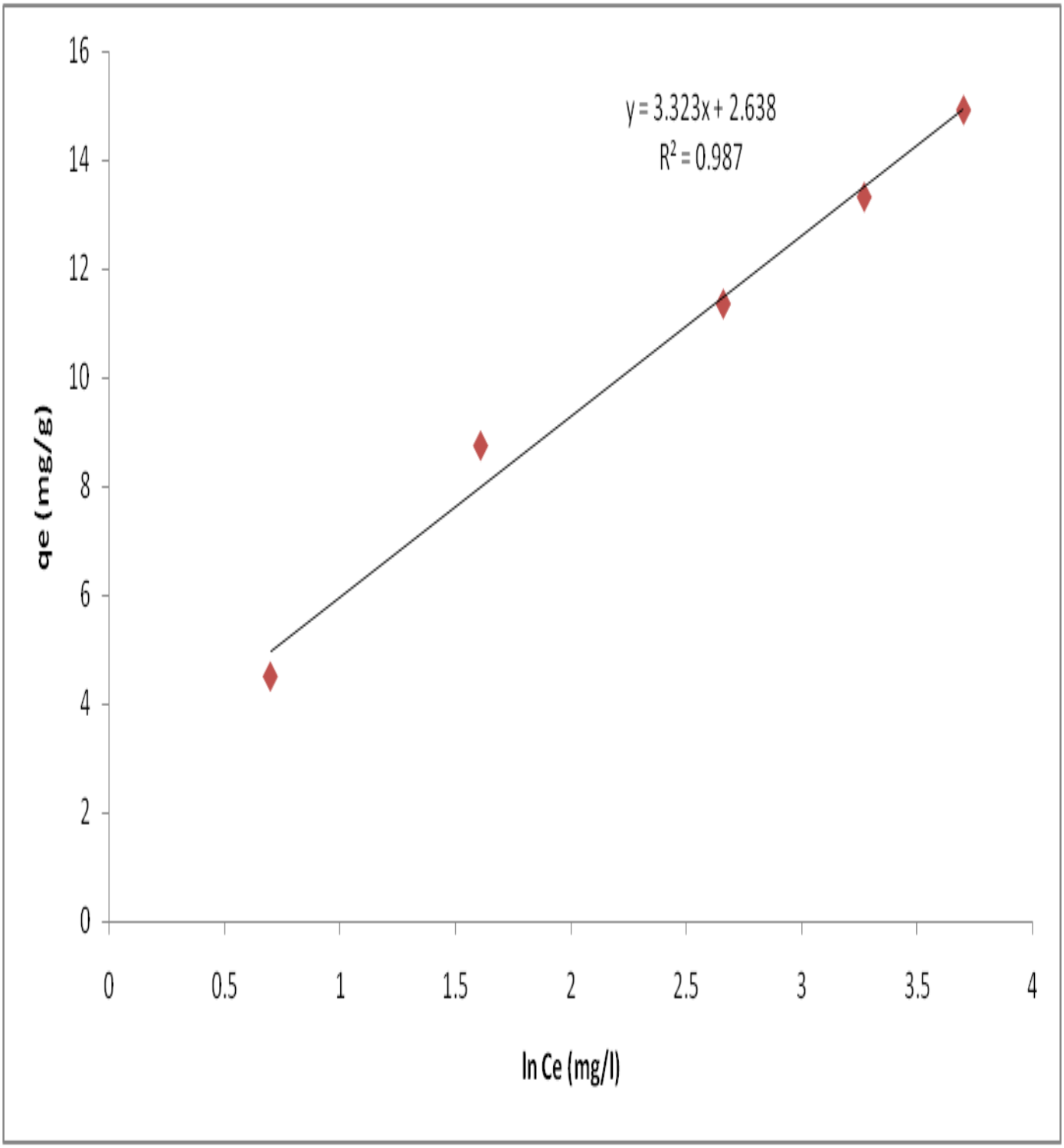


Figure 4.44: Temkin Isotherm for AR1 Adsorption on TKP at 328 K

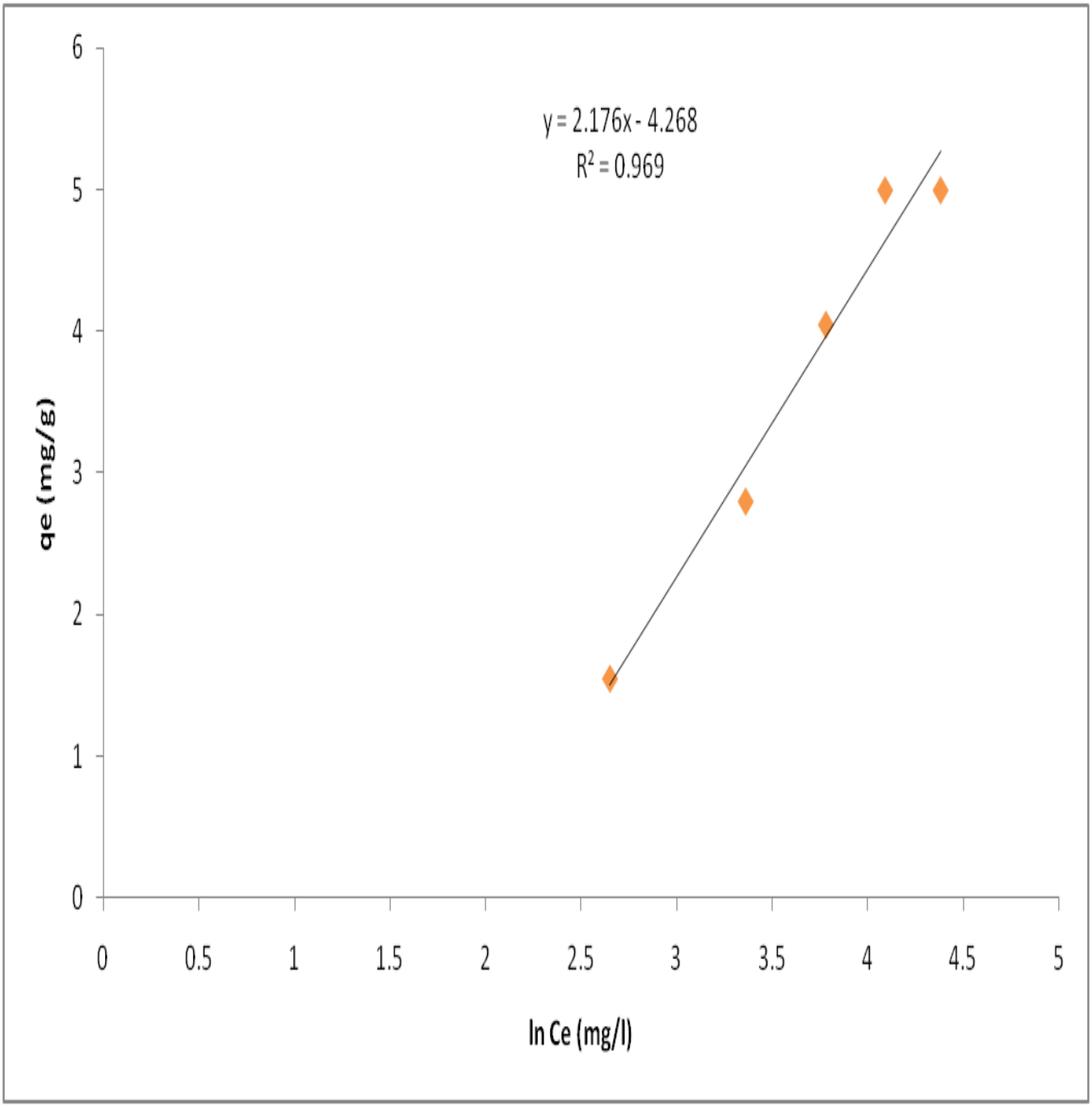


Figure 4.45: Temkin Isotherm for RO20 Adsorption on TKP at 298 K

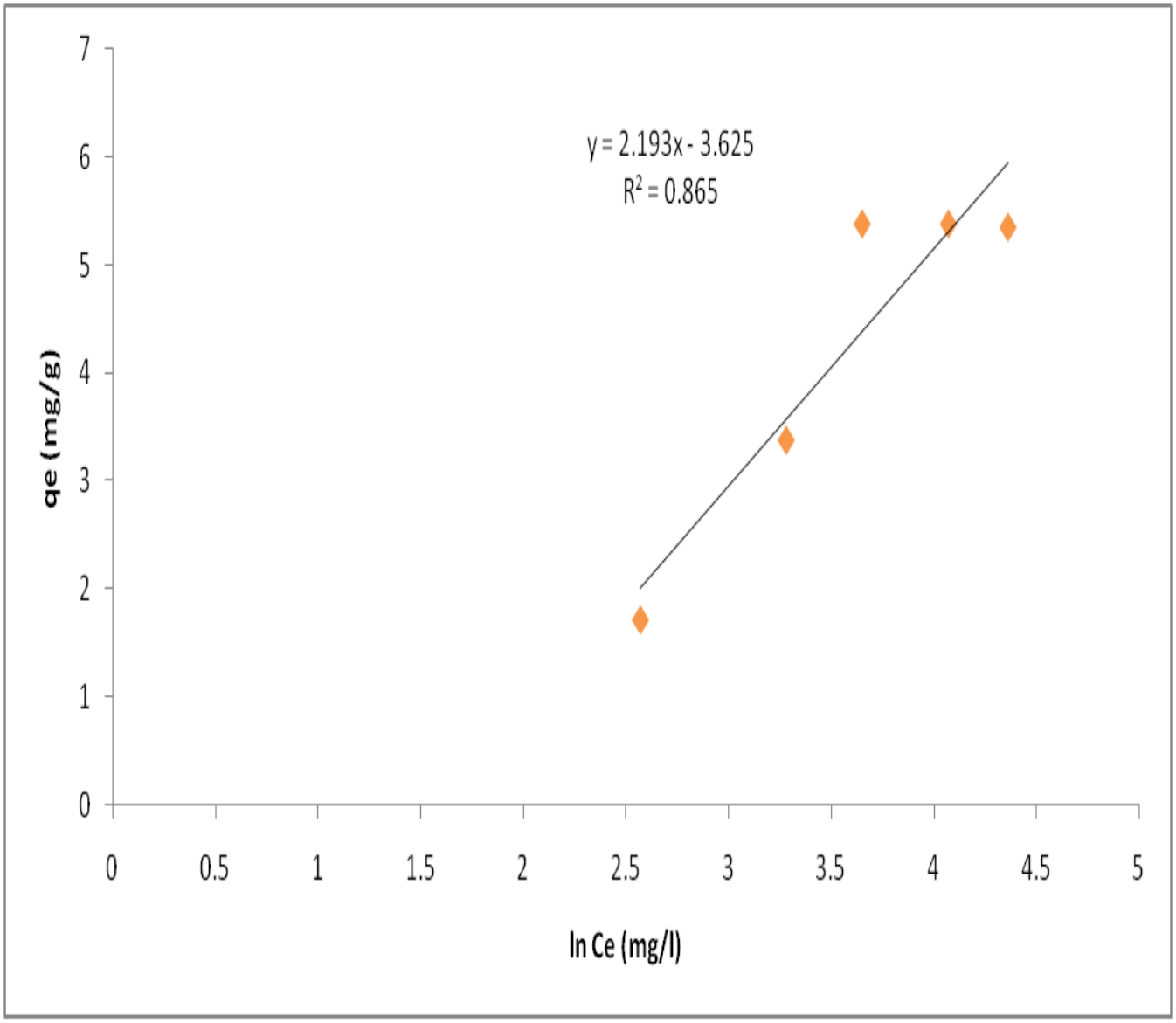


Figure 4.46: Temkin Isotherm for RO20 Adsorption on TKP at 308 K

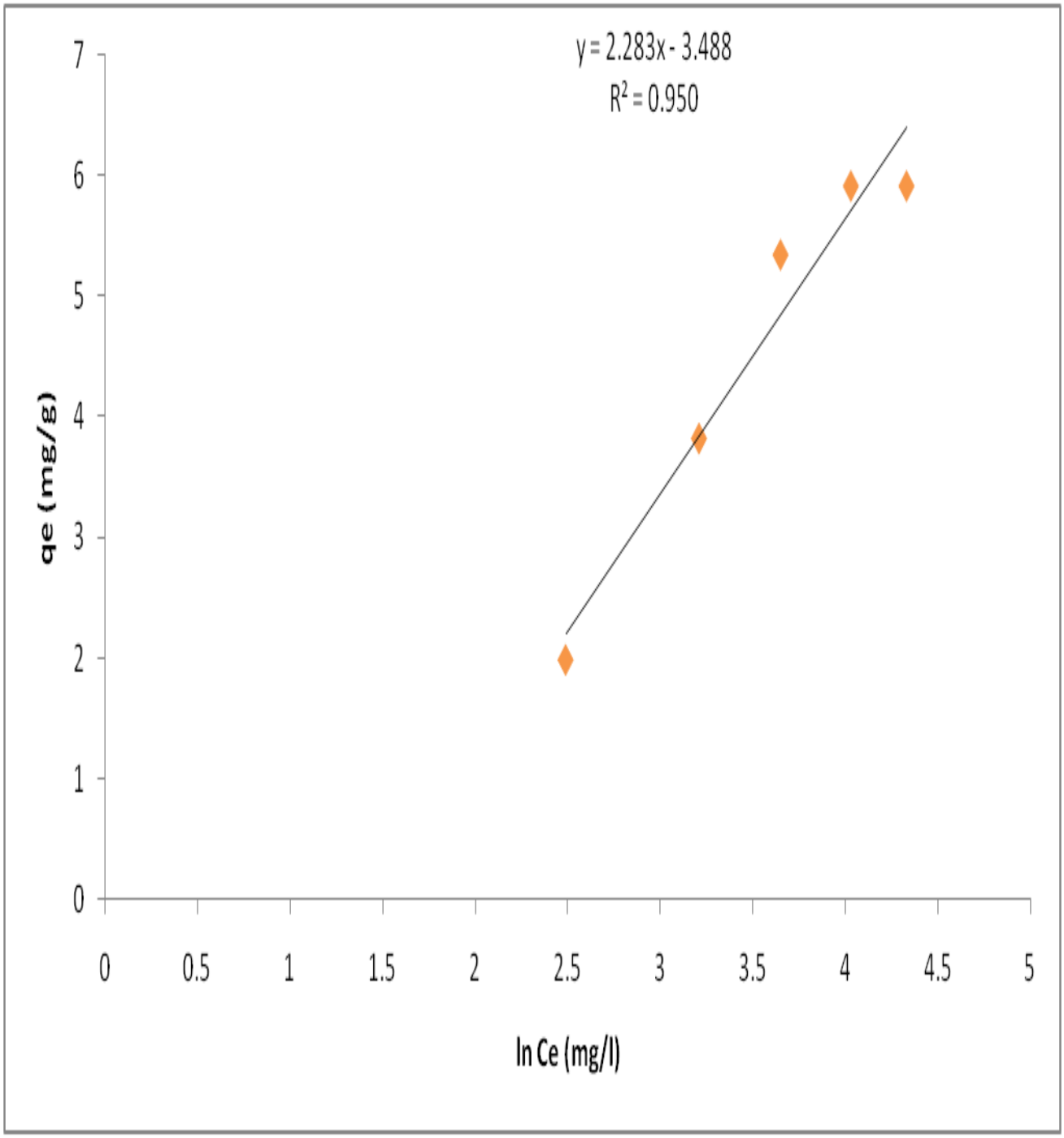


Figure 4.47: Temkin Isotherm for RO20 Adsorption on TKP at 318 K

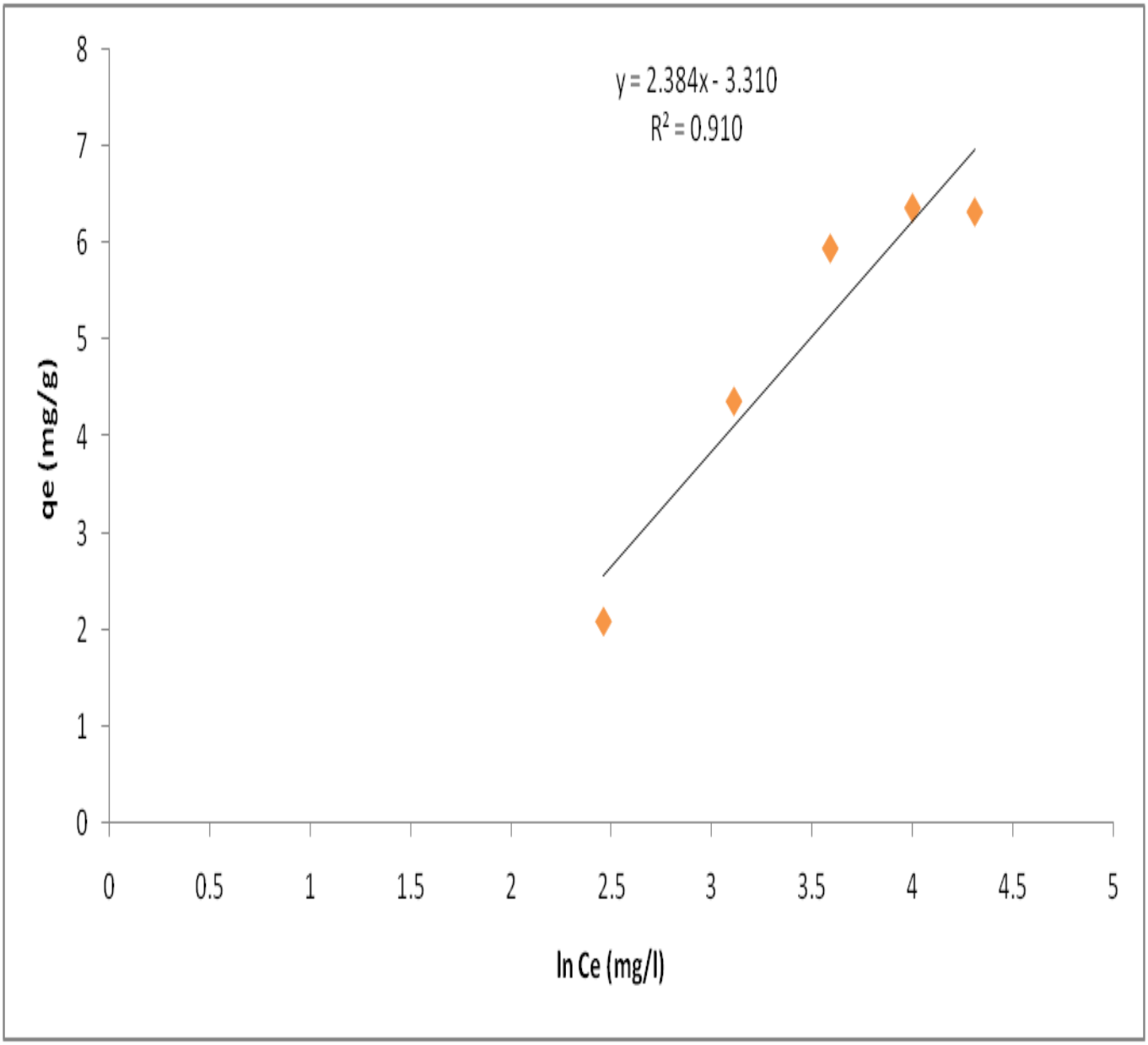


Figure 4.48: Temkin Isotherm for RO20 Adsorption on TKP at 323 K

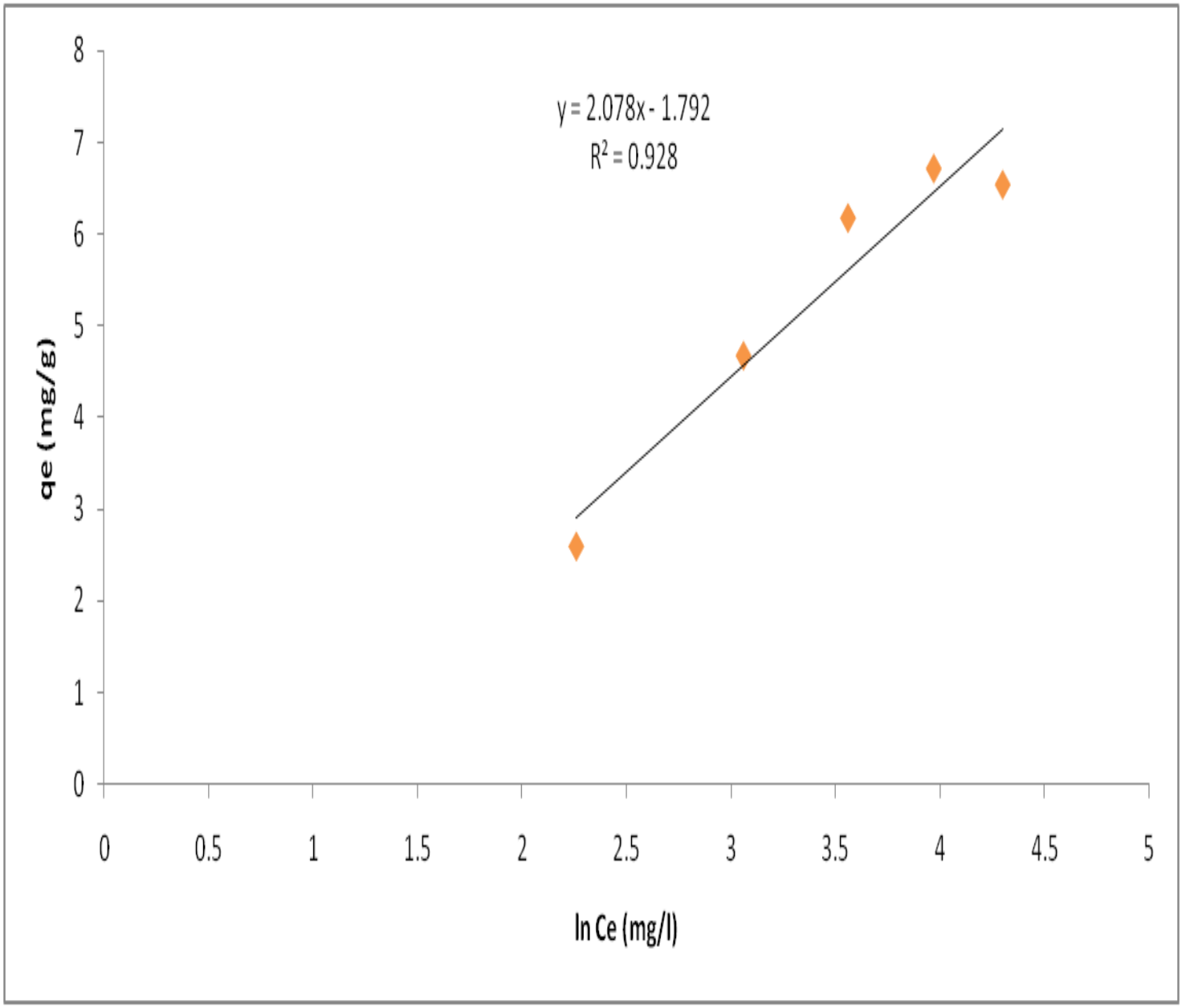


Figure 4.49: Temkin Isotherm for RO20 Adsorption on TKP at 328 K

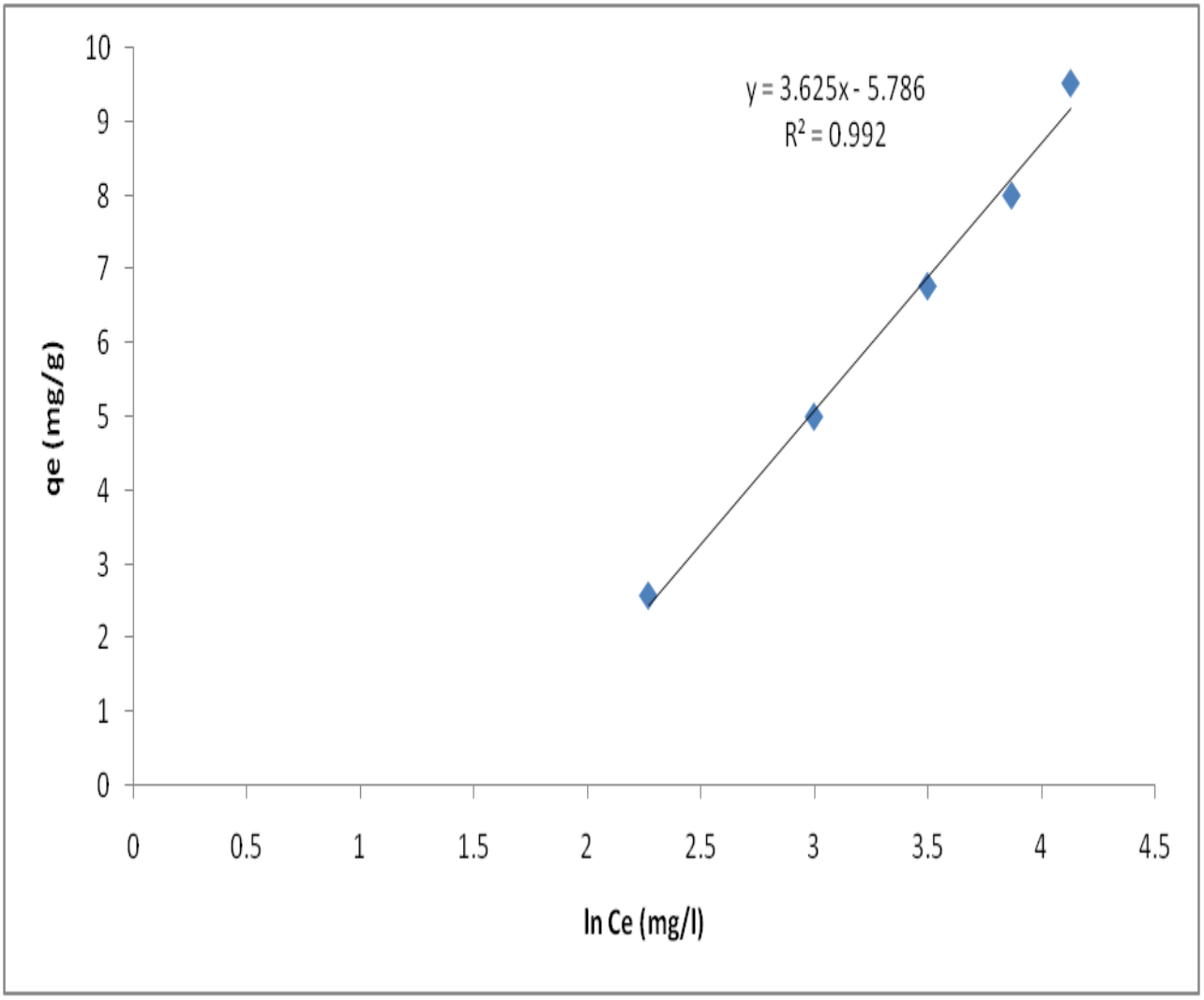


Figure 4.50: Temkin Isotherm for RB29 Adsorption on TKP at 298 K

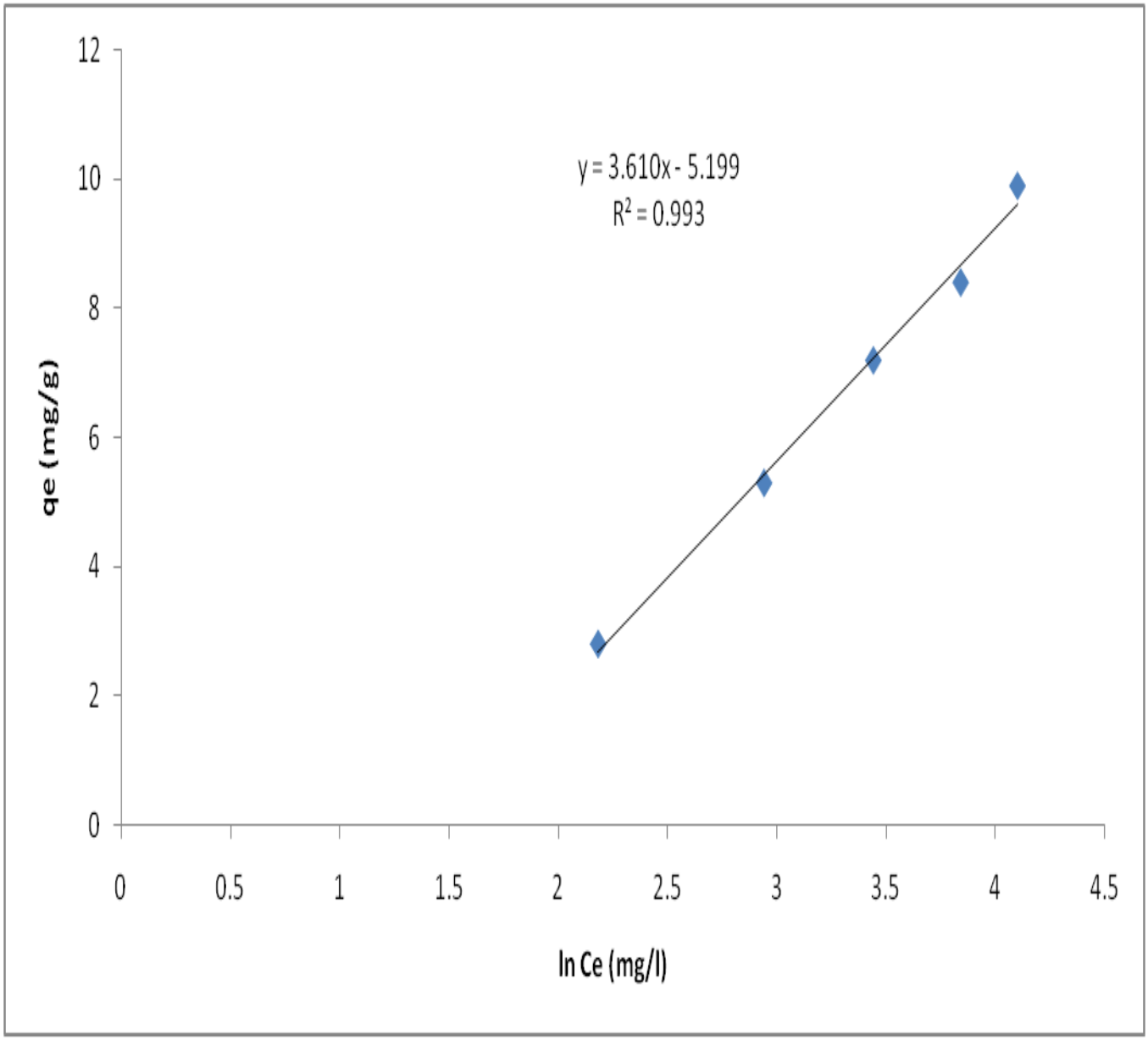


Figure 4.51: Temkin Isotherm for RB29 Adsorption on TKP at 308 K

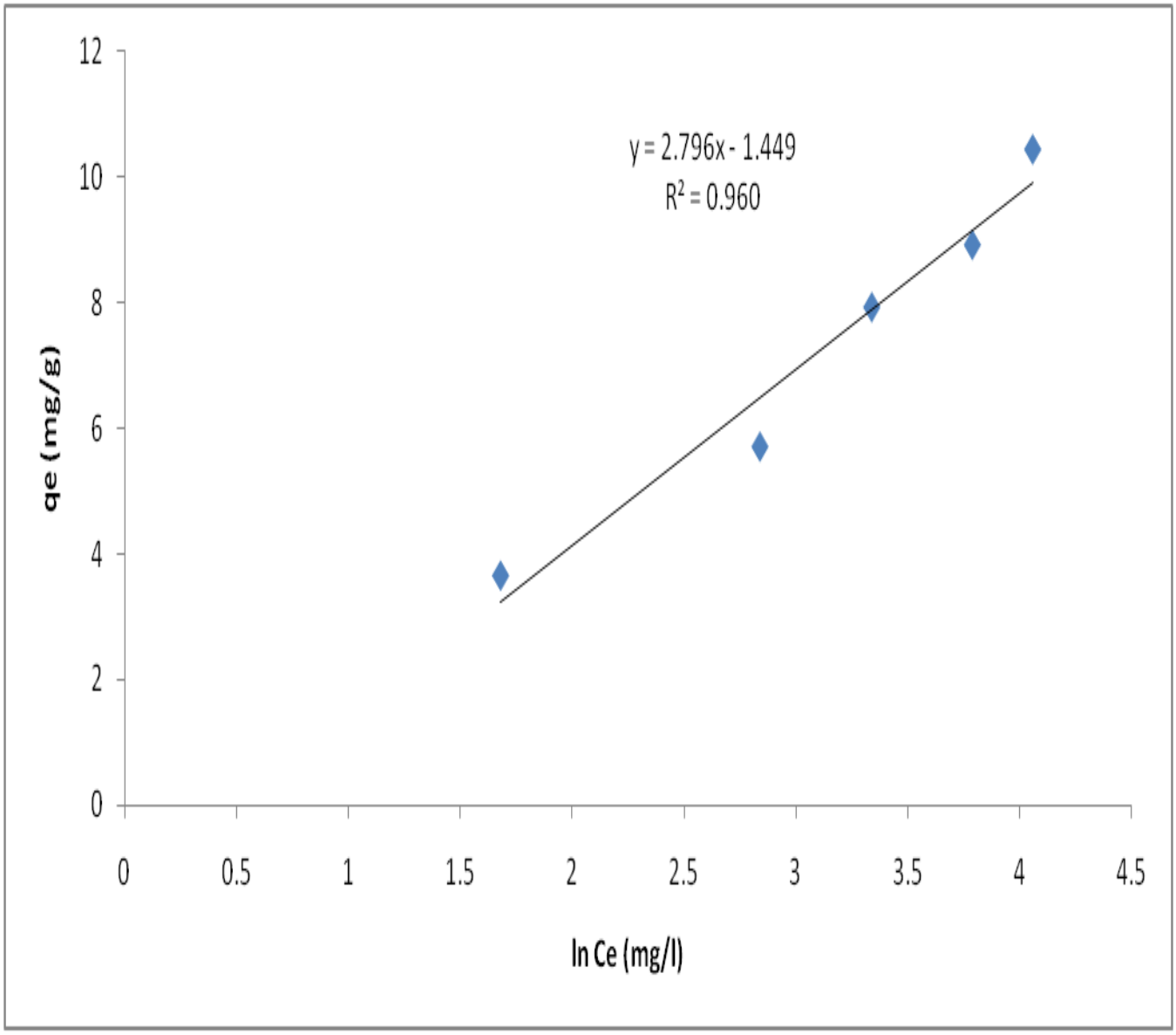


Figure 4.52: Temkin Isotherm for RB29 Adsorption on TKP at 318 K

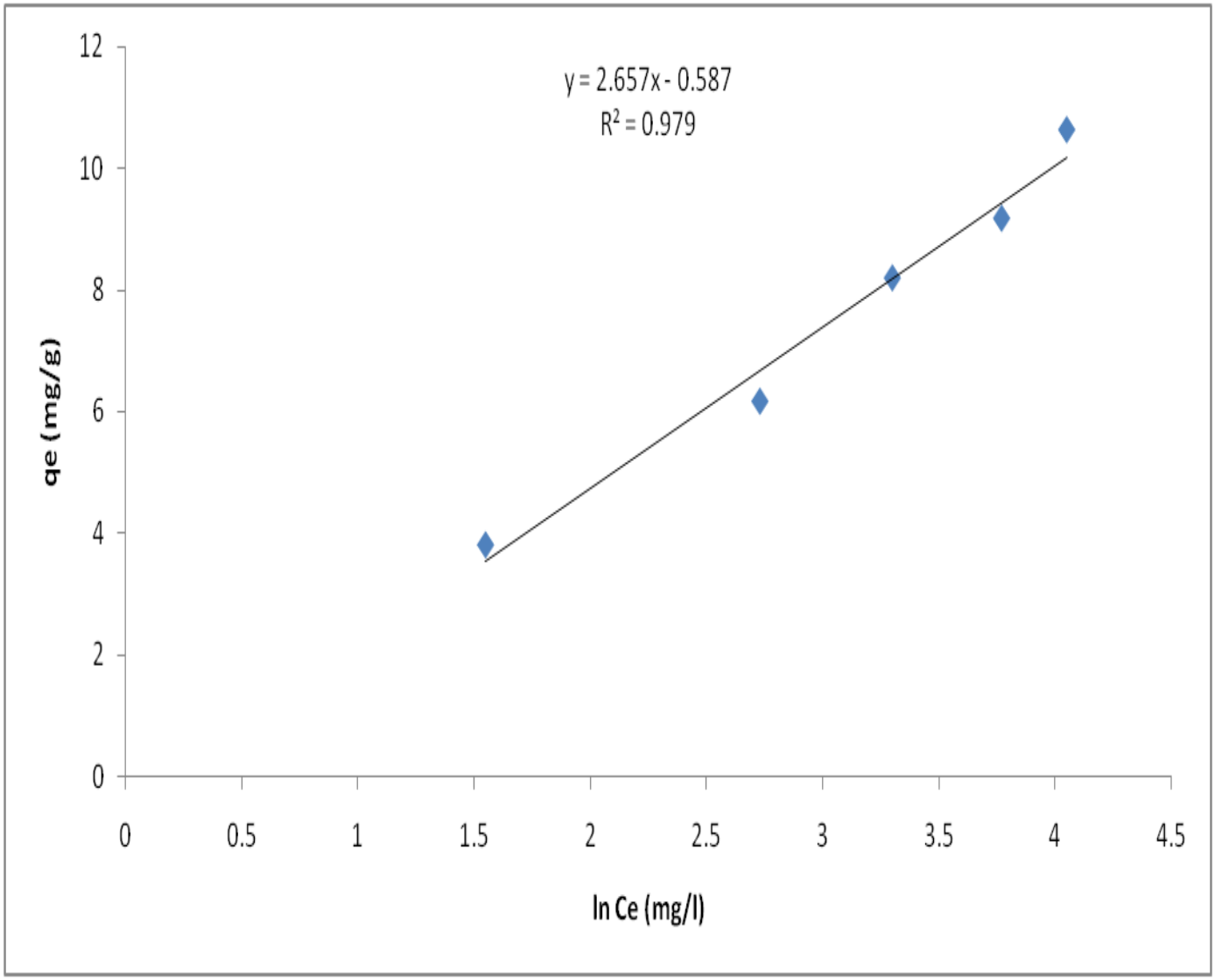


Figure 4.53: Temkin Isotherm for RB29 Adsorption on TKP at 323 K

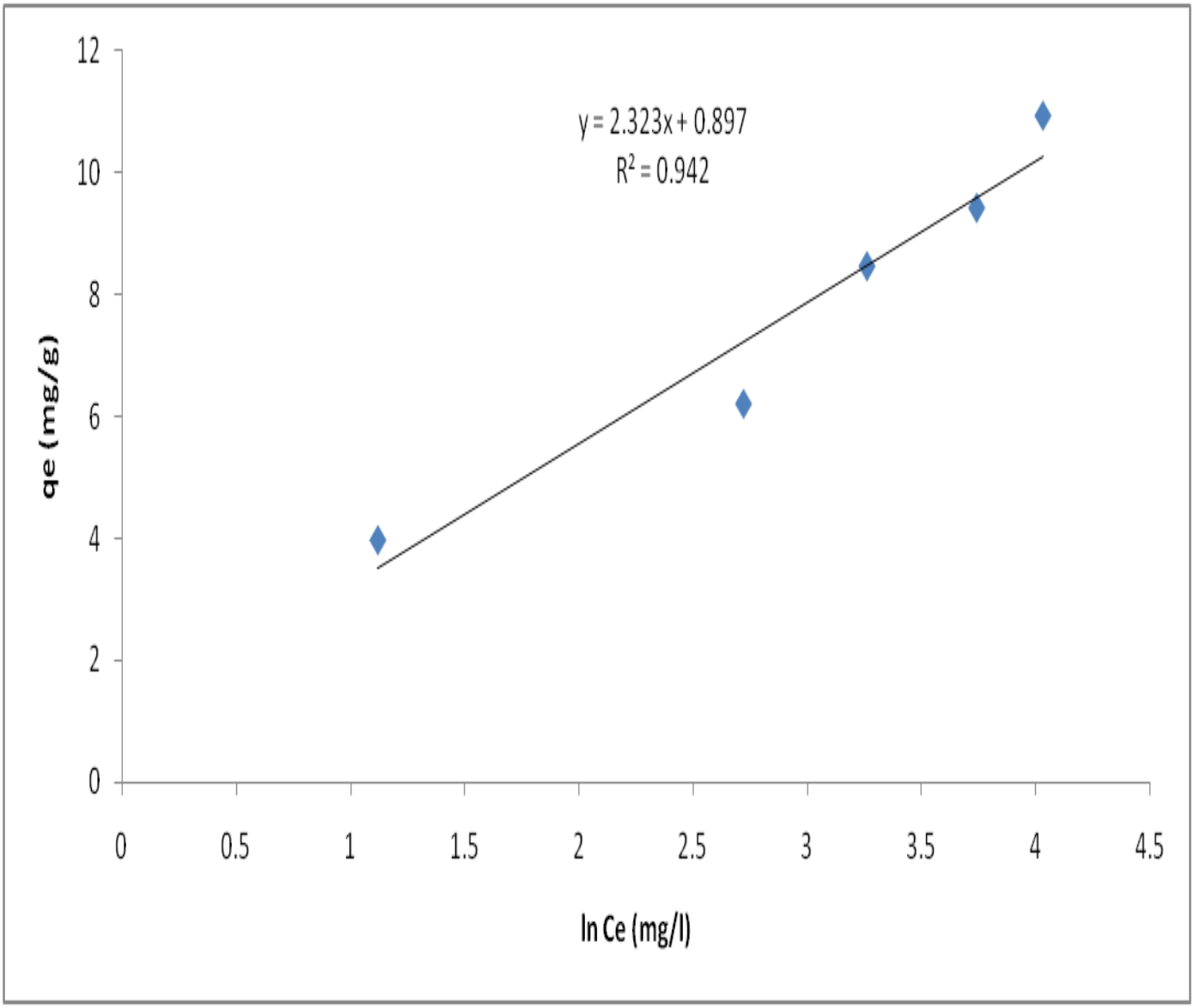


Figure 4.54: Temkin Isotherm for RB29 Adsorption on TKP at 328 K

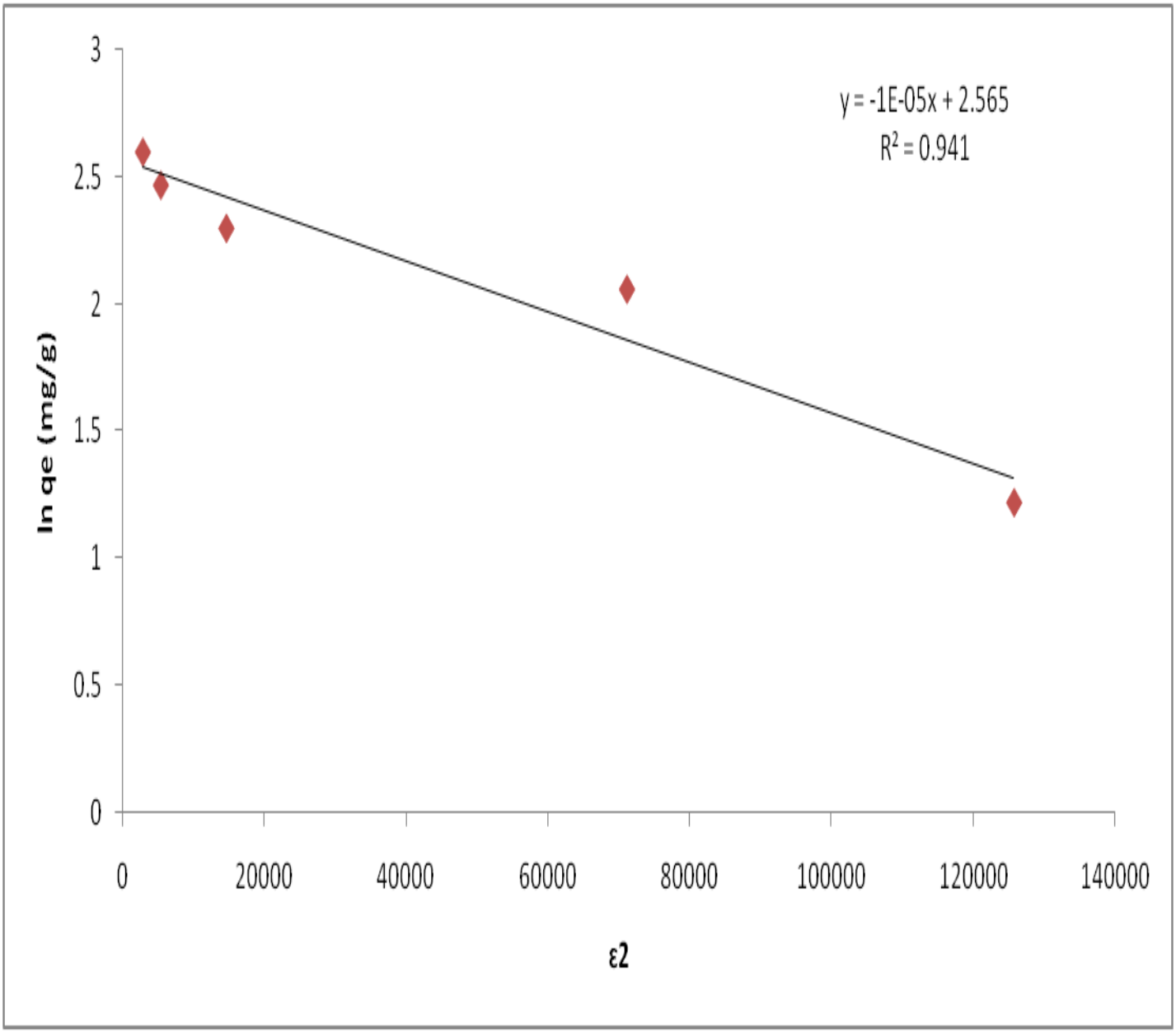


Figure 4.55: D-R Isotherm for AR1 Adsorption on TKP at 298 K

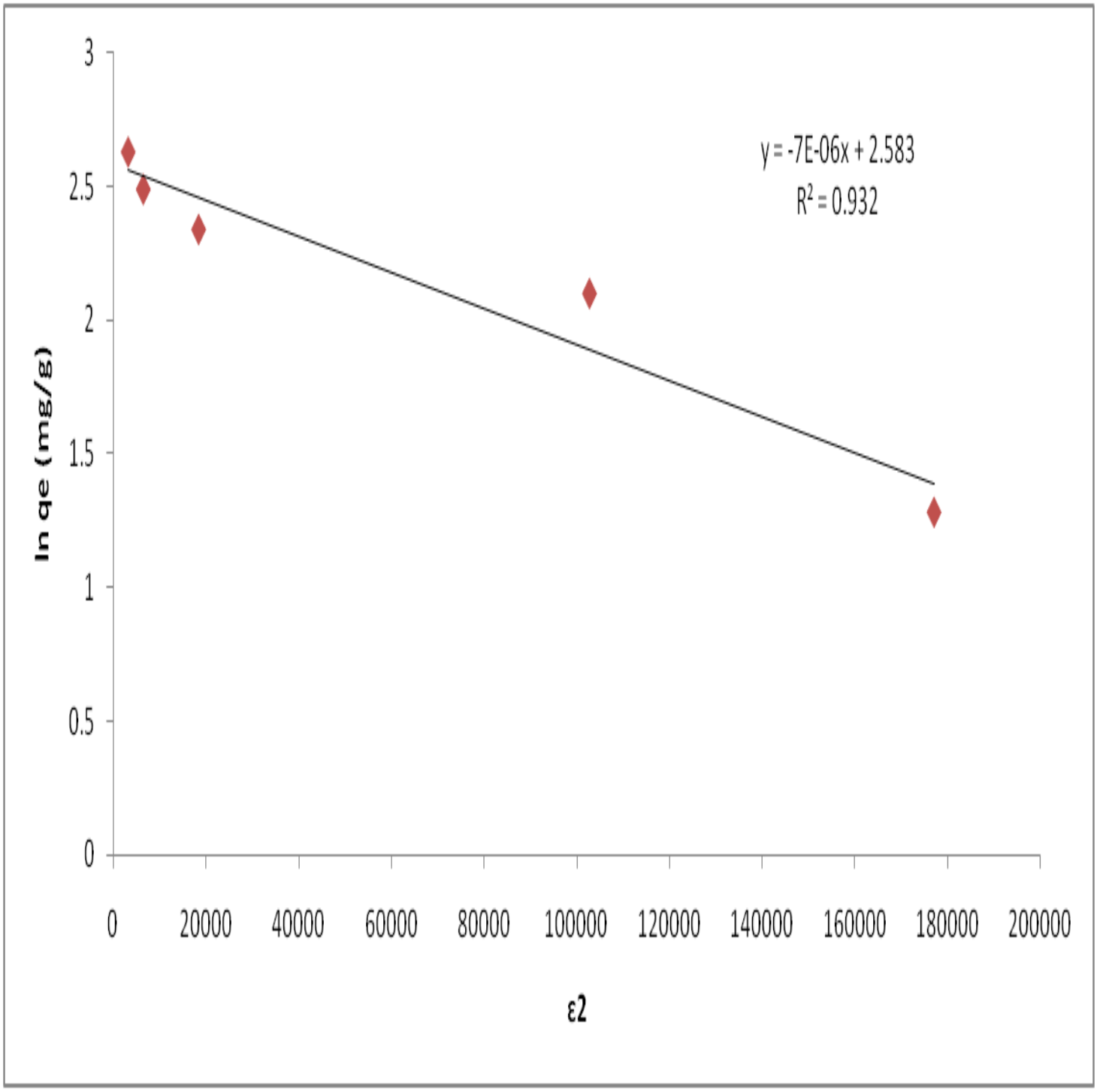


Figure 4.56: D-R Isotherm for AR1 Adsorption on TKP at 308 K

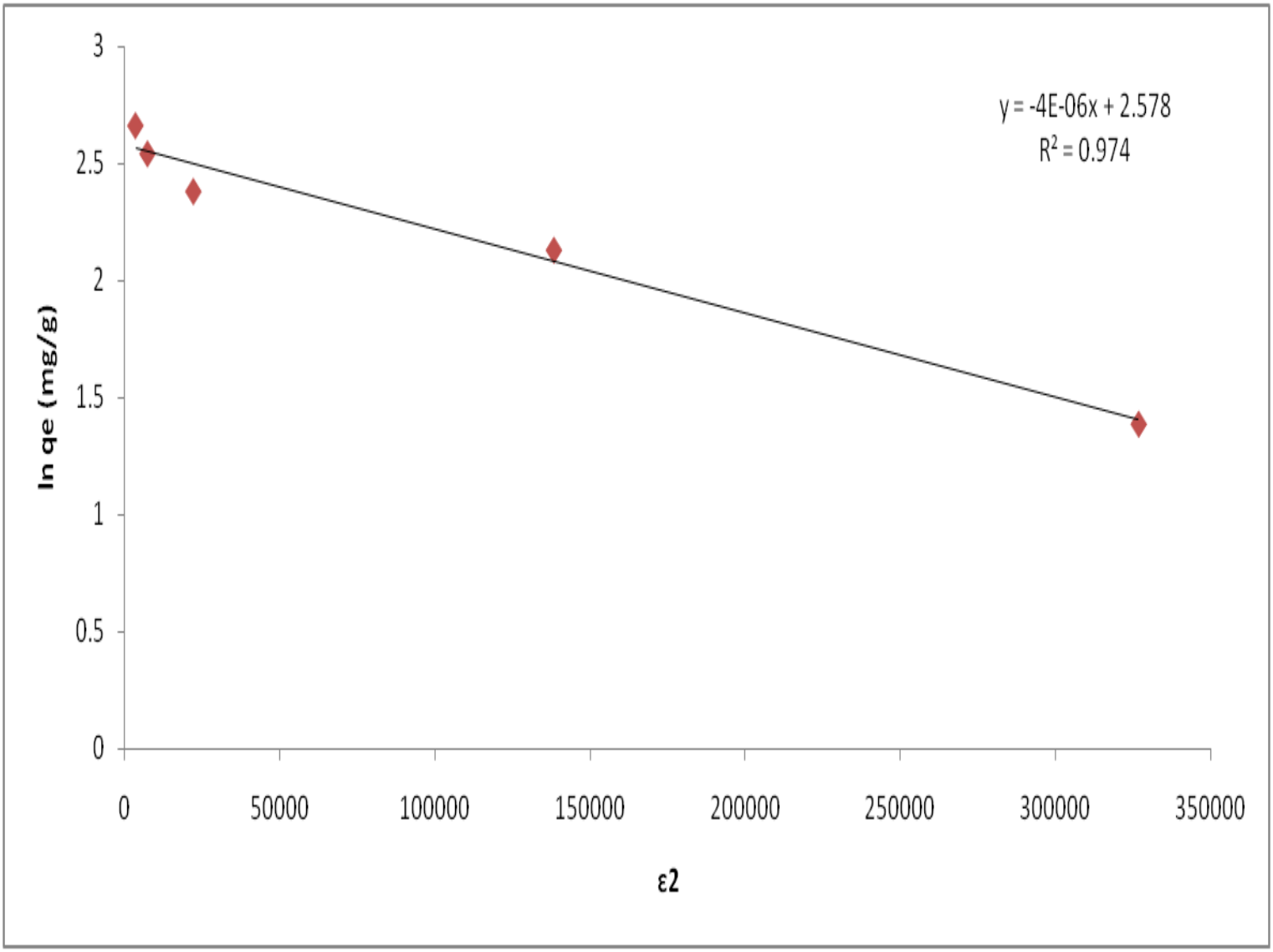


Figure 4.57: D-R Isotherm for AR1 Adsorption on TKP at 318 K

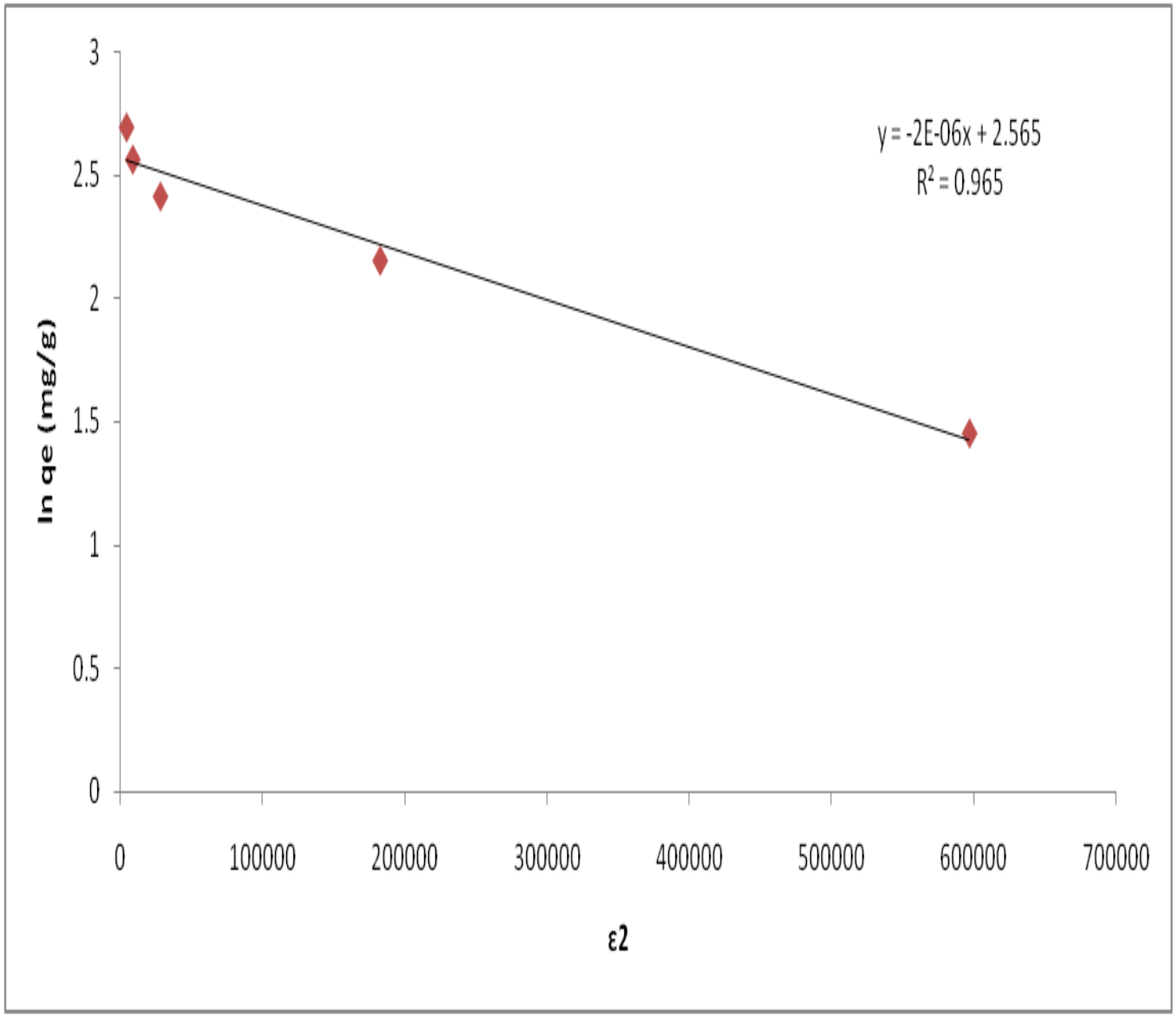


Figure 4.58: D-R Isotherm for AR1 Adsorption on TKP at 323 K

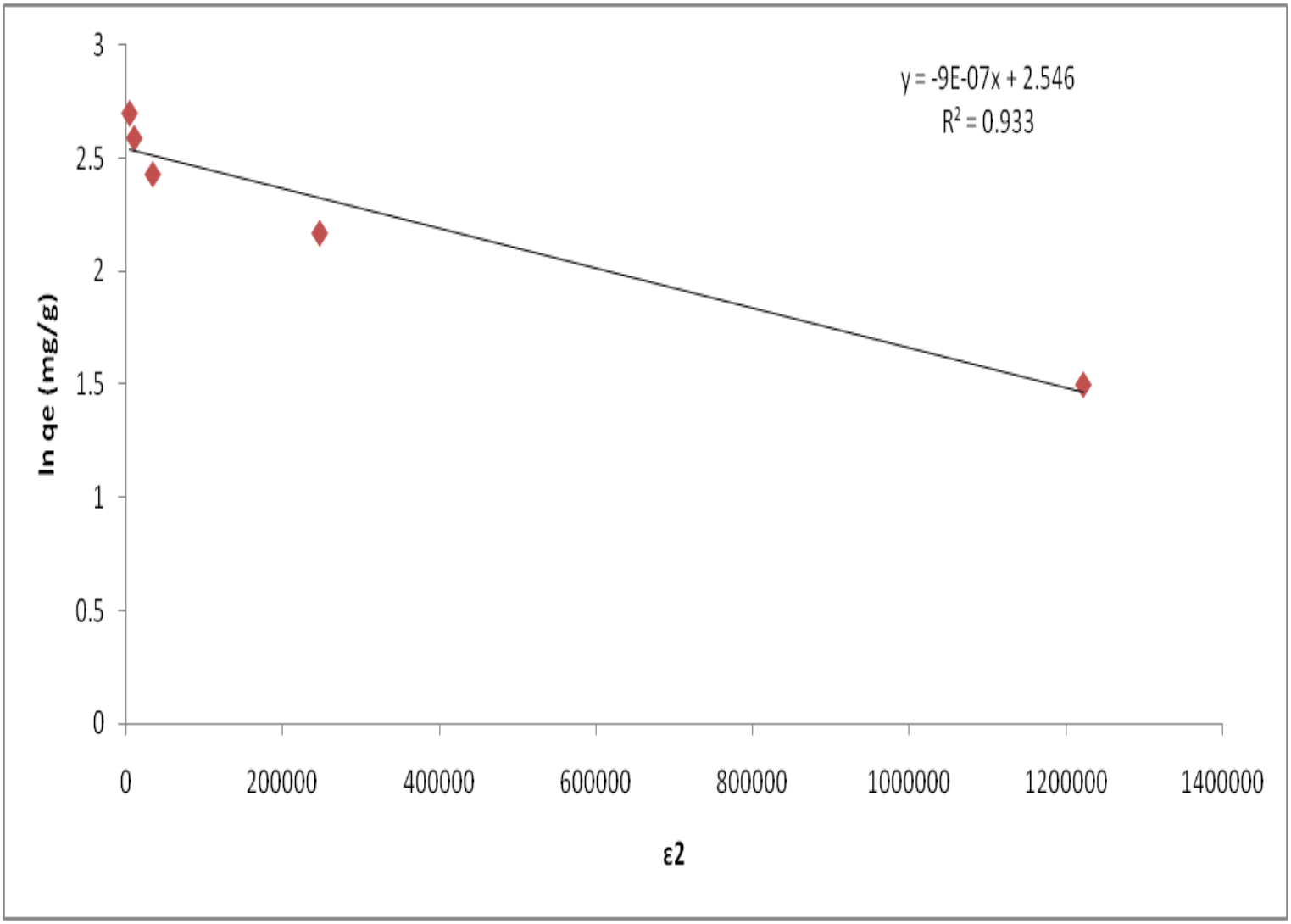


Figure 4.59: D-R Isotherm for AR1 Adsorption on TKP at 328 K

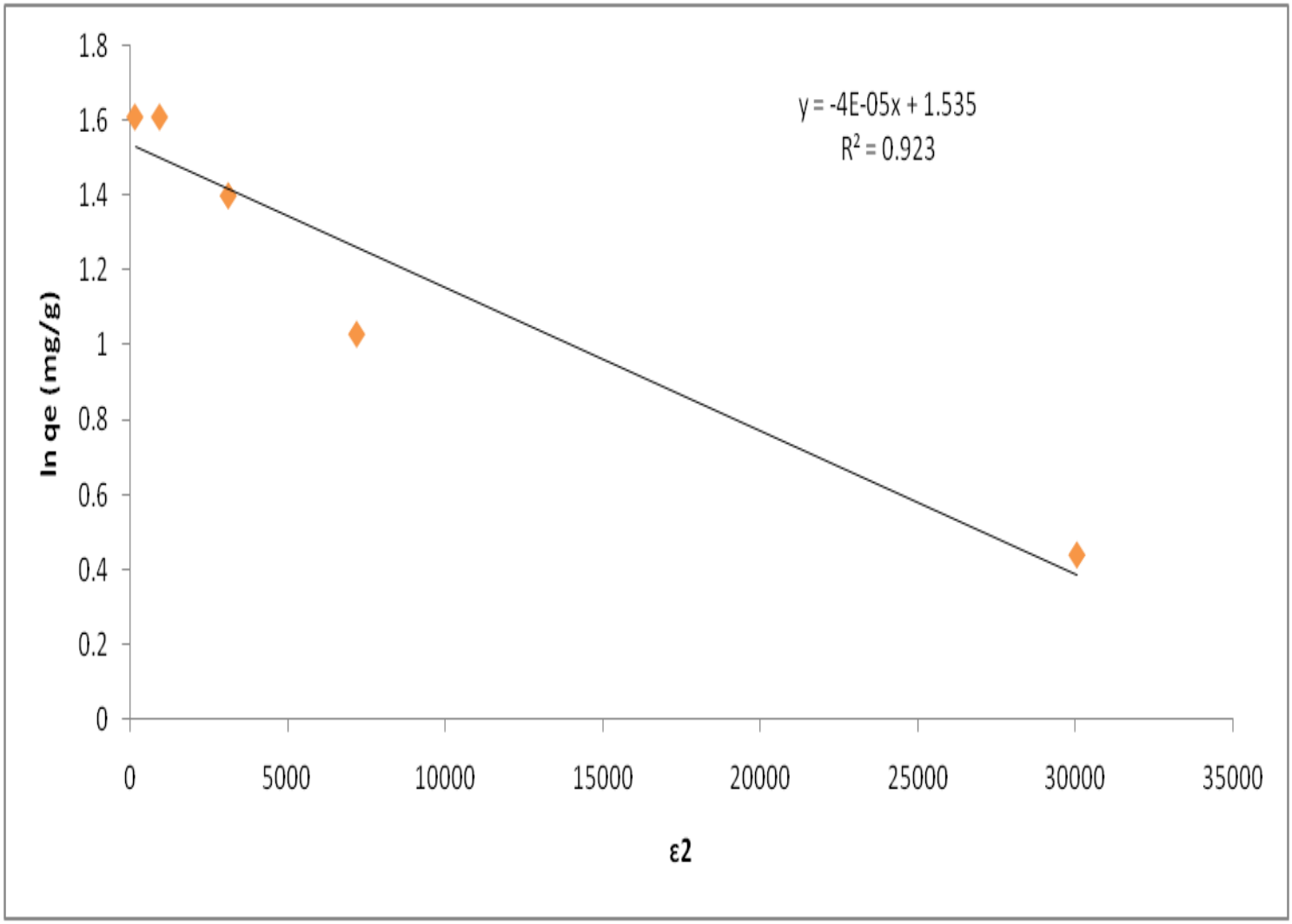


Figure 4.60: D-R Isotherm for RO20 Adsorption on TKP at 298 K

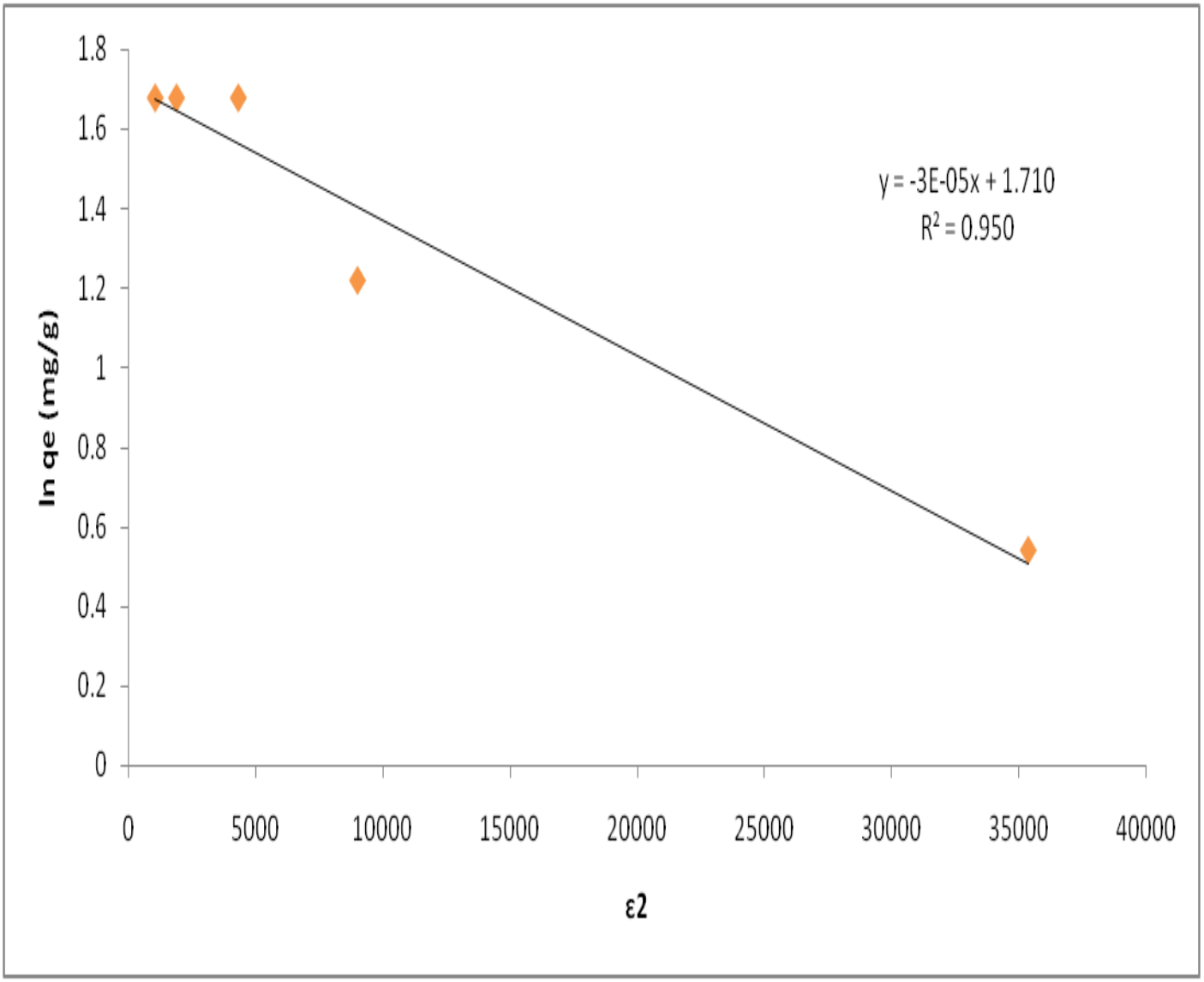


Figure 4.61: D-R Isotherm for RO20 Adsorption on TKP at 308 K

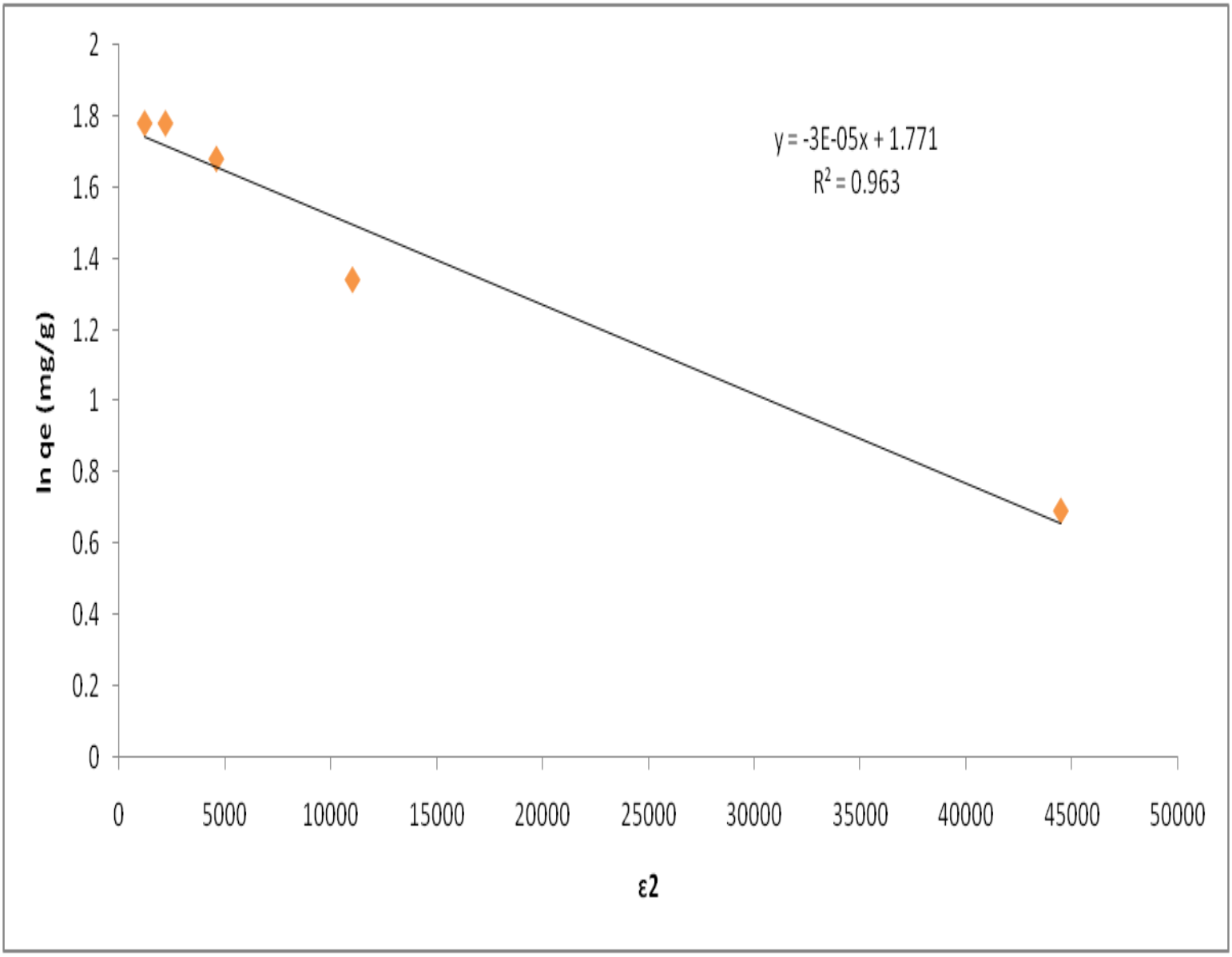


Figure 4.62: D-R Isotherm for RO20 Adsorption on TKP at 318 K

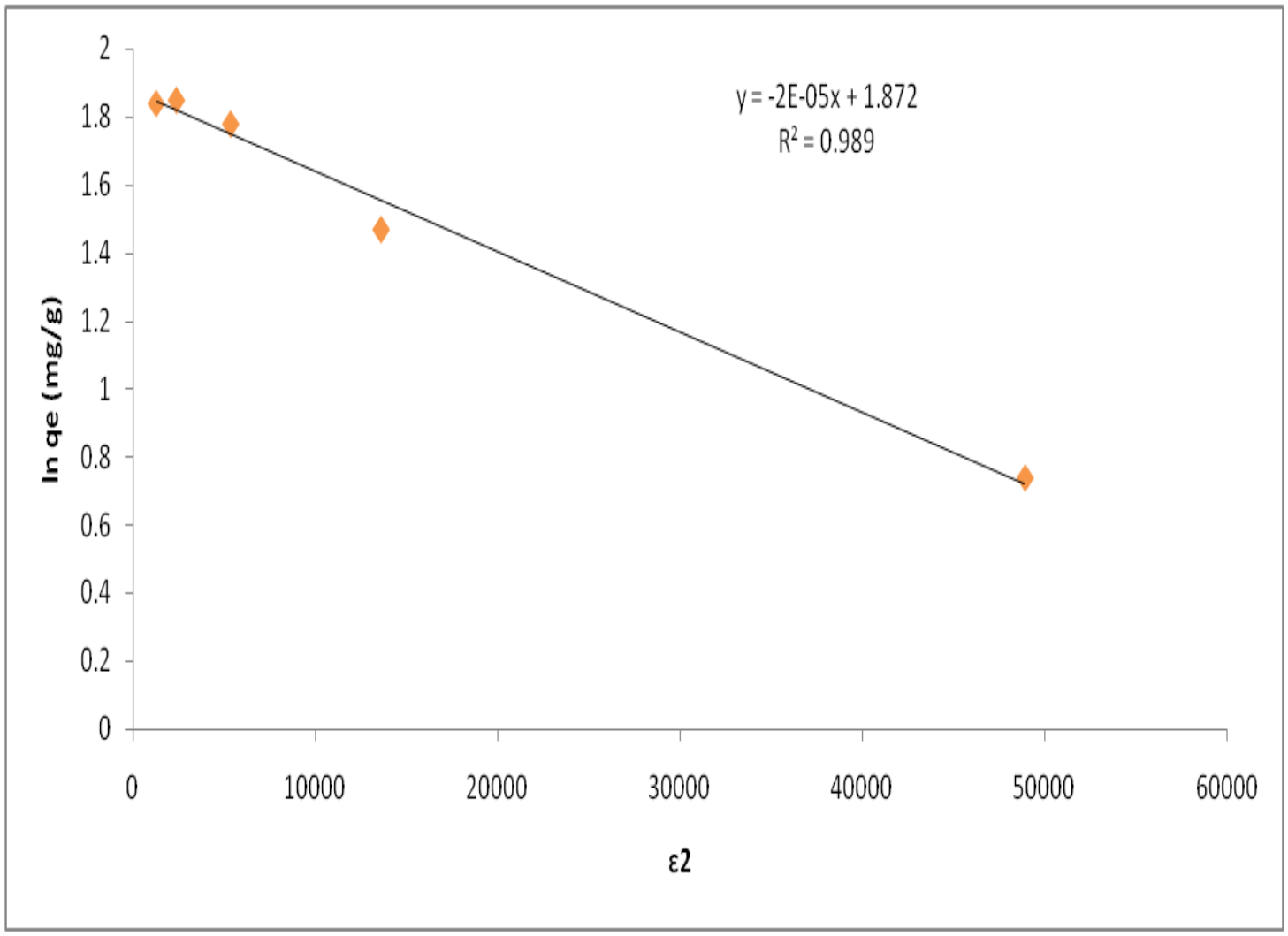


Figure 4.63: D-R Isotherm for RO20 Adsorption on TKP at 323 K

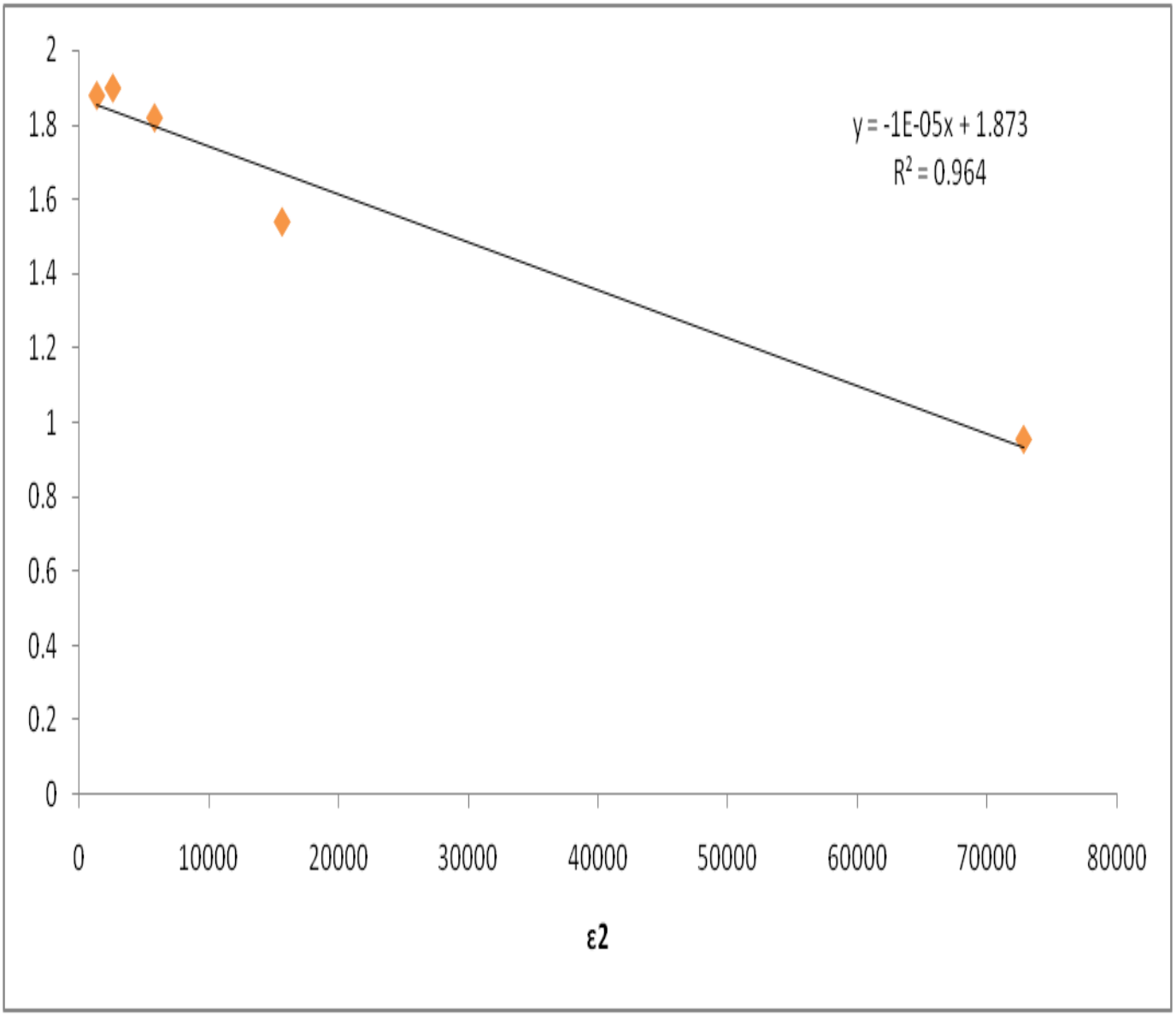


Figure 4.64: D-R Isotherm for RO20 Adsorption on TKP at 328 K

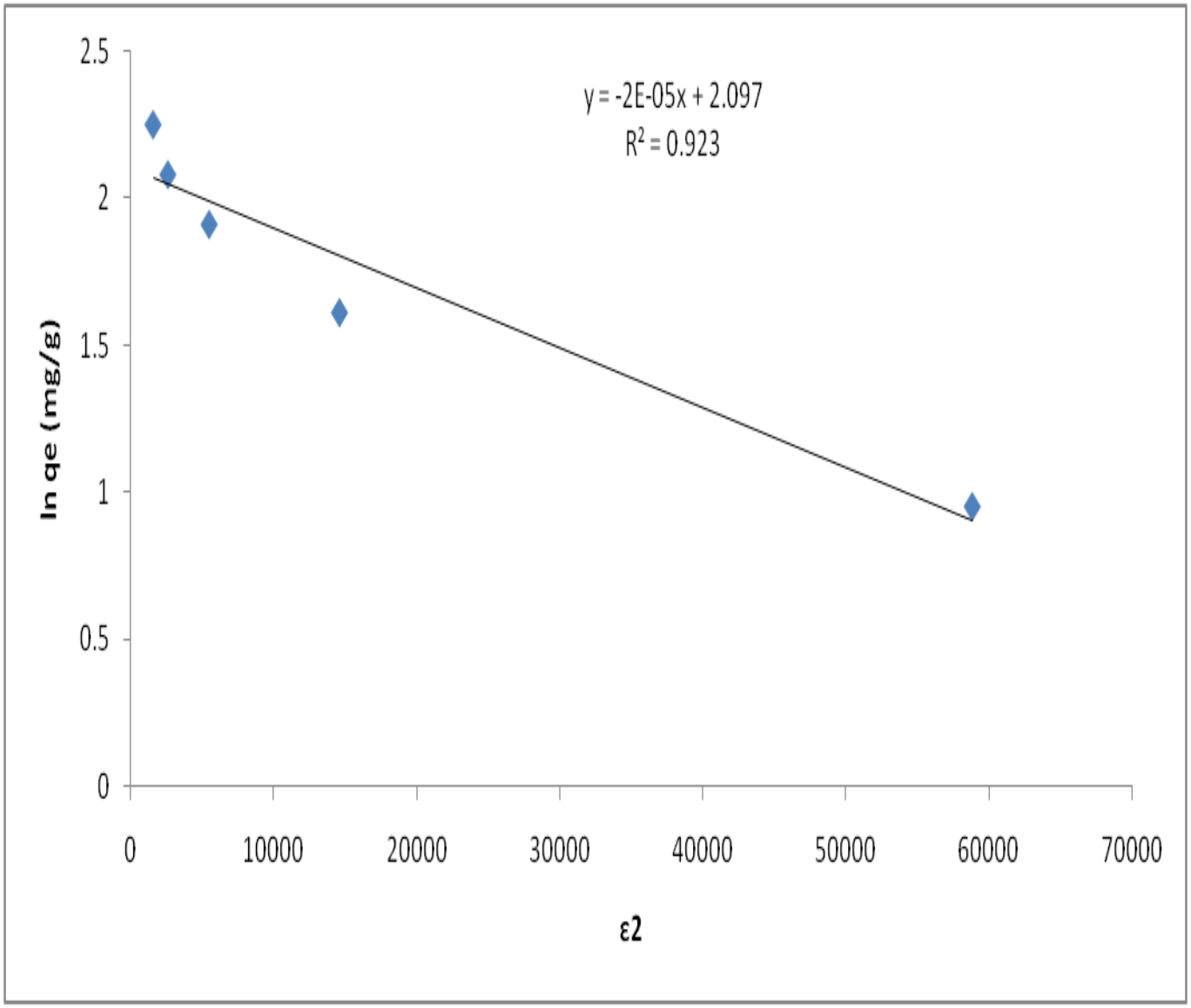


Figure 4.65: D-R Isotherm for RB29 Adsorption on TKP at 298 K

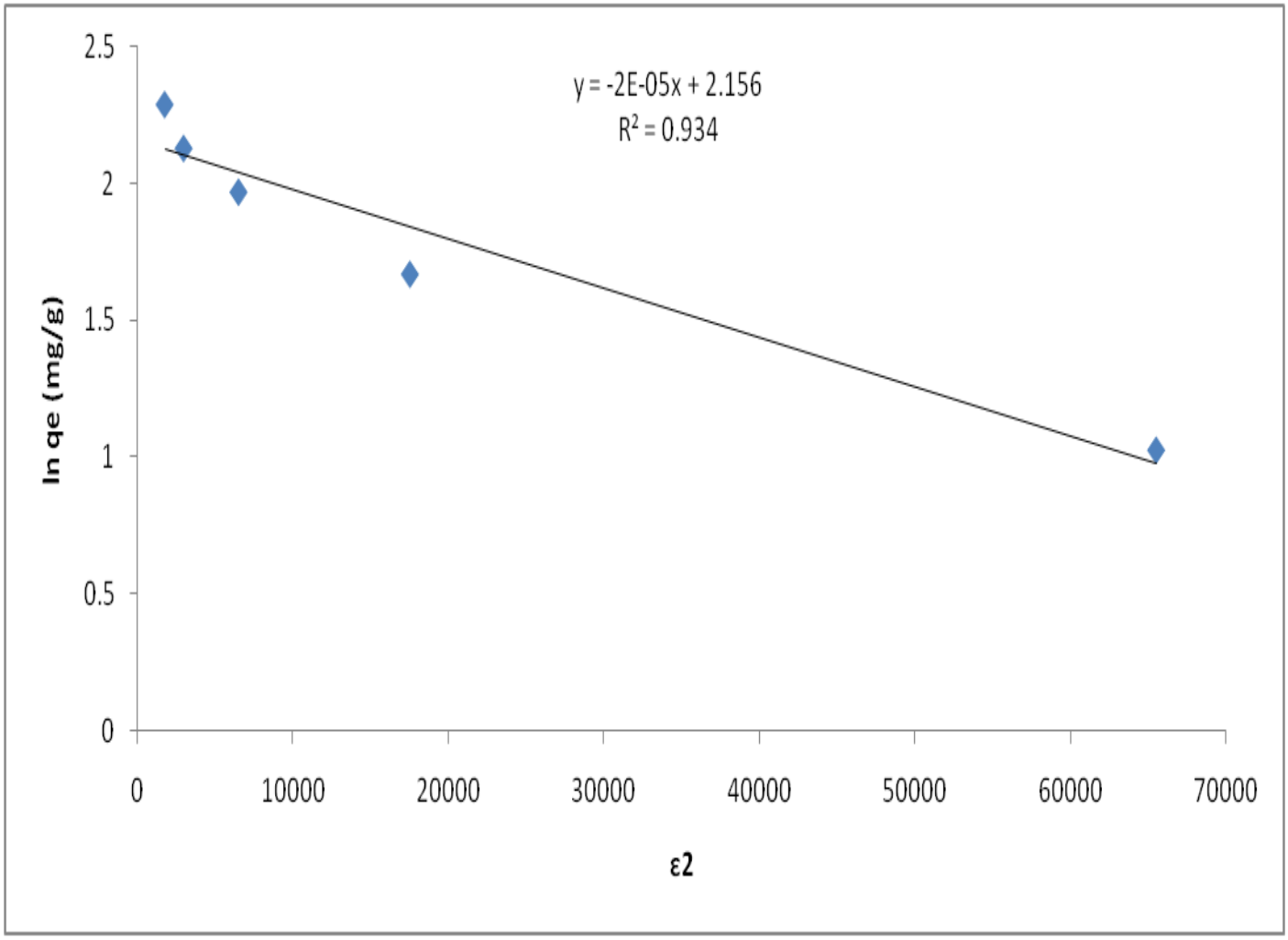


Figure 4.66: D-R Isotherm for RB29 Adsorption on TKP at 308 K

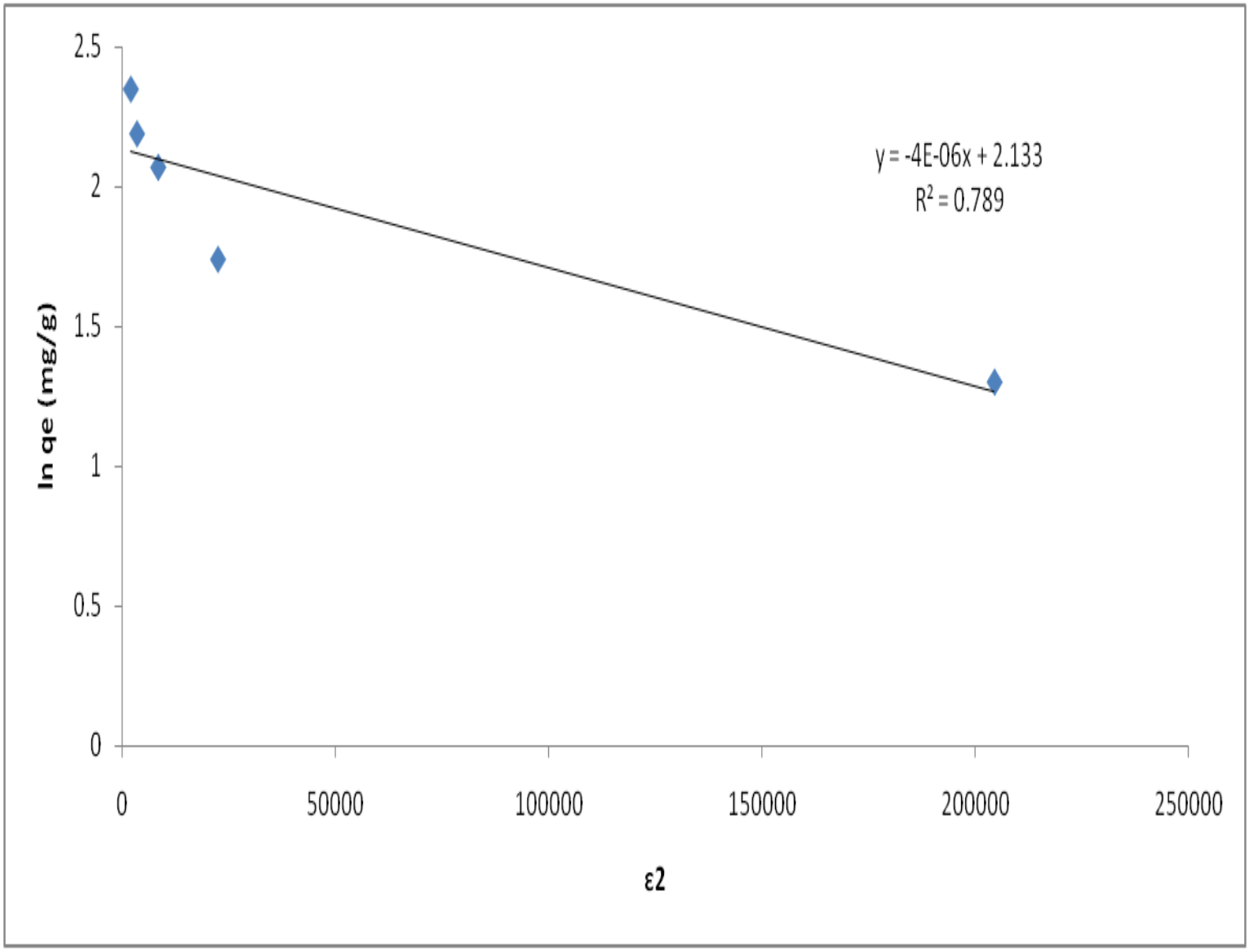


Figure 4.67: D-R Isotherm for RB29 Adsorption on TKP at 318 K

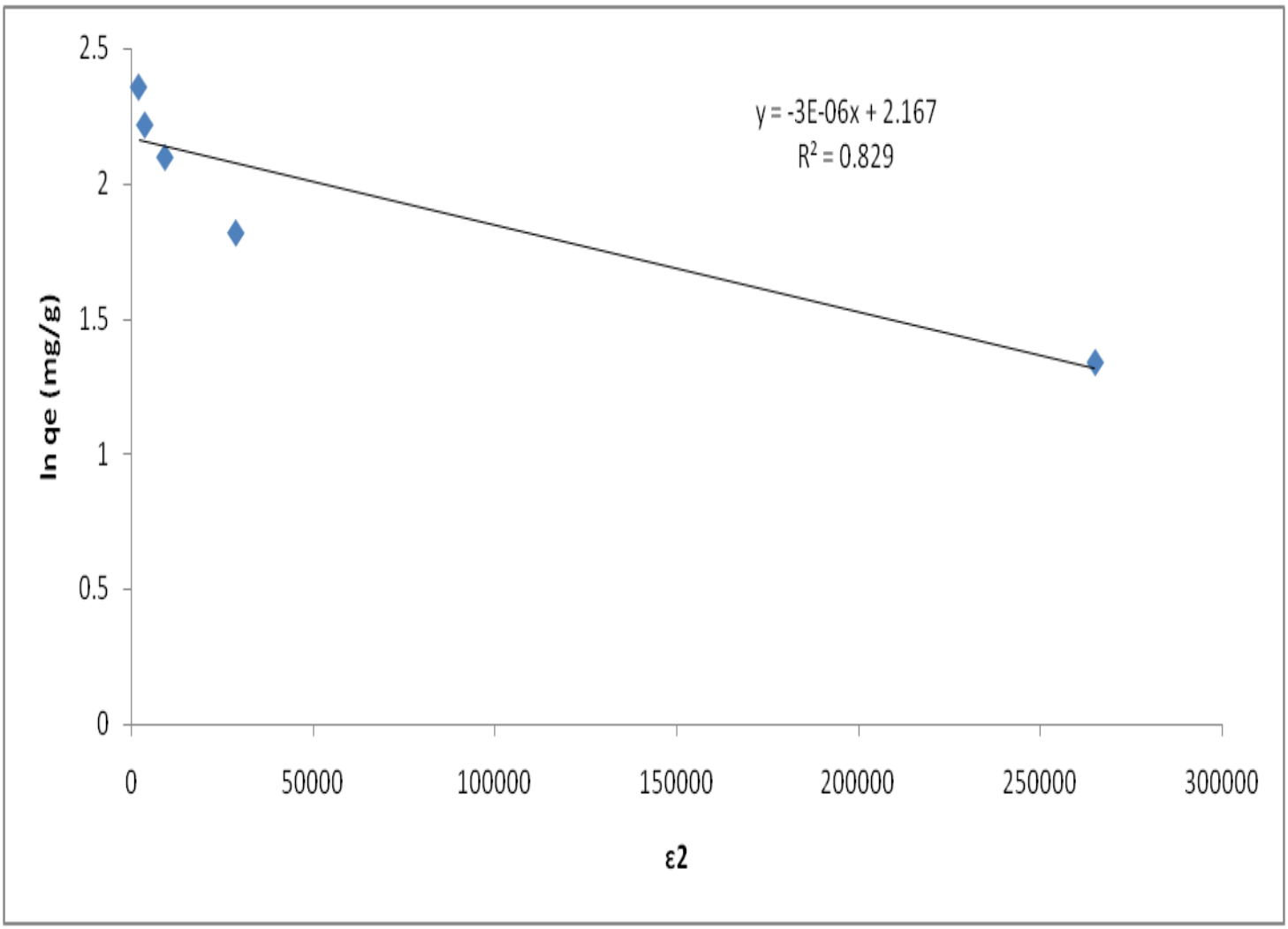


Figure 4.68: D-R Isotherm for RB29 Adsorption on TKP at 323 K

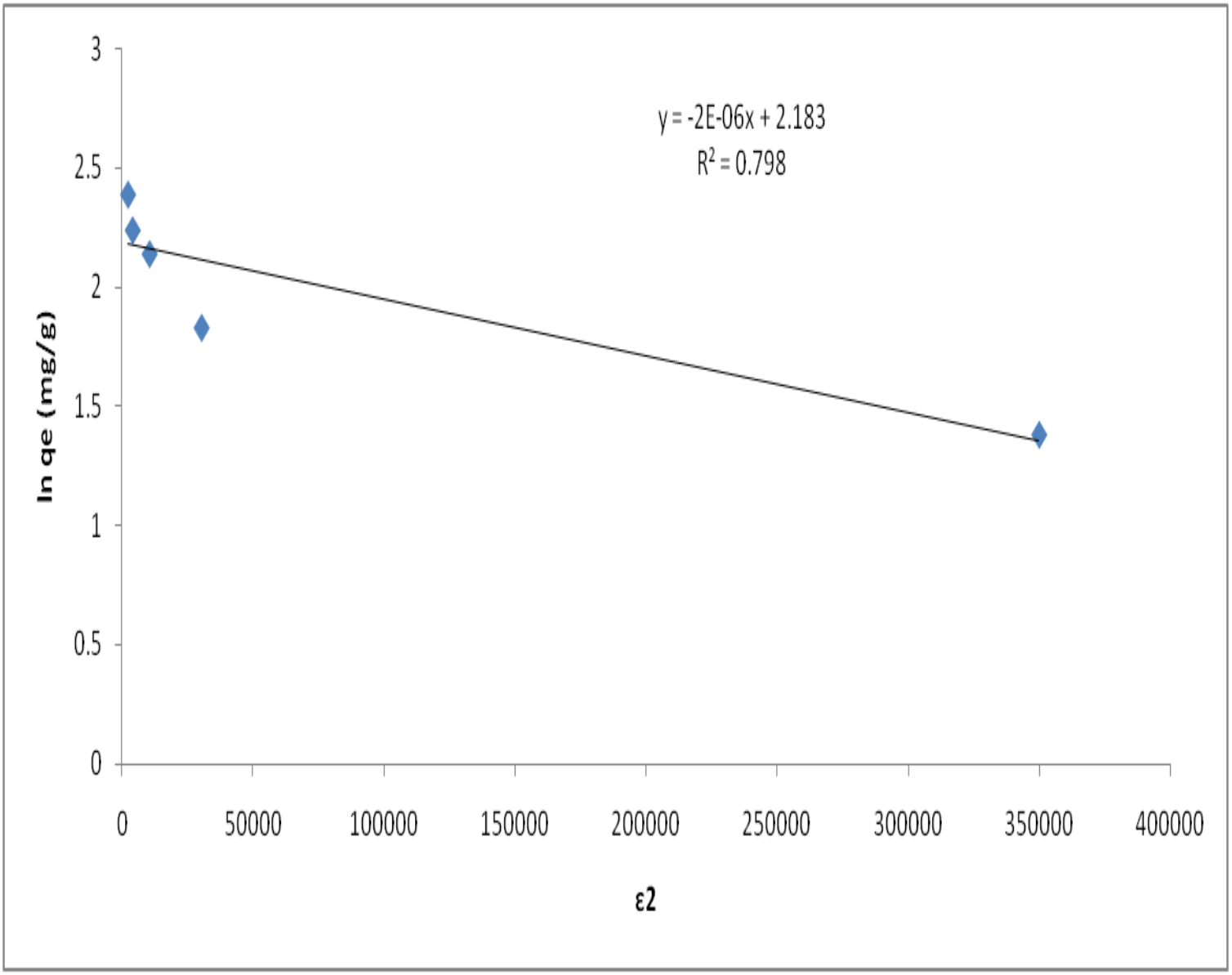


Figure 4.69: D-R Isotherm for RB29 Adsorption on TKP at 328 K

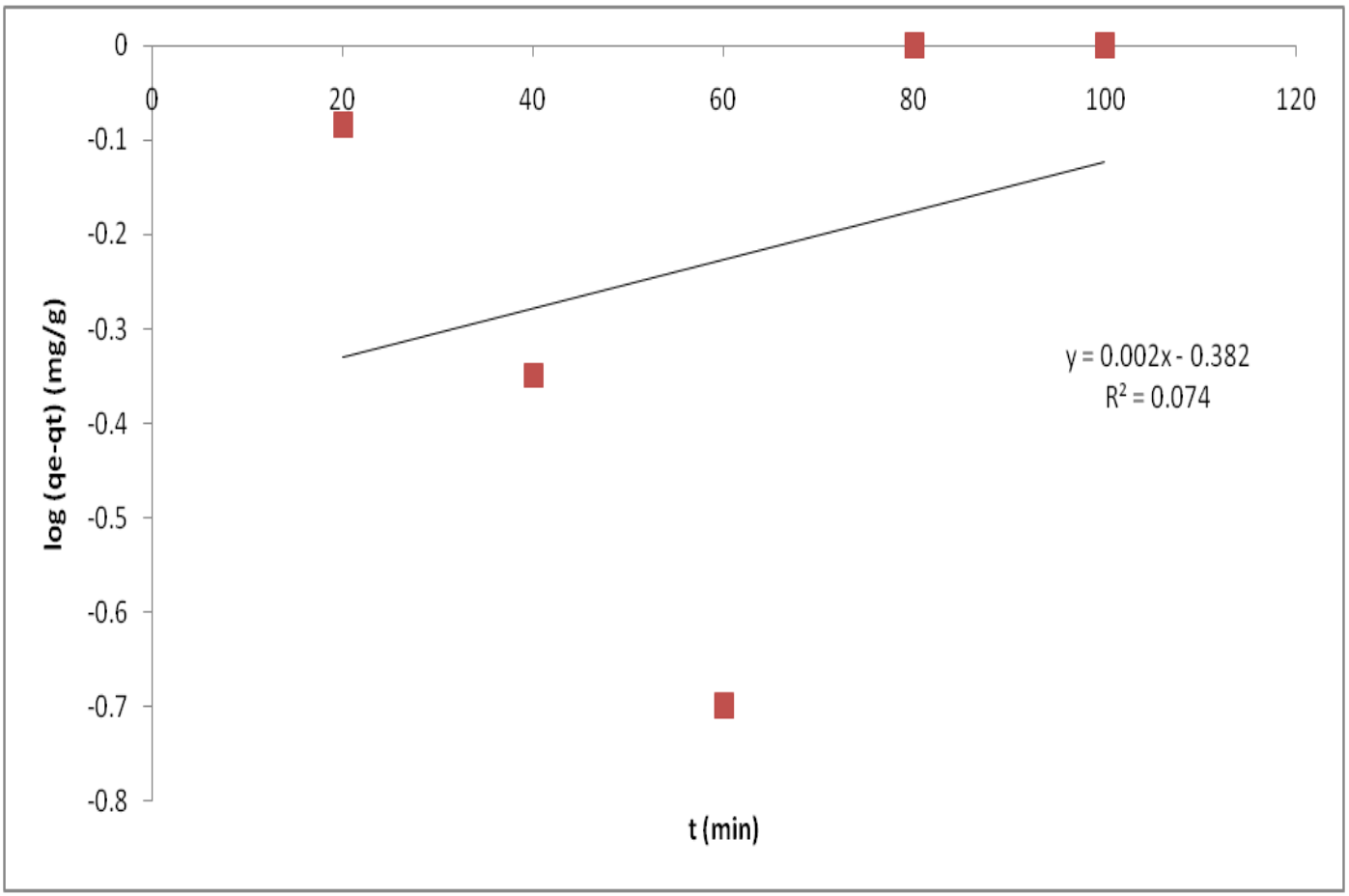


Figure 4.70: Pseudo-First Order Plot for AR1 Adsorption on TKP

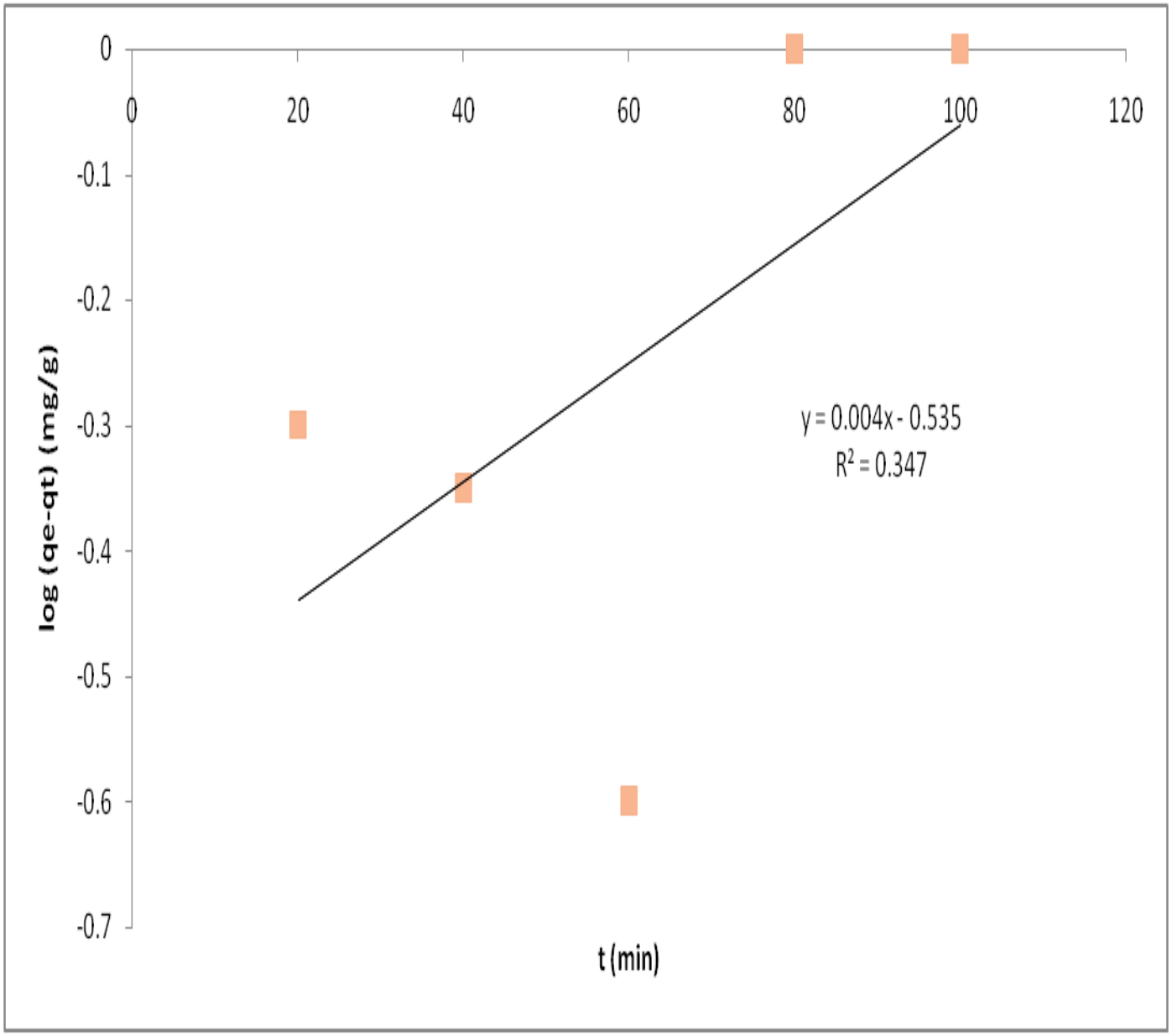


Figure 4.71: Pseudo-First Order Plot for RO20 Adsorption on TKP

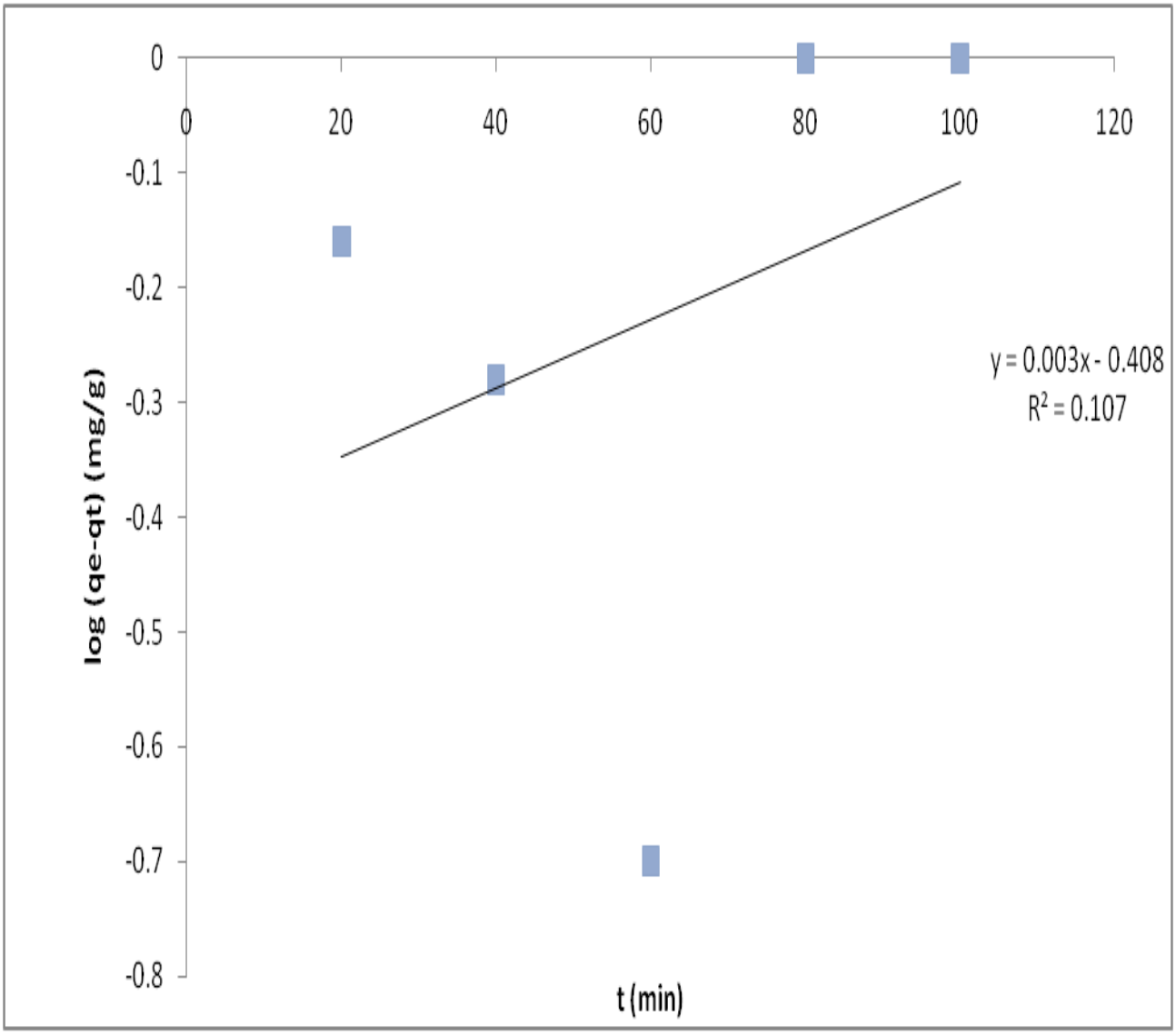


Figure 4.72: Pseudo-First Order Plot for RB29 Adsorption on TKP

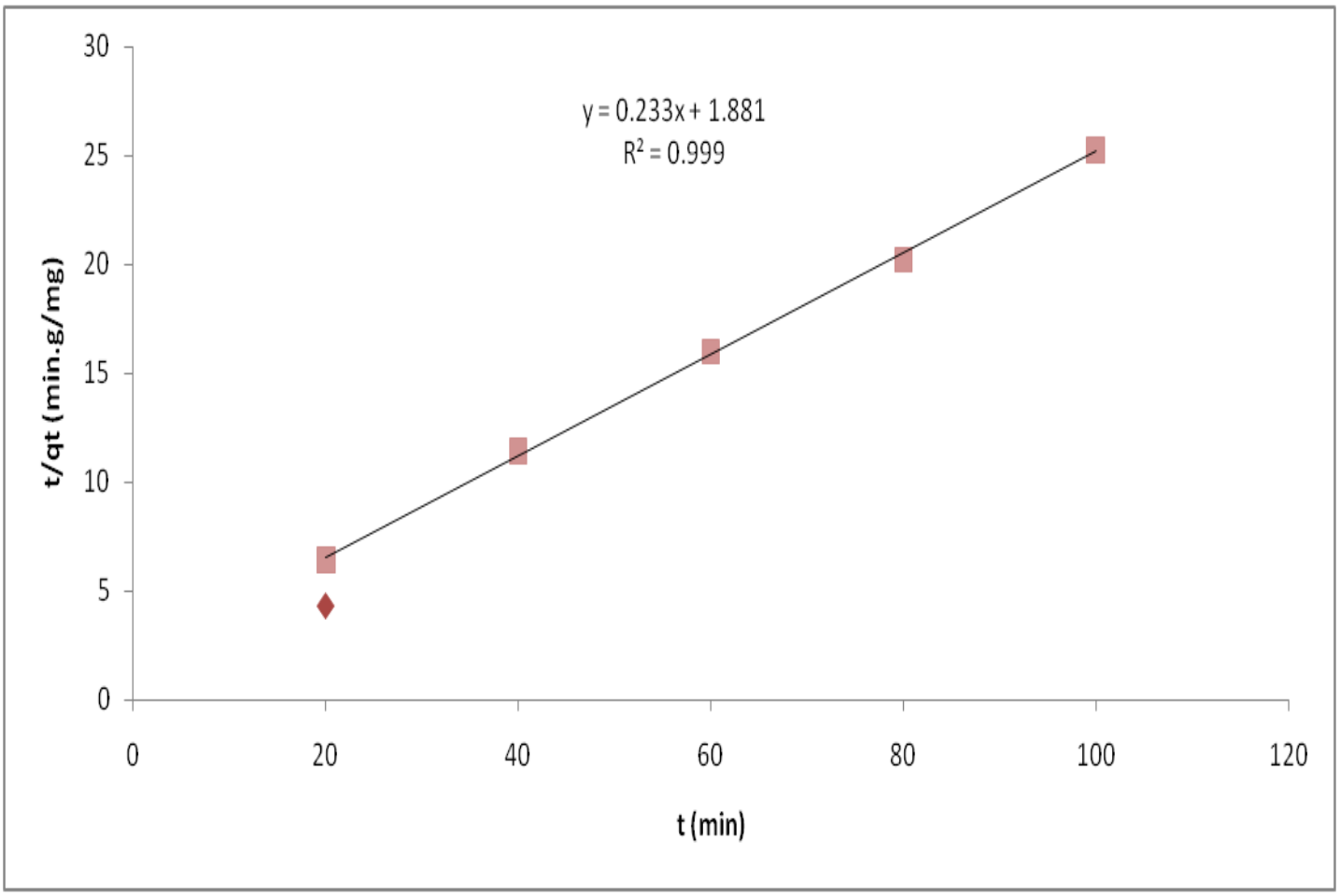


Figure 4.73: Pseudo-Second Order Plot for AR1 Adsorption on TKP

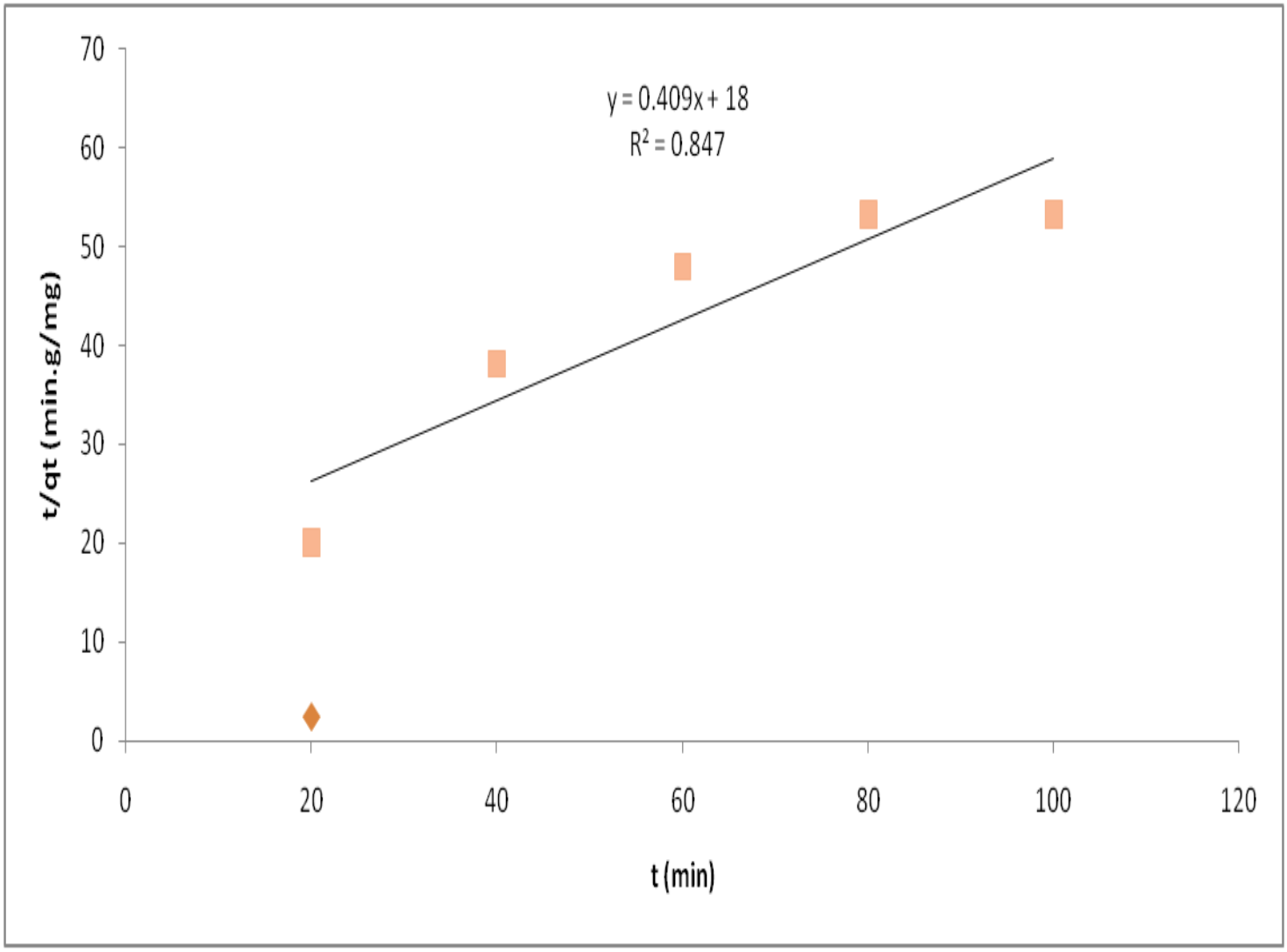


Figure 4.74: Pseudo-Second Order Plot for RO20 Adsorption on TKP

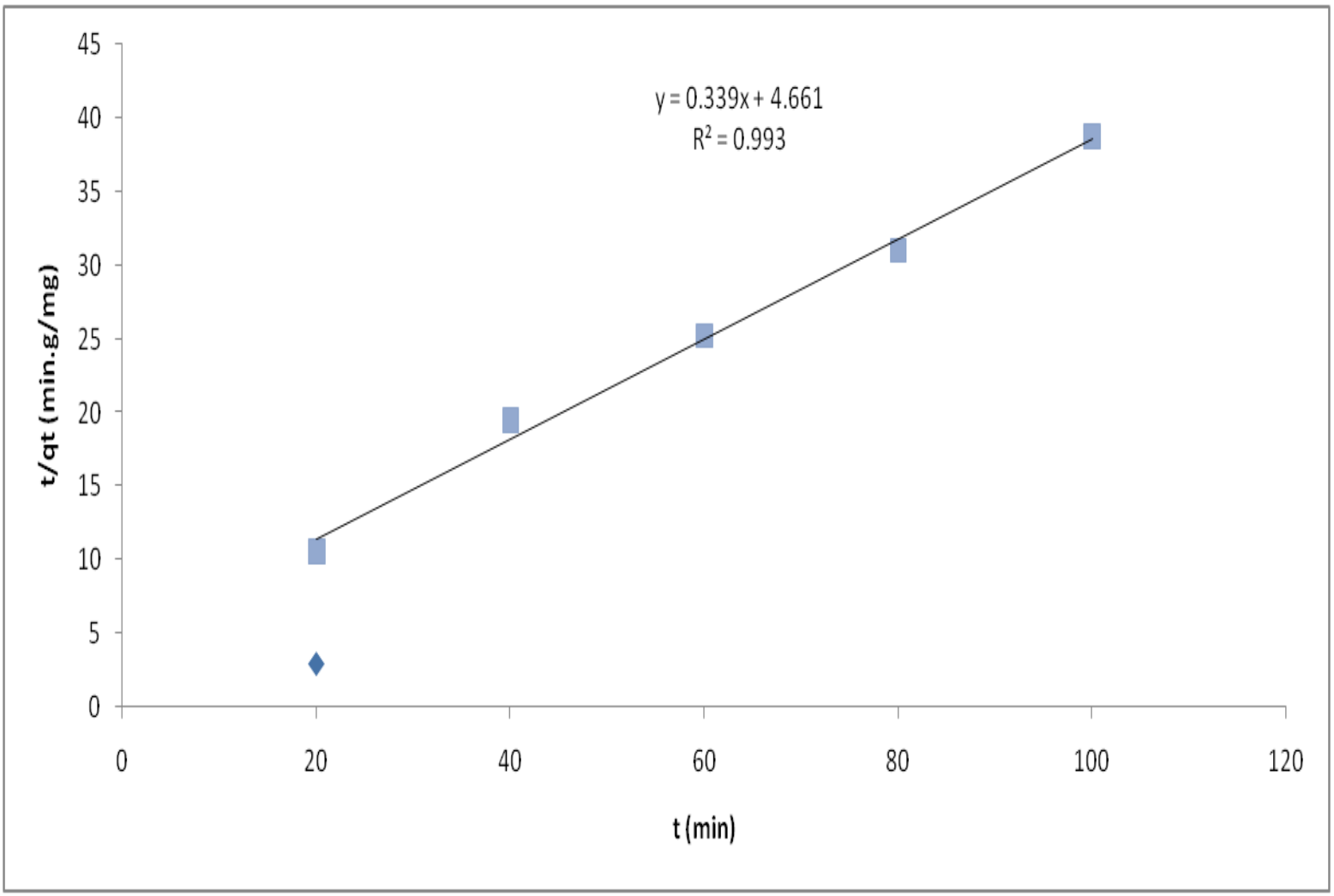


Figure 4.75: Pseudo-Second Order Plot for RB29 Adsorption on TKP

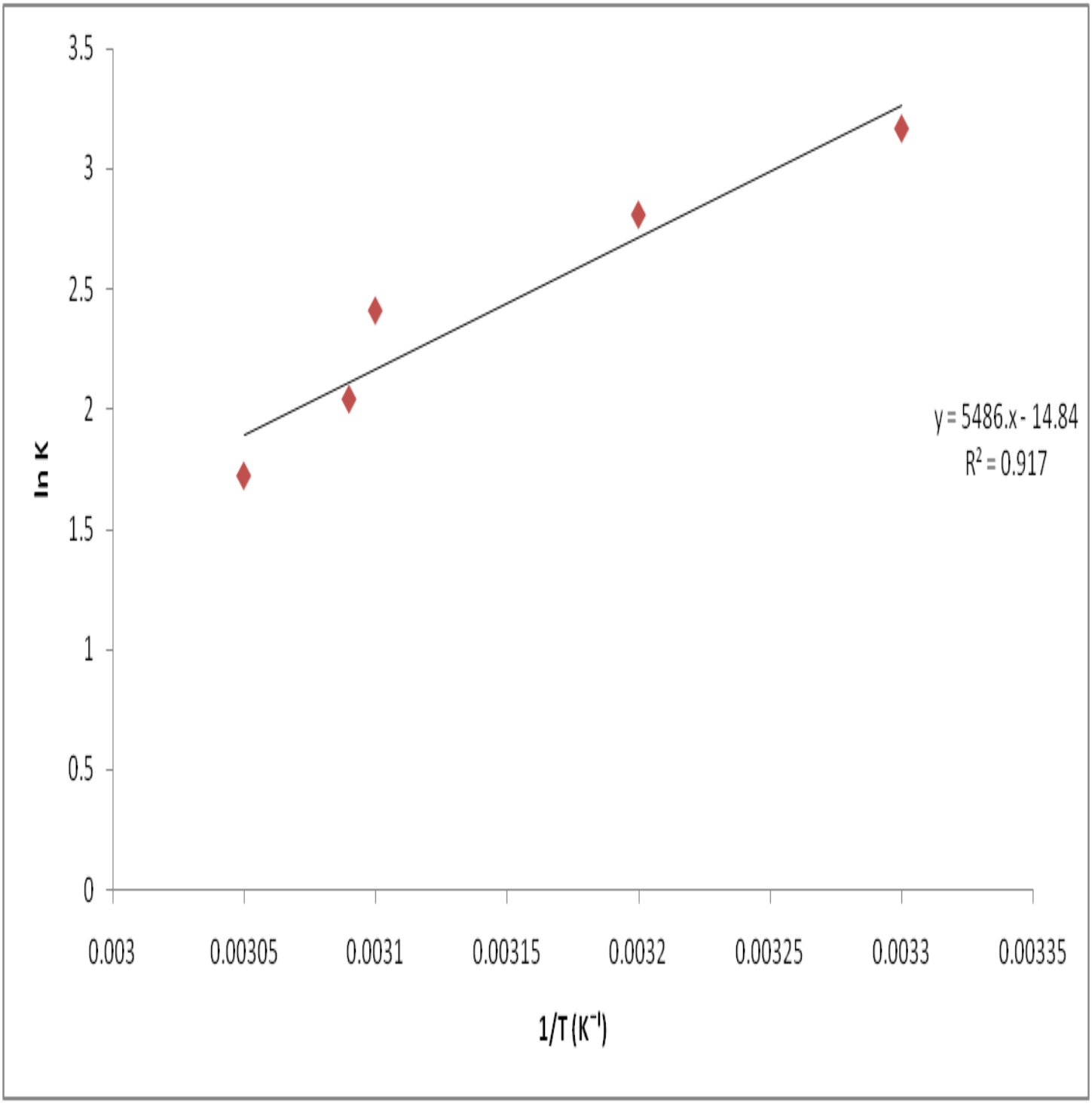


Figure 4.76: Van't Hoff Plot for AR1 Adsorption on TKP

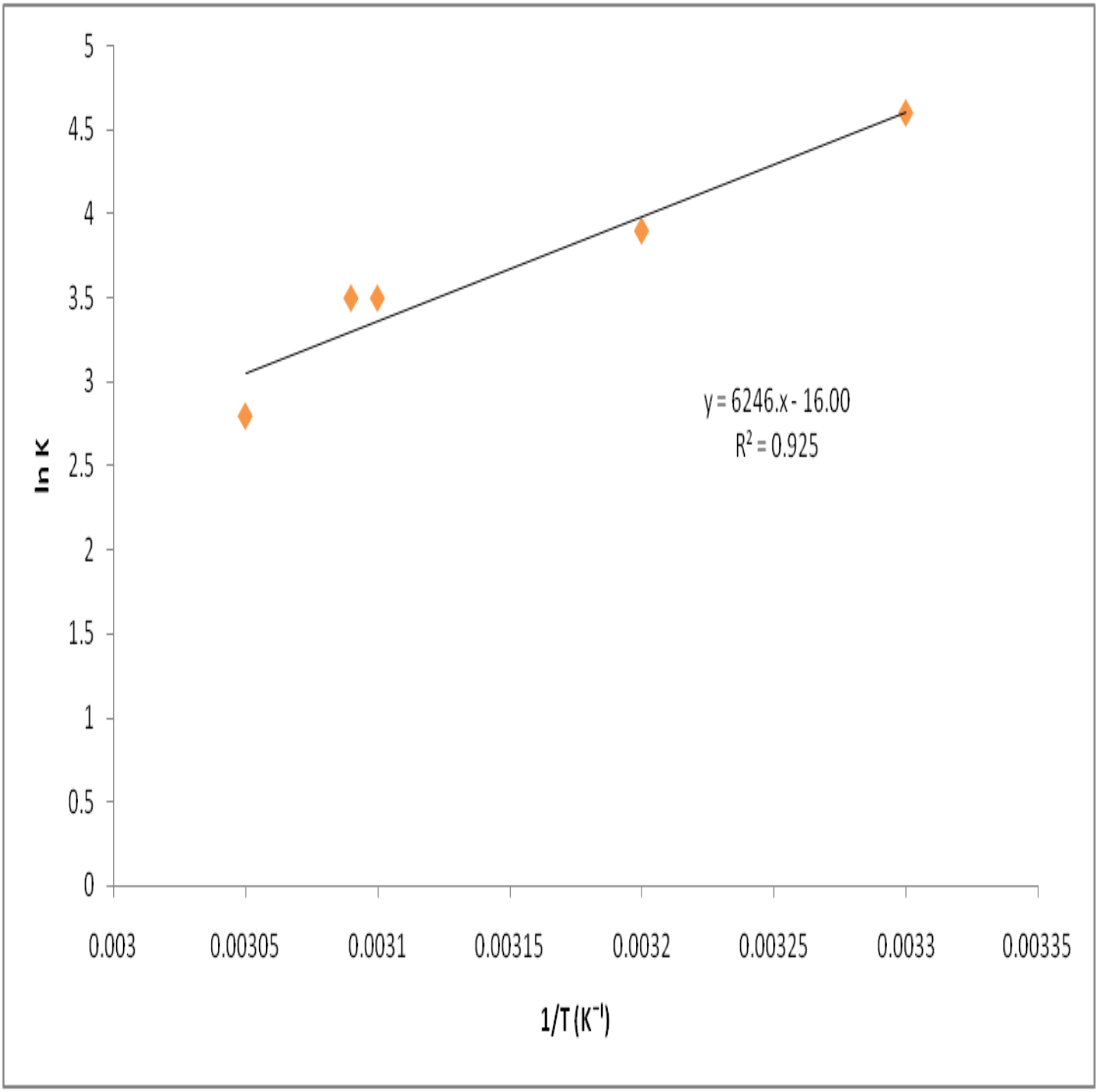


Figure 4.77: Van't Hoff Plot for RO20 Adsorption on TKP

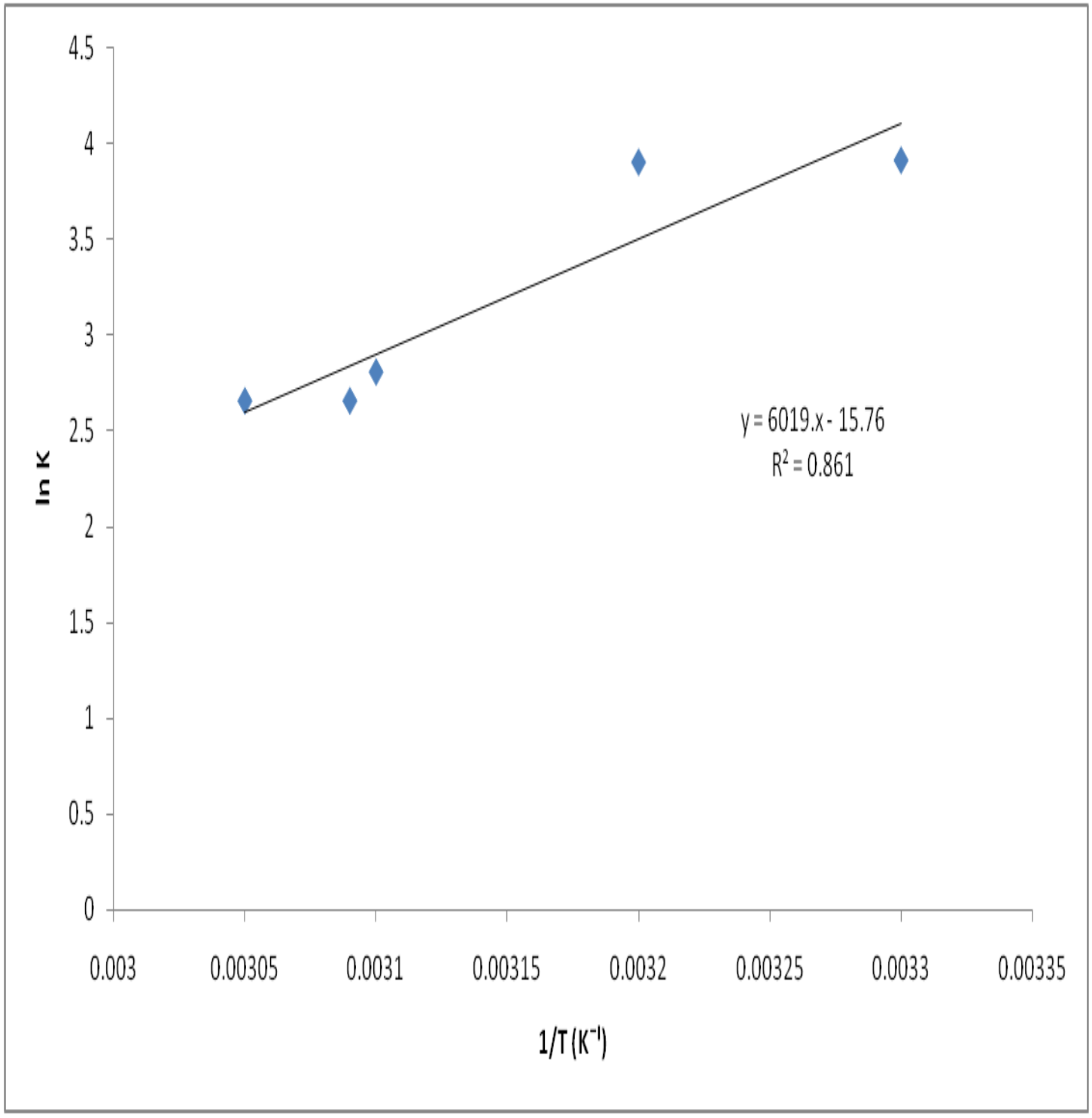


Figure 4.78: Van't Hoff Plot for RB29 Adsorption on TKP

CHAPTER FIVE

DISCUSSION

5.1 Characterization of Activated Tamarind Kernel Powder (ATKP)

5.1.1 Moisture and Dry matter content of ATKP

The moisture content of activated TKP is seen to possess 3.45% of moisture and 96.55% of Dry matter. The percentage of moisture was lower when compared to values obtained from *Khaya senegalensis* fruit (6.17 %), walnut shell (4.18 %), *Delonix regia* (6.286 %), and Locust bean husk (8.20 %) as reported by Gimba *et al.*, (2009); Abechi, (2006); Ocholi, (2006); and Oladunni *et al.*, (2012) respectively. It was also lower than that obtained from *Euphorbia antiquorum* (7.56 %) Rice husk (6.62 %) reported by Palanisamy and Sivakumar (2009) and Malik (2003) respectively. The low moistureand high dry matter content of the ATKP indicates that the adsorbent is an excellent material for adsorption processes.

5.1.2 Bulk Density of TKP

The bulk density of activated tamarind kernel powder (Table 4.1) was found to be 0.4g/cm^3 which showed some variation with that reported by Oladunni *et al*., (0.49 g/cm^3) for locust bean husk, 0.26 g/cm^3 for saw dust of *Dalbergia sisso* (Shakirullah *et al*., 2006); 0.81 g/cm^3 for *Khaya senegalensis* fruits (Gimba *et al*., 2009); 1.1034 g/cm^3 for walnut shell (Abechi, 2006); 0.563 g/cm^3 for *Delonix regia* pods (Ocholi, 2006); 0.73 g/cm^3 for rice husk carbon (Malik, 2003); 0.48 g/cm^3 for *Euphorbia antiquorum* (Palanisamy and Sivakumar, 2009); 0.28 g/cm^3 for *Enteromorpha prolifera* (Sun and Yang 2003); and 0.5494 g/cm^3 for mosambi peel (Ladhe *et al*., 2011).Abram (1973) reported that the bulk density of an adsorbent determines to a very large extent the length of itsfiltration cycle. Okiemmen*et al*., (2008) also reported that bulk density is an important parameter as far as the investigation into the filterability of an adsorbent is concerned because it determines the amount of adsorbent that can be contained in a filter of a given solid's capacity and the amount of treated liquid that

can be retained by the filter cake. Oladunni *et al*., (2012) also reported that when the bulk density of an adsorbent is high, greater volume activity is provided which is an indication of better adsorbent quality.

5.1.3 Ash Content of ATKP

The percentage ash content of the activated tamarind kernel powder (Table 4.1) was found to be 5.30%. Thus, the low ash content value indicates that theATKP has low inorganic content and high fixed carbon. 2.08 % was reported for Cornelian cherry, 2.21 % for Apricot stone and 2.14 % for Almond shells by Erhan *et al*., (2004); 23.0 % was reported for Mosambi peel by Ladhe *et al*., (2011); 3.72 % for *Enteromorpha prolifera* by Deshuai *et al*., (2013); 6.5 % for saw dust carbon and 45.97 % for Rice husk carbon by Malik (2003); 13.4 % for *Euphorbia antiquorum L* by Palanisamy and Savikumar (2009); 2.58 % for Wheat shells by Bulut and Aydin (2006) and 3.50 % for locust bean husk by Oladunni *et al*., (2012).

5.1.4 pH of ATKP

The pH of the activated tamarind kernel powder was 6.45 as presented in table 4.1, and this fell within the acceptable pH range for an ideal adsorbent. Dada *et al.*, (2012), reported pH 6.30 for rice husk carbon; pH 7.7 for Mosambi peel by Ladhe *et al*., (2011). Erhan *et al*., (2004); reported pH 6.20, 6.25 and 5.80 for Cornelian cherry, Apricot stone and Almond shell respectively.

5.2 FTIR Analysis of ATKP

Fourier Transform Infrared Spectroscopy (FTIR) study was carried out to study and identify the functional groups present in the adsorbents ranging from 650cm^{-1} to 4000cm^{-1}. The adsorption capacity or potential of an adsorbent depends upon its porosity as well as the chemical reactivity of the functional groups at the adsorbent surface (Suresh, 2013). The spectra showing the functional groups and their peaks on the activated tamarind kernel powder and dyetreated activated tamarind kernel powder are presented in Figures 4.1 – 4.4.

Furthermore, the results presented in Tables 4.2-4.5 show the presence of Phosphates (P-O-C), (-C=C-Stretch alkenyl), (-C=C-Stretch conjugated), alkanes (C-H stretch), alkenes (=C-H stretch), alkynes (-C≡C-), carboxylic acids (O-H bend), aromatic amines (C-N), nitrites (C≡N stretch), aromatics (C-H stretch), alkyl halides, (C-O Stretch, Primary alcohol) etc. An observed shift in the wave number of dominant peaks associated with the spectra indicatesthe various functional groups activities on the activated tamarind kernel powder surface as reported by Okoli *et al*., (2015). These activities have been characterized by the interaction between the functional groups on the surface of the adsorbent and the functional groups in the dye molecule. A shift from 3261.4 cm^{-1} on the ATKP spectrum (O-H stretch, carboxylic acid) to 3257.7 cm^{-1} on RB29 spectrum signifying an O-H (broad) stretch H-bonded, Hydroxyl group and 3343.4 cm^{-1} on the RO20 spectrum signifying O-H stretch H-bonded hydroxyl group. A shift from 2922.2 cm^{-1} on the ATKP and RO20 spectra signifying H-C-H stretch alkanes to 2926.4 cm^{-1} on the AR1 and RB29 spectra indicating methyl C-H asymmetric/symmetric stretch. A shift from 2109.7 cm^{-1} on the ATKP and RB29 spectra indicating - C≡C – stretch alkynes to 2113.4 cm^{-1} on the AR1and RO20 spectra indicating methyl C-H asymmetric/symmetric stretch. A shift from 1699.7 cm^{-1} on ATKP and AR1 spectra indicating the presence of -C=C-stretch alkenyl to 1703.4 cm^{-1} on RB29 and RO20 spectra indicating the presence of aromatic combination bands. A shift from 1606.5 cm^{-1} on ATKP, AR1 and RB29 spectra indicating the presence of an aromatic ring stretch/quinone or conjugated ketone/open chain azo/primary amine, NH bend/secondary amine NH bend to 1617.7 cm^{-1} on RO20 spectrum indicating the presence of an open chain azo. A shift from 1237.5 cm^{-1} on ATKP spectrum indicating the presence of C-N stretch aromatic amines to 1241.2 cm^{-1} on ARI, RB29 and RO20 spectra indicating the presence aromatic ethers, Aryl-O stretch or aromatic phosphates (P-O-C stretch). The presence of hydroxyl groups, carbonyl groups, ethers, and aromatic compounds is an evidence of the lingo-cellulosic structure of

tamarind kernel powder which was also observed in other materials such as coconut shell (Andre *et al*., 2011) and cotton stalks (El-Hendawy *et al*., 2008; In: Okoli *et al*., 2015).

5.3 Adsorption Studies

5.3.1 Effect of pH on the Adsorption Process

pH controls the degree of ionization and speciation of the adsorbate (in this case the dye solutions) as such it is regarded as an important parameter in adsorption studies. Initial solution pH determines the surface charge of the adsorbent and the degree of ionization and speciation of the adsorbate (Deshuai *et al*., 2013), which in turn affects its adsorption on the adsorbent material. Moreover,the adsorption of other ions depends to a very large extent the adsorption of hydrogen (H^+) and hydroxyl ion (OH^-).The effect of pH on the adsorption of dye unto activated tamarind kernel powder was studied between the ranges of 2-10. The percentages of dye adsorbed as presented in table 4.2.1, were between the range of 95.00% to 61.00% for Acid Red 1dye, 80.00% to 9.00% for Reactive Orange 20 dye and 85.00% to 20.00% for Reactive Blue 29 dye. The result showed that the amount (%) of AR1, RO20 and RB29 dyes adsorbed decreased with increase in the pH value of all three dyes (Figure 4.5). This indicates that a low pH was favourable for the adsorption of AR1, RO20, and RB29 by the adsorbent, due to the anionic nature of AR1, RO20 and RB29 dyes. This phenomenon is as a result of the increase in the number of positively charged sites due to a decrease in the number of negatively charged sites resulting from a decrease in the pH of the system. These in effect made the adsorption of the negatively charged dye anions favourable due to electrostatic attraction. Similar outcomes were reported by Singh *et al*. (2011) and Okoli *et al*.,(2015).

5.3.2 Effect of Adsorbent Dosage on the Adsorption Process

The resultsobtained from this experiment indicated that as the adsorbent dosage increased (from 0.4g to 1.2g), the percentage of dye adsorbed increased also from 65.0 % to 86.5% for AR1, 40.0% to 64.0% for RO20 and 40.0% to 54.0% for RB29. The percentage of adsorption increased up to 1.0g of adsorbent after which no significant changes in the percentages of dye was adsorbed with an increasing amount of the adsorbent. Joseph and Philomena, (2011) reported that for every given initial concentration of an adsorbate, the adsorbent dosage determines the capacity of an adsorbent. Okoli *et al.*, (2015) also reported that the increase in adsorption efficiency is as result of the increased number of adsorption sites and surface. However, from the experiment, it was observed that equilibrium was attained after 1.0 g of adsorbent was used for the analysis. This confirmed what was reported by Okoli *et al.,* (2015) where it was stated that "most of the adsorbents studied attained equilibrium around 1.0g of dosage" but further increase in the adsorbent dose resulted in the reduction in the amount of dye removed from the solution. This resulted from the overlapping of the adsorption sites as a result of overcrowding of the highest adsorbent dosage which has imposed a screening effect on the dense outer layer of the cells, thereby shielding the binding site from the dyes (Pons and Fuste, 1993; In: Oladunni, 2012).

5.3.3 Effect of Contact Time

The effect of batch contact time on the percentage removal of dye was investigated. It was observed that the percentage removal of dye increases rapidly with an increase in contact time initially, and thereafter, beyond a contact time of about 80 min, no noticeable change in the percentage removal was observed. When the contact time was increased from 20 min to 100 min the percentage dye removal increased from 62.5% to 79.0% for AR1, 20.0% to 30.0% for RO20 and 37.5% to 51.5% for RB29. Therefore, the optimum contact time is considered to be 80 min. This is also taken as the equilibrium time of the batch adsorption

experiment, since beyond a contact time of 80 min;the rate of adsorption is not affected. From the results, a rapid removal of dye at the beginning of the contact time was observed; this is due to the presence of large number of binding sites available for adsorption and also due to the initial concentration gradients between the adsorbate in solution and the number of vacant sites available on the TKP surface at the beginning (Oladunni, 2012). The progressive increase in adsorption and consequently the attainment of equilibrium adsorption may be due to limited mass transfer of the molecules from the bulk liquid to the external surface of the adsorbent as reported by Oladunni, (2012). At this time, the adsorption mainly occurred on the surface of the adsorbent. Furthermore, the slow removal rate is due to the saturation of the binding sites by the dye molecules as reported by Papita *et al.*, (2010).

5.3.4 Effect of Initial Dye Concentration

Okoli *et al.,* (2015) reported that the percentage of dye removal is dependent upon the initial concentration. Adsorption of ARI, RO20 and RB29 dyes usinginitial concentrationsof 20, 40, 60, 80 and 100 mg/l each of AR1, RO20 and RB29at constant adsorbent dose and pH were investigated at different operating temperatures.

The initial concentration of adsorbate plays an important role, as a given mass of adsorbent can adsorb only a certain amount of a solute. As presented in Figure 4.2.4 the % removal of the dyes depreciated with increase in initial dye concentration i.e. from 76.0% to 54.0% for Acid Red 1, 31.0% to 20.0% for Reactive Orange 20 and then 51.5% to 38.0% for Reactive Blue 29. The result indicated that the more the concentration of the solution, the smaller the percentage of dye that a given mass of adsorbent can adsorb as reported by Okoli *et al.,* (2015). In a low concentration range, the fractional adsorption is higher compared to the high concentration range. This is due to the fact that at lower concentrations, the amount of available adsorption sites are more, while at higher concentrations, the available sites become less. The adsorption sites take the available dye molecules more rapidly at lower

concentrations while at higher concentrations the molecules are required to diffuse to the adsorbent surface by intra particle diffusion (Bhatti*et al*., 2006; Saradhi *et al.*, 2010 In: Oladunni, 2012). Thus, the percentage of dye removal was dependent upon the initial concentration. However, similar cases have been observed and reported by Himanshu and Vashi (2010).

5.3.5 Adsorption Isotherm Modelling

The adsorption isotherm data revealed that the amount of dye adsorbed increased with increasing equilibrium concentration of dyes. However, the adsorption reached a maximum capacity due to nearly complete coverage of the active sites at high dye concentrations. For solid-liquid system, adsorption isotherm is important in the description of adsorption behavior (Sun and Yang 2003). In this work, Freundlich, Langmuir, Temkin and Dubinin-Radushkevich isotherm were evaluated.

5.3.5.1 Langmuir Isotherm

The monolayer coverage of the adsorbate on anadsorbent surface at a constant temperature is represented by the Langmuir isotherm. The basic assumption is that the forces exerted by chemically unsaturated surface atoms do not extend further than the diameter of one adsorbed molecule. The Langmuir isotherm hints towards surface homogeneity (Oladoja *et al*., 2008). Langmuir constants b and q_m represent the adsorption equilibrium constant and the maximum adsorption capacity, respectively. A straight line graph with slope of $1/q_m$ and intercept b was obtained when C_e/q_e was plotted against C_e. Figures 4.9 – 4.13 represent the Langmuir adsorption isotherm models for Acid Red 1 at a temperature range of 298K to 328K respectively. From the figures it could be seen that the plotsare linear and the correlation coefficient (R^2) values were found to be 0.859, 0.917, 0.978, 0.991, and 0.995at 298K, 308K, 318K, 323K and 328K respectively which indicate that the graphs follow the Langmuir isotherm model. The maximum adsorbate uptake (q_m) for Acid Red 1 were 20.8 (mg/g),

18.87 (mg/g), 17.86 (mg/g), 17.24 (mg/g), 16.67 (mg/g) at 298K, 308K, 318K, 323K and 328K respectively. From the results it could be seen that q_m,which also signifies the number of sites available for adsorption,is decreasingas the temperature increased from 298K to 328K. The constant b relating to the coefficient of affinity of Acid Red 1 to activated tamarind kernel powder at 298K, 308K, 318K, 323K and 328K is 0.04 (l/mg), 0.06 (l/mg), 0.09 (l/mg), 0.13 (l/mg), 0.18 (l/mg) respectively.

Figures 4.14 – 4.18 represent the Langmuir adsorption isotherm models for Reactive Orange 20 at a temperature range of 298K to 328K respectively. From the figures it could be seen that the plots are linear and the correlation coefficient (R^2) values were found to be 0.907, 0.825, 0.930, 0.901, and 0.975 at 298K, 308K, 318K, 323K and 328K respectively which indicate that the graphs follow the Langmuir isotherm model. The maximum adsorbate uptake (q_m) for Reactive Orange 20 were 10.10 (mg/g), 9.01 (mg/g), 9.35 (mg/g), 9.61 (mg/g), and 8.54 (mg/g) at 298K, 308K, 318K, 323K and 328K respectively. From the results it could be seen that q_m decreased as the temperature increased from 298K to 328K. The constant b relating to the coefficient of affinity of Acid Red 1 to activated tamarind kernel powder at 298K, 308K, 318K, 323K and 328K is 0.04 (l/mg), 0.06 (l/mg), 0.09 (l/mg), 0.13 (l/mg), 0.18 (l/mg) respectively.

Figures 4.19 – 4.23 represent the Langmuir adsorption isotherm models for Reactive Blue 29 at a temperature range of 298K to 328K respectively. From the figures it could be seen that the plots are linear and the correlation coefficient (R^2) values were found to be 0.986, 0.989, 0.971, 0.983, and 0.977 at 298K, 308K, 318K, 323K and 328K respectively which indicate that the graphs follow the Langmuir isotherm model. The maximum adsorbate uptake (q_m) for Reactive Blue 29 were 16.67 (mg/g), 16.67 (mg/g), 13.16 (mg/g), 12.82 (mg/g), 12.98 (mg/g) at 298K, 308K, 318K, 323K and 328K respectively. From the results, q_m is seen to decrease as the temperature increased from 298K to 328K. The constant b relating to the

coefficient of affinity of Reactive Blue 29 to activated tamarind kernel powder at 298K, 308K, 318K, 323K and 328K is 0.02 (l/mg), 0.02 (l/mg), 0.06 (l/mg), 0.07 (l/mg), 0.07 (l/mg) respectively.

The decrease in the maximum adsorbate uptake (q_m) might be as a result of an increase in the number of dye molecules migrating from the dye solution to the surface of the adsorbent at increased temperatures. The b values were seen to increase with an increase in the temperature of the system which might be due to an increase in the activity of the dye molecules as they are kinetically energized.

The R_L values issued from this study were ranged from 0.05 to 0.35 for Acid Red 1dye, 0.125 to 0.45 for Reactive Orange 20 dye and 0.11to 0.42 for Reactive Blue 29, while the correlation coefficients (R^2) ranged from 0.825 to 0.995 for Acid Red 1 dye, 0.859 to 0.974 for Reactive Orange 20 dye and 0.971 to 0.989 for Reactive Blue 29 with the increase in temperature from 298K to 328K. The results obtained from separation factor (R_L) calculation showed that adsorption of Acid Red 1, Reactive Orange 20 and Reactive Blue 29 are favourable on activated tamarind kernel powder. Similar results are reported by Himanshu and Vashi (2010), and Okoli *et al*., (2015).

5.3.5.2 Freundlich Isotherm

The Freundlich isotherm is an empirical equation employed to describe heterogeneous systems. It is a most popular model for a single solute system, based on the distribution of solute between the solid phase and aqueous phase at equilibrium (Freundlich, 1928). The Freundlich constants K_f and n corresponding respectively to adsorption capacity of adsorbent and adsorption intensity have been obtained from the intercepts and slopes of the linear plot of $\ln q_e$ against $\ln C_e$as shown in Figures 4.25 – 4.39. The magnitude of adsorption intensity n gives an indication of the favourability of the adsorption process. Ho and Chang, (2001) reported that the favourability of the process is achieved if n lies in the range of 1–10. This

shows that the adsorption of the dyes on the adsorbent followed Freundlich isotherm but not as much as that of the Langmuir equilibrium Isotherm plot where a higher correlation was obtained. However, the results obtained are in line with the findings of Okoli *et al*., (2015).

Figures 4.25 – 4.29 represent the Freundlich adsorption isotherm models for Acid Red 1 at a temperature range of 298K to 328K respectively. From the figures it could be seen that the plots are linear and the correlation coefficient (R^2) values were found to be 0.803, 0.793, 0.863, 0.797, and 0.931 at 298K, 308K, 318K, 323K and 328K respectively which indicate that the graphs follow the Freundlich isotherm model. The adsorption capacity (K_f) of the activated tamarind kernel powder for Acid Red 1 were 1.57 (l/g), 1.98 (l/g), 2.93 (l/g), 3.32 (l/g), and 3.97 (l/g) at 298K, 308K, 318K, 323K and 328K respectively. From the results it could be seen that K_f,which also signifies the adsorption capacity of the adsorbent, is increasing as the temperature increased from 298K to 328K. The constant n relating to the adsorption efficiency of activated tamarind kernel powder for Acid Red 1 at 298K, 308K, 318K, 323K and 328K is 1.73, 1.88, 2.12, 2.27, and 2.66 respectively.

Figures 4.30 – 4.34 represent the Freundlich adsorption isotherm models for Reactive Orange 20 at a temperature range of 298K to 328K respectively. From the figures it could be seen that the plots are linear and the correlation coefficient (R^2) values were found to be 0.964, 0.860, 0.915, 0.856, and 0.898 at 298K, 308K, 318K, 323K and 328K respectively which indicate that the graphs follow the Freundlich isotherm model. The adsorption capacity (K_f) of the activated tamarind kernel powder for Reactive Orange 20 were 4.09 (l/g), 2.75 (l/g), 2.06 (l/g), 1.72 (l/g), and 1.00 (l/g) at 298K, 308K, 318K, 323K and 328K respectively. From the results it could be seen that K_f decreased as the temperature increased from 298K to 328K. The constant n at 298K, 308K, 318K, 323K and 328K is 1.39, 1.51, 1.63, 1.68, and 2.12 respectively.

Figures 4.35 – 4.39 represent the Freundlich adsorption isotherm models for Reactive Blue 29 at a temperature range of 298K to 328K respectively. From the figures it could be seen that the plots are linear and the correlation coefficient (R^2) values were found to be 0.982, 0.981, 0.989, 0.995, and 0.984 at 298K, 308K, 318K, 323K and 328K respectively which indicate that the graphs follow the Freundlich isotherm model. The adsorption capacity (K_f) of activated tamarind kernel powder for Reactive Blue 29 were 1.71 (l/g), 1.36 (l/g), 1.72 (l/g), 2.05 (l/g), and 2.63 (l/g) at 298K, 308K, 318K, 323K and 328K respectively. From the results it could be seen that K_f increased as the temperature increased from 298K to 328K. The constant n at 298K, 308K, 318K, 323K and 328K is 1.46, 1.55, 2.27, 2.46, and 2.90 respectively.

The magnitude of the adsorption intensity n gives an insight into the favourability of the adsorption process. This is achieved when n lies in the range of 1-10 (Ho and Chang, 2001). The Freundlich adsorption isotherm is useful for predicting the adsorption capacity of an activated tamarind kernel powder for Acid Red 1, Reactive Orange 20 and Reactive Blue 29. The steeper the isotherm, the more effective is the adsorbent (Ho and Chang, 2001).

5.3.5.3 Temkin Isotherm

The Temkin isotherm equation assumes that the heat of adsorption of all the molecules in a unit layer decreases linearly with coverage due to adsorbent-adsorbate interactions, and that the adsorption is characterized by a uniform distribution of the bonding energies, up to some maximum binding energy (Temkin, 1940).

Temkin isotherm constant b_T and Temkin isotherm equilibrium binding constant A_T were obtained from the intercepts and slopes of the linear plot of q_e versus $\ln C_e$ as shown in Figures 4.40 – 4.54.

Figures 4.40 – 4.44 represent the Temkin adsorption isotherm models for Acid Red 1 at a temperature range of 298K to 328K respectively. From the figures it could be seen that the

plots are linear and the correlation coefficient (R^2) values were found to be 0.803, 0.793, 0.863, 0.797, and 0.931 at 298K, 308K, 318K, 323K and 328K respectively which indicate that the graphs follow the Temkin isotherm model. The adsorption capacity (A_T) of the activated tamarind kernel powder for Acid Red 1 were 2.27 (l/g), 1.69 (l/g), 1.12 (l/g), 1.33 (l/g), and 2.21 (l/g) at 298K, 308K, 318K, 323K and 328K respectively. From the results it could be seen that A_T,which also signifies the equilibrium bindingconstant corresponding to the maximum binding energy of the adsorbent, is decreasing as the temperature increased from 298K to 328K. The constant b_T relating to the heat of adsorption of activated tamarind kernel powder for Acid Red 1 at 298K, 308K, 318K, 323K and 328K is 552.4 (J/mg), 600.4 (J/mg), 668.8 (J/mg), 808.1 (J/mg), and 820.6 (J/mg) respectively.

Figures 4.45 – 4.49 represent the Temkin adsorption isotherm models for Reactive Orange 20 at a temperature range of 298K to 328K respectively. From the figures it could be seen that the plots are linear and the correlation coefficient (R^2) values were found to be 0.969, 0.865, 0.950, 0.910, and 0.928 at 298K, 308K, 318K, 323K and 328K respectively which indicate that the graphs follow the Temkin isotherm model. The adsorption capacity (A_T) of the activated tamarind kernel powder for Reactive Orange 20 were 7.11 (l/g), 5.22 (l/g), 4.61 (l/g), 4.01 (l/g), and 2.37 (l/g) at 298K, 308K, 318K, 323K and 328K respectively. From the results it could be seen that A_T,which also signifies the equilibrium binding constant corresponding to the maximum binding energy of the adsorbent, is decreasing as the temperature increased from 298K to 328K. The constant b_T relating to the heat of adsorption of activated tamarind kernel powder for Reactive Orange 20 at 298K, 308K, 318K, 323K and 328K is 1138.0 (J/mg), 1167.7 (J/mg), 1158.1 (J/mg), 1292.3 (J/mg), and 1312.0 (J/mg) respectively.

Figures 4.50 – 4.54 represent the Temkin adsorption isotherm models for Reactive Blue 29 at a temperature range of 298K to 328K respectively. From the figures it could be seen that the

plots are linear and the correlation coefficient (R^2) values were found to be 0.992, 0.993, 0.960, 0.979, and 0.942 at 298K, 308K, 318K, 323K and 328K respectively which indicate that the graphs follow the Temkin isotherm model. The adsorption capacity (A_T) of the activated tamarind kernel powder for Reactive Blue 29 were 4.93 (l/g), 4.22 (l/g), 1.68 (l/g), 1.25 (l/g), and 1.47 (l/g) at 298K, 308K, 318K, 323K and 328K respectively. From the results it could be seen that A_T,which also signifies the equilibrium binding constant corresponding to the maximum binding energy of the adsorbent, is decreasing as the temperature increased from 298K to 328K. The constant b_T relating to the heat of adsorption of activated tamarind kernel powder for Reactive Blue 29 at 298K, 308K, 318K, 323K and 328K is 683.5 (J/mg), 709.3 (J/mg), 945.6 (J/mg), 995.1 (J/mg), and 1173.0 (J/mg) respectively.

5.3.5.4 Dubinin-Radushkevich (D-R) Isotherm

The Dubinin-Radushkevich parameters B_D and q_D (theoretical isotherm saturation capacity) were calculated from the slopes and intercepts of the linear plots of $\ln q_e$ versus ε^2 as shown in Figures 4.55 – 4.69.

Figures 4.55 – 4.59 represent the Dubinin Radushkevich adsorption isotherm models for Acid Red 1 at a temperature range of 298K to 328K respectively. From the figures it could be seen that the plots are linear and the correlation coefficient (R^2) values were found to be 0.941, 0.932, 0.974, 0.965, and 0.933 at 298K, 308K, 318K, 323K and 328K respectively which indicate that the graphs follow the Dubinin Radushkevich isotherm model. The saturation capacity constant (q_D) of the activated tamarind kernel powder for Acid Red 1 were 13.0 (mg/g), 13.2 (mg/g), 13.1 (mg/g), 13.0 (mg/g), and 12.76 (mg/g) at 298K, 308K, 318K, 323K and 328K respectively. From the results it could be seen that q_D, is decreasing as the temperature increased from 298K to 328K. The constant B_D relating to the mean free energy of adsorption of Acid Red 1 on activated tamarind kernel powder at 298K, 308K, 318K,

323K and 328K is $-1x10^{-5}$ (mol^2/J^2), $-7x10^{-6}$ (mol^2/J^2), $-4x10^{-6}$ (mol^2/J^2), $-2x10^{-6}$ (mol^2/J^2), and $-9x10^{-7}$ (mol^2/J^2) respectively.

Figures 4.60 – 4.64 represent the Dubinin Radushkevich adsorption isotherm models for Reactive Orange 20 at a temperature range of 298K to 328K respectively. From the figures it could be seen that the plots are linear and the correlation coefficient (R^2) values were found to be 0.923, 0.950, 0.963, 0.989, and 0.964 at 298K, 308K, 318K, 323K and 328K respectively which indicate that the graphs follow the Dubinin Radushkevich isotherm model. The saturation capacity constant (q_D) of the activated tamarind kernel powder for Reactive Orange 20 were 4.64 (mg/g), 5.53 (mg/g), 5.88 (mg/g), 6.50 (mg/g), and 6.51 (mg/g) at 298K, 308K, 318K, 323K and 328K respectively. From the results it could be seen that q_D, is increasing as the temperature increased from 298K to 328K. The constant B_D relating to the mean free energy of adsorption of Reactive Orange 20 on activated tamarind kernel powder at 298K, 308K, 318K, 323K and 328K is $-4x10^{-5}$ (mol^2/J^2), $-3x10^{-5}$ (mol^2/J^2), $-3x10^{-5}$ (mol^2/J^2), $-2x10^{-5}$ (mol^2/J^2), and $-1x10^{-5}$ (mol^2/J^2) respectively.

Figures 4.65 – 4.69 represent the Dubinin Radushkevich adsorption isotherm models for Reactive Blue 29 at a temperature range of 298K to 328K respectively. From the figures it could be seen that the plots are linear and the correlation coefficient (R^2) values were found to be 0.923, 0.934, 0.789, 0.829, and 0.798 at 298K, 308K, 318K, 323K and 328K respectively which indicate that the graphs follow the Dubinin Radushkevich isotherm model. The saturation capacity constant (q_D) of the activated tamarind kernel powder for Reactive Blue 29 were 8.14 (mg/g), 8.63 (mg/g), 8.44 (mg/g), 8.73 (mg/g), and 8.87 (mg/g) at 298K, 308K, 318K, 323K and 328K respectively. From the results it could be seen that q_D, is increasing as the temperature increased from 298K to 328K. The constant B_D relating to the mean free energy of adsorption of Reactive Blue 29 on activated tamarind kernel powder at

298K, 308K, 318K, 323K and 328K is $-2x10^{-5}$ (mol^2/J^2), $-2x10^{-5}$ (mol^2/J^2), $-4x10^{-5}$ (mol^2/J^2), $-3x10^{-5}$ (mol^2/J^2), and $-2x10^{-5}$ (mol^2/J^2) respectively.

The activation energy (E_A) value reveals the nature of adsorption. Thus, if the value of adsorption energy (E_A) is less than 8kJ/mol, adsorption process is physical (physisorption); but if it is ranged from 8 to 16kJ/mol, it is a chemical adsorption or chemisorption (Okoli *et al*., 2015). The E_A values obtained for Acid Red 1 dye adsorption on activated tamarind kernel powder were 0.22kJ/mol, 0.27kJ/mol, 0.35kJ/mol, 0.50kJ/mol and 0.74kJ/mol at system temperature of 298K, 308K, 318K, 323K and 328K respectively.

The E_A values obtained for Reactive Orange 20 dye adsorption on activated tamarind kernel powder were 0.11kJ/mol, 0.13kJ/mol, 0.13kJ/mol, 0.16kJ/mol and 0.22kJ/mol at system temperature of 298K, 308K, 318K, 323K and 328K respectively.

The E_A values obtained for Reactive Blue 29 dye adsorption on activated tamarind kernel powder were 0.16kJ/mol, 0.16kJ/mol, 0.35kJ/mol, 0.41kJ/mol and 0.50 kJ/molat system temperature of 298K, 308K, 318K, 323K and 328K respectively.

The mean free energyvalues obtained are less than 8kJ/mol, indicating that Acid Red 1 dye, Reactive Orange 20 and Reactive Blue 29 adsorption on activated tamarind kernel powder is a physical process or physisorption.

5.4. Adsorption Kinetics

In this study, two different models were used such as the pseudo-first-order (Hashem and El-Khiraigy, 2013) and the pseudo-second-order (Ho and McKay, 2003; Hameed *et al*., 2008). Pseudo-first order and pseudo-second order kinetic models described above were used to test the equilibrium data in order to investigate the mechanism of adsorption and potential rate controlling step of the adsorption process. However, in selecting optimum conditions for carrying out full scale batch dye removal processes,information on the kinetics of dye

adsorption is required. A kinetic study at different time intervals, constant initial dye concentration and adsorbent dosage was performed.

The pseudo-first and pseudo second order kinetics modelling of Acid Red 1, Reactive Orange 20 and Reactive Blue 29 dyes adsorption unto TKP are represented in Figures 4.70 – 4.72, and 4.73 – 4.75; respectively. The experimental adsorption capacities of Acid Red 1, Reactive Orange 20 and Reactive Blue 29 are 3.95 mg/L, 1.50 mg/L and 2.58 mg/L respectively. Their adsorption capacities by using pseudo-first order model were calculated and presented as 2.41 mg/L, 3.53 mg/L and 2.56 mg/L respectively while that of pseudo-second order model are 4.29 mg/L 2.44 mg/L and 2.95 mg/L respectively. The calculated adsorption capacities of all the dyes by pseudo-second order model were seen to be very close to their respective experimentally determined adsorption capacities. But whenthe adsorption capacities obtained from the pseudo-first order kinetics were compared with the experimentally determined values, a large difference was observed.

The values obtained for the correlation coefficients, R^2, of the pseudo-first order adsorption model for Acid Red 1, Reactive Orange 20 and Reactive Blue 29dyes were 0.074, 0.347 and 0.107 respectively. For pseudo-second order kinetics we have R^2 values as follows: 0.999, 0.847 and 0.993 for Acid Red 1, Reactive Orange 20 and Reactive Blue 29dyes respectively. From the above results it could be seen that the R^2 values obtained from the Pseudo-second order kineticplot are higher than that obtained from the Pseudo-first order adsorption kinetic plot. Thus, the correlation coefficient values and calculated adsorption capacities of all the dyes did not follow the pseudo-first order kinetic model, which suggests that theadsorption of Acid Red 1, Reactive Orange 20 and Reactive Blue 29 on activated tamarind kernel powder are dependent on initial concentration. Hence, pseudo-second order adsorption model is more suitable to describe the adsorption kinetics of Acid Red 1, Reactive Orange 20 and Reactive Blue 29 unto ATKP and this relies on the assumption that adsorption may be the rate-limiting

step (Gupta and Rastogi, 2007). The obtained kinetic information has a significant practical value for technological applications, since kinetic modelling successfully replaces time and material consuming experiments necessary for process equipment design (Bhatti *et al*., 2006; Gupta and Rastogi, 2007; Mahamadi and Torto, 2007; Krishnaiah *et al*., 2008; Oladunni *et al*., 2012).

5.5 Adsorption Thermodynamics

The temperatures used in the thermodynamic study were 298K, 308K, 318K, 323K and 328K. The values of the thermodynamic parameters obtained from adsorption of Acid Red 1 dye, Reactive Orange 20 dye and Reactive Blue 29 dye on activated tamarind kernel powder are listed in Table 4.5 and the Van't Hoff plots of lnK against T^{-1} AR1, RO20 and RB29 dyes are presented as figures 4.76 to 4.78 respectively. The heat change (ΔH) and entropy change (ΔS) valuesand were obtained from the slopes and intercepts respectively of the Van't Hoff plots. The negative Gibbs free energy change (ΔG) values indicate that the process is thermodynamically feasible and spontaneous. The negative ΔH values indicate that the nature of the adsorption process is exothermic indicating that heat is released during the adsorption process. This is also supported by the decrease in the value of adsorption capacity of the adsorbent with the increase in temperature. The negative values of ΔS pointed to a decreased disorder of the solid/solution interface during the adsorption process. However, similar results were obtained by Okoli *et al*., (2015).

CHAPTER SIX

SUMMARY, CONCLUSION AND RECOMMENDATIONS

6.1 Summary and Conclusion

In this research, adsorption of C.I Acid Red 1, C.I Reactive Orange 20 and C.I Reactive Blue 29using activated carbonized tamarind kernel powder was successfully carried out.The characterization analysis carried out on the activated carbon indicated that all parameters namely: bulk density, pH, ash content and dry matterwere within acceptable range. The Fourier transform infrared spectroscopic analysis carried out on the raw activated tamarind kernel powder indicated the presence of functional groups which include: Hydroxyl, alkanes, alkenes, alkynes, carboxyl, phenols, phosphates, carbonyl, primary and secondary amines,etc.; which constitute very important adsorption sites on the adsorbent surface. The FTIR analysis carried out on the dye-adsorbed activated tamarind kernel powder indicated the presence of some functional groups which did not appear in the FTIR spectrum of raw ATKP. They include: open chain azo groups, quinones, conjugated ketones, sulphonates, aromatic ethers, aromatic nitro groups and others. The effect of the different parameters namely: pH, adsorbent dosage, initial dye concentration, contact time and temperature indicated that the adsorption of Acid Red 1, Reactive Orange 20 and Reactive Blue 29 from the simulated dye based wastewater using activated tamarind kernel powder isdependent on these factors. From the four equilibrium isotherms tested in this research the order in which the data obtained best fits the isotherm models are Langmuir >Temkin > Dubinin Radushkevich >Freundlich.

From the Adsorption kinetic models, Pseudo-Second order kinetic model offered the best description of the adsorption kinetics modelling carried out.From the thermodynamic studies, it could be inferred that the adsorption of Acid Red 1, Reactive Orange 20 and Reactive Blue 29 on activated tamarind kernel powder is a physical process (physisorption) due to the fact

that the activation energy (E_A) value was less than 8kJ/mol and hence the adsorbent can be easily regenerated and re-used. It is also feasible and spontaneous due to negative value of the Gibb's free energy (ΔG).The negative change in enthalpy (ΔH) value revealed the exothermic nature of the adsorption process.The negative change in entropy (ΔS) values of the system suggests the decrease in adsorbate concentration in solid-solution interface indicating thereby the increase in adsorbate concentration onto the solid phase. This is the normal consequence of the physical adsorption phenomenon, which takes place through electrostatic interactions as reported by Saswati and Uday, (2005).

6.2 Recommendations

From this work, it is evident that activated tamarind kernel powder has the capacity to remove Acid Red 1, Reactive Orange 20 and Reactive Blue 29. Therefore, it is imperative to explore the following areas so as to help reveal some of the latent potentials of tamarind kernel powder that have not been reported in this or any other research:

i. The adsorption potential of regenerated activated tamarind kernel powder.
ii. The potential of tamarind kernel powder as filler in polymer composites.
iii. The heavy metals adsorption capacity of tamarind kernel powder.
iv. The adsorptive capacity of tamarind kernel powder obtained from different locations.
v. The variation in adsorptive capacity of tamarind kernel powder activated via different means.
vi. The adsorptive potential of nano particles obtained from tamarind kernel powder.

6.3 Contributions to Knowledge

This research has presented us with the following information

i. The adsorption of Acid Red 1 (AR1), Reactive Orange 20 (RO20) and Reactive Blue 29 (RB29) on activated tamarind kernel powder (ATKP) is a physicochemical process

ii. The adsorption of AR1, RO20 and RB29 on ATKP is more dependent on heat of adsorption which decreases linearly with coverage due to adsorbate-adsorbent interaction.

iii. The adsorbed dye molecules are not so tightly held unto the ATKP due to the reduced binding energies observed with increased in the temperature of the system. This indicates that ATKP can be easily regenerated and reused.

REFERENCES

Abechi, S.E. (2006). Adsorption Characteristics of Ti (IV) and Zn(II) Oxide Coated Activated Carbon from Walnut Shells. An M.Sc. Thesis, Department of Chemistry, Ahmadu Bello University, Zaria.

Abram, J.C. (1973). The Characteristics of Activated Carbon. A paper Presented at a conference on "Activated carbon in Water Treatment, organized by the Walter Research Association held at the University of Reading, Malaysia. Pp. 1-29.

Abdessalem, O., Ahmed, W., and Mourad, B., (2012). Adsorption of Bentazon on Activated Carbon Prepared from Lawsonia Inermis Wood. Equilibrium and Thermodynamic studies, *Arabian Journal of Chemistry*. 10, 1016.

Aharoni, C. and Sparks, D. L. (1991). 'Kinetics of Soil Chemical Reaction-A Theoretical Treatment' in D. L. Sparks and D. L. Suarez (eds), Rates of soil chemical processes, Soil Science society of America, Madison, Wi, pp1-18.

Ahmed, A.I., (1995).Reactive Dyes Development- A Review.*Textile Dyer & Printer*, 28(16): 19.

Ahalya N., Kanamadi R.D. and Ramchendra T.V. (2005). *Electronic Journal of Biotechnology*. 3(3), 258-264.

Al-degs, Y.S., Musa I.E., Annjad H.E., and Gavin M.W., (2007). Effect of Solution pH, Ionic Strength, and Temperature on Adsorption Behaviour of Reactive Dyes on Activated Carbon. *Elsevier Journal of Dyes and Pigments*,1-8.

Al-Degs, Y. S. M. I. El-Barghouthi, M. A. Khraisheh, M. N. Ahmad and S. J. Allen, (2004). "Effect of Surface Area, Mi- cropores, Secondary Micropores and Mesopores Volumes of Activated Carbons on Reactive Dyes Adsorption from Solution," *Separation Science and Technology*, 39(1): 97-111.

Allen, S.G. (1974) "Chemical Analysis of Ecological Materials". Blackwell, Oxford.Pp565-566.

Andre, L. C., Alexandro, M. M., Eurica, M. N., Marcos, H. K., Marcos, R.G., Alessandro, C. N., Tais, L. S., Juliana, C. G., and Victor, C. A. NaOH (2011). Activated Carbon of High Surface Area Produced from Coconut Shell: Kinetics and Equilibrium Studies from the Methylene Blue Adsorption. *Chemical Engineering Journal*, 174: 117-125.

Aspland, J.R., (1997).Application of Anions to Nonionic Fibres: Dyeing Cellulosic Fibres. "*Textile Dyeing and Coloration*", AATCC, pp105-141.

Atkins, W. (2003). Physical chemistry. Oxford University Press (7^{th} edition). Pp. 988-989.

Arita I.H., Castano V.M., and Wilkinson D.S. (1995). Synthesis and Processing of Hydroxyapatite Ceramic Tapes with Controlled Porosity. *Journal of Materials Science;* 6(1): 19-23.

Arun S. (2002). Adsorption of organic pollutants onto Natural adsorbent. MSc Thesis. Department of Chemical engineering, Mississippi State University,pp32-35

Anonymous, (1976).*Tamarindus indica* L. The Wealth of India (Raw Material). Volume X. Council of Scientific and Industrial Research, New Delhi, pp144-122.

ASTM Committee on Standards, (1986). American Society for Testing and Materials: Standard for Method for Moisture in Activated Carbon. Philadelphia, PA: ASTM Committee on Standards.

American Society for Testing and Materials (1996): Standard Method for the Determination of pH value in Biomass, Philadelphia, P.A.: 11, (05).

American Society for Testing and Materials (2003): Standard Method for the Determination of Ash in Biomass, Philadelphia, P.A.: 11, (05).

Baban, A.; Yediler, A. andCiliz, N.K. (2010). Integrated Water Management and CP Implementation for Wool and Textile Blend Processes. *Clean*, 38 (1): 84-90

Bapat, P., Nandy, S. K., Wangikar, P., andVenkatesh, K. V. (2006). Quantification of metabolically active biomass using Methylene Blue dye Reduction Test (MBRT): Measurement of CFU in about 200 s. *Journal ofMicrobiological Methods*, 65: 107–116.

Beech, W.F., (1970). "Fibre Reactive Dyes", Logos Press Limited, London,pp175-176.

Bertea, A. and Bertea, A.P. (2008).Decolorisation and Recycling of Textile Wastewater.In: Romanian,Performantica (Ed) Iasi, Romania,pp978-973.

Bhatia, S.C. (2006). Environmental Pollution and Control in Chemical Process Industries, Khanna publishers, Darya gay, New Delhi. pp. 1184-1191

Bhattacharya, P.K. (1974). A Note on the Precence of Anthocyanine Pigment in the Stem of Red Fruited Variety of Tamarind. Indian Forester 100 (4).pp 255-258.

Bhattacharya, S.D. and Panchal, H.M., (1984).Tamarind.*Indian Textile Journal*, 95(3), 109.

BohumilVolesky, and Jinbai Yang (1999). Biosorption of Uranium on *Sargassum* Biomass. *Water Research*. 33(15). 3357-3363.

Bhatti, I., Qureshi, K., Kazi, R. and Ansari, A.K (2007) Physical and Chemical Analysis of Activated Carbon Prepared from sugarcare Dagasse and Use for sugar Decolonization. World Academy of Science, Engineering and Technology.34:194-198.

Bhavin P., (2009). Evaluation of Tamarind Seed Polysaccharide as a Mucoadhesive and Sustained Release Component of Nifedipine Buccoadhesive Tablet and Comparison with HPMC and NACMC. *International Journal of Pharmaceutical TechnologyResearch*,1(3): 404-410.

Bisschops, I.A.E. and Spanjers, H. (2003). Literature Review on Textile Wastewater Characterisation. *Environmental Technology Journal*, 24, 1399-1411

Brenan, J.P.M. (1967). Leguminosae, Sub family Caesalpinoidae. In: Milne-Red head, E. and Polhill, R.M. (eds). Flora of Tropical East Africa Agents for Overseas Governments and Administration, London.pp151-153.

Bottari F. Di Colo G., Nannipieri E., Seattone M.F., and Serafini M.F. (1975). Evaluation of a Dynamic Permeation Technique for Studying Drug-Macromolecule Interactions. *Journal of Pharmaceutical Science*. 946-949.

Bueso C.E. (1980) Soursop, Tamarind and Chironka. In: Nagy, S. and shaw, P.E., (Eds.) Tropical and Substropical Fruits. AVI Publishing, WestPort, Conn., 375.

Burgalassi S., Panichi L., Saettone M. F., Jacobsen J., and Rassing M. R.(1996). Development and In vitro/In vivo Testing of Mucoadhesive Buccal Patches Releasing Benzydamine and Lidocaine. *International Journal of Pharmaceutical Sciences* (133), 1-7.

Bulut E., Ozacar M. and Sengil I.A., (2008).Adsorption of Malachite Green onto Bentonite: Equilibrium and Kinetic Studies and Process Design. *Journal of Hazardous Materials*, 154, 613-622.

Bulut, Y., and Aydin H., (2006). A Kinetics and Thermodynamics Study of Methylene Blue Adsorption on Wheat Shells. *Elsevier Journal of Desalination,* 194: 259-267.

Chapman, K.R. (1984) Tamarind. In: page, P.E. (compiled) Tropical Tree Fruits for Australia. Queensland Department of Primary Industries. Information series Q183018, Brisbane: 83-86.

Chandrasekhar, S., and Pramada, N. P. (2006). Rice husk Ash as an Adsorbent for Methylene Blue—Effect of AshingTemeparature. *Adsorption*, 12, 27–43.

Charley H. (1970) Food Science. John Wiley and Sons. New York. Cheremisinoff, P. and Ellerbusch, F. (1976). Carbon Adsorption Handbook. Ann Arbor Science Publisher Inc. London 72, pp689-690.

Cheremisinoff, N. P. and Chermisinoff, P.N. (1993). Carbon Adsorption for Pollution Control; Prentice Hall, Englewood Cliffs, NJ.pp167-169.

Chaturvedi, A.N., (1985). Firewood Farming on the Degraded Lands of the Gangetic Plain. U.P. Forest Bulletin. Government of India Press, Lucknow, India.756-758.

Christie, R.M., (2001), "Colour Chemistry", *The Royal Society of Chemistry*, U.K., 135-147.

Chye S., Loo J., Siew Y.E., Ho S., Boey F.Y.C., and Ma J. (2008). Synthesis and Hydrothermal Treatment of Nanostructured Hydroxyapatite of Controlled Sizes. *Journal of Material Science and Material Medicine*.19: 1387-1397.

Chilton N. Jack N. L. , Wayne E. M., and R. Rao (2002).Freundlich Adsorption Isotherms of Agricultural By-product-based Powdered Activated Carbons in a geosmin–water System. *Bioresource Technology*. 85(2): 131-135.

Contino-Rodriguez, R., Hernande4z-Cruz, P. and Giles-Rios, H. (2001). Lectins in Fruits having Gastrointestinal Activity: their Participation in the Hemagglutinating Property of *Escherichia coli*. *Archives of Medical Research* 32(4): 251-257.

Cooney, D.O., 1999. Adsorption Designer for Wastewater Treatment. Lewis Publishers, London, England, 150-190.

Coronel, R.E. (1991) *Tamarindus indica* L. In: Verheiji, E.W.M. and Edible Fruits and Nuts. PROSEA Foundation, Bogor Indonesia,pp298-301

Correia, V.M.; Stephenson, T. and Judd, S.J. (1994). Characterization of Textile Wastewaters – a Review. *Environmental Technology*, 15: 917-929

Cote, L.G., (1986). A Study of the Kinetics of Cold Pad Batch Dyeing with Fibre Reactive Dyes Using High Performance Liquid Chromatography, Ph.D. Dissertation, Clemson University, University Microfilms International, pp252-256.

Crini, G., andBadot, P. M. (2008). Application of Chitosan, a Natural Polysaccharide, for Dye Removal from Aqueous Solutions by Adsorption Processes using Batch studies: A Review of Recent Literature. *Progress in Polymer Science*, 33: 399–447.

Dada, A.O., Olalekan A.P., Olatunya, A.M., and Dada, O., (2012). Langmuir, Freundlich, Temkin and Dubinin-Radushkevich Isotherms Studies of Equilibrium Sorption of Zn^{2+} unto Phosphoric Acid Modified Rice Husk. *IOSR Journal of Applied Chemistry*, 3(1): 38-45.

Daintith, J., (2000). A dictionary of Chemistry. 4th edition. Oxford University Press,pp15.

Datta R.,and Bandopadhyay A.K. (2006). A New Nasal Drug Delivery System for Diazepam using Natural Mucoadhesive Polysaccharide Obtained from Tamarind Seeds. *Saudi Pharmaceutical Journal*, 14(2); 115-119.

Deshuai, S., Zhongyi Zhang, Mengling W., and Yude W., (2013). Adsorption of Reactive Dyes on Activated Carbon Developed from *Enteromorpha prolifera*. *American Journal of Analytical Chemistry,* 4: 17-26.

Deveswaran R. (2009). Design and Characterization of Dichlofenac Sodium Tablets containing Tamarind Seed Polysaccharide as Release Retardants. *International Journal of Pharmaceutical Technology Research*, 1 (2): 191-195.

Dickerson, R. E., and Geis, I. (1976). *Chemistry, Matter, and the Universe*. USA: W. A. Benjamin Inc.) ISBN 0-19-855148-7,pp354-355.

Dolby, P.J, (1977), Reactive Dyes. In: Textile Chemist and Colorist, *Dyeing Prima-a Series of Short Papers on the Fundamentals of Dyeing*. American Society of Textile Chemists and Colorists, North Carolina, USA, 12(9), pp231.

Dogan, M., Abak, H., andAlkan, M. (2008). Biosorption of methylene blue from quesous solutions by hazelnut shells: equilibrium, parameters and isotherms. Water, Air, and Soil Pollution, 192, pp 141–153.

Dorian A. H. H., M. G.,Wojciech C.,and Yixiang G. (2014). Scalable Surface Area Characterization by Electrokinetic Analysis of Complex Anion Adsorption. *Langmuir American Chemical Society Journal*, 30: 15143-15152.

Duane A.J. (1978). Clarified Tamarind Powder.United States Patent, pp 442.

El-Hendawy, A. A., Alexander, R. J., and Andrews, G. F., (2008). Effect of Activation Schemes on Porous Surface and Thermal Properties of Activated Carbons Prepared from Cotton Stalk, *Journal of Analytical Applicationin Pyrolysis*, 82: 272-278.

El-Siddig. K., Gunasena, H.P.M., Prasad, B.A., Pushpakumara, O,K,N,G., Ramana, K.V.R., Vijayanand, P. and Williams, J.T. (2006). Tamarind: *Tamarindus indica* L.Southampton Centre for Underutilized Crops, Southampton, UK,pp735-736.

Erhan, D., Kobya, M., Elif, S., and Tuncay, O., (2004). Adsorption Kinetics for the Removal of Chromium (VI) from Aqueous Solutions on the Activated Carbons Prepared from Agricultural Wastes. *Journal of Water Research* 30 (4): 533-540.

FAO (1988) Fruit bearing Trees. Technical notes. FAO-SIDA Forestry Paper 34: 165-167.

Feungchan, S., Yimsawat, T., Chindaprasat, S. and Kitpowosong, P. (1996a) Tamarind (*Tamarindus indica* L.) Plant Genetic Resources in Thailand. *Thai Journal of Agricultural Science*, Special issue 1, 1-11

Ford J.L., Ribinstein M.H., McCaul F., Hogan J.E., and Edgar P.J. (1987). Importance of Drug Type, Tablet Shape and added Diluents on Drug Release Kinetics from Hydroxymethyl cellulose Matrix Tablets. *International Journal of Pharmaceutical Science*, (40), 223-234.

Freundlich and Halfield. (1926): Adsorpion in Solution. *Journal of Physical Chemical Society*, 40: 1361-1368.

Feungchan, S., Yimsawat, T., Chindaprasat, S. and Kitpowosong, P. (1996b) Evaluation of Tamarind Cultivars on the Chemical Composition of Pulp.*Thai Journal of Agricultural Science* Special issue 1, 28-33.

Gamal G.A., Al- mufadi, and Said A.H. (2013). Effect of Iron Additives on the Microstructure of Hydroxyapatite. Engineering, *Technology and Applied Research*. 3(6): 532-539.

Gerard T. (1980). Tamarind Gum in Handbook of Water Soluble Gums and Resins. In: Davidson R.L., (Ed). USA: McGraw-Hill Book Co.,pp1-23.

Ghelardi E., Tavanti A., Celandroni F., Lupetti A., Blandizzi C., and Boldrini F., (2000). Effect of a Novel Mucoadhesive Polysaccharide Obtained from Tamarind Seeds on the Intraocular Penetration of Gentamicin and Ofloxacin in Rabbits. *Journal of Antimicrobial Chemotherapy*, 46: 831-834.

Ghelardi E., Tavanti A., Davini P., Celandroni F., Salvetti S., and Parisio E., (2004). A Mucoadhesive Polymer Extracted from Tamarind Seed Improves the Intraocular Penetration and Efficiancy of Rufloxacin in Topical Treatment at Experimental Bacterial Keratitis. *Antimicrobial Agents Chemotherapy Journal*. 48: 3396-33401.

Gimba, C.E. Ocholi, O.J., Egwaikhide, P.A., Muyiwa, T. and Akporhonor, E.E., (2009) New Raw Material for Activated Carbon. I. Methylene Blue Adsorption on Activated Carbon Prepared from *Khaya senegalensis* fruits. *Nigerian Journal of Scientific Research*, 36(1): 107-114.

Giriraj T., Kulkarni K., and Gawthamarajan, (2003). Development of Controlled Release Spheroids Using Natural Polysaccharides as Biomater Artif Organs. 17, pp41-46.

Glenn MR. Activated carbon application in the food and pharmaceutical industries.First Edn.Technomic Publishing coy.inc., USA, 1993; pp177-179

Glicksman M. (1996). Tamarind Seed Gum. In: Glicksman M., (Ed). Food Hydrocolloids. Boca Raton, Florida, USA: CRC Press Inc.pp191-202.

Grosch W., and Belitz (1987). Food Chemistry. Springer, Verlag. New York,pp735-752.

Gupta, V.K. and Rastogi, A. (2007). Biosorption of Lead from Aqueous Solutions by Green Algea Spirogyra Species. Kinetics and Equilibrium Studies. *Journal of Colloid and Interface Science*, 296: 59-63.

Gupta, V. K., andSuhas. (2009). Application of low cost adsorbents for dye removal—A review. *Journal of Environmental Management*, 90: 2313–2342.

Gunasena, H.P.M. and Hughes, A. (2000). Fruits for the future-1. Tamarind (*Tamarindus indica* L) International Centre for Underutilized Crops, Southhampton, UK, pp256-258.

Gurses, A., Dogar, C., Yalc-in, M., Acikyildiz, M., and Bayrak, R. (2006). The Adsorption Kinetics of Cationic Dye Methylene Blue onto Clay. *Journal of Hazardous Materials*. 131: 217-228.

Hamdaoui, O., andChiha, M. (2007). Removal of Methylene Blue from Aqueous Solutions by Wheat Bran. *Acta Chimica Slovenica Journal*, 54, 407–418.

Han, R. (2006). Removal of Methylene Blue from Aqueous Solution by Chaff in Batch Mode.*Journal of Hazardous Materials*, 137, 550–557.

Han, R. (2007). Biosorption of Methylene Blue from Aqueous Solution by Fallen Phoenix Tree's Leaves. *Journal of Hazardous Materials*, 141, 156–162.

Hao, O.J.; Kim, H. and Chang, P.C. (2000). Decolorization of Wastewater. *Critical Reviews in Environmental Science and Technology*, Vol.30, 449-505

Hameed, B. H., Tan, I. A. W. and Ahmad, A. L., (2008). Adsorption isotherm, kinetic modeling and mechanism of 2,4,6-trichlorophenol on coconut husk-based activated carbon. *Chemical Engineering Journal*, 144, 235-244.

Hashem, A. and El-Khiraigy, K. (2013) Bioadsorption of Pb(II) onto Anethumgraveolens from Contaminated Wastewater: Equilibrium and Kinetic Studies. *Journal of Environmental Protection*, 4, 108-119.

Hilkens J., Ligtenberg M.J., Vos H.L. and Litvinov S.V. (1992). Cell Membrane-Associated Mucins and their Adhesion Modulating Property. *Trends in Biochemical Science*. 17, pp359-363.

Himanshu P. and Vashi R.T. (2010). Adsorption of Crystal violet dye onto Tamarind Seed powder. *Electronic Journal of Chemistry*, 7(3): 973-984.

Hindum M.P., Sri Maryani E.F., Nur Alifar and Sucipto, (2001). Tamarind Kernel Powder (*Tamarindus indica*) Pocessing (Reviews on Roasting Temperature and Roasting Duration). *Journal TeknologiPertanian*, 2 (3): 150-158.

Ho, Y.S. (2005). Isotherms for the sorption of lead onto peat: Comparison of linear and non-linear methods. *Polish Journal of Environmental Studies*, 15: 81–86.

Ho, Y. S., and Chang, C. C. (2001). Sorption Studies of Acid Dye by Mixed Sorbents. *Journal of Adsorption*, 7: 139-147.

Ho, Y.S. and G. McKay, (2003). Pseudo-second order model for Sorption Processes. *Process Biochemistry Journal*, 34(5): 451-465.

Ibrahim, S. I. Fatimah, H. Ang and S.Wang, (2010). Adsorption of Anionic Dyes in Aqueous Solution Using Chemically Modified Barley Straw. *Water Science and Technology*, 62(5): 1177-1182.

Ibrahim N.A., Abo-shosha M.H., Allan E.A., and El-Zairy E.M., (2010). New Thickness Agents Based on Tamarind Seed Gum and Karaya Gum Polysaccharides. *Carbohydrate Polymers*. 81: 402-408.

Ishola, M.M., Agbaji, E.B. and Agbaji, A.S. (1990). A Chemical Study of *Tamarindus indica* (Tsamiya) Fruits Grown in Nigeria. *Journal of Science, Food and Agriculture* 51: 141-143.

Jani G.K., Shah D.P., Prajapati V., and Jain V., (2009). Gums and Mucilages: Versatile Excipients for Pharmaceutical Formulations. *Asian Journal of Pharmaceutical Science*. 4: 309-328.

Jayaweera, D.M.A. (1981). Medicinal Plants (Indigenous and Exotic) used in Ceylon. Part III. Flacourtiaceae- Lytharaceae. A Publication of the National Science council of Sri Lanka,pp244-246

Jean M.S., (2015). The Van't Hoff equation. Chemistry 360 Lecture Notes, Department of Chemistry, Illinois State University,pp1-3.

Jothibas M., Manoharan S., Dhanapandian and Johnson J. (2013). Influence of Precursor Concentration on Sprayed In_2O_3 Thin Films. *Asian Journal of Chemistry*; 25, Supplementary issue. 59-64.

Joseph. T. N. and Philomena, K. I., (2011). Copper (II) Uptake by Adsorption Using Palmyra Palm Nut. Adv. Appl. Sci. Res. 2(6), 166-175.

Khelendra A., Gurbhinder S., Devendra P., and Satya P. (2011). Synthesis and Characteristerization of Hydroxyapatite Powder by Sol-Gel Method for Biomedical Application. *Journal of Minerals and Materials Characterization and Engineering.*10(8): 727-734.

Karadag D., Turan M., Akgul E., Tok S. and Aysegul F. (2007).Adsorption Equilibrium and Kinetics of Reactive Black 5 and Reactive Red 239 in Aqueous Solution onto Surfactant-Modified Zeolite. *Journal of Chemical. Engineering Data*. 52, 1615-1620.

Kadirvelu, K. M. Kavipriya, C. Karthika, M. Radhika, N. Vennilamani, and S. Pattabhi, (2003).Utilization of various agricultural wastes for activated carbon preparation and application for the removal of dyes and metal ions from aqueous solutions.*Bioresources Technology Journal*. 87 (1) 129.

Kannan, N.M., and M. Sundaram, (2001).Kinetics and Mechanism of Removal of Methylene Blue by Adsorption on various Carbons – a comparative study.*Dyes and Pigments Journal*, 51(1): 25.

Kesari, K. K., Verma, H. and N., Behari, J. (2011), Physical Methods in Wastewater Treatment: Sono Chemistry: Environmental Science and Engineering Application in Wastewater, LAP LAMBERT Academic Publishing, pp152.

Khullar P., Khar R.K., and Agarwal S.P. (1998). Evaluation of Guar Gum in the Preparation of Sustained Release Matrix Tablets. *Drug Development and Industrial Pharmacy Journal* 24: 1095-1099.

Kittiya K., Janya P., Wanchang S., and Rattanaphol M., (2012). Thickening Agent Based on Tamarind Seed Gum for Dispersed Printing of Polyester. RMUTP International Conference: Textile and Fashion. Bangkok, Thailand, 325-330.

Kinniburgh, D.G. (1986). General Purpose Adsorption Isotherms. *Environmental Science Technology Journal*, 20: 895–904.

Kulkarni D., Ddwivedi D.K., Sarin J.P.S., and Singh S., (1997). Tamarind Seed Polyose: A Potential Polysaccharide for Sustained Release of Verapamil Hydrochloride as a Model Drug. *Indian Journal Pharmaceutical Science* (59): 1-7.

Krishnaiah, A., Kayani, F., Sankara R.V.S., Boddu, V.M. and Subbaiah, M.V., (2008). Biosorption of Cr(VI) from Aqueous Solutions using *Trametes versicolor* Polyporus Fungi. *Electronic Journal of Chemistry*, 5(3): 499-510.

Kumar, K.S. Lyle, S. Gierke, A. Matov,G. Danuser, and T. Wittmann (2009). GSK3β Phosphorylation Modulates CLASP–Microtubule Association and Lamella Microtubule Attachment. *The Journal of Cell Biology*.184 (6): 895-908

Ladhe, U.V., Wankhede, S.K., Patil, V.T., and Patil P.R., (2011). Adsorption of Erichrome Black T from Aqueous Solutions on Activated carbon Prepared from Mosambi peel. *Journal of Applied Sciences in Environmental Sanitation*, 6: 149-154.

Lagergren, S. (1898).About the Theory of So-called Adsorption of Soluble Substance. In: Xunjun C., Modelling of Experimental Adsorption Isotherm Data. *Information Journal*, 6: 14-22.

Langmuir, I. (1916). The constitution and fundamental properties of solids and liquids.In: Xunjun C., Modelling of Experimental Adsorption Isotherm Data. *Information Journal*, 6: 14-22.

Lewis, D.M., (1982), The Dyeing of Wool with Reactive Dyes. *Journal of the Society of Dyers and Colourists*, 98(5/6): 165.

Liu C., Wang W., Shen W., Chen T., Hu L., and Chen Z. (1997). Evaluation of Biocompatibility of Anonceramic Hydroxyapatite. *Journal of Endodontics*. 23, 490-493.

LaGrega M., Buckingham P.L., and Evans J.C. (1994). Hazardous Waste Management, McGraw-Hill, New York, pp340-343.

Macmillan, H.F. (1943). Handbook of Tropical plants. Medicinal plants. Anmol Publications, New Delhi, India,pp362.

Mark B. (2011). Carbohydrate Chemistry and Nomenclature, 60.In: Xunjun C., Modelling of Experimental Adsorption Isotherm Data. *Information Journal*, 6: 14-22.

Malviya R., Srivasteva P., and Kulkarni G. (2011). Applications of Mucilages in Drug Delivery - A Review. *Advance Biological Research Journal*. 5: 1-7.

Mckay, G., 1995. Use of Adsorbents for the Removal of Pollutants from Waste Water. CRC Press Inc., Boca Raton, USA, pp 72-74.

Mckay, G. and Ho, Y.S. (1999). The Sorption of Lead(II) Ions on Peat Response to Comment. *Journal of Water Research,* 33: 578-584.

Morton, J. (1987). Fruits of Warm Climates. Miami, Florida. Pp. 115-121

Macmillan, H.F. (1943). Handbook of Tropical plants. 362. Medicinal plants. Anmol Publications, New Delhi, India, pp146-150.

Mahony, T. O., Guibal, E., and Tobin, J. M. (2002). Reactive Dye Biosorption by Rhizopus Arrhizus Biomass. *Enzyme and Microbial Technology Journal*, 31, 456–463.

McCabe, W. L, Smith, J. C., and Harriott, P. (2005). Unit Operations of Chemical Engineering, 7th edn. New York: McGraw Hill International Edition, pp836.

Mondal, S. (2008). Methods of Dye Removal from Dye House Effluent—An Overview. *Environmental Engineering Science*, 25, 383–396.

Makfoeld D., (1982) Dsikripsi Pengolahan Hasil Pertanian I. Departmen Ilmu Dan Tecknologi Makanan. FTPUGM Yogyarkarta, pp 50.

Meffert R.M. Thomas J.R. Hamilton K.M. Brownstein C.N. (1985). Hydroxyapatite as an Periodontol. 56, pp63-73.

Munting E., Verhelpen M., Li F., and Vincent A. (1990). Contribution of Hydroxyapatite Coatings to Implant Fixations. Handbooks of Bioactive Ceramic. Vol. 2 Boca Raton, FLA. USA: CRC Press; pp143-148.

Mane S.M., Vanjara A.K. and Sawart M.R., (2005). Liquid-Liquid Extraction of Phenol from Simulated Sebacic Acid Wastewater. *Journal of the Chinese Chemical Society*, 52(6) 1117-1122.

Mahamadi, C., and Torto, N., (2007). A Comparative Study of the Kinetics of Nickel Biosorption by River System. *Electronic Journal of Environmental Science and Technology*, 5(2): 275-285.

Mishra M.U.,and Khandare J.N. (2007). Tamarind Seed Polysaccharides: Biodegradable Polymer for Colonic Drug Delivery. Second Int. Conference and Indo-Canadian Satellite Symposium on Pharmaceutical Science, Technology, Practice and Natural Products, Conference Chronicle. DDS, 35, pp206.

Malik, P.K. (2003). Use of Activated Carbons Prepared from Sawdust and Rice Husk for Adsorption of Acid Dyes: a Case Study of Acid Yellow 36. *Elsevier Journal of Dyes and Pigments*, 56: 239-249.

Malviya R., Srivasteva P., and Kulkarni G. (2011). Applications of Mucilages in Drug Delivery - A Review. *Advance Biological Research Journal*. 5: 1-7.

Nkeonye, P.O., (1988). Introductory Textiles for Home Economist, Students of art &Beginners Generally. *Textile Dyer & Printer*, 21(17), 20.

National Academy of Science (NAS), (1979).*Tropical Legumes: Resources for the Future*. (NAS), Washington DC,pp117-121.

Nagarajan, B., Nicodemus, A., Mandal, A.K., Verma, R.K., Gireesan, K. and Mahadevan N.P. (1997). Phenology and Controlled Pollination Studies in Tamarind. *Silvae Genetica-Journal of Forest Genetics* 47: 237.

Ocholi, O. (2006). Studies on the preparation and adsorption of activated carbon matrices from Delonix regia pods and Khaya senegalensis fruits. An M.Sc. Thesis, Department of Chemistry, Ahmadu Bello University, Zaria.

Oei, B. C. S. Ibrahim, S. Wang and H. Ang; (2009). Surfactant Modified Barley Straw for Removal of Acid and Reactive Dyes from Aqueous Solution, *Journal of Bioresource Technology*, 100(18): pp4292-4295.

Oladoja, N.A., Aboluwoye and Olademeji (2008). Kinetics and Isotherm Studies on Methylene blue Adsorption onto Ground palm Kernel Coat. *Turkish Journal of engineering and Environmental Science*. 32: 303-312.

Oladunni, N., (2012). Removal of selective heavy metals from aqueous solutions by adsorption onto activated locust bean (*Parkia Biglobosa*) husk. An M.Sc. Thesis, Department of Chemistry, Ahmadu Bello University, Zaria.

Oladunni, N., Agbaji, E.B., and Idris, S.O., (2012). Removal of Pb^{2+} and Ni^{2+} from aqueous solutions by adsorption onto activated locust bean (*Parkia Biglobosa*) husk. *Archives of Applied Science Research*, 4(5): 2161-2173.

Olugbenga S.B, Oladipo M.A, Misbaudeen A.H, and Olalekan A.M.P (2010) Kinetic and Equilibrium Studies of Methylene Blue Removal from Aqueous Solution by Adsorption on Treated Sawdust. *Macedonian Journal of Chemistry and Chemical Engineering*, 29(1): 77–85.

Okoli, C.A., Onukwuli, C.D., Okey-Onyesolu, C.E. and Okoye C.C., (2015). Adsorptive Removal of Dyes from Synthetic Waste water using Activated Carbon from Tamarind Seed. *European Scientific Journal*, 11(18): 190-221.

Okiemmen, F., Okiemen, C., and Wuana, A. (2008). Preparation and Characterization of Activated Carbon from Rice Husk.*Journal of Chemical Society of Nigeria*, 32, 126-136.

OMRI (2002). Activated carbon processing. National Organic standards board of technical advisory panel review for the USDA. National Organic Program, 1-14.

Orhon, D.; Babuna, F.G. andInsel, G. (2001). Characterization and modelling of denimprocessing wastewaters for activated sludge. *Journal of Chemical Technology andBiotechnology*, 76: 919-931

Ozacar M. and Sengil I.A. (2003).Adsorption of reactive dyes on calcined alunite from aqueous solutions. *Journal Hazardous Materials*, 98: 211-224.

Özcan, A.S. S. Tetik, A. Özcan, (2004). Adsorption of acid dyes from aqueous solutions onto sepiolite.*Journal of Separation Science and Technolology*. 39 (2) 301.

Orthman, J. H.Y. and Zhu, G.Q. L., (2003).Use of Anion Clay Hydrotalcite to Remove Coloured Organics from Aqueous Solutions. *Journal of Separation and Purification Technology*, 31 (1) 53.

Palanisamy P.N., Agalya A. and Sivakumar P., (2013). Equilibrium uptake and sorption Dynamics for the Removal of Reactive Dyes from Aqueous Solution using Activated Carbon prepared from *Euphobia tirucalli* L wood. *Indian Journal of Chemical Technology*. 20: 245-251.

Palanisamy, P.N., and Sivakumar P. (2009). Kinetic and Isotherm Studies of the Adsorption of Acid Blue 92 using Low-cost non-conventional Activated Carbon. *Elsevier Journal of Desalination*, 249: 388-397.

Papita S., Shamik C., S. Gupta, I. Kumar, and R. Kumar (2010).Assessment on the Removal of Malachite Green Using Tamarind Fruit Shell as Biosorbent. *CLEAN-Soil, Air, Water;* 38(5-6): 437-445.

Papita S. and Shamik C. (2011). Insight Into Adsorption Thermodynamics, Thermodynamics, Prof. Mizutani Tadashi (Ed.), InTech, Shanghai, pp 23-27.

Patel, R.S., Patel, P.S., Patel, K.C. and Patel, S.K. (2002).Synthesis of non-benzidine Reactive dyes and their application on various fibres,*Asian Journal of Chemistry*,14(1): 420.

Patel H. and Vashi R. (2010).Treatment of Textile Wastewater by Adsorption and Coagulation. E-Journal of Chemistry, 7(4): 1468-1476.

Patnaik, K.K. (1974). Seasonal Pattern of Tartaric Acid Metabolism Underlying the Phasic Development in *Tamarindus indica*. Biological Plant pp 161.

Palanivelu R.A., Rubankumar.(2011). Synthesis and Spectroscopic Characterization of Hydroxyapatite by Sol-Gel Method.*International Journal of Chemical Technology Research* 5(6): 2965-2969.

Phani K., Gangarao D., Kotha N.S., and L. Raju.(2011). Isolation and Evaluation of Tamarind Seed Polysaccharide being used as a Polymer in Pharmaceutical Dosage forms.*Research Journal of Pharmaceutical, Biological and Chemical Sciences*. 2(2): 274-289.

PiccinJ. S., DottoG. L. and PintoL. A. A. (2011). Adsorption Isotherms and Thermochemical Data of Fd&C Red N° 40 Binding by Chitosan. *Brazilian Journal of Chemical Engineering*. 28, (02):295 – 304

Piecuch J.F. (1986). Augmentation of the Atrophic Edentulous Ridge with Porous Replamineform Hydroxyapatite (Interpore-200). Deutclin North America. 30: pp291-305.

Pons, M.P. and Fuste, C.M. (1993). Uranium uptake by immobilized cells of pseudomonas strain. *Journal of Applied Microbiology and Biotechnology*, 39: 4-5, 661-665.

Purseglove, J.W. (1987). Tropical Crops. Dicotyledons. Longman Science and Technology, Singapore,pp204-206

Rama Rao, M. (1975). Flowering Plants of Travancore. Bishen Singh Mahendra Pal Singh, Dehra Dun India: pp 484.

Rao P.S. and Srivastava (1983). Tamarind Packaging of Heat Preserved Foods. Blackie Academic and Professional. New York, pp244-254.

Rao P.S.,and Srivastava H.C. (1973). Tamarind. In: Whistler R.L. editor. Industrial Gums. 2nd edition New York: Academic Press;pp369-411.

Ratee, I.D., (1984), Review of Progress in Coloration and Related Topics, 14:pp50.

Rauli R.A., Adnan R., Bakar M.A., and Masudi S.M., (2011). Synthesis and Characterization of Pure Nanoprous Hydroxyapatite. *Journal of Physical Science,* 22: 25-37.

Ramakrishna,R. Ramkrishna,D., and Allan E. K. (1997). Microbial growth on substitutable substrates: Characterizing the consumer-resource relationship. *Biotechnology and Bioengineering*. 54(1): 77-90.

Risk S., Duru D., Gandy D., and Jacob M. (1994). Natural Polymer Hydrophilic Matrix. Influencing Drug Release Factors. *Journal of Drug Development and Industrial Pharmocology*, (20): 2563-2564.

Robinson, T.Chandran, and P. Nigam, (2002).Effect of Pre-treatments of three waster residues, wheat straw, corncobs and barley husks on dye adsorption *Journal of Bioresources Technology* 85(2): 119.

Robinson, T.; McMullan, G.; Marchant, R. and Nigam, P. (2001). Remediation of dyes in textile effluent: a critical review on current treatment technologies with a proposed alternative. *Journal of Bioresources Technology*, 77: 247-255.

Rudd, V.E. (1991). Fabaceae (Leguminoseae): Sub Family Caesalpinoideae. In: Dassanayake, M.D. and Fosberg, F.R. (Ed): A Revised Handbook to the Flora of Ceylon. Vol. VII. Oxford and IBH Publishing Company (Pvt). Ltd. New Delhi, pp108-235.

Saha, P., and Datta, S. (2009). Assessment on Thermodynamics and Kinetics Parameters on Reduction of Methylene Blue Dye using Flyash. *Journal of Desalination and water treatment,* 12, 219–228.

Sano M., Miyata E., Tamano S., Hagiwara A., Ito N., and Shirai T. (1996). Lack of Carcinogenicity of Tamarind Seed Polysaccharide in B6C3F Mice. *Journal of Food and Chemical Toxicolology*, (34): 463-467.

Sanosh K.P., Chu M.C., Balakrishnan A., Kim T.N., and Cho S.J., (2009) Preparation and Characterization of Nano Hydroxyapatite Powder using Sol-Gel Technique. *Bull Material Science.* 32(5). 465-470.

Saswati G., and Uday C.G., (2005).Studies on adsorption behaviour of Cr(VI) onto Synthetic Hydrous Stannic Oxide. *Water Resources*, 13(4): 597-602

Saradhi, B.V., Rao, S.R.K., Kumar, Y.P., Vijetha, P., Rao, K.V., and Kalyami, G. (2010). Applicability of Langmuir and Freundlich theory for Biosorption of Chromium from Aqueous Solution using test of Sea Urchins. *International Journal of Chemical Engineering Research*, 2(2): 139-148

Shakirullah, M., Habib-ur-Rehman, I.A., Sher, S., and Hameedullah, G. (2006). Sorption studies of nickel ions onto sawdust of *Dalbergia sisso*. *Journal of the Chinese Chemical Society*, 53: 1045-1052.

Shoba B., Sakthiganesh R., and Raju S., (2015).Treatment of Diary Wastewater using Tamarind Kernel Adsorbent.*Internetional Journal of Innovative Research in Engineering and Management*, 3(1): 221-223.

Shanthi and T. Mahalakshmi (2012) Studies on the Removal of Malachite Green and Methylene Blue Dyes from Aqueous Solutions of their Binary Mixture by Adsorbtion over Commercial Activated Carbon and Tamarind Kernel Powd*er. International Journal of Research in Pharmacy and Chemistry.* 2 (2): 289-298

Singh, K.P., D. Mohan, S. Sinha, G.S. Tandon and D. Ghosh, 2003. Colour removal from wastewater using low cost activated carbon derived from agricultural waste material. Ind. Eng. Chem. Res., 42: pp1965-1976.

Singh, J., Mishra, N. S., and Sushmita, B. (2011).Comparative Studies of Physical Characteristics of Raw and Modified Sawdust for their Use as Adsorbents for Removal of Acid Dye.*BioResouirces,*6(3): 2732-2743.

Suresh J. (2013). SEM, FTIR and XRD Studies for the Removal of Cu(II) from Aqueous Solution Using Marine Green Algae. *Journalof Global Research Analysis* 2(11): 2277-8160.

Simons, A.J., Salim, A.S., Orwa, C., Munjuga M. and Mutua, A. (2005). Agroforestry Tree Database: A Tree Species Reference and Selection Guide. World Agroforestry Centre, Nairobi Kenya, pp254-257.

Sougata J., (2010). Evaluation of Epichlorohydrin Cross-Linked Mucoadhesive Patches of Tamarind Seed Polysaccharide for Buccal Application. *International Journal of Pharmaceutical Science and Drug Research,* 2(3): 193-198.

Soloman, P.A.; Basha, C.A.; Ramamurthi, V.; Koteeswaran, K. and Balasubramanian, N. (2009). Electrochemical degradation of Remazol Black B dye effluent. *Clean*, 37(11): pp.889-900

Sun, Q. andL. Yang, (2003).The Adsorption of Basic Dyes from Aqueous Solution on Modified Peat-Resin Particle. *Elsevier Journal of Water Research*, 37 (7): 1535.

Sujja-areevath J., Munday D.L., Cox P.J. and Khan K.A. (1996). Release Characteristics of Diclofenac Sodium from Encapsulated Natural Gum Mini-Matrix Formulations. *International Journal of Pharmaceutical Science*, 139: 53-62.

Suresh, D.S., Thomas, K. A., Mohan, P. N., and Damodaran, A. D. (1994). Alteration of Ilmenite in the Manavalakurichi Deposit, India.*Journal of Clays and Minerals*, 42 (5): 567 - 571.

Sumathi S., and Ray A.R., (2002). Release Behaviour of Drugs from Tamarind Seed Polysaccharide Tablets. *Journal of Pharmacy and Pharmaceutical Science* 5(1): 50-53.

Suteu, D.; Zaharia, C.; Bilba, D.; Muresan, A.; Muresan, R. andPopescu, A. (2009a). Decolorization wastewaters from the textile industry – physical methods, chemical methods. *Industria TextilaJournal*, 60 (5): pp.254-263

Steve,K.,and ErikaT.,(1998).Unit Operations and Processes of Activated Carbon-Environmental Engineering", 2nd Ed. PWS Publishing, pp235.

Taylor, J.A., Pasha, K. and Phillips D.A.S, (2001), The Dyeing of Cotton with Hetero bi-functional Reactive dyes Containing both a Monochlorotriazinyl and a Chloroacetylamino Reactive Group. *Elsevier Journal of Dyes and Pigments*, 51(23): 145.

Talukdar M.M., Plaizer and Vercammen J. (1993). Evaluation of Xanthan Gum as a Hydrophilic Matrix for Controlled Release Dosage form Preparations. *Journal of Drug Development Industrial Pharmacology*, (19), 1037-1046.

Temkin, M. and Pyzhev, V. (1940) Kinetics of Ammonia Synthesis on Promoted Iron Catalysts.*ActaPhysicochimica URSS*, 12, 217-222.

Tucker, S.C. (2000). Floral Development in Tribe Detariae (*Leguminosae Caesalpinoideae*): Amherstia, Brownea and *Tamarindus indica*. *American Journal of Botany* 87: 1385-1407.

Tailor, P. T. Tamura and K. Ozato (2006). IRF Family Proteins and Type I Interferon Induction in Dendritic. *Cell Research*. Cells 16: 134-140

Ucello-Berrata G., Nazzi S., Balzano F., Dicolo G., Zambito Y., and Zaino C. (2008). Enhanced Affinity of Ketotifen Towards Tamarind Seed Polysaccharide in Comparison with Hydroxyethylcellulose and Hyaluronic Acid: A Nuclear Magnet Resonance Investigation. *Journal of Bioorganic and Medicinal Chemistry* (16): 7371-7376.

Vidic D. R., Suidan M.S., and Brenner R.C., (1993).Oxidative coupling of phenols on activated carbon: impact on adsorption equilibrium. *Environmental Science and Technology*. 27(10): pp 2079-2085.

Vadivelan, V., and Vasanth, K. K. (2005). Equilibrium, Kinetics, Mechanism and Process Design for the Sorption of Methylene Blue onto Rice Husk. *Journal of Colloid and Interface Science*, 286: 90–95.

Vijayaraghavan, K. S. W. Won and Y. Yun, (2009). Treatment of Complex Remazol Dye Effluent Using Sawdust- and Coal-Based Activated Carbons, *Journal of Hazardous Materials*, 167 (1-3): pp. 790-796.

Volesky, B., andYang J. (1999). Biosorption of Uranium on *Sargassum* Biomass.*Water Research*. 33(15), Pp. 3357-3363.

Walker, G.M., and L.R. Weatherley, (1999).Kinetics of Acid Dye Adsorption on GAC. *Journal of Water Resources*, 33(8): 1895.

Walker, G.M., and L.R.Weatherley, (2000). Textile Wastewater Treatment Using Granular Activated Carbon Adsorption in Fixed Beds. *Journal of Separation Science and Technology* 35(9): 1329.

Wang, S. Y. Boyjoo, A. Choueib and H. Zhu, (2005). Removal of Dyes from Solution Using Fly Ash and Red Mud. *Journal ofWater Research*, 39(1): pp. 129-138.

Wang S., Li H., Xie S., Li S. and Xu L. (2006). Physical and Chemical Regeneration of Zeolitic Adsorbents for Dye Removal in Wastewater Treatment. *Chemosphere Journal*,65: 82-87.

Waranusantigul, P., Pokethitiyook, P., Kruatrachue, M., and Upatham, E. S. (2003). Kinetic of basic dye (methylene blue) biosorption by giant duckweed (Spirodela polyrrhiza). *Journal of Environmental Pollution*, 125, 385–387.

Waring D.R, (1990). Dyes for Cellulosic Fibres, Chapter 3, 49-63, in: "The Chemistry and Application of Dyes" (Waring, D.R. and Hallas, G., eds.), Plenum Press, New York, pp49-62.

Weber, W.J. (1973). The prediction of the performance of activated carbon for water treatment. A paper presentation at a conference organized by the water research association held at the University of Reading, Malaysia pp. 53-71.

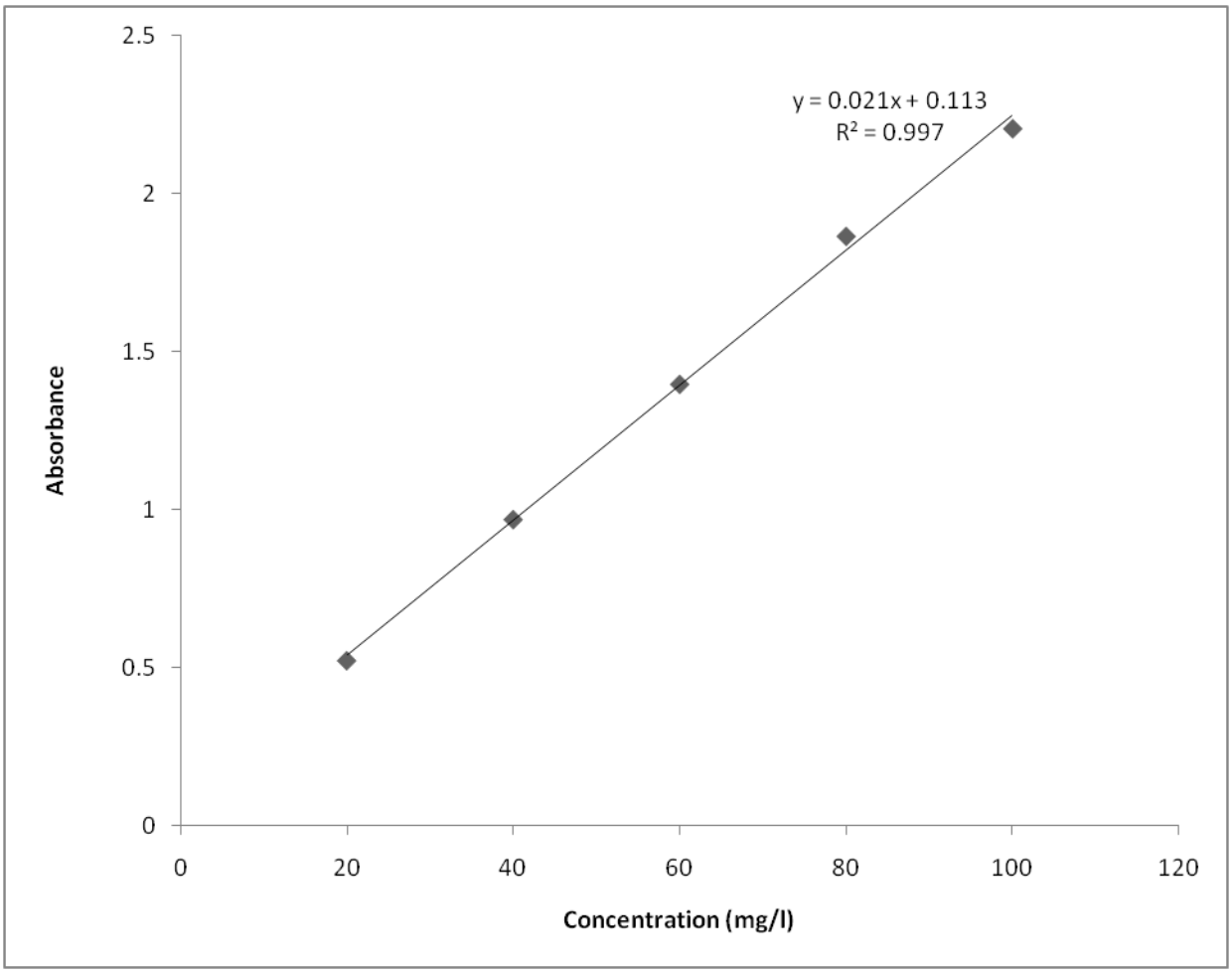
Won, S., Han, M. H., and Yon, Y. S. (2008). Different binding mechanisms in biosorption of Reactive dyes according to their reactivity. *Journal of Water Research*, 42: pp. 4847–4855.

Yang Y., Ong J.L., and Tian J. (2002). Rapid Sintering of Hydroxyapatite by Microwave Processing. *Journal of Materials Science Letters*, 21: 67-69.

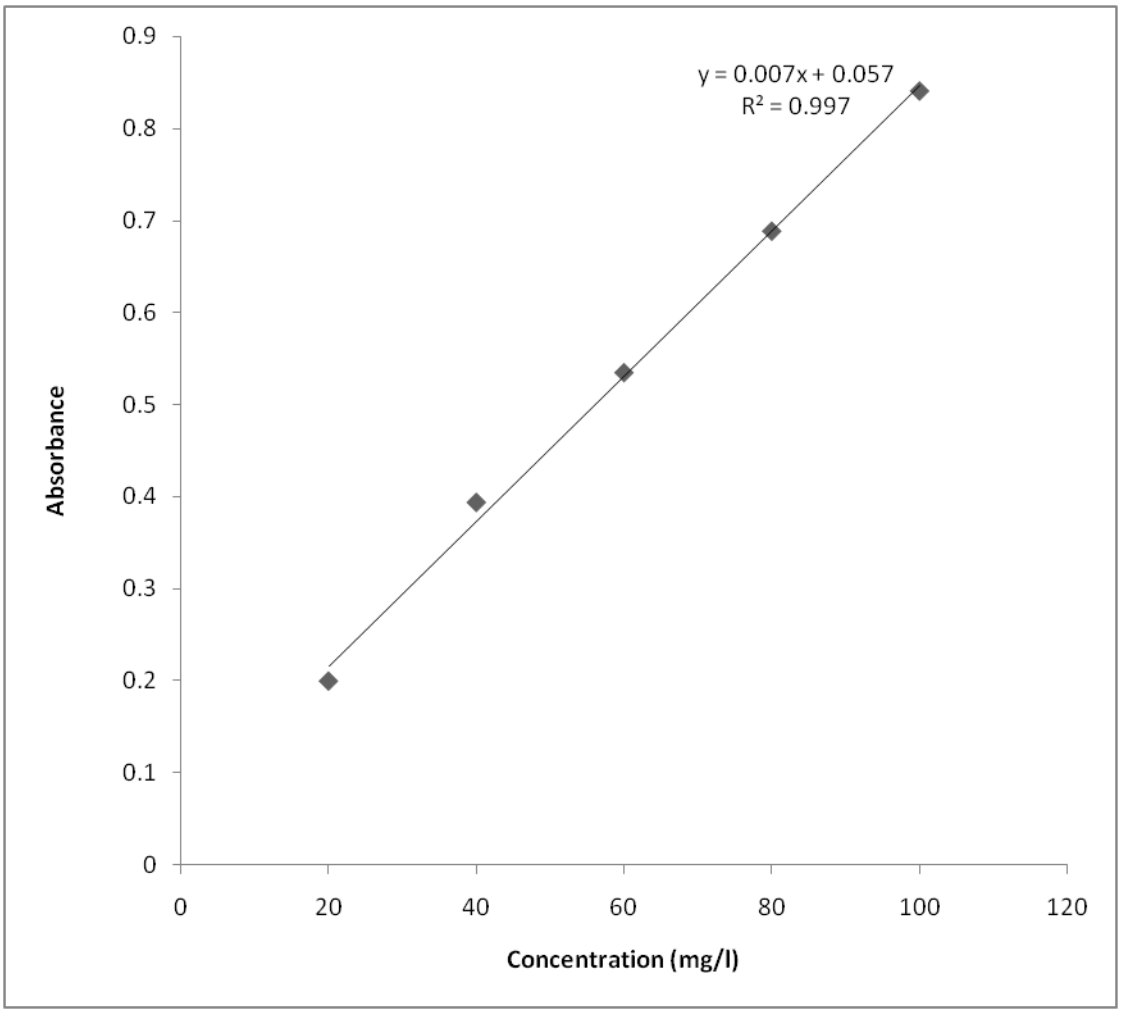
Yoshimura M., Suda H., Okamoto K., and Ioku K. (1994). Hydrothermal Synthesis of Biocompatible Whiskers. *Journal of Materials Science*. 29(13): pp. 3399-3402.

Zaharia, C.; Suteu, D.; Muresan, A.; Muresan, R. andPopescu, A. (2009). Textile wastewater treatment by homogenous oxidation with hydrogen peroxide. *EnvironmentalEngineering and Management Journal*, 8 (6): 1359-13

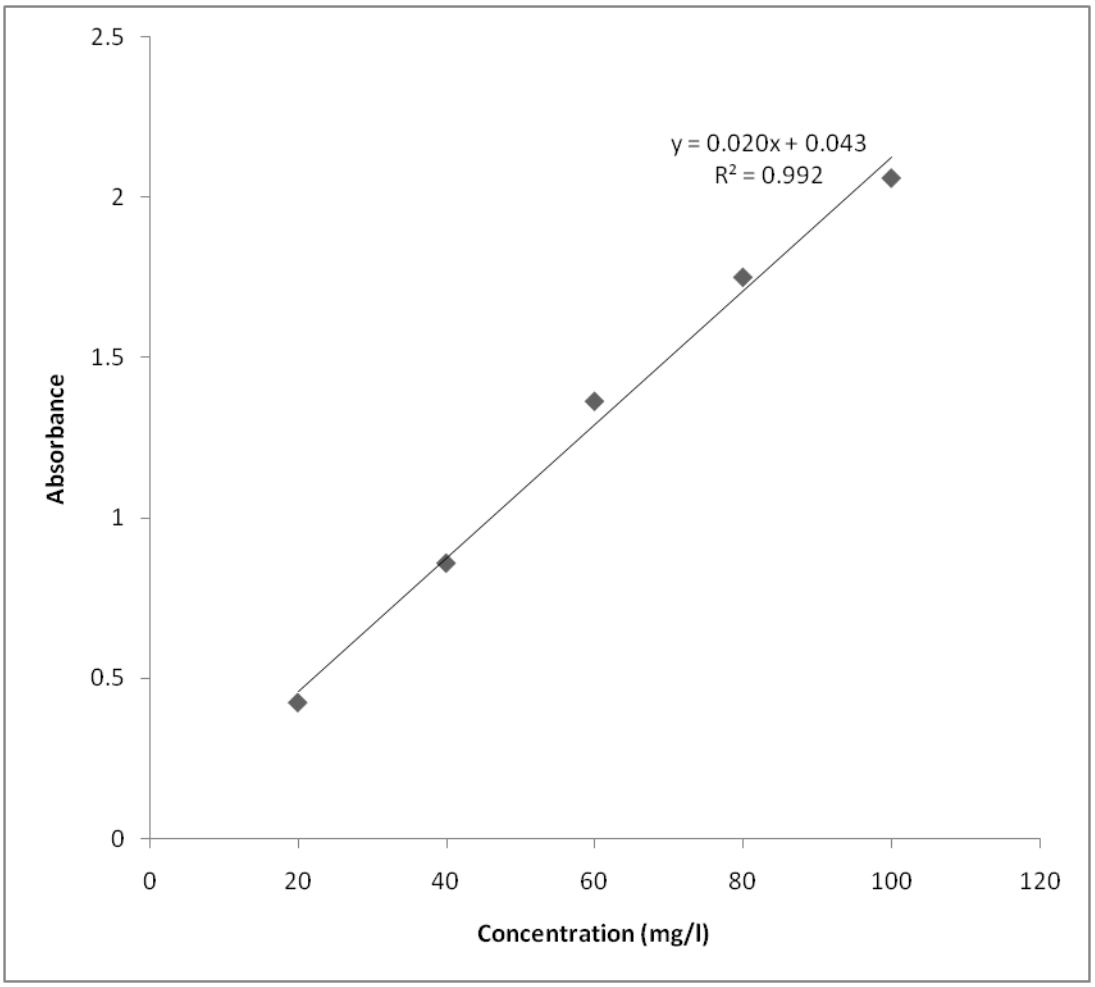
APPENDICES



Appendix 1: Standard Calibration Curve for Acid Red 1



Appendix 2: Standard Calibration Curve for Reactive Blue 29 Dye



Appendix 3: Standard Calibration Curve for Reactive Orange 20 Dye

Appendix 4: Experimental Data obtained from AR1 Dye adsorption on ATKP

	C_o (mg/l)	C_e (mg/l)	q_e (mg/g)	% Removal	
Effect of varying initial concentration	20	4.8	3.8	76.0	
	40	8.7	7.8	78.3	
	60	20.0	10.0	66.7	
	80	33.0	11.8	58.8	
	100	46.0	13.5	54.0	
					Dosage (g)
Effect of varying Adsorbent Dosage	20	7.0	1.6	65.0	0.4
	20	5.5	1.2	72.5	0.6
	20	4.0	1.0	80.0	0.8
	20	2.8	0.9	86.0	1.0
	20	3.0	0.7	85.0	1.2
					pH
Effect of varying initial solution pH	20	1.0	4.75	95.0	2.0
	20	3.4	4.15	83.0	4.0
	20	4.6	3.85	77.0	6.0
	20	6.0	3.50	70.0	8.0
	20	7.8	3.05	61.0	10.0
					Time (min)
Effect of varying Contact time	20	7.5	3.1	62.5	20
	20	6.0	3.5	70.0	40
	20	5.0	3.8	75.0	60
	20	4.2	4.0	79.0	80
	20	4.2	4.0	79.0	100
					Temperature (K)
Effect of varying Temperature	20	6.5	3.4	67.5	298
	20	5.6	3.6	72.0	308
	20	4.0	4.0	80.0	318
	20	3.2	4.3	85.0	323
	20	2.0	4.5	90.0	328

Appendix 5: Experimental Data obtained from RO20 Dye adsorption on ATKP

	C_o (mg/l)	C_e (mg/l)	q_e (mg/g)	% Removal	
Effect of varying initial concentration	20	13.8	1.6	31.0	
	40	28.8	2.8	28.0	
	60	43.8	4.1	27.0	
	80	60.0	5.0	25.0	
	100	80.0	5.0	20.0	
					Dosage (g)
Effect of varying Adsorbent Dosage	20	12.0	1.0	40.0	0.4
	20	11.3	0.7	43.5	0.6
	20	9.0	0.7	55.0	0.8
	20	7.5	0.6	62.5	1.0
	20	8.0	0.5	60.0	1.2
					pH
Effect of varying initial solution pH	20	4.0	4.0	80.0	2.0
	20	14.0	4.9	30.0	4.0
	20	15.8	1.1	21.0	6.0
	20	17.0	0.8	15.0	8.0
	20	18.2	0.5	9.0	10.0
					Time (min)
Effect of varying Contact time	20	16.0	1.0	20.0	20
	20	15.7	1.1	21.5	40
	20	15.0	1.3	25.0	60
	20	14.0	1.5	30.0	80
	20	14.0	1.5	30.0	100
					Temperature (K)
Effect of varying Temperature	20	14.0	0.3	30.0	298
	20	11.6	0.4	42.0	308
	20	9.2	0.5	54.0	318
	20	7.8	0.6	61.0	323
	20	4.0	0.8	80.0	328

Appendix 6: Experimental Data obtained from RB29 Dye adsorption on ATKP

	C_o (mg/l)	C_e (mg/l)	q_e (mg/g)	% Removal	
Effect of varying initial concentration	20	9.7	2.6	51.5	
	40	20.8	4.8	48.0	
	60	33.0	6.8	45.0	
	80	48.0	8.0	40.0	
	100	62.0	9.5	38.0	
					Dosage (g)
Effect of varying Adsorbent Dosage	20	12.0	1.0	40.0	0.4
	20	11.2	0.7	44.0	0.6
	20	10.1	0.6	49.5	0.8
	20	9.3	0.5	53.5	1.0
	20	9.8	0.4	52.0	1.2
					pH
Effect of varying initial solution pH	20	3.0	4.3	85.0	2.0
	20	9.8	2.6	51.0	4.0
	20	12.0	2.0	40.0	6.0
	20	15.1	1.2	24.5	8.0
	20	16.0	1.0	20.0	10.0
					Time (min)
Effect of varying Contact time	20	12.5	1.9	37.5	20
	20	11.8	2.1	41.0	40
	20	10.5	2.4	47.5	60
	20	9.7	2.6	51.5	80
	20	9.7	2.6	51.5	100
					Temperature (K)
Effect of varying Temperature	20	14.0	0.3	30.0	298
	20	12.0	0.4	40.0	308
	20	11.2	0.4	44.0	318
	20	10.3	0.5	48.5	323
	20	9.2	0.5	54.0	328

Appendix 7: Equilibrium Data for Plotting Langmuir Isotherm for AR1 Dye adsorption on ATKP

Tempt. (K)	C_o (mg/l)	C_e (mg/l)	q_e (mg/g)	C_e/q_e (g/l)
298	20	6.5	3.4	1.9
	40	8.8	7.8	1.1
	60	20.0	10.0	2.0
	80	33.3	11.8	2.8
	100	46.0	13.5	3.4
308	20	5.6	3.6	1.6
	40	7.5	8.1	0.9
	60	18.4	10.4	1.8
	80	31.25	12.1	2.6
	100	44.4	13.9	3.3
318	20	4.0	4.0	1.0
	40	6.4	8.4	0.8
	60	16.7	10.9	1.5
	80	29.4	12.7	2.3
	100	42.9	14.3	3.0
323	20	3.0	4.3	0.7
	40	5.8	8.6	0.7
	60	15.6	11.1	1.4
	80	28.6	13.0	2.2
	100	41.16	14.7	2.8
328	20	2.0	4.5	0.4
	40	5.0	8.8	0.6
	60	14.3	11.4	1.3
	80	26.3	13.3	2.0
	100	40.3	14.9	2.7

Appendix 8: Equilibrium Data for Plotting Langmuir Isotherm for RO20 Dye adsorption on ATKP

Tempt. (K)	C_o (mg/l)	C_e (mg/l)	q_e (mg/g)	C_e/q_e (g/l)
298	20	13.8	1.6	8.9
	40	28.7	2.8	10.2
	60	43.8	4.1	10.8
	80	60.0	5.0	12.0
	100	80.0	5.0	16.0
308	20	13.1	1.7	7.6
	40	26.5	3.4	7.8
	60	38.5	5.4	7.2
	80	58.5	5.4	10.9
	100	78.6	5.4	14.7
318	20	12.0	2.0	6.1
	40	24.7	3.8	6.5
	60	38.6	5.3	7.2
	80	56.3	5.9	9.5
	100	76.3	5.9	12.9
323	20	11.7	2.1	5.6
	40	22.5	4.4	5.2
	60	36.2	6.0	6.1
	80	54.5	6.4	8.6
	100	74.7	6.3	11.8
328	20	9.61	2.6	3.7
	40	21.3	4.7	4.6
	60	35.3	6.2	5.7
	80	53.2	6.7	7.9
	100	73.9	6.5	11.3

Appendix 9: Equilibrium Data for Plotting Langmuir Isotherm for RB29 Dye adsorption on ATKP

Tempt. (K)	C_o (mg/l)	C_e (mg/l)	q_e (mg/g)	C_e/q_e (g/l)
298	20	9.7	2.6	3.5
	40	20.0	5.0	4.0
	60	32.9	6.8	4.7
	80	48.0	8.0	6.0
	100	61.9	9.5	6.5
308	20	8.8	2.8	3.2
	40	18.8	5.3	3.6
	60	31.2	7.2	4.3
	80	46.4	8.4	5.5
	100	60.4	9.9	6.1
318	20	5.4	3.7	1.5
	40	17.1	5.7	3.0
	60	28.3	7.9	3.6
	80	44.3	8.9	5.0
	100	58.2	10.45	5.6
323	20	4.7	3.8	1.2
	40	15.3	6.2	2.5
	60	27.2	8.2	3.3
	80	43.3	9.2	4.7
	100	57.5	10.6	5.4
328	20	4.1	4.0	1.0
	40	15.2	6.2	2.4
	60	26.1	8.5	3.1
	80	42.3	9.4	4.5
	100	56.2	11.0	5.1

Appendix 10: Equilibrium Data for Plotting Freundlich Isotherm for ARI Dye adsorption on ATKP

Tempt. (K)	C_o (mg/l)	C_e (mg/l)	q_e (mg/g)	ln C_e(g/l)	ln q_e (mg/g)
298	20	6.5	3.4	1.9	1.2
	40	8.8	7.8	2.2	2.1
	60	20.0	10.0	3.0	2.3
	80	33.3	11.8	3.5	2.5
	100	46.0	13.5	3.8	2.6
308	20	5.6	3.6	1.7	1.3
	40	7.5	8.1	2.0	2.1
	60	18.4	10.4	2.9	2.3
	80	31.3	12.1	3.4	2.5
	100	44.4	13.9	3.8	2.6
318	20	4.0	4.0	1.4	1.4
	40	6.4	8.4	1.9	2.1
	60	16.7	10.9	2.8	2.4
	80	29.4	12.7	3.4	2.5
	100	42.9	14.3	3.8	2.7
323	20	3.0	4.3	1.1	1.5
	40	5.8	8.6	1.8	2.2
	60	15.6	11.1	2.8	2.8
	80	28.6	13.0	3.4	2.6
	100	41.2	14.7	3.7	2.7
328	20	2.0	4.5	0.7	1.5
	40	5.0	8.8	1.6	2.2
	60	14.3	11.4	2.7	2.4
	80	26.3	13.3	3.3	2.6
	100	40.3	14.9	3.7	2.7

Appendix 11: Equilibrium Data for Plotting Freundlich Isotherm for RO20 Dye adsorption on ATKP

Tempt. (K)	C_o (mg/l)	C_e (mg/l)	q_e (mg/g)	$\ln C_e$ (mg/l)	$\ln q_e$ (mg/g)
298	20	13.8	1.6	2.7	0.4
	40	28.7	2.8	3.4	1.0
	60	43.8	4.1	3.8	1.4
	80	60.0	5.0	4.1	1.6
	100	80.0	5.0	4.4	1.6
308	20	13.1	1.7	2.6	0.5
	40	26.5	3.4	3.3	1.2
	60	38.5	5.4	3.7	1.7
	80	58.5	5.4	4.1	1.7
	100	78.6	5.4	4.4	1.7
318	20	12.0	2.0	2.5	0.7
	40	24.7	3.8	3.2	1.3
	60	38.6	5.4	3.7	1.7
	80	56.3	5.9	4.0	1.8
	100	76.3	5.9	4.3	1.8
323	20	11.7	2.1	2.5	0.7
	40	22.5	4.4	3.1	1.5
	60	36.2	6.0	3.6	1.8
	80	54.5	6.4	4.0	1.9
	100	74.7	6.3	4.3	1.8
328	20	9.6	2.6	2.3	1.0
	40	21.3	4.7	3.1	1.5
	60	35.3	6.2	3.6	1.8
	80	53.2	6.7	4.0	1.9
	100	73.9	6.5	4.3	1.9

Appendix 12: Equilibrium Data for Plotting Freundlich Isotherm for RB29 Dye adsorption on ATKP

Tempt. (K)	C_o (mg/l)	C_e (mg/l)	q_e (mg/g)	lnC_e (mg/l)	ln q_e (mg/g)
298	20	9.7	2.6	2.3	1.0
	40	20.0	5.0	3.0	1.6
	60	32.9	6.8	3.5	1.9
	80	48.0	8.0	3.9	2.1
	100	61.9	9.5	4.1	2.3
308	20	8.8	2.8	2.2	1.0
	40	18.8	5.3	2.9	1.7
	60	31.2	7.2	3.4	2.0
	80	46.4	8.4	3.8	2.1
	100	60.4	9.9	4.1	2.3
318	20	5.4	3.7	1.7	1.3
	40	17.1	5.7	2.8	1.7
	60	28.3	7.9	3.3	2.1
	80	44.3	9.0	3.8	2.2
	100	58.2	10.5	4.1	2.4
323	20	4.7	3.8	1.6	1.3
	40	15.3	6.2	2.7	1.8
	60	27.2	8.2	3.3	2.1
	80	43.3	9.2	3.8	2.2
	100	57.5	10.6	4.1	2.4
328	20	4.1	4.0	1.1	1.4
	40	15.2	6.2	2.8	1.8
	60	26.1	8.5	3.3	2.1
	80	42.3	9.4	3.7	2.2
	100	56.2	11.0	4.0	2.4

Appendix 13: Equilibrium Data for Plotting Temkin Isotherm for AR1 Dye adsorption on ATKP

Tempt. (K)	C_o (mg/l)	C_e (mg/l)	q_e (mg/g)	$\ln C_e$ (mg/l)
298	20	6.5	3.4	1.9
	40	8.8	7.8	2.2
	60	20.0	10.0	3.0
	80	33.3	11.8	3.5
	100	46.0	13.5	3.8
308	20	5.6	3.6	1.7
	40	7.5	8.1	2.0
	60	18.4	10.4	2.9
	80	31.3	12.1	3.4
	100	44.4	13.9	3.8
318	20	4.0	4.0	1.4
	40	6.4	8.4	1.9
	60	16.7	10.9	2.8
	80	29.4	12.7	3.4
	100	42.9	14.3	3.8
323	20	3.0	4.3	1.1
	40	5.8	8.6	1.8
	60	15.6	11.1	2.8
	80	28.6	13.0	3.4
	100	41.2	14.7	3.7
328	20	2.0	4.5	0.7
	40	5.0	8.8	1.6
	60	14.3	11.4	2.7
	80	26.3	13.3	3.3
	100	40.3	14.9	3.7

Appendix 14: Equilibrium Data for Plotting Temkin Isotherm for RO20 Dye adsorption on ATKP

Tempt. (K)	C_o (mg/l)	C_e (mg/l)	q_e (mg/g)	$\ln C_e$ (mg/l)
298	20	13.8	1.6	2.7
	40	28.7	2.8	3.4
	60	43.8	4.1	3.8
	80	60.0	5.0	4.1
	100	80.0	5.0	4.4
308	20	13.1	1.7	2.6
	40	26.5	3.4	3.3
	60	38.5	5.4	3.7
	80	58.5	5.4	4.1
	100	78.6	5.4	4.4
318	20	12.0	2.0	2.5
	40	24.7	3.8	3.2
	60	38.6	5.4	3.7
	80	56.3	5.9	4.0
	100	76.3	5.9	4.3
323	20	11.7	2.1	2.5
	40	22.5	4.4	3.1
	60	36.2	6.0	3.6
	80	54.5	6.4	4.0
	100	74.7	6.3	4.3
328	20	9.6	2.6	2.3
	40	21.3	4.7	3.1
	60	35.3	6.2	3.6
	80	53.2	6.7	4.0
	100	73.9	6.5	4.3

Appendix 15: Equilibrium Data for Plotting Temkin Isotherm for RB29 Dye adsorption on ATKP

Tempt. (K)	C_o (mg/l)	C_e (mg/l)	q_e (mg/g)	$\ln C_e$ (mg/l)
298	20	9.7	2.6	2.3
	40	20.0	5.0	3.0
	60	32.9	6.8	3.5
	80	48.0	8.0	3.9
	100	61.9	9.5	4.1
308	20	8.8	2.8	2.2
	40	18.8	5.3	2.9
	60	31.2	7.2	3.4
	80	46.4	8.4	3.8
	100	60.4	9.9	4.1
318	20	5.4	3.7	1.7
	40	17.1	5.7	2.8
	60	28.3	7.9	3.3
	80	44.3	8.9	3.8
	100	58.2	10.5	4.1
323	20	4.7	3.8	1.6
	40	15.3	6.2	2.7
	60	27.3	8.2	3.3
	80	43.3	9.2	3.8
	100	57.5	10.6	4.1
328	20	4.1	4.0	1.1
	40	15.2	6.2	2.7
	60	26.1	8.5	3.3
	80	42.3	9.4	3.7
	100	56.2	11.0	4.0

Appendix 16: Equilibrium Data for Plotting D-R Isotherm for AR1 Dye adsorption on ATKP

Tempt. (K)	C_o (mg/l)	C_e (mg/l)	q_e (mg/g)	lnq_e (mg/l)	ε^2
298	20	6.5	3.4	1.2	125700.5
	40	8.8	7.8	2.1	71109
	60	20.0	10.0	2.3	14612.3
	80	33.3	11.8	2.5	5373.8
	100	46.0	13.5	2.6	2844.0
308	20	5.6	3.6	1.3	177016.1
	40	7.5	8.1	2.1	102724.6
	60	18.4	10.4	2.3	18443.4
	80	31.3	12.1	2.5	6505.9
	100	44.4	13.9	2.6	3247.1
318	20	4.0	4.0	1.4	326505.2
	40	6.4	8.4	2.1	138212.4
	60	16.7	10.9	2.4	22125.8
	80	29.4	12.7	2.5	7330.6
	100	42.9	14.3	2.7	3484.8
323	20	3.0	4.3	1.5	596830.1
	40	5.8	8.6	2.2	182462.1
	60	15.6	11.1	2.4	27977.9
	80	28.6	13.0	2.6	8535.3
	100	41.2	14.7	2.7	4155.6
328	20	2.0	4.5	1.5	1222573.0
	40	5.0	8.8	2.2	247197.3
	60	14.3	11.4	2.4	34022.2
	80	26.3	13.3	2.6	10348.4
	100	40.3	14.9	2.7	4472.2

Appendix 17: Equilibrium Data for Plotting D-R Isotherm for RO20 Dye adsorption on ATKP

Tempt. (K)	C_o (mg/l)	C_e (mg/l)	q_e (mg/g)	lnq_e (mg/g)	ε^2
298	20	13.8	1.6	0.4	30042.4
	40	28.7	2.8	1.0	7200.7
	60	43.8	4.1	1.4	3128.1
	80	60.0	5.0	1.6	167.7
	100	80.0	5.0	1.6	947.3
308	20	13.1	1.7	0.5	35380.0
	40	26.5	3.4	1.2	9003.6
	60	38.5	5.4	1.7	4316.0
	80	58.5	5.4	1.7	1885.1
	100	78.6	5.4	1.7	1048.1
318	20	12.0	2.0	0.7	44497.9
	40	24.7	3.8	1.3	11010.0
	60	38.6	5.4	1.7	4572.7
	80	56.3	5.9	1.8	2165.1
	100	76.3	5.9	1.8	1184.5
323	20	11.7	2.1	0.7	48906.1
	40	22.5	4.4	1.5	13601.1
	60	36.2	6.0	1.8	5354.8
	80	54.5	6.4	1.9	2382.4
	100	74.7	6.3	1.8	1276.0
328	20	9.6	2.6	1.0	72845.4
	40	21.3	4.7	1.5	15639.0
	60	35.3	6.2	1.8	5799.8
	80	53.2	6.7	1.9	2582.8
	100	73.9	6.5	1.9	1344.9

Appendix 18: Equilibrium Data for Plotting D-R Isotherm for RB29 Dye adsorption on ATKP

Tempt. (K)	C_o (mg/l)	C_e (mg/l)	q_e (mg/g)	lnq_e (mg/g)	ε^2
298	20	9.7	2.6	1.0	58863.3
	40	20.0	5.0	1.6	14612.3
	60	32.9	6.8	1.9	5496.7
	80	48.0	8.0	2.1	2609.8
	100	61.9	9.5	2.3	1575.5
308	20	8.8	2.8	1.0	65505.3
	40	18.8	5.3	1.7	17538.9
	60	31.2	7.2	2.0	6518.2
	80	46.4	8.4	2.1	2982.9
	100	60.4	9.9	2.3	1768.1
318	20	5.4	3.7	1.3	204547.2
	40	17.1	5.7	1.7	22465.3
	60	28.3	7.9	2.1	8454.8
	80	44.3	8.9	2.2	3485.5
	100	58.2	10.5	2.3	2028.7
323	20	4.7	3.8	1.3	265060.1
	40	15.3	6.2	1.8	28877.6
	60	27.2	8.2	2.1	9392.6
	80	43.3	9.2	2.2	3845.6
	100	57.5	10.6	2.4	2144.4
328	20	4.1	4.0	1.4	349927.2
	40	15.2	6.2	1.8	30360.0
	60	26.1	8.5	2.1	10512.5
	80	42.3	9.4	2.2	4066.8
	100	56.2	11.0	2.4	2313.9

Appendix 19: Equilibrium Data for Plotting Pseudo First and Second Order Kinetics for AR1, RO20 and RB29 Dye adsorption on ATKP

Dye	Time (min)	q_t (mg/g)	q_e (mg/g)	$q_e - q_t$ (mg/g)	log ($q_e - q_t$) (mg/g)	t/q_t (min.g/mg)
AR1	20	3.1	4.0	0.8	-0.1	6.4
	40	3.5		0.5	-0.4	11.4
	60	3.8		0.2	-0.7	16.0
	80	4.0		0	0	20.3
	100	4.0		0	0	25.3
RO20	20	1.0	1.5	0.5	-0.3	20.0
	40	1.1		0.5	-0.4	38.1
	60	1.3		0.3	-0.6	48.1
	80	1.5		0	0	53.3
	100	1.5		0	0	53.3
RB29	20	1.9	2.6	0.7	-0.2	10.6
	40	2.1		0.5	-0.3	19.5
	60	2.4		0.2	-0.7	25.3
	80	2.6		0	0	31.1
	100	2.6		0	0	38.8

Appendix 20: Equilibrium Data for Plotting Van't Hoff Isotherms for AR1, RO20 and RB29 Dye adsorption on ATKP

Dye	Tempt. (K)	$T^{-1}(K^{-1})$	K	lnK
AR1	298	0.0033	23.8	3.2
	308	0.0032	16.7	2.8
	318	0.0031	11.1	2.4
	328	0.00309	7.7	2.0
	323	0.00305	5.6	1.7
RO20	298	0.0033	100.0	4.6
	308	0.0032	50.0	3.9
	318	0.0031	33.3	3.5
	328	0.00309	33.3	3.5
	323	0.00305	16.7	2.8
RB29	298	0.0033	50.0	3.9
	308	0.0032	49.8	3.9
	318	0.0031	16.7	2.8
	328	0.00309	14.3	2.7
	323	0.00305	14.3	2.7

Appendix 21: Effect of Initial pH on Dye Adsorption onto TKP

	Acid Red 1		Reactive Orange 20		Reactive Blue 29	
pH	q_e (mg/l)	R(%)	q_e (mg/l)	R(%)	q_e (mg/l)	R(%)
2	4.75	95.0	4.00	80.0	4.25	85.0
4	4.15	83.0	4.93	30.0	2.55	51.0
6	3.85	77.0	1.05	21.0	2.00	40.0
8	3.50	70.0	0.75	15.0	1.23	24.5
10	3.05	61.0	0.45	9.0	1.00	20.0

Appendix 22: Effect of Adsorbent Dose (A.D.) on Dye Adsorption onto TKP

	Acid Red 1		Reactive Orange 20		Reactive Blue 29	
A.D. (g)	q_e (mg/l)	R(%)	q_e (mg/l)	R(%)	q_e (mg/l)	R(%)
0.4	1.63	65.0	1.00	40.0	1.00	40.0
0.6	1.21	72.5	0.73	43.5	0.73	44.0
0.8	1.00	80.0	0.69	55.0	0.62	49.5
1.0	0.86	86.0	0.63	62.5	0.54	53.5
1.2	0.70	85.0	0.50	60.0	0.43	52.0

Appendix 23: Effect of Contact Time on Dye Adsorption onto TKP

	Acid Red 1		Reactive Orange 20		Reactive Blue 29	
Time (min)	q_e (mg/l)	R(%)	q_e (mg/l)	R(%)	q_e (mg/l)	R(%)
20	3.1	62.5	1.0	20.0	1.9	37.5
40	3.5	70.0	1.08	21.5	2.1	41.0
60	3.8	75.0	1.3	25.0	2.4	47.5
80	4.0	80.0	1.5	30.0	2.6	51.5
100	4.0	80.0	1.5	30.0	2.6	51.5

Appendix 24: Effect of Initial Concentration on Dye Adsorption onto TKP

	Acid Red 1		Reactive Orange 20		Reactive Blue 29	
C_o (mg/l)	q_e (mg/l)	R(%)	q_e (mg/l)	R(%)	q_e (mg/l)	R(%)
20	3.8	76.0	1.6	31.0	2.6	51.5
40	7.8	78.3	2.8	28.0	4.8	48.0
60	10.0	66.7	4.1	27.0	6.8	45.0
80	11.8	58.8	5.0	25.0	8.0	40.0
100	13.5	54.0	5.0	20.0	9.5	38.0

Appendix 25: Langmuir Isotherm constants for AR1, RB29 and RO20

Tempt (K)	Dye	q_m(mg/g)	B(l/g)	R^2	R_L
	Acid Red 1				
298		20.8	0.04	0.859	0.35
308		18.87	0.06	0.917	0.23
318		17.86	0.09	0.978	0.14
323		17.24	0.13	0.991	0.08
328		16.67	0.18	0.995	0.05
	Reactive Blue 29				
298		16.67	0.02	0.986	0.42
308		16.67	0.02	0.989	0.36
318		13.16	0.06	0.971	0.18
323		12.82	0.07	0.983	0.13
328		12.98	0.07	0.977	0.11
	Reactive Orange 20				
298		10.10	0.01	0.907	0.45
308		9.01	0.02	0.825	0.36
318		9.35	0.03	0.930	0.26
323		9.61	0.03	0.901	0.23
328		8.54	0.06	0.974	0.13

Appendix 26: Freundlich Isotherm constants for AR1, RB29 and RO20

Tempt (K)	Dye	K_f(l/g)	N	R^2
	Acid Red 1			
298		1.57	1.72	0.803
308		1.98	1.88	0.793
318		2.93	2.12	0.863
323		3.32	2.27	0.797
328		3.97	2.66	0.931
	Reactive Orange 20			
298		4.09	1.39	0.964
308		2.75	1.51	0.860
318		2.06	1.63	0.915
323		1.72	1.68	0.856
328		1.00	2.12	0.898
	Reactive Blue 29			
298		1.71	1.46	0.982
308		1.36	1.55	0.981
318		1.72	2.27	0.989
323		2.05	2.46	0.995
328		2.63	2.90	0.984

Appendix 27: Temkin Isotherm constants for AR1, RB29 and RO20

Tempt (K)	Dye	A_T(J/mg)	b_T (l/g)	R^2
	Acid Red 1			
298		2.24	552.4	0.921
308		1.69	600.4	0.913
318		1.12	668.8	0.953
323		1.33	808.1	0.971
328		2.21	820.6	0.987
	Reactive Orange 20			
298		7.11	1138.0	0.969
308		5.22	1167.7	0.865
318		4.61	1158.1	0.950
323		4.01	1292.3	0.910
328		2.37	1312.0	0.928
	Reactive Blue 29			
298		4.93	683.5	0.992
308		4.22	709.3	0.993
318		1.68	945.6	0.960
323		1.25	995.1	0.979
328		1.47	1173.0	0.942

Appendix 28: Dubinin Radushkevich Isotherm constants for AR1, RB29 and RO20

Tempt (K)	Dye	B_D (mol^2/J^2)	q_D (mg/g)	R^2
	Acid Red 1			
298		$-1x10^{-5}$	13.0	0.941
308		$-7x10^{-6}$	13.2	0.932
318		$-4x10^{-6}$	13.1	0.974
323		$-2x10^{-6}$	13.0	0.965
328		$-9x10^{-7}$	12.76	0.933
	Reactive Orange 20			
298		$-4x10^{-5}$	4.64	0.923
308		$-3x10^{-5}$	5.53	0.950
318		$-3x10^{-5}$	5.88	0.963
323		$-2x10^{-5}$	6.50	0.989
328		$-1x10^{-5}$	6.51	0.964
	Reactive Blue 29			
298		$-2x10^{-5}$	8.14	0.923
308		$-2x10^{-5}$	8.63	0.934
318		$-4x10^{-6}$	8.44	0.789
323		$-3x10^{-6}$	8.73	0.829
328		$-2x10^{-6}$	8.87	0.798

Appendix 29: Pseudo-First order Kinetic constants for AR1, RO20 and RB29

Dye	$k_1(min^{-1})$	q_e (mg/g) (calculated)	R^2
Acid Red 1	0.005	2.41	0.074
Reactive Orange 20	0.0092	3.43	0.347
Reactive Blue 29	0.0069	2.56	0.107

Appendix 30: Pseudo-Second order Kinetic constants for AR1, RO20 and RB29

Dye	k_2 (g/mg.min)	q_e (mg/g) (calculated)	R^2
Acid Red 1	0.03	4.29	0.999
Reactive Orange 20	0.009	2.44	0.847
Reactive Blue 29	0.002	2.95	0.993

Appendix 31: Thermodynamic Parameters for AR1, RO20 and RB29 Adsorption onto TKP

Acid Red 1	Tempt. (K)	ΔG (KJ/mol)	ΔH (kJ/mol)	ΔS (J/mol K)	E (kJ/mol)
	298	-7.85	-45.61	-123.4	0.22
	308	-7.2			0.27
	318	-6.37			0.35
	323	-5.48			0.50
	328	-4.69			0.74
Reactive Orange 20					
	298	-11.4	-51.9	-133.0	0.11
	308	-10.0			0.13
	318	-9.3			0.13
	323	-9.4			0.16
	328	-7.6			0.22
Reactive Blue 29					
	298	-9.69	-50.0	-131.0	0.16
	308	-9.99			0.16
	318	-7.43			0.35
	323	-7.14			0.41
	328	-7.3			0.50



Plate I: Coloured Effluent discharged from an Industry into the Environment

(http://indicportal.org/tag/development/)



Plate II: A Dye Polluted Water body(http://inhabitat.com/why-we-need-earth-day-7-most-pressing-environmental-problems-we-need-to-solve/why-we-need-earth-day-energy-5)



Plate III: Prepared Stock Solutions of Acid Red 1, Reactive Orange 20 and Reactive Blue 29



Plate IV: Prepared concentrations of Acid Red 1, Reactive Orange 20 and Reactive Blue 29 Dyes before Adsorption Treatment on Activated TKP



Plate V: Treatment of Dye samples using Activated Tamarind Kernel Powder

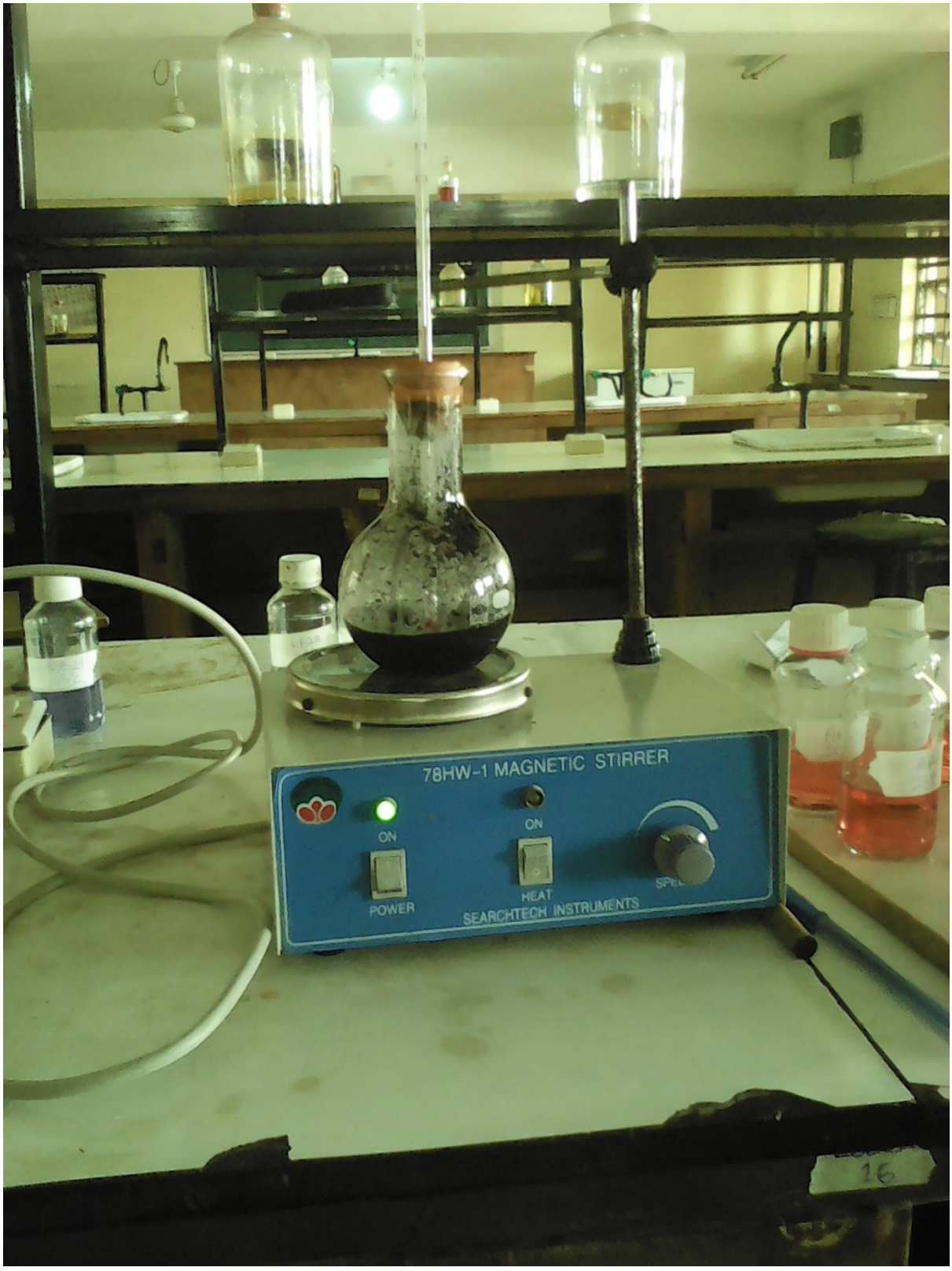


Plate VI: Temperature controlled treatment of Acid Red 1, Reactive Orange 20 and Reactive Blue 29 using TKP



Plate VII: UV/Visible Spectrophotometric Analysis of Treated Dye Samples